INTERNATIONAL ENERGY AGENCY
energy conservation in buildings and
community systems programme
Annex XII
Windows and fenestration

Step 2

Thermal and Solar Properties of Windows

EXPERT GUIDE

December 1987

INTERNATIONAL ENERGY AGENCY

Energy Conservation in Buildings and
Community Systems Programme

Annex XII, WINDOWS AND FENESTRATION

Report from Step 2

THERMAL AND SOLAR PROPERTIES OF WINDOWS

EXPERT GUIDE

This report is part of the work of the IEA Energy Conservation in Buildings & Community Systems Programme

Annex XII - Windows and Fenestration

Participants in this task:

Belgium, FR-Germany, Italy, The Netherlands (Operating Agent), Norway, Switzerland, United Kingdom, United States of America.

The complete list of representatives who have contributed to this report is given in chapter 7.

Document	: Report on work carried out under Step 2 of the project.
Distribution	: Unrestricted.
Editor	: H.A.L. van Dijk and K.Th. Knorr TNO Institute of Applied Physics P.O. Box 155 2600 AD DELFT The Netherlands.
Additional copies:	TNO Institute of Applied Physics.
Approximate price:	Dfl 85.--.

Delft, December 1987

LIST OF CONTENTS

PREFACE

International Energy Agency

In order to strengthen co-operation in the vital area of energy policy, an Agreement of an International Energy Programme was formulated among a number of industrialized countries in November 1974. The International Energy Agency (IEA) was established as an autonomous body within the Organization for Economic Co-operation and Development (OECD) to administer that agreement. Twenty-one countries are currently members of the IEA, with the Commission of the European Communities participating under special arrangement.

As one element of the International Energy Programme, the Participants undertake co-operative activities in energy research, development and demonstration. A number of new and improved energy technologies which have the potential of making significant contributions to our energy needs were identified for collaborative efforts. The IEA Committee on Energy Resarch and Development (CRD) assisted by a small Secretariat staff, co-ordinates the energy research, development and demonstration programme.

Energy Conservation in Buildings and Community Systems

As one element of the Energy Programme, the IEA encourages research and development in a number of areas related to energy. In one of these areas, energy conservation in buildings, the IEA is encouraging various exercises to predict more accurately the energy use of buildings, including comparison of existing computer programmes, building monitoring, comparison of calculation methods, as well as air quality and inhabitant behaviour studies.

The Executive Committee

Overall control of the R&D programme energy conservation in buildings and community systems is maintained by an Executive Committee, which not only monitors existing projects but identifies new areas where collaborative effort may be beneficial. The Executive Committee ensures all projects fit into a predetermined strategy without unnecessary overlap or duplication but with effective liaison and communication.

ANNEX XII

In June 1982 the Executive Committee approved Annex XII, 'Windows and Fenestration' as a new joint effort project, with the Netherlands acting as 'Operating Agent' to co-ordinate the work.
The following countries are participating in this project:

BELGIUM, FEDERAL REPUBLIC OF GERMANY, ITALY, THE NETHERLANDS, NORWAY, SWITZERLAND, UNITED KINGDOM, UNITED STATES.

The project consists of 5 steps:

Step 1: Survey the state-of-the-art in all types of existing windows and future designs (including glazing and combinations of glazing and insulating and/or sunshading systems).

Step 2: Survey the state of the art in thermal and solar properties of windows and compare definitions, test methods, calculation procedures and measured, calculated or assumed data, wherever possible converted to one or several sets of standardized conditions. The aim: to try and cover all existing (and sometimes conflicting) information in this field in an extensive report for 'expert groups'.
A separate report contains summarized information for general use among architects, consultants and manufacturers.

Step 3: Review and analyse existing simplified steady-state calculation methods dealing with gains and losses through window systems. These methods can provide a preliminary and global figure for the influence of the window on energy consumption without considering the interaction with the builing, occupants and climate in a detailed way.

Step 4: Adapt and compare existing dynamic calculation methods dealing with the influence of window type, size and orientation on energy consumption and thermal comfort in buildings.
Normally, a good window design will often be treated with a global approximation, with the consequence that specific features of the design cannot be revealed properly. With a study specifically focused on windows complex systems also can be simulated, like multi-layer systems with foils, coatings and/or gas fillings and e.g. systems at which the control of an openable window, insulation panel, or sunshading is associated with indoor temperature and/or time and/or intensity of solar radiation. A thorough consideration of the effect of windows calls for a calculation model that can handle such simulation.

Step 5: Apply unsteady state models in a series of selected, general sensitivity studies and thereby produce extensive information on optimal window design from an energy point of view for different buildings (mass, insulation), occupants' behaviour schemes (control of equipment, internal heat) and climatic zones. The results are aimed at groups like architects, manufacturers and policy makers.

This publication is the main result of the efforts within Step 2.

1. INTRODUCTION

H.A.L. van Dijk
TNO Institute of Applied Physics
P.O. Box 155
2600 AD DELFT
The Netherlands

LIST OF CONTENTS

1. BACKGROUND

From the point of view of functioning windows are the most complex constructive elements of a building.
The window is a part of the building envelop. In that function it acts as a physical barrier against climatic phenomena like wind and rain, heat or cold, noise and dust, and as a physical and psychological barrier between the occupants and the world outside.
On the other hand the window has the special function of communicating controlled amounts of light, air, view and sound from and to the outside. It is this combination of functions, which - together with esthetic or other cultural considerations - has led to specific designs for different regions and times, restricted by the technical, political and economic situation.

A number of the above-mentioned functions have been taken over in the last two decades by separate facilities, in the expectation of a permanent flow of cheap fossil energy. The result has been an excessive use of artificial lighting and HVAC-installations.
Since the problems on the energy market in the last decade the multi-functional character of the window has been regaining its original place.

The thermal and solar properties of windows became crucial elements in an energy efficient design. The lack of international agreement on terminology, calculation procedures and testing, however, led to significant discrepancies in this field.
As this report will show, there are a great many conditions that influence the values for the thermal and solar performance of a window.

Different conditions assumed in calculations or applied during experiments lead to different results. Moreover, differences occur due to various simplifications in calculation or in the evaluation of test results.

This confusion concerning the window properties affects the prediction of the performance of an energy-efficient design.
It affects e.g. the result of a complex hour by hour computer calculation where precise and detailed hourly values of the window properties are needed. It also affects the result of a simplified design tool where realistic mean values are requested.
Furthermore, similar products on the market receive different ratings purely as a result of differences in the determination procedure for the properties of the window or window component. In the selection of products even minor differences may have a decisive influence on the actual choice.
Better knowledge and more international agreement concerning thermal and solar properties of windows will strongly benefit the rational selection and use of windows in an energy-efficient design.

2. AIM

The aim of this publication is to survey the state-of-the-art in thermal and solar properties of windows; to compare definitions, test methods, calculation procedures and measured, calculated or assumed data; to illustrate the influence of assumed or actual conditions and simplifying approximations.

The target group for such an extensive report is necessarily limited to experts in the field of window physics.
A separate report summarizes the information for general use among architects, consultants and manufacturers.

3. METHOD

The research project Annex XII, Windows and Fenestration started in October 1982 at a first experts meeting in Delft by defining a general workplan for each of the five steps mentioned in the Preface.
With the actual work within the project a gradual start was made in the course of 1983. Early 1984 the final list of participants was established and the group then accelarated its activities.

For Step 2 the initial approach was to present the state-of-the-art on the basis of comparison of results on a number of selected window examples.
The results would contain the values for the thermal and solar properties derived by the participants in a wide variety of different ways.
Soon, however, it became clear that a separate document was needed. This document should serve as a kind of extensive glossary of terms.
First drafts from the Operating Agent were discussed at successive experts meetings and modified and extended according to the suggestions from the participants.

Late 1984 it had become clear that, to meet the aim of Step 2, the proposed document would have to grow in depth and size more than originally expected.
This necessitated a reorganisation of the work; the drafting of the various chapters of the report - now called Thermal and Solar Properties of Windows - was distributed among the participants.
The work on the comparison of the selected examples received a more limited scope: a comparison for thermal resistances and U-values only; see list of other publications.

The year 1985 was used for writing the first draft chapters of the report on Thermal and Solar Properties, discussing the contents and identifying overlaps and gaps. By the end of that year, at the 10th meeting in Stuttgart, it was decided to divide the report into two separate parts:

<u>Part 1</u>:
A short report for "users" (e.g. architects, consultants, manufacturers), with a qualitative description of window properties, definitions, test and calculation methods and the relation between windows and energy consumption, with only simplified formulae, but with many references to part 2.

<u>Part 2</u>:
An extensive report for "experts", presenting detailed information on windows and their thermal and solar properties.

Part 2 consists of independent contributions (sections) in the form of an article, with an individual responsibility by each main author.

During the final year of the project, the draft chapters were completed; an extensive set of guidelines was used to ensure uniformity in the presentations. The individually written sections were reviewed by the experts group of participants in Annex XII, listed at the end of this introduction. The first complete draft of the publication was discussed at the final experts meeting in October 1986 in Brussels. At this meeting arrangements were made for the final editing.

Notwithstanding the reviewing procedure, the responsibility for the contents of the sections, however, remains with the individual authors.

The short version of the report was edited by the Operating Agent on the basis of summaries provided by the authors of the various chapters.

4. ENERGY-EFFICIENT WINDOWS

Just as the window itself may be considered to be an architectural compromise between the occupant's desire to be separated and protected from outdoor environment and yet maintain connection with and derive benefit from the outdoors, the energy-efficient window is a compromise on an expanded perspective: a compromise between the user's needs, the ambient energy flows and the building's energy budget.
Because ambient energy occurs in great varieties - solar gain, air movement, temperature difference - each of significant magnitude and associated with amenities (light, ventilation, thermal comfort) which the building must provide in any case, there are both opportunities for and constraints on using the window to improve the building's energy budget. Solar gain in winter may provide useful heat and light, but may also cause glare or local overheating. Solar gain in summer may provide unwanted heat, but may also be a cooler light source than electrical alternatives.

Different combinations of sources may provide new opportunities: ventilation may be used in a window system to reduce thermal losses or re-distribute solar heat gains. Moreover, combinations and tradeoffs may be inherent in a particular window technology: reflective glazing to reduce solar heating in summertime may also reduce beneficial wintertime heating; multiple glazing may reduce thermal losses but also desirable daylighting.
Given this inherent complexity, understanding and improving fenestration performance require familiarity with a broad range of phenomena. This report is intended as a discussion and summary of those phenomena.

Although this publication is focussed on the window properties, the effect on energy consumption is touched upon frequently. Extensive studies within the context of Annex XII on the influence of window design, size and orientation on energy consumption are reported separately as listed under heading 6 of this Introduction.

5. FROM HEAT TRANSPORT PHENOMENA TO WINDOW PROPERTIES

5.1. Introduction

The overall energy transfer through a window is in general the combined effect on three different types of energy transport.

Heat transmission: the temperature difference across the window is the driving force for the transmission of heat. The transmission is in fact the collective noun for any combination of the following mechanisms: conduction, convection, thermal radiation and condensation/evaporation.

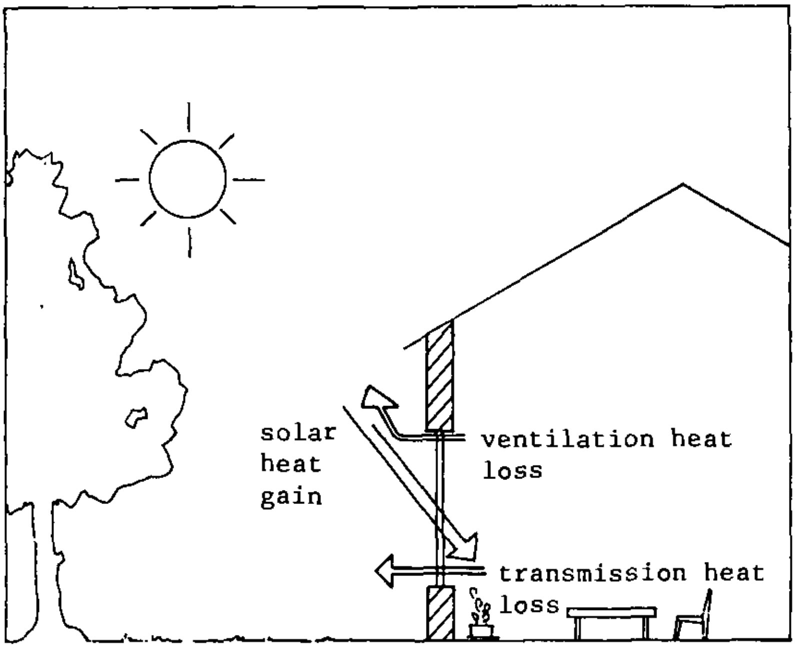

Figure 1: The three types of heat transfer through a window.

Solar radiation: radiation directly from the sun and/or indirectly from the sky and surroundings reaches the window and is partly reflected and absorbed. The remaining part is transmitted to the indoor space. The radiation absorbed in the window is released as heat to the indoor and outdoor environment.
Part of the transmitted solar radiation is visible light.
Daylighting through windows is therefore strongly related to the solar properties of windows.

Ventilation: through cracks and openings in the window air moves from indoor to outdoor environment and vice versa. In case of a temperature difference heat or cold is transferred with the air.

The division into chapters follows the distinction of different types of energy transport:
thermal properties of windows (chapter 3);
solar properties of windows (chapter 4);
daylighting (chapter 5);
air infiltration (chapter 6).

The interaction between these different phenomena is a typical aspect of windows.
This interaction is shown in the following sections where the energy transfer through windows is introduced somewhat more extensively. Many references to the various parts of chapters 3 to 6 serve to introduce the reader to this publication.

5.2. Heat Transmission

Heat transmission is the common name for any combination of the following heat transfer mechanisms: conduction, convection, thermal radiation and condensation/evaporation. Convection not along but across or through window components is introduced here separately as air circulation.

a. Conduction: the amount of heat transferred by conduction through a solid, liquid or gas is determined by the conductivity of and the temperature difference across the medium.
   Still air is a well-known insulator. The conductivity of glass is for instance thirty times as high; of most metals even more than a thousand times as high.

In general the conductivity is a temperature dependent material property. For window components the temperature dependency is usually not more than a second order effect.
Conductivity plays a major role in air or gasfilled cavities between window panes (section 3.2.2.), in window frames (section 3.2.3.) and in shutters provided with insulative material (section 3.6.).

b. Convection: heat from a fluid or gas to a surface and vice versa can also be transferred by convection if the fluid near the surface is not in rest. "Free convection" is the movement of fluid or gas governed by local temperature differences, "forced convection" is caused by external sources, e.g. the wind or an induction-unit of the HVAC-installation.
The amount of convective heat transfer is determined by the rate of convection near the surface and - again - the temperature difference between surface and fluid.
If convection occurs, then often the conductive heat transfer through the air (or gas) can be neglected.
Convection is a major problem area with respect to the determination of window properties. Convection between panes and at the indoor and outdoor window surfaces is discussed in section 3.2.2. Free convection behind shutters affects their efficiency as night insulation (section 3.6.).
Free convection is governed by local temperature differences. Local temperature differences in windows are often strongly influenced by the heat from absorbed solar radiation. In sections 4.3. and 4.5. it is shown how this influences the window properties.

c. Thermal radiation: each surface emits radiation; the energy and the wavelength distribution (spectrum) depends on the temperature and emissivity of the emitting surface.

For sources at ambient temperature the spectrum lies within the far infra-red, hence it is called IR, long-wave or thermal radiation. The receiving body can in general transmit, absorb or reflect the incident radiation. The transmissivity, absorptivity and reflectivity is a material property which is in general dependent on wavelength (thus temperature of the emitting surface) and angle of incidence. For example, normal clear glass is highly transparent to solar radiation, but intransparent to IR-radiation from objects at room temperature; the major part of this thermal radiation is absorbed, the remaining part is reflected.
Section 3.2.1. deals with the heat transfer in windows due to thermal radiation. Section 3.5. shows the influence of thermal radiation on the thermal transmission properties of windows.
The radiative heat transfer coefficients are not so strongly temperature dependent as the free convective coefficients. The main field of interaction between the thermal radiative and the solar properties of windows is in the treatment of surfaces to change the optical properties, sections 4.3. and 4.5.

d. Air circulation: apart from infiltration or natural ventilation through window cracks and openings, and the already described convection along surfaces, air can also flow across a single window component. For instance, the air flow behind a curtain or behind and between venetian blinds. Here again both 'free' and 'forced' convection can be found: slats of venetian blinds heated by the sun, a curtain caught by the hot air flow from a radiator underneath, or wind leaking behind outdoor shutters, etc. This type of heat flow often acts as a short-cut for the overall transmission of heat.

The air circulation in window systems is very difficult to model. In experiments the influece of air circulation on the thermal and solar properties is determined. Available results are presented in section 3.6. (thermal) and sections 4.3. and 4.5. (solar).

e. Condensation/evaporation: during evaporation of fluid particles, either at a surface or free in the air, evaporation heat is taken from the surface or ambient. When the vapour condensates e.g. on a cold surface, the same amount of heat is released. Thus, heat is transferred from a warm to a colder environment. Because the heat content in the vapour is not accompanied by an increased temperature, this type of heat is called latent heat, in contrast to the sensible heat transfer mechanisms described above.
However, although condensation on window surfaces is a classic and sometimes major problem area, the accompanying heat transfer can usually be neglected in comparison with the transfer of heat by one or more of the above mentioned sensible heat transfer mechanisms.
Section 3.4. deals with the risk of condensation on windows.

In section 3.1. the major properties, relations and problem areas with respect to heat transmission through windows are introduced. Section 3.2. presents a review on the IR-radiative and conductive/convective heat transfer phenomena. Section 3.3. gives a survey on test methods on window components and complete window systems.
The section on condensation (3.4.) is followed by two sections on practical window design, where the possibilities, the problem areas and actual data, with respect to windows with low heat transmission, are presented.

5.3. Solar Radiation

Radiation from the sun and/or diffuse radiation from sky and surroundings falls on the window and is partly reflected and absorbed. The rest is transmitted through the window and reaches the indoor surfaces of the room as short wave radiation (direct or primary transmission). As for thermal radiation, the surface properties are dependent on wavelength and angle of incidence. The spectrum of the solar radiation ranges from UV and visible to the near infra-red.
Daylighting results from the visible part of the solar radiation which explains the strong relation between solar and daylighting properties of windows.

A second aspect of the solar radiation, but often very significant for the window performance, is the way absorbed solar heat is released from the window. For instance, a single glass pane absorbs about 12% of the incident radiation. This absorbed heat is released at both surfaces to the indoor and outdoor environment by convection and thermal radiation. So, eventually part of this heat will be brought into the room (secondary transmission).

In section 4.1. the solar properties of windows are introduced. A presentation of the solar radiation itself (4.2.) is followed by a review on the solar properties of windows (4.3.). The section on measurement techniques (4.4.) gives a survey of the various techniques to obtain experimental data. The final section (4.5.) reviews the possibilities to achieve efficient control of solar heat.

5.4. Daylighting

The reduction of solar radiation in most cases also leads to a reduction in the amount of visible light in the building. It often takes a well thought-out integrated design of building and window to minimize solar heat without the need for (extra) artificial lighting. Artificial lighting not only costs electricity, but also increases the discomfort in or the cooling load of the building.
This was sufficient justification to dedicate a separate chapter to daylighting and more in particular to the daylighting properties of windows (chapter 5).

5.5. Ventilation

The heat or cold which is transferred through cracks and openings of the window from inside to outside and vice versa: heat flow by air infiltration and natural ventilation; this heat flow is determined by the air flow through and the temperature difference across the window.

Chapter 6 presents an extensive introduction on the air infiltration through windows. Wherever applicable the discussion is placed in the context of building ventilation where alongside energy conservation, comfort and air quality are major focal points.
Many references are made to publications by the Air Infiltration Centre and other initiatives on ventilation within the IEA R&D Programme on Energy Conservation in Buildings and Community Systems. Nevertheless, chapter 6 gives an extensive review on the theory on ventilation (section 6.2.), on existing measurement techniques (6.3.) and present standard values (6.4.).

Section 6.5. describes the importance of the window leakage as part of the total building leakage.
The next section 6.6. reviews the possibilities to achieve airtight joints while section 6.7. describes the influence of the inhabitants on the use of a window to control natural ventilation.
The final section 6.8. summarizes briefly the possibilities on the market of special ventilation provisions, like grills, exhaust windows and such.

6. OTHER PUBLICATIONS FROM ANNEX XII

The following publications have been prepared as final products of the project:

Step 1:

The State-of-the-art in Existing Windows and New Window Designs: A survey from eight countries, ed. H.A.L. van Dijk, September 1986.

Building Regulations, Standards and Codes concerning Thermal and Solar Performance of Windows; A survey of eight countries, ed. H.A.L. van Dijk, September 1986.

Step 2:

Thermal Transmission through Windows, Selected Examples to Illustrate the Need for a More Standardized Approach, ed. H.A.L. van Dijk, 1987.

Thermal and Solar Properties of Windows; summary, ed. H.A.L. van Dijk and K.Th. Knorr, 1987.

Step 3:

Calculation of Seasonal Heat Loss and Gain through Windows: A Comparison of Some Simplified Models, ed. H.A.L. van Dijk, September 1986.

Step 4:

Comparison of Six Simulation Codes: DEROB, DYWON, PASSIM, DOE-2.1C, SERI-RES, HELIOS1, ed. T. Frank and T.W. Püntener, 1987.

Step 5:

National reports on sensitivity studies concerning the influence of windows on energy consumption, prepared by the participants from Germany, the Netherlands, Switzerland and USA.

2. TERMINOLOGY AND SYMBOLS

H.A.L. van Dijk
TNO Institute of Applied Physics
P.O. Box 155
2600 AD DELFT
The Netherlands

LIST OF CONTENTS

1. INTRODUCTION

The quantities and symbols are listed at the beginning of each section. In order to facilitate the reading of the report a general list of definitions and symbols has been adopted for the main quantities. This general list is, wherever possible, based on ISO draft standard DIS 7345/1 [1].

2. LIST OF GENERAL TERMINOLOGY AND SYMBOLS

	symbol	unit
Heat: quantity of heat	Q	J
Heat flow rate: The quantity of heat transferred to or from a system per unit time: $\phi = \frac{dQ}{dt}$	ϕ	W
Density of heat flow rate: Heat flow rate divided by area: $q = \frac{d\phi}{dA}$	q	W/m^2

	symbol	unit
<u>Thermal conductivity:</u> Quantity defined by the following relation: $\bar{q} = \lambda \text{ grad } T$	λ	W/(m.K)
<u>Thermal resistance</u>: Temperature difference divided by the areal density of heat flow rate in the steady state condition: $R = \dfrac{T_1 - T_2}{q}$ NOTE: For a plane layer for which the concept of thermal conductivity applies and when this property is constant or linear with temperature: $R = \dfrac{d}{\lambda}$ where d is the thickness of the layer.	R	$(m^2.K)/W$

These definitions assume the definition of two reference temperatures, T_1 and T_2, and the area through which the density of heat flow rate is uniform.

Thermal resistance can be related either to the material, structure of surface. If either T_1 or T_2 is not the temperature of a solid surface, but that of a fluid, a reference temperature must be defined in each specific case (with reference to free or forced convection and radiation from surrounding surfaces, etc.).
When quoting values of thermal resistance, T_1 and T_2 must be stated.

<u>Surface coefficient of heat transfer</u>: Density of heat flow rate at a surface in the steady state divided by the temperature difference between that surface and the surroundings:

symbol	unit
h	$W/(m^2.K)$

$$h = \frac{q}{T_s - T_a}$$

NOTE: This assumes the definition of the surface through which the heat is transferred, the temperature of the surface, T_s, and the ambient temperature, T_a, (with reference to free or forced convection and radiation from surrounding surfaces, etc.).

	symbol	unit
<u>Thermal conductance</u>: The reciprocal of thermal resistance from surface to surface under conditions of uniform density of heat flow rate:	Λ	$W/(m^2.K)$
$\Lambda = \frac{1}{R}$		
<u>Thermal transmittance</u>: The heat flow rate per unit area in the steady state divided by the temperature difference between the surroundings on each side of a system:	U	$W/(m^2.K)$
$U = \frac{\phi}{(T_1 - T_2)A}$		
NOTE: This assumes the definition of the system, the two reference temperatures, T_1 and T_2, and other boundary conditions. The reciprocal of the thermal transmittance is the total thermal resistance between the surroundings on each side of the system.		
<u>Thermodynamic temperature</u>	T	K
<u>Celsius temperature</u>	θ	°C
<u>Area</u>	A	m^2

	symbol	unit
<u>Volume</u>	V	m^3
<u>Emissivity</u>: The ratio of the emitted radiant intensity to the radiant intensity emitted by a black body at the same temperature and in the same direction or with the same angular distribution. NOTE: This definition implies that the direction or angular distribution (e.g. hemispherical) must be defined in each specific case.	ε	--
<u>Total solar energy transmission coefficient</u>: or: total solar energy transmittance or: solar factor		
for glazing:	g	--
in general :	SF	--
The density of transmitted total solar energy through a window divided by the intensity of incident solar radiation. NOTE: For explanation, see chapter 1 of the report.		

SUBSCRIPTS (optional):

interior	i
exterior	e
surface or sky	s
interior surface	si
exterior surface	se
convection	c
radiation	r
ambient or air (!)	a
window	w
glass	g
frame	f

3. REFERENCES

[1] ISO: DIS 7345/1, Thermal insulation - Vocabulary - Part 1.

3. THERMAL PROPERTIES OF WINDOWS

3.1. Introduction

H.A.L. van Dijk
TNO Institute of Applied Physics
P.O. Box 155
2600 AD DELFT
The Netherlands

In the general introduction, chapter 1, the various heat transport mechanisms were presented in brief.
For the thermal transmission through windows the following quantities play a major role:

- The surface-to-surface thermal resistance of a window (-component), R_w in m²K/W, or its reciprocal value, the conductance Λ_w.

- The surface heat transfer coefficients (in W/m²K):

indoor	convective	h_{ci}	sum: $h_i = h_{ci} + h_{ri}$
	radiative	h_{ri}	
outdoor	convective	h_{ce}	sum: $h_e = h_{ce} + h_{re}$
	radiative	h_{re}	

Sometimes the reciprocal values are used, the surface film resistances R_i, etc.

- The total heat transmission q_w through the window can be described with equation:

$$q_w = A_w \cdot U_w \cdot (\theta_i - \theta_e) \qquad (W) \qquad (1)$$

where:

q_w is the steady state heat transmission caused by the temperature difference $(\theta_i - \theta_e)$;

A_w is the window area (m^2);

θ_i, θ_e are the indoor and outdoor environmental temperatures (°C).

The coefficient U_w is the <u>heat transmission coefficient</u> or <u>thermal transmittance</u>, or simply: U-value of the window.
The U-value can be derived from the summation of the series of resistances:

$$U = \frac{1}{R_w + h_i^{-1} + h_e^{-1}} \qquad (W/m^2K) \qquad (2)$$

On the other hand: if the U-value and the surface coefficients are known, equation (2) yields the value for the window resistance.

The thermal resistance of the window or a window component can often be described as a network of parallel and serial resistances. In figure 1 this is illustrated for double glazing: the window resistance is composed of the (small) resistances by conduction through the panes and the parallel resistances for radiative and convective heat transfer across the cavity.

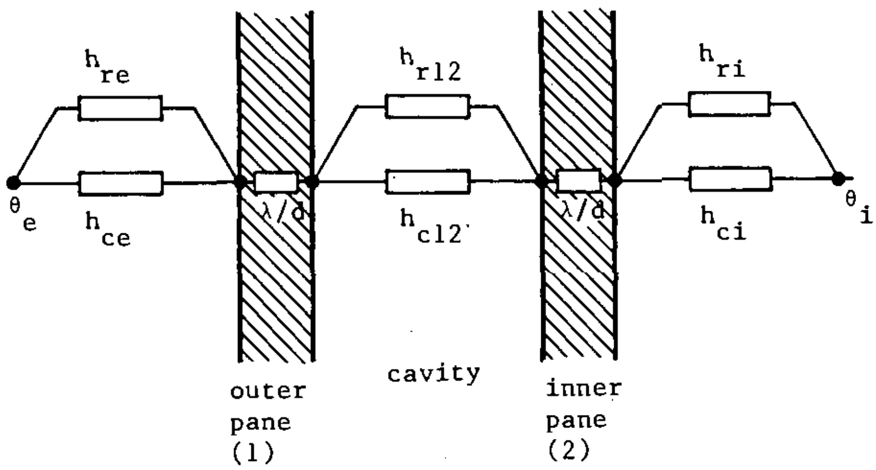

<u>Figure 1</u>: Network presentation of thermal resistances, example for double glazing.

In fact, the environmental temperatures θ_i and θ_e should be divided into:

for convection: the indoor, resp. outdoor air temperatures;

for thermal radiation: the weighted mean surface temperature of the indoor surroundings and the weighted mean sky and surroundings temperature outside respectively.

Moreover, when for instance indoor venetian blinds are added to the window, an extra term is to be introduced to model the heat transfer by air circulation from room air to air cavity between blinds and inner pane, see figure 2. In figure 2 the resistance of each pane has been neglected. Nevertheless, the scheme is already too complicated for a simple calculation of the U-value.

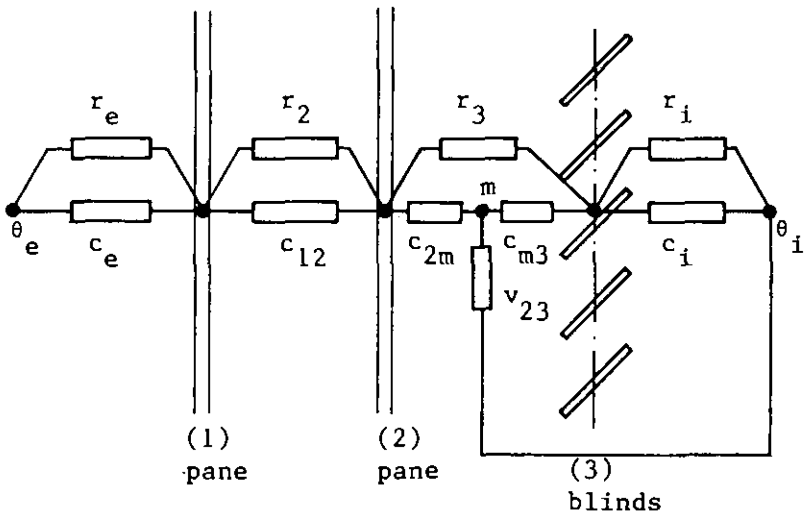

e: outside
i: inside
r: radiation (thermal)
c: convection
v: ventilation

Figure 2: Network presentation of thermal resistances; example for double glazing with blinds.

Already for this type of window the surface-to-surface thermal resistance can no longer be derived with a relation as simple as equation (2).

In general, the surface heat transfer coefficients and the cavity conductances, are dependent on the boundary conditions such as:

- exterior:
  climatic conditions: sky radiation, wind speed, temperature, etc.;

- interior:
  room conditions: air temperature, surface temperature of the walls, air movement, geometry of the room;

- cavity:
  cavity conditions: surface temperatures and temperature difference.

Obviously, the properties of the window components themselves play a major role, such as:
- emissivity of pane or other surfaces;
- cavity distances;
- shutters: thermal resistance, air tightness;
- frames: composition, thermal bridges.

In this chapter 3 the thermal transmission properties of windows are introduced.
In section 3.2. the heat transfer mechanisms are presented. The sections 3.2.1. and 3.2.2. contain basic theoretical considerations and comparison of existing empirical formulae for the radiative and convective heat transfer coefficients.

Section 3.2.3. gives a presentation on thermal bridges; in the first part calculation methods and evaluation techniques are introduced, in the second part case studies are discussed.

Section 3.3. presents various measurement techniques, to obtain basic window (component) properties (3.3.1.) or the values for thermal resistance and/or U-value (3.3.2. and 3.3.3.). The discussions presented in this section give a clear illustration that it is important to accurately define and state the test conditions.

Section 3.4. gives a short but clear presentation on the risk of condensation on window surfaces and the ways to eliminate the risk. Practical solutions to diminish heat losses through windows are presented in sections 3.5. and 3.6. These sections also contain graphs and tables with actual data from calculations or tests.

3.2. Thermal transmission

3.2.1. Thermal radiative heat transfer

J.B. Gay, N. Morel
Ecole Polytechnique Fédérale
Groupe de Recherches en Energie Solaire
CH - 1015 LAUSANNE (Switzerland)

Th. Frank, T.W. Püntener
EMPA
Ueberlandstrasse 129
CH - 8600 DUBENDORF (Switzerland)

LIST OF SYMBOLS

Φ	: Radiative heat flow	[W]
A	: Area	[m^2]
q_s	: Long wave irradiance from the sky	[W/m^2]
ε	: Surface emissivity	[-]
σ	: Boltzmann constant (=5.67 x 10^{-8})	[W/m^2K^4]
T	: Absolute temperature	[K]
Θ	: Celcius temperature	[^oC]
H_G	: Horizontal global solar radiation	[W/m^2]
H_{DIF}	: Horizontal diffuse solar radiation	[W/m^2]
C_F	: Cloud cover fraction (1/10)	[-]
E	: Effective emittance	[-]
h_r	: Radiative heat transfer coefficient	[W/m^2K]
F_s	: View factor of the sky from the window	[-]
$F_{i \rightarrow j}$	: Form factor (from surface i to j)	[-]
α	: Global heat transfer coefficient	[W/m^2K]
G	: Equivalent conductance	[W/K]

Indices

s	: sky	e	: exterior
w	: window	i	: interior
g	: glass		
R	: radiometer		
a	: ambient		
dp	: dew point		

1. INTRODUCTION

When considering the thermal radiative heat transfer of a window, four components can be identified (see fig. 1) :

a) The radiation between the external glazing surface and the sky
b) The radiation between the external glazing surface and the surroundings
c) The radiation between two parallel glazing surfaces (for double or multilayer windows)
d) The radiation between the internal glazing surface and the room surfaces

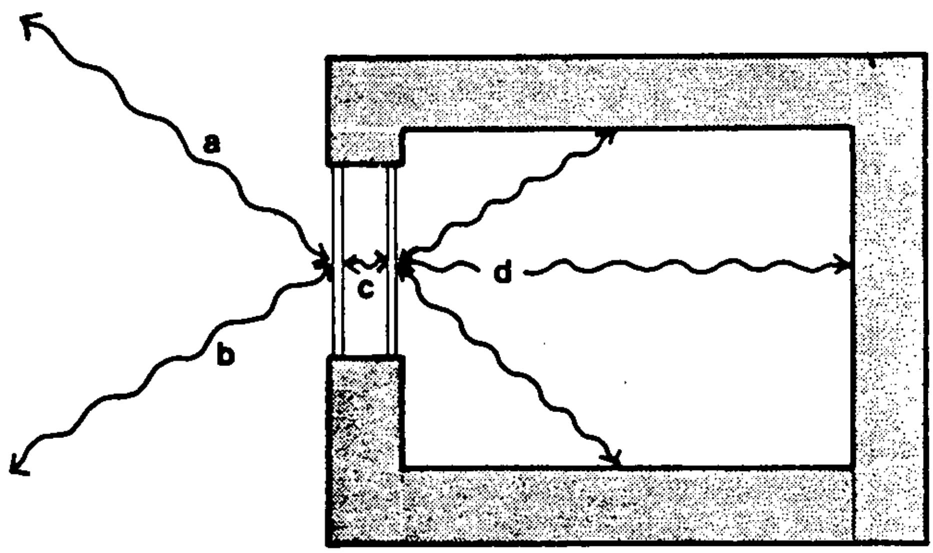

Figure 1 : Thermal radiative heat transfer related to a window. This figure relates to glazed units, it may be different for plastic films which are transparent to the infrared radiation.

2. RADIATION TO THE SKY

Neglecting second order terms the net radiative exchange between the external glazing surface and the sky may be written as follows :

$$\Phi_s = A_g F_s(\varepsilon_g \sigma T_g^4 - \varepsilon_g q_s) \qquad [W] \qquad (1)$$

where : F_s = view factor of the sky from the window
ε_g = emissivity of the external glazing surface
T_g = absolute temperature of the external glazing surface
q_s = long wave irradiance from the sky to the glazing surface

In order to compute q_s, the values of two parameters are required: the sky temperature and the sky emissivity. Since these parameters are unknown, one of the following approaches is generally adopted :

a) The sky is considered as a black body (ε_s = 1) at a given equivalent sky temperature (T_s). The net radiation between the glazing surface and the sky can then be expressed as :

$$\Phi_s = A_g F_s \varepsilon_g \sigma(T_g^4 - T_s^4) \qquad [W] \qquad (2)$$

b) The sky temperature is assumed to be the same as the ambient temperature ($T_s = T_a$), and a sky emissivity (ε_s) is used. This emissivity is defined as the ratio of the sky radiance to σT_a^4 :

$$\varepsilon_s = \frac{q_s}{\sigma T_a^4} \qquad [-] \qquad (3)$$

T_a being the absolute air temperature near the ground.

Then :

$$\Phi_s = A_g F_s \varepsilon_g \sigma(T_g^4 - \varepsilon_s T_a^4) \qquad [W] \qquad (4)$$

One notices that both approaches are equivalent.

2.1. Sky temperature

An equivalent blackbody sky temperature (T_s) is used to account for the fact that the atmosphere is not at an uniform temperature, and that the emission is strongly dependent on the wavelength.

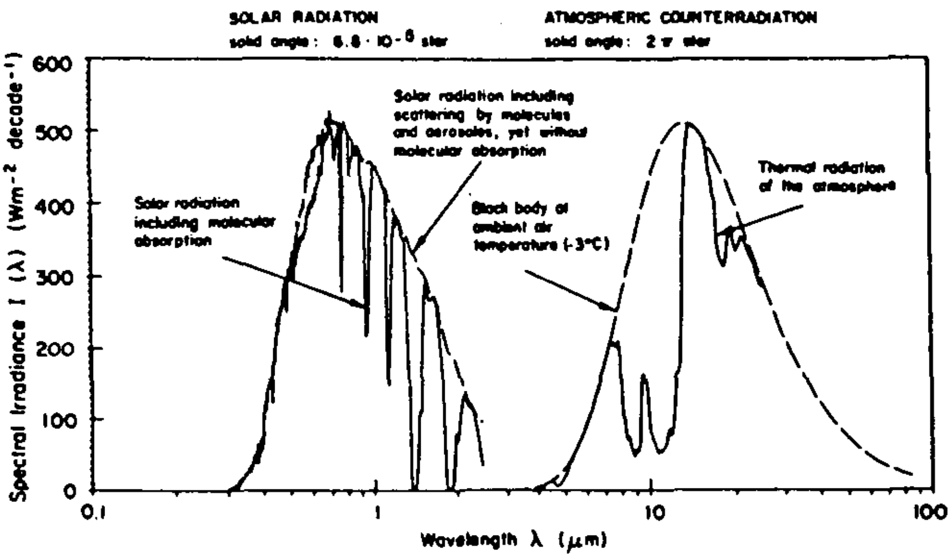

Figure 2 : Solar radiation and atmospheric counter-radiation on a horizontal surface element. Midlatitude winter, 600 m above sea level, ambient air temperature - 3°C, elevation 20 °.

In order to determine this sky temperature, several methods may be considered :

a) Direct measurement :

The best solution is to measure the sky IR radiation with a radiometer (for exemple a PIR pyrgeometer from Eppley Laboratory).

The calibration constant given by the manufacturer is defined as :

$$\sigma\ (T_R^4 - T_s^4) = kV \qquad (5)$$

where : T_R = Radiometer absolute temperature [K]
T_s = Sky absolute temperature [K]
k = Calibration constant of the radiometer [$W/m^2 mV$]
V = Output voltage of the radiometer [mV]

Rearranging equation (5) gives :

$$T_s = \sqrt[4]{T_R^4 - \frac{kV}{\sigma}} \quad [\mathrm{K}] \qquad (6)$$

However such a measurement is not generally available.

b) Empirical relations :

Several empirical relations have been proposed to relate the sky temperature to the outdoor air temperature (T_a). Swinbank has proposed [1] :

$$T_s = 0.0552\ T_a^{1.5} \quad [\mathrm{K}] \qquad (7)$$

and more recently Whillier [2] gave the relation :

$$T_s = T_a - 6.0 \quad [\mathrm{K}] \qquad (8)$$

Both these relations are very crude however and do not account for the effect of the sky cloudiness.

c) Correlation methods :

As the sky temperature is strongly correlated to the sky cloudiness, Ineichen et al [3] have made an attempt to correlate the sky temperature with two measured quantities : the ambient temperature and the normalized diffuse solar radiation By plotting $\Delta\Phi = \Phi_a - \Phi_s = \sigma\ (T_a^4 - T_s^4)$ versus $z = (1-H_{DIF}/H_G)$ a rather good correlation was found with the following parameters :

$$\Delta\Phi = 22 + 175\ z \quad \text{if} \quad z < 0.1 \tag{9}$$

$$\Delta\Phi = 34 + 63\ z \quad \text{if} \quad z \geqslant 0.1 \tag{10}$$

H_{DIF} and H_G are averaged daily values for the horizontal diffuse and global solar radiation.

d) Practical comparison of the presented algorithms :

In order to compare and evaluate the algorithms, the sky temperature was computed for two typical periods (each one presenting cloudy and clear days) and compared with measurements.

Figures 3 and 4 present the horizontal global and diffuse radiation together with the measured air and sky temperature for the two typical periods : one in winter (Feb. 8th to Feb. 12th) and one in summer (July 2nd to July 6th).

The measurements were performed by the University of Geneva [3] It is noticable that there are significant differences between air and sky temperatures, which sometime exceed 25 ^{o}C.

The graph of temperature vs. time may be used to compare the different algorithms.One may also use the mean value of the temperatures for the selected period since the energy loss due to sky radiation only is roughly proportional to the difference $\bar{T}_g - \bar{T}_s$ and this heat loss is the quantity which is of greatest interest.

Therefore, we will give both the graph of temperature versus time and the mean value for every algorithm discussed next.

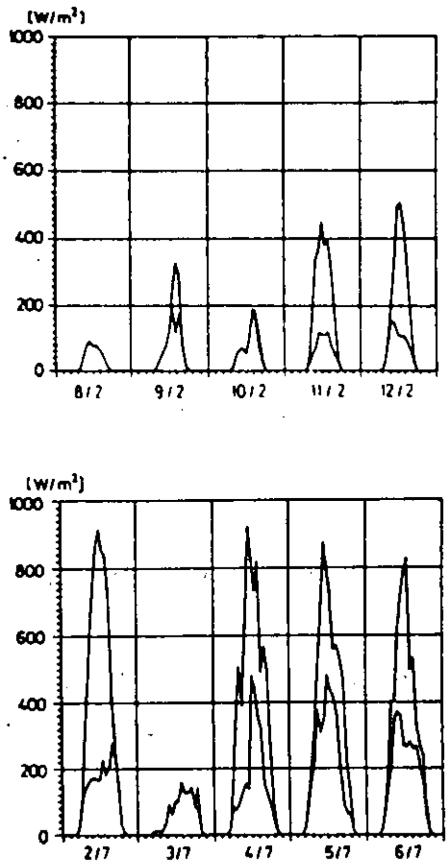

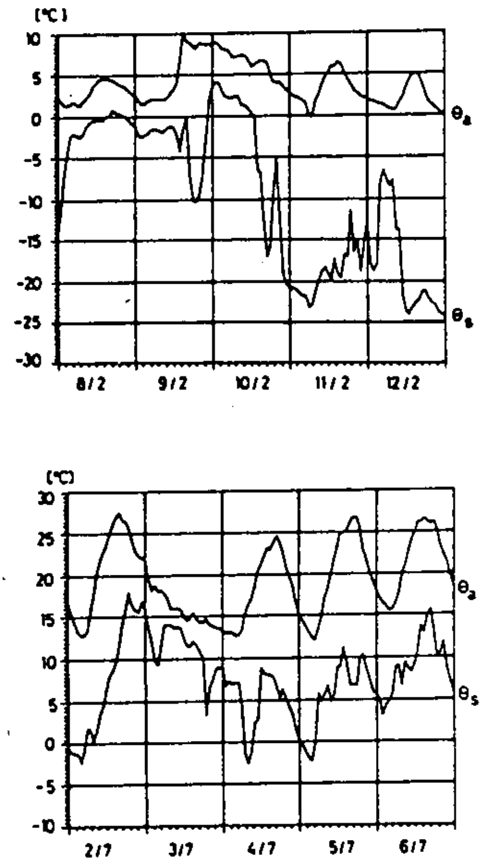

Figure 3 : Global and diffuse horizontal solar radiation.

Figure 4 : Measured air and sky temperature.

Swinbank and Whillier models

Figures 5 and 6 compare the empirical relations of Swinbank and Whillier, for the whole 5 days periods. The average results are as follows :

	θ_s [°C]			θ_a [°C]
	Swinbank	Whillier	Measured	
Winter	- 18.6	- 2.0	- 9.3	4.0
Summer	2.8	13.3	7.6	19.3

It can be seen that the Swinbank relation systematically underestimates the sky temperature while the Whillier relation overestimates it.

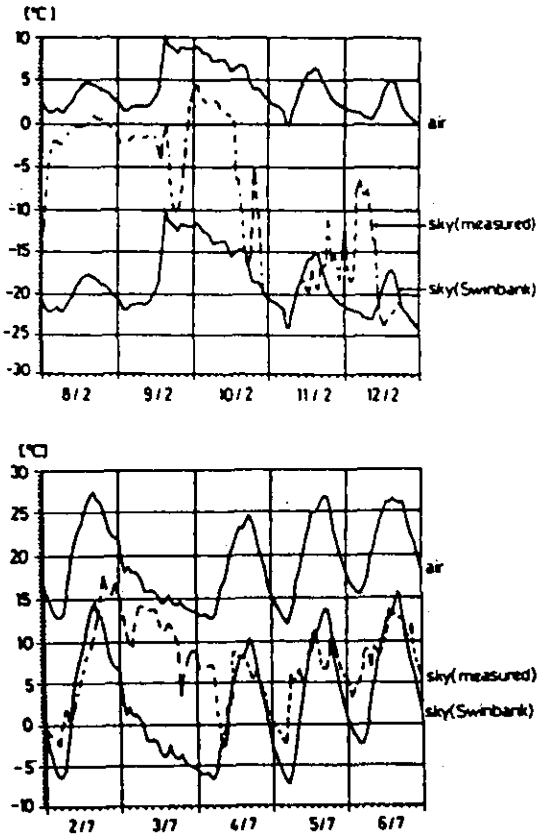

Figure 5 : Sky temperature using the Swinbank relation.

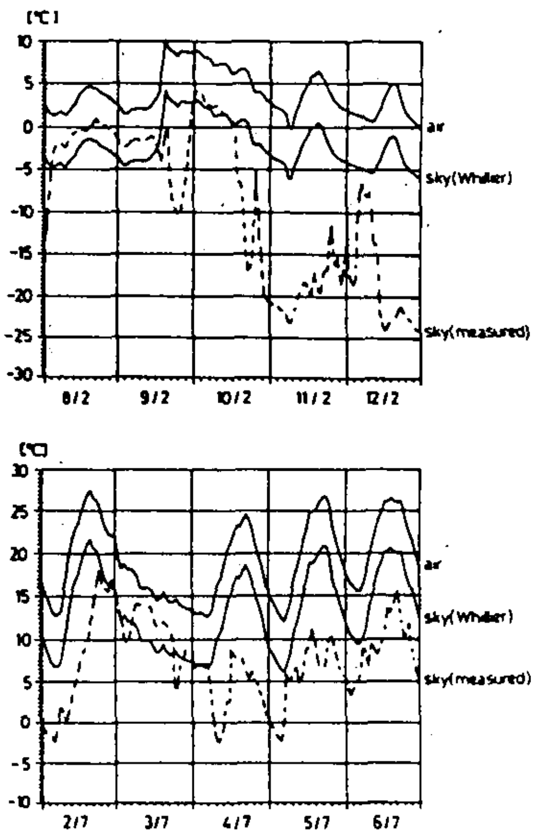

Figure 6 : Sky temperature using the Whillier relation.

Comparing the data on an hourly basis one notices that the Swinbank relation is rather good for sunny days while the Whillier relation gives a correct approach only for cloudy periods.

Correlation with the solar radiation

The correlation model between the sky temperature and the solar radiation [3] was also examined. Since diffuse radiation is generally not available, two tests were made : one using the measured diffuse radiation (fig. 7) and one using the computed radiation using Liu and Jordan correlation (fig. 8).

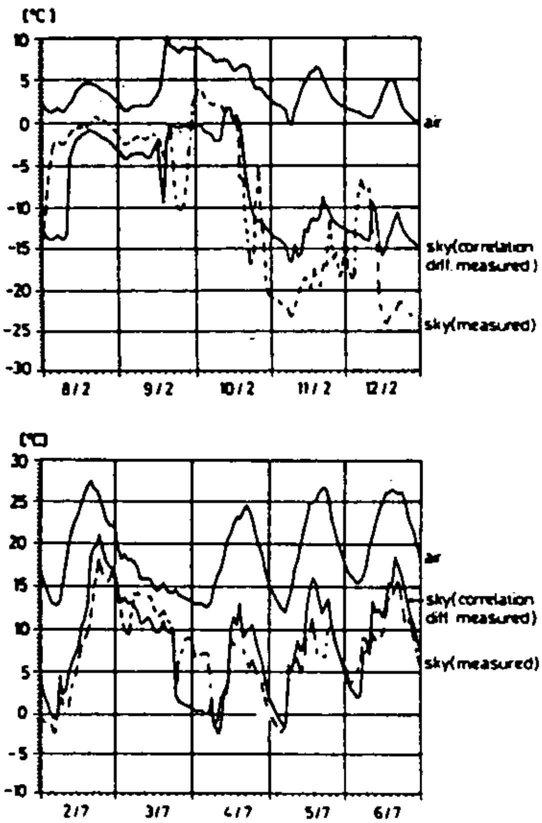

Figure 7 : Sky temperature computed with the global horizontal and the measured diffuse radiation.

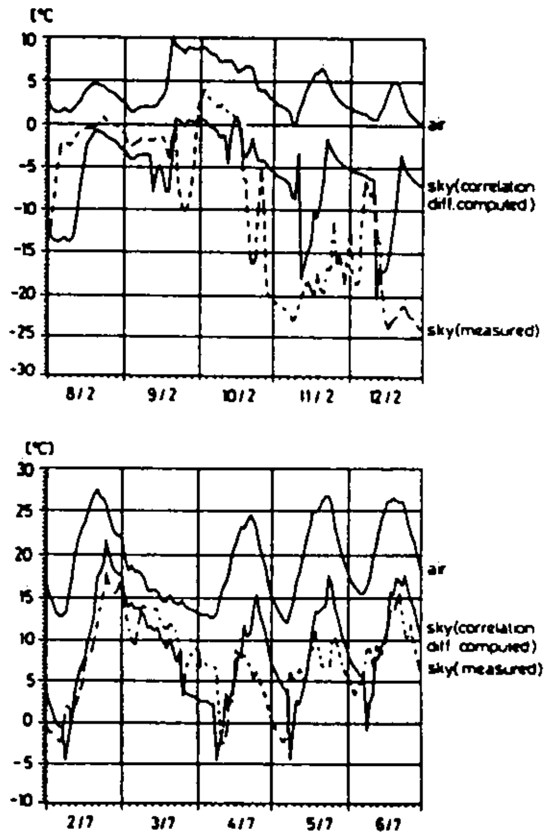

Figure 8 : Sky temperature computed with the global horizontal and the Liu and Jordan diffuse radiation.

The average values for the considered periods are as follows :

	Θ_s [°C]			Θ_a [°C]
	using the measured diffuse radiation	using the computed diffuse radiation	measured value	
Winter	- 7.8	- 5.6	- 9.3	4.0
Summer	8.5	8.8	7.6	19.3

The results show that the use of the computed diffuse component of the solar radiation does not greatly affect the results, at least for the mean values. The correlation model offers a good way for estimating the real sky temperature.

2.2. Sky Emissivity

As mentioned above, instead of defining a sky temperature, several authors have proposed the use of a sky emissivity. This emissivity may be correlated to the dew-point temperature (Θ_{dp}, see fig. 9) and to the cloud cover fraction (C_F).

For clear sky conditions :

$$\varepsilon_s \ (0) = 0.75 + 0.005 \ \Theta_{dp} \tag{11}$$

For cloudy sky conditions, Unsworth and Monteith [8] proposed the following relation :

$$\varepsilon_s \ (c) = (1 - 0.84 \ C_F) \ \varepsilon_s \ (0) + 0.84 \ C_F \tag{12}$$

The cloud cover fraction, expressed in 1/10, and the dew point temperature are available on an hourly time step base in most of the airport weather stations.

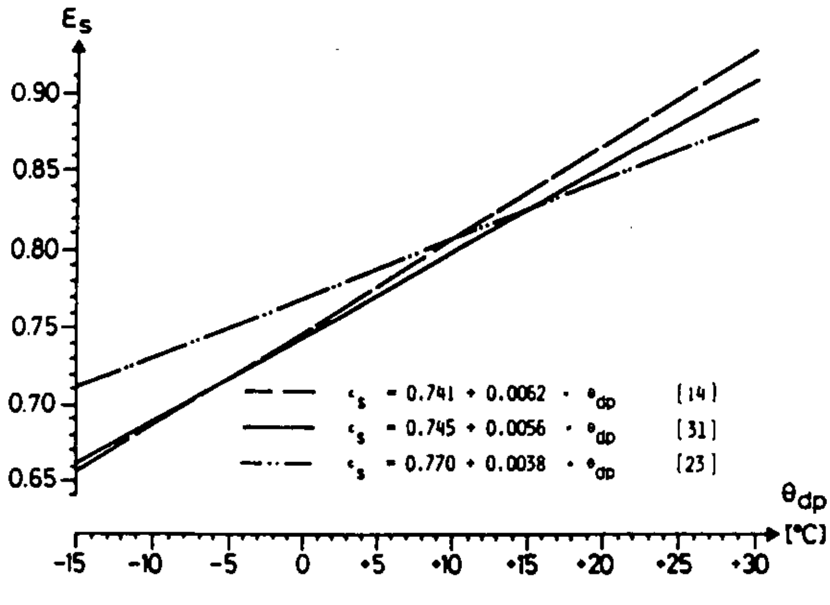

Figure 9 : Correlation between the clear sky emissivity and the dewpoint temperature.

3. RADIATION TO THE SURROUNDING

A window, as does any vertical surface, also exchanges heat by radiation with the ground and the surrounding. It is generally assumed that the temperature of the environment is the same as the outdoor temperature near the ground (T_a).

The thermal irradiance to the environment excluding sky may then be expressed as :

$$\Phi_E = A_g \ (1 - F_s) \ \varepsilon_g \sigma \ (T_g^4 - T_a^4) \qquad [\,W\,] \qquad (13)$$

Adding the sky and the ground components, the following expression is obtained for the global thermal irradience (Φ_{tot}) :

Total radiation to the outside

Adding the sky and the ground components, the following expression is obtained for the global thermal irradiance :

$$\Phi_{tot} = \Phi_s + \Phi_E = A_g \varepsilon_g \ \sigma \left\{ T_g^4 - [\ 1 - F_s(1 - \varepsilon_s)\,] \ T_a^4 \right\} \qquad (14)$$

Using typical values for winter conditions and a view factor of ½, the following average radiative transfer coefficient is obtained :

$h_r \approx 9 \quad [\,W/m^2K\,]$

One notices that 3/4 of this value are due to the radiative transfer to the sky.

4. RADIATIVE EXCHANGES BETWEEN TWO GLAZED PANES

The emissivity of glass and of coated surfaces depends on the angle of emission, as presented in figure 10 : emission is stronger in directions close to the normal, and drops to zero as the emission angle approaches 90 °.

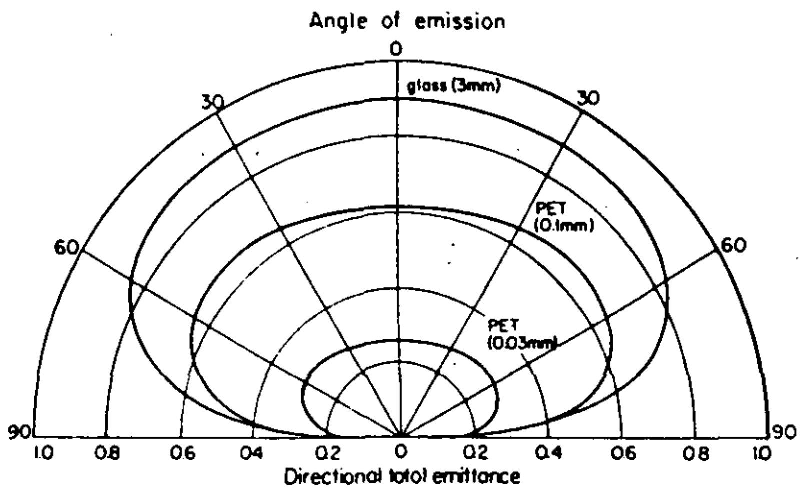

Figure 10 : Directional total emittance of window glass (3mm) and PET films (0.1 and 0.03 mm) at 293° K. The horizontal axis represents the surface of the material : the angle of emission is measured from the normal to the surface.

However, when calculating the radiative heat exchanges between two glass panes, it is generally assumed that the glass acts as a grey surface with an weighted average emissivity of 0.85.

The net radiative heat balance between the two parallel surfaces can then be given by

$$\Phi_I = A_g \frac{\sigma\ (T_1^4 - T_2^4)}{\frac{1}{\varepsilon_1} + \frac{1}{\varepsilon_2} - 1} = A_g\, \sigma\, E\ (T_1^4 - T_2^4) \qquad [W] \qquad (15)$$

Where : $E = \left(\frac{1}{\varepsilon_1} + \frac{1}{\varepsilon_2} - 1 \right)^{-1}$ = effective emittance

ε_i = average emissivity of surface i [-]

T_i = surface temperature of surface i [K]

Since the temperatures of the two panes do not differ greatly, the following approximation can be made.

$$\Phi_{net} = A_g \, 4 \, \sigma \, E\bar{T}^3 \, (T_1 - T_2) = A_g h_r \, (T_1 - T_2) \qquad [W] \qquad (16)$$

$$\text{Where : } h_r = 4 \, \sigma \, E\bar{T}^3 \quad [W/m^2K] \quad \text{and } \bar{T} = \frac{T_1 + T_2}{2} \quad [K] \qquad (17)$$

This is the surface coefficient of heat transfer by radiation between two parallel surfaces. It depends strongly on the emissivity of the surfaces as shown in fig. 11.

These formula are only valid for panes which are opaque to the IR-radiation (e.g. for glasses).

<u>Selective surfaces</u>

A "heat mirror" is a coating which is predominately transparent in the visibile and near IR (0.3 - 2.0 μm) and reflective in the infrared (2 - 100 μm)).

Heat mirrors can be classified under two broad categories :

1) single layer materials (In_2O_3 : Sn, SnO_2 : F, Cd_2 : SnO_4...)

and

2) multilayer metal-based films (SiO_2/Ag, Zns/Cu/Zns, TiO_2/Ag/TiO_2 ......)

The coatings can be physically deposited on the glass by a variety of methods including physical vapor deposition (vacuum evaporation, sputtering [26] or chemical procedures (immersion, chemical vapor deposition, pyrolysis ....).

In order to classify a heat mirror it is important to consider both the solar transmittance and the infrared reflectance (R = 1 - ε).

Figure 11 demonstrates the advantages of a "heat mirror", it shows the variation of the radiative heat transfer coefficient (h_r) as a function of the surfaces emissivities.

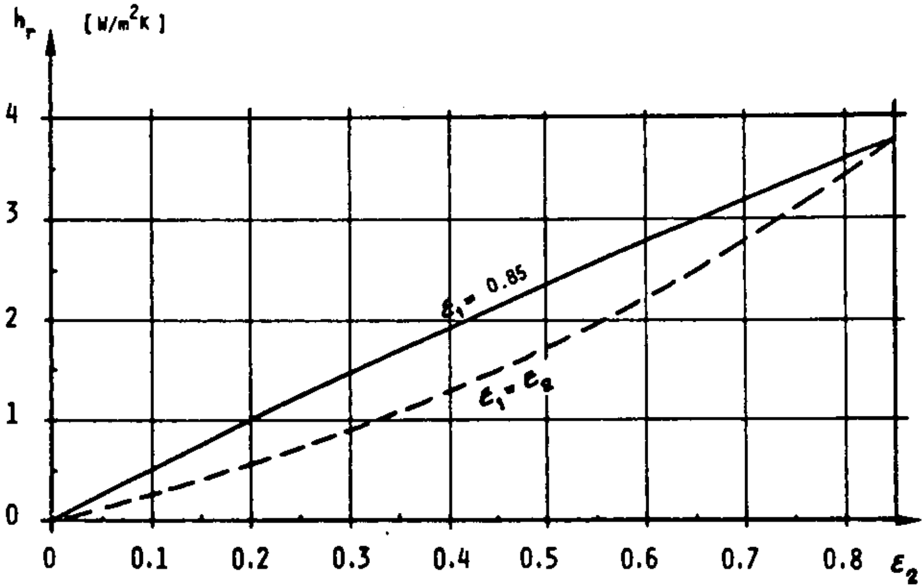

Figure 11 : Variation of the radiative heat transfer coefficient between two glazings with the surface emissivity.

a) for a coated surface and an uncoated one (full line)

b) for two coated surfaces : $\varepsilon_1 = \varepsilon_2$ (dotted line)

RADIATIVE COUPLING BETWEEN WINDOW AND INSIDE

In a real situation, the exact computation of radiative coupling between window (inside pane) and inside surfaces is a rather complicated task.

In order to be able to evaluate the heat transfer, many methods use the following simplifying assumptions.:

- all surfaces are grey, i.e. the radiation properties are independant of wavelength;
- every surface diffuses isotropically the IR radiation;
- the temperature of every surface is uniform;
- the incident energy over every surface is uniform.

Under these conditions, the net heat flux from surface i to surface j is given by the expression :

$$\Phi_{i\to j} = \sigma\,(T_i^4 - T_j^4).\,\frac{1}{\dfrac{1-\varepsilon_i}{\varepsilon_i.A_i} + \dfrac{1-\varepsilon_j}{\varepsilon_j.A_j} + \dfrac{1}{A_i.F_{i\to j}}} \quad [W] \qquad (18)$$

Where ε_i, ε_j are the emissivity of surfaces i and j respectively, A_i, A_j the areas, and $F_{i\to j}$ is the form factor, which accounts for geometrical position of both surfaces ([28] , [29]).

The form factor is given by :

$$A_i F_{i\to j} = A_j F_{j\to i} = \int_{s_i}\int_{s_j} \frac{\cos(\Theta_i).\cos(\Theta_j)}{\pi\;.\;r_{ij}}\, dA_i dA_j \qquad (19)$$

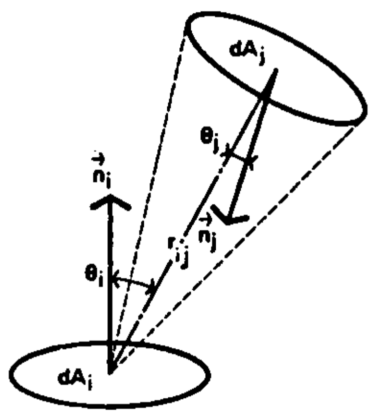

Figure 12 : Radiative heat exchanges between two surface elements i and j.

Most construction materials (bricks, mortar, wood, etc. ....) have an emissivity of 0.8 - 0.9, and may be considered as grey surfaces emitting and reflecting isotropically, for infrared radiation. The only remaining problem is the calculation of form factors. We discuss two cases in the following text.

5.1. Inside surfaces at uniform temperature

All the inside surfaces are considered to be at the same temperature except the internal surface of the window. We have then the situation of part of the enclosure (the window) looking at the rest of the enclosure (walls + floor + ceiling). In that case, the form factor $F_{w \to i}$ is unity, and the formula giving the heat exchange may be written:

$$\Phi_{i \to w} = \sigma\ (T_i^4 - T_w^4) \cdot \frac{A_w \cdot \varepsilon_w}{1 + \frac{A_w}{A_i} \cdot \frac{\varepsilon_w}{\varepsilon_i}(1 - \varepsilon_i)} \qquad [W] \qquad (20)$$

Where the index i stands for "inside surfaces", and w for "window". Usually, the ratio of window area to inside walls area is rather small, and the term $1-\varepsilon_i$ near to zero, so the expression reduces to :

$$\Phi_{i \to w} \simeq \sigma\ (T_i^4 - T_w^4) \cdot A_w \cdot \varepsilon_w \qquad [W] \qquad (21)$$

The equivalent conductance (i.e. the ratio $\frac{\Phi_{i \to w}}{T_i - T_w}$) may be written :

$$G_{iw} = 4\,\sigma\,\bar{T}^3 \,.\, A_w \,.\, \varepsilon_w \qquad \left(\text{with } \bar{T} = \frac{T_i + T_w}{2}\right) \tag{22}$$

For $\varepsilon_w = 0.85$ and $\bar{T} = 290$ K, the following radiative transfer coefficient is obtained :

$$h_r = \frac{G_{iw}}{A_w} = 4.7\ [\,W/m^2K\,] \tag{23}$$

The contribution of the radiation coupling is therefore important. The usual calculation, using $\alpha_i = 8\,[W/m^2K]$ (radiation + convection) introduces a coupling only to the inside air, when in reality the most important part of this coupling, i.e. the radiative part, takes place with inside surfaces, which may be at different temperatures.

5.2. Inside surfaces at different temperatures

The general case considers that all inside surfaces may be at different temperatures. One has then to use the general formula, using the form factors. An equivalent conductance may be deduced from the general expression :

$$G_i = \frac{\Phi_{i \to j}}{T_i - T_j} = \underbrace{\sigma(T_i + T_j)(T_i^2 + T_j^2)}_{\sim\ 4\,\sigma\,\bar{T}^3} \,.\, \frac{1}{\frac{1-\varepsilon_i}{\varepsilon_i A_i} + \frac{1-\varepsilon_j}{\varepsilon_j A_j} + \frac{1}{A_i F_{i \to j}}} \tag{24}$$

Computing of form factors may be done either using graphical methods and combination of elementary cases (see for example [29] , pp 223), or using a numerical computer code [30] .

6. CONCLUSIONS

A large fraction of the heat losses through windows is dominated by radiative exchanges. This has practical consequences either in the development of new windows, or for detailed calculations.

- The use of low emissivity coated surfaces or films allows a strong reduction of the heat losses of a window.
- As soon as detailed calculations are required, radiative and convective exchanges have to be considered separately.
- Attention has to be paid to the outdoor heat exchanges with the sky. Depending on the sky equivalent temperature, this heat exchange may be rather important. For this reason several empirical methods have been developed, which allow practical calculations starting with experimental parameters which are generally available.

7. REFERENCES

[1] Swinbank, W.C. et al, "Long wave radiations from clear skies", J. Royal Meteorological Society 89, (1963)

[2] Whillier, A., " Design Factors Influencing Solar collectors", ASHRAE, (1967)

[3] Ineichen, P. et col., "Infrared sky radiation in Geneva", Solar Energy 32 No 4 (1984)

[4] Liu, B.H., Jordan, R.C., "The interrelationship and characteristic distribution of direct, diffuse and total solar radiation", Solar Energy, vol. 4 (1960)

[5] Parmelee, G.V., et al., "Radiant energy emission of atmosphere and ground : A design factor in heat gain and loss", American Society of Heating and Ventilating Engineers, (1952)

[6] Bliss, R.W., "Atmospheric radiation near the surface of the ground : "A summary for engineers", Solar Energy, (1961)

[7] Leduc, R. et al., "A heat loss index incorporating solar, temperature, wind and cloud cover effects", Energy and Buildings, (1979)

[8] Unsworth, M.H. et al, "Longwave radiation at the ground", Quarterly Journal of the Royal Meteorological Society, (1975)

[9] Roch, H.A. et al., "Möglichkeiten zur Berücksichtigung von Sonnen- und Wärmestrahlungseinflüssen auf Geländeoberflächen", Gesundheitsingenieur, (1977)

[10] Cole, R.J., "The longwave radiation environment around buildings" Building and Environment, (1976)

[11] Cole, R.J., "The longwave radiation incident upon the external surface of buildings", B.S.E., (1976)

[12] Cole, R.J., "The longwave radiation incident upon inclined surfaces ", Solar Energy, (1979)

[13] Wolfseher, "Der Wärmetransport an Bauteroberflächen unter Berücksichtigung des langwelligen Strahlungsaustausches", Gesundheitsingenieur, (1981)

[14] Berdall, P. et al, "The thermal radiance of clear skies", Solar Energy, (1982)

[15] Fanger, G. et al, "Verbesserungen des Energie haushaltes von Gebäuden durch Verminderung der Wärmeabstrahlung von Fenstern und Fassaden", Schweizer Ing. und Arch., (1979)

[16] Reagan, J.R. et al, "Solar reflectivity of common building materials and its inlfuence on the roof heat gain", Energy and Buildings, (1979)

[17] Sagelsdorff, R. et al, "Einfluss der Strahlungsvorgänge an der Gebäudehülle auf den Energie verbrauch", IVBH Kongress Wien, (1980)

[18] Frank, Th. et al, "Testkabinen Maugwil", EMPA Bericht, ('82)

[19] Zürcher, Ch. et al, "The influence of thermal and solar radiation on the energy consumption of buildings", Infrared Physics, (1982)

[20] Frank Th.,"Passive solar heat gain of opaque building structures", CIB - Congress Stockholm, (1983)

[21] Frank, Th. et al, "Meteo-Data measurements Maugwil", EMPA Report, (1981)

[22] Liebot J.E. et al, "Some results of thermal atmospheric radiation measurements in Manresa (Spain)", Solar Energy, (1984)

[23] Berger, K. et al, "About the equivalent radiative temperature for clear skies", Solar Energy, (1984)

[24] Paltridge, G.W. "Day-time longwave radiation from the sky" Quarterly Journal of the Royal Meteorological Society, (1970)

[25] Kimura, K., "Scientific Basis of Air Conditioning", Applied Science Publishers, (1977)

[26] "Coating architectural glass", Leybold Heraeus 14 - 100.1 (1980)

[27] Forsch. Gebeite Ingenieurwesen 6 (1935)

[28] Duffie & Beckmann, "Solar Energy Thermal Processes", (1974)

[29] Kreith, "Transmission de chaleur et thermodynamique", (1967)

[30] Ch. Eriksson, "AIRES, A computer Code to Compute Form Factors and Radiation Couplings", GRES internal report, (1984)

[31] Püntener, T.W., Frank, Th., "Oberflächentemperaturen von besonnten Fensterglasscheiben und ihre Auswirkungen auf Raumklima und Komfort", NEFF-Projekt Nr. 266 - EMPA (1986)

[32] Rubin, M. , "Calculating heat transfer through windows" Energy Research Vol. 6, 1982

3.2.2. Convective/conductive heat transfer

K.Th. Knorr
TNO Institute of Applied Physiscs
P.O. Box 155
2600 AD DELFT
THE NETHERLANDS

LIST OF CONTENTS

LIST OF SYMBOLS

h	Heat transfer coefficient	W/m^2K
V	Wind speed	m/s
a	Wind direction	degrees
d	Wall azimuth	degrees
λ	Thermal conductivity	W/mK
w	The width of the gap	m
Nu	Nusselt number	--
Gr	Grashoff number	--
Pr	Prandtl number	--
Ra	Rayleigh number	--
g	Gravitational accelleration	m/s^2
β	Coefficient of thermal expansion	K^{-1}
ρ	Density	kg/m^3
μ	Dynamic viscosity	kg/m.s
θ	Temperature	K
A	Aspect ratio	--
ε	Emissivity	--
M	Molar mass	g/mole
C_p	Specific heat at constant pressure	J/kgK
H	Height	m

Subscripts

e	Exterior
s	Surface
r	Radiative
c	Convective
m	Meteorological
h	Hemispherical

1. CONVECTIVE HEAT TRANSFER AT THE EXTERIOR SURFACE OF BUILDINGS

In product information the U-value of glazings is given, taking into account a standardized value for the combined (convective and radiative) heat transfer coefficient h_e. ISO [5] recommends $h_e = 23$ W/m^{2}K, assuming a meteorological wind speed of 3 to 4 m/s, while ASHRAE [6] recommends to make a distinction for winter and summer design conditions $h_e = 34$ W/m^{2}K and $h_e = 23$ W/m^{2}K respectively.
The U-values given in product information are also often used to determine the capacity of the heating plant and for global energy analyses.
For more detailed calculations based upon hourly weather data, either measured on site (above the roof) or at a meteorological station in the vicinity, the combined h_e can be divided into a convective part $h_{e,c}$ and a radiative part $h_{e,r}$.
How to deal with $h_{e,r}$ is described in chapter 3.2.1. Theoretically the convective heat transfer coefficient $h_{e,c}$ is dependent upon the air flow velocity near the wall.
Only a few full scale experiments to quantify the convective component of the external surface energy balance are known from literature.
Two of these experiments are described here.
The results of the experiments Ito et al [1] carried out at a six storey building with an open L shaped plan situated in Tokyo have gained international recognition. From this work the ASHRAE Task Group [1] has derived an algorithm to calculate the convective heat transfer coefficient $h_{e,c}$ taking into account the meteorological windspeed V_m.

The following measurements have been carried out:

- wind speed and wind direction at a height of 8 m above the roof;
- air flow velocities at 30 cm from the wall at centre part and edge part positions according to figure 1;
- convective heat transfer in the same positions by means of two heat flux sensor panels side by side, maintained at slightly different temperatures.

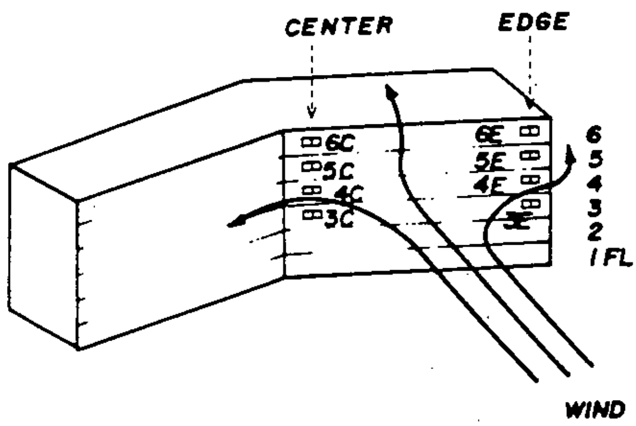

Figure 1: Positions and symbols of the measurement done at the north wall surface of the test building.

The conclusions were:

1. the air flow velocity near the surface was 1/3 - 1/5 times the wind speed when the surface is windward and 1/18 - 1/11 when it is leeward;
2. the convective heat transfer is more closely related to the air flow velocity near the surface than to the wind speed;
3. the test results from an actual building did not agree with the conventional relations between convective heat transfer coefficient and air flow velocity, if the wind speed was used instead of air flow velocity along the surface;
4. the relation between wind speed and convective heat transfer can be broken down into two characteristic parts:

   a. relation between wind speed and air flow velocity near the surface;

   b. relation between the convective heat transfer coefficient and the air flow velocity near the surface;

   When the wind speed is low or when the surface is leeward, the convective heat transfer coefficient often turns out to be as low as about 6 W/m^2K.

Kimura [2] derived from the experiments an algorithm for computer calculation:

Input V = wind speed in general (m/s), here the meteorological wind speed V_m is taken;

a = wind direction (angle measured clockwise from north) (degrees);

b = wall azimuth (positive degrees westward from south and negative eastward).

Output V_s = air velocity near the outside surface (m/s);

$h_{e,c}$ = convective heat transfer coefficient (W/m^2K).

Calculation sequence

(1) Calculate wind direction relative to the wall surface γ

$$d = b + 180 - a$$

If $|d| > 180$, $d = 360 - |d|$

(2) Calculate air velocity near the outside surface V_s

(i) If the surface is windward:

for $V_m > 2$ $\quad V_s = 0.25\ V_m$
for $V_m < 2$ $\quad V_s = 0.5.$

(ii) If the surface is leeward:

$$V_s = 0.3 + 0.05\ V_m.$$

(3) Calculate convective heat transfer coefficient $h_{e,c}$

$$h_{e,c} = 3.5 + 5.6\ V_s.$$

As an example: windspeed 4 m/s,
$h_{e,c} = 9.1\ W/m^2K$ windward side
$h_{e,c} = 6.3\ W/m^2K$ leeward side.

This plotted back to the results of the experiments indicates that the algorithm is valid for the center parts on the third and fourth floor of the building in figure 1, although for the leeward side and calm conditions ($V_m < 3$ m/s) a lower value for $h_{e,c}$ can be derived than was found with the experiments ($h_{e,c} \simeq 6\ W/m^2K$).

The ASHRAE Task Group [1] took the same algorithms as Kimura to calculate V_s from V_m but derived for $h_{e,c}$, $h_{e,cl} = 18.6\ V_s^{0.65}$.

According to Rubin [3], Lokmanhekim, derived the following formulas from Ito's experiments:

$h_{e,c} = 8.07\ V_m^{0.605}$ windward side

$h_{e,c} = 18.64\ (0.3 + 0.05\ V_m)^{0.605}$ leeward side

These formulas lead to the same results as the ASHRAE approach and give for $V_m = 4$ m/s:

$h_{e,c} = 18.7\ W/m^2K$ windward side
$h_{e,c} = 12.3\ W/m^2K$ leeward side

These values are more in accordance with the results of Ito's measurements for the top floor.

Sharples [8] carried out measurements on the north façade of the 18 storey Arto Tower at Sheffield University, U.K., based upon the same principles as the ITO experiments. Sharples derived relationships between $h_{e,c}$ and the meteorological wind speed V_m, the wind speed above the roof V_r and the air velocity near the wall V_s for the center parts of the 6th, 14th and 18th floor and for the edge part of the 18th floor. The algorithm he derived from the experiments for the worst case (18th floor edge site) takes the form:

windward surface $V_s = 1.8\ V_m + 0.2$ m/s
leeward surface $V_s = 0.2\ V_m + 1.7$ m/s
for either surface $h_{e,c} = 1.7\ V_s + 5.1\ W/m^2K$.
For $V_m = 4$ m/s, this algorithm leads to:
windward surface $h_{e,c} = 17.7\ W/m^2K$
leeward surface $h_{e,c} = 9.4\ W/m^2K$.

These figures are somewhat lower than those found by the ASHRAE algorithm.
For the 6th floor center part even lower values ($h_{e,c} \approx 6$ W/m^{2}K) than can by derived by the Kimura algorithm were found.
This shows that $h_{e,c}$ for a given wind speed increases with the height, decreases with the distance from the edge of a building and is strongly dependent upon the façade location.
Figures for lower floors than the sixth are not available.

In literature (e.g. 4, see figure 2) results from wind tunnel experiments can be found which confirms that the local conditions near the façade strongly vary with position on the façade, with building geometry, position of adjacent buildings and roughness of the surroundings (mean height of buildings or other obstructions). The quantity derived from these types of experiments is the local wind pressure, related to the meteorological wind speed. However, although the low air velocity is related to the local wind pressure, this relation may not be unique for all circumstances (flow direction).

The conclusion that can be drawn is that in order to carry out very detailed calculations of the energy balance of windows one must be aware that the values for the convective heat transfer coefficients for differently situated parts of the façade of a building with a specific geometry only can be derived at the moment from a few full scale experiments each with their own limitations and uncertainties.
Taking the highest value (top floor, edge site) for all parts of the façade can lead to an overestimation of the heat transmission through a single glazing of about 10% and for a double glazing of about 6%.

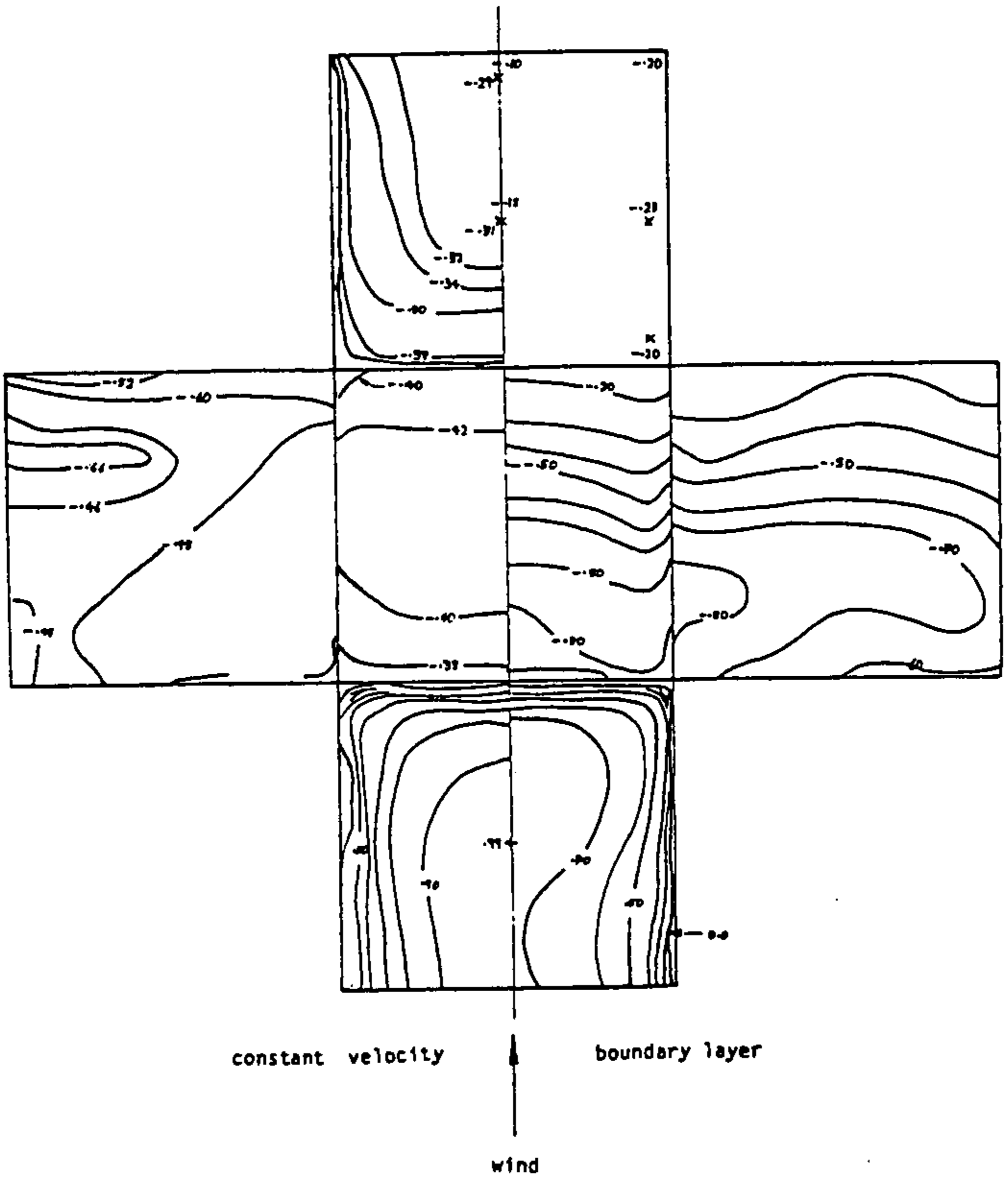

Figure 2: Comparison of pressure coefficients on a cube for constant velocity and boundary layer flow (after Hamilton).

2. CALCULATION OF THE CONDUCTIVE AND CONVECTIVE HEAT TRANSFER IN GAPS OF MULTIPLE GLAZINGS

The conductance h in a gap between two parallel panes is given by the relation $h = \lambda/w\ Nu$, where

λ = thermal conductivity of the gas or gasmixture of the gap in W/mK;

w = the width of the gap in m;

Nu = Nusselt number $Nu = h.w/\lambda$; (1)

h = heat transfer coefficient in W/m^2K.

The Nusselt number depends on the occurring flow regime. Three flow regimes exist.

1. pure conduction $\overline{Nu} = 1$
2. transition
3. boundary layer.

Which flow regime occurs is according to Eckhart and Carlson [9] dependent on the Grashof number Gr_w on the aspect ratio A_x.

The Grashoff number Gr_w is given by:

$$Gr_w = \frac{g.\beta.\rho^2.w^3}{\mu^2}.\Delta\theta \qquad (2)$$

g = gravitational acceleration, 9.81 m/s^2

β = coefficient of thermal expansion, K^{-1}

ρ = density in kg/m^3

μ = dynamic viscosity in kg/m.s

$\Delta\theta$ = temperature difference across the region in K

w = gap width in m

A_x is the aspect ratio, the ratio between the height and the width.

TABLE 1: Some heat transfer relations for vertical gaps.

relation number / author	RELATION	Ra	Ax	Pr	remarks	REF.
1. Jacob	$\bar{N}u = 0.18 \; Gr^{0.25} \, Ax^{-0.111}$ $\bar{N}u = 0.065 \; Gr^{0.333} Ax^{-0.111}$	$1.4*10^3 - 1.4*10^4$ $>1.4 * 10^5$	3-42 3-42	0.71 0.71	data of Mull and Reiher (caloric)	[10] [11]
2. De Graaf and Van der Held	$\bar{N}u = 0.0436 \; Ra^{0.37}$ $\bar{N}u = 0.036 \; Ra^{0.37}$	$0.7*10^4 - 5.6*10^4$ $> 2.4 * 10^5$	3-48 3-48	0.71 0.71	caloric for $Ra > 2.4*10^5$ data of Mull and Reiher [2]	[12]
3. Rubin	$\bar{N}u = 0.0424 \; Ra^{0.37}$ $\bar{N}u = 0.43 \; Ra^{0.16}$ $\bar{N}u = 0.0354 \; Ra^{0.37}$	$5*10^3 < Ra < 6*10^4$ $6*10^4 < Ra < 1.5*10^5$ $Ra > 1.5*10^5$			derived from De Graaf and Van der Held	[3]
4. Eckert and Carlsson	$\bar{N}u = 0.132 \; Ra^{0.3} \; Ax^{0.1}$	$>10^5$	2.5-47	0.6-0.8	interferometric	[9]
5. Jannot and Mazeas	$\bar{N}u = 0.0835 \; Ra^{0.315}$	$10^5 - 10^{10}$	3.5-100	0.71	interferometric	[13]
6. Mynett and Duxbury	$\bar{N}u = 0.216 \; Ra^{0.263} Ax^{-0.21}$	$10^3 - 6.5*10^6$	1.25-20	0.71	interferometric	[14]
7. Yin, Wung, Cheng	$\bar{N}u = 0.210 \; Ra^{0.269} Ax^{-0.13}$	$1.5*10^3 - 9*10^6$	5-78	0.71	caloric	[15]
8. Randall	$\bar{N}u = 0.096 \; Ra^{0.29}$	$3*10^3 - 2*10^5$	9-36	0.71	interferometric	[16]
9. Gläser	$\bar{N}u = 0.11 \; Ra^{0.333} Ax^{-0.111}$	$Ra Ax^{-0.333} > 5*10^2$			data from Linke [18]	[11]
10. Schinkel	$\bar{N}u = 0.106 \; Ra^{0.29}$	$10^4 < Ra < 4*10^4$	27.5	0.71		[19]
11. Elshirbiny, Raithby, Hollands	$\bar{N}u = [Nu_1, \, Nu_2, \, N_3]_{max}$	*)	5-110	0.71	caloric	[20]
12. Owens	$\bar{N}u = 0.035 \; Ra^{0.38}$	$Ra > 6.783*10^3$		0.71	caloric, derived from Robinson, Powlitch, Dill	[21]

*) $Nu_1 = 0.0605 \; Ra^{0.333}$

$$Nu_2 = \left[1 + \left(\frac{0.104 \times Ra^{0.293}}{1 + \left(\frac{6310}{Ra}\right)^{1.36}} \right)^3 \right]^{0.333}$$

$$Nu_3 = 0.242 \; . \; \left(\frac{Ra}{Ax}\right)^{0.272}$$

Thus the conductance in the gap is dependent on: properties of the gas in the gap, the temperature level, the temperature difference and the dimensions.

According to many authors the convective heat transfer between panes can be described by a relation as

$\bar{N}u = a.(Gr.Pr)^b.A_x{}^c$ (3)

where Pr = Prandtl number = $c_p\mu/\lambda$ (4)

where c_p = specific heat at constant pressure in J/kg.K

The product Gr.Pr is also called the Rayleigh number.

In table 1 a review is given of $\bar{N}u$-Ra relations for vertical gaps,which authors derived from measurements either caloric or inter-ferometric.

As can be seen most of the experiments have been carried out at low aspect ratios comparing with the aspect ratios for normal multiple glazings. At a height of the glazing of 1 m and a width of the gap between 6 mm and 24 mm A_x varies between 167 and 42. Some authors find a dependency on the A_x with c in (2) of -0.10 tot -0.29, and some do not (De Graaf and Van der Held [12], Jannot and Mazeas [13]).

For normal glazings in a winter situation a Ra-number greater than 10^5 only occurs with heavy gases like SF_6.

It is important to select a set of relations that cover all practical situations. That means also the situations with low emissivity coatings, where the gasconductance is of main importance and the same in combination with other gases than air or gasmixtures.

As all the relations in table 1 were derived from experiments it is interesting to compare calculations with measurements on real glazings either with the hot plate method or with the hot box method.

Rubin [3] showed that his relations are in good correspondence with the hot-box measurements he carried out with normal non-coated glazings and air spaces (see figure 3).

Gläser [17] measured with the hot plate apparatus also glazings with low emissivity coatings and gasfillings.

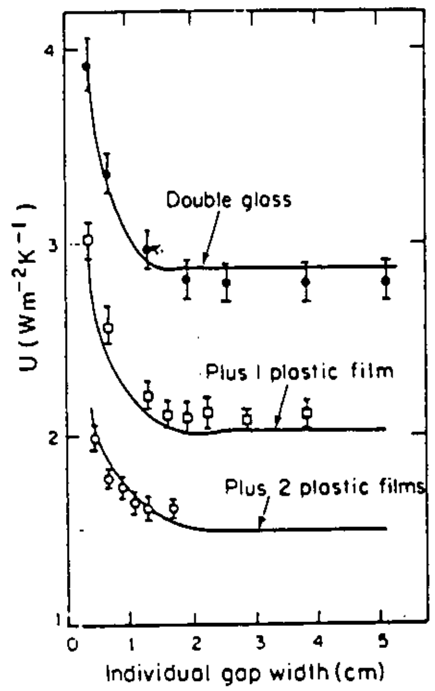

Figure 3: Overall thermal conductance measured in a calibrated hot-box vs. individual gap widths for double glazing alone, and double glazing with one or two polyester films suspended vertically in the air gap. The solid lines represent calculated values.

In figure 4 the measurements of Gläser on glazings with air space and a low emissivity ε = 0.065 are compared with calculations using some relations of table 1 for exactly the same conditions and sizes.

The calculations with Nu = 1 (so no convection) result in a somewhat lower U-value than the measurements. The cause is not yet clear but the shape of the curve is of vital importance.
The relations of Gläser, Yin Wung Chen and Randall result in a higher U-value than the others.
The relations of Jacob give the same shape of the curve as the measurements. The relation of Owens gives the lowest U-value and a shape of the curve that can be compared with the measurements. It is also clear that all the relations indicate that convection is occurring, see Nu = 1.
In a recent study Mrs E. Keizer-Boogh, [25] calculated in a theoretical way local Nu-numbers in gaps with air and with argon. She also found a good corresponding course with the measurements. From this study Nu-Ra relations have not been derived yet.

In figure 5 the same has been given for the gas SF_6. Now it can be seen that the results of the measurements are lower than the calculated results with the Gläser relation and higher than with the Owens and Jacob relations. The Owens and Rubin relations give the same shape as the measurements. The Jacob relation gives a remarkable difference.
In the calculations figures 2 and 3 are based on, the effect of the infrared absorption of the gas fillings has been neglected. That can certainly be done for gases as air and argon. However, it is known that sulphur hexafluoride SF_6 has a strong absorption band in the important wave length region of 10 µm to 11 µm. On the one hand the absorption causes a less radiant heat exchange, on the other hand the onset of convection starts earlier and higher $\bar{Nu}$-numbers occur.
Which effect prevails depends on the temperature difference between the panes and the temperature level.

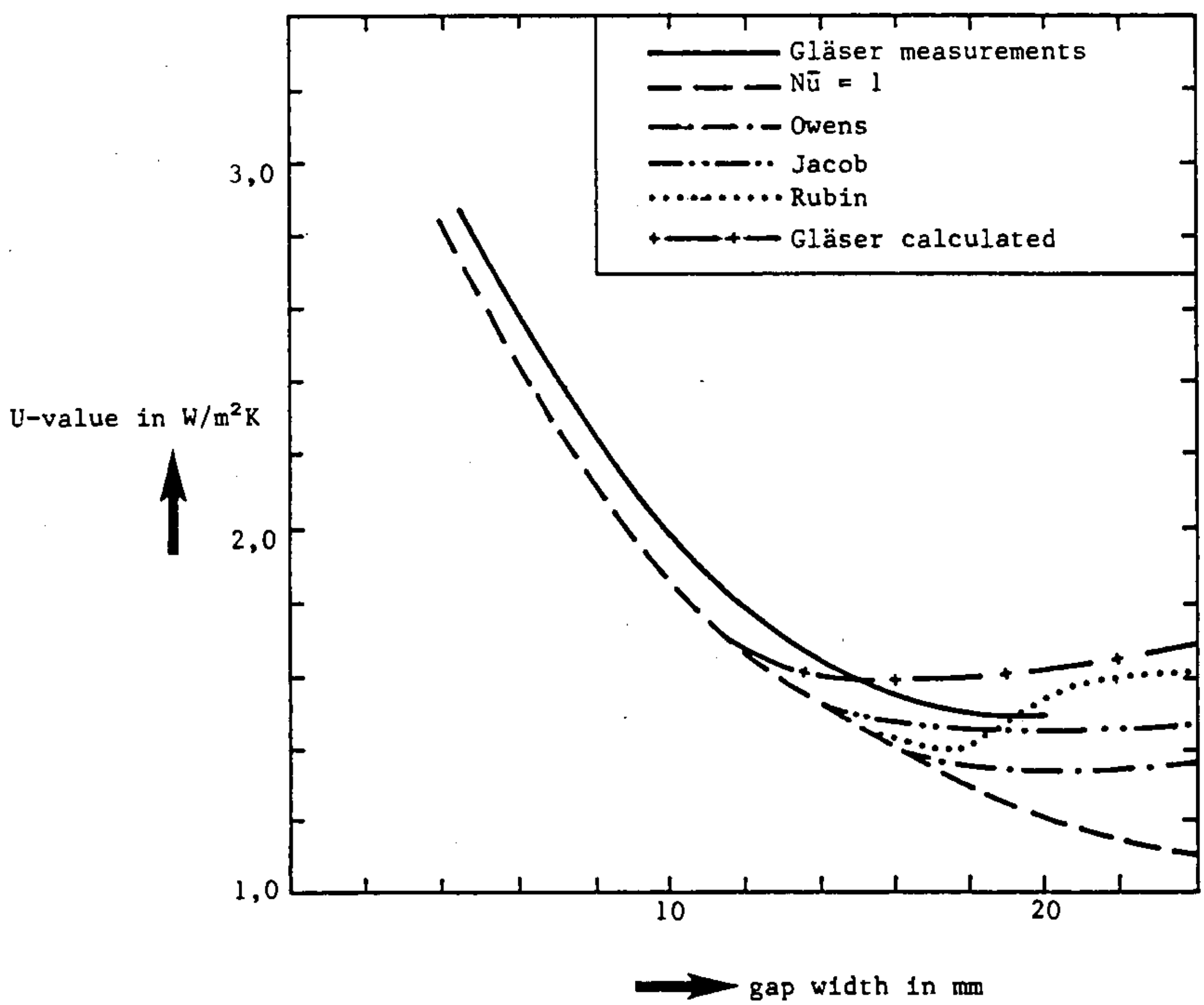

Figure 4: Comparison of measured and calculated U-values, hot plate conditions
outer pane 5 °C, 4 mm, height 0.77 m
inner pane 15 °C, 4 mm, height 0.77 m

$\varepsilon_{h1} = 0.84$, $\varepsilon_{h2} = 0.065$

$h_e = 23\ W/m^2K$, $h_i = 8\ W/m^2K$

A I R
=====

In figure 5 it can be seen that the deviation between the measurements of Gläser and the Owens relation is relatively small. This could indicate that the effect on the convection is slightly larger than the effect on the radiant heat exchange.
The computation of the radiant heat exchange in a multiple glazing with an infrared absorbing gas can be based on the same idealized and approximated model as with a non-absorbing gas, but is considerably complicated.
To describe the convective heat transfer in gas with an i.r. absorbing gas further research is needed.

For this moment the conclusion can be drawn that for all practical situations the relation of Owens corresponds best with known measurements. The Rubin relations only fit with the high Ra-numbers and the Jacob relation only fits with Ra < 20.000. The use of the Owens and Rubin relations has the advantage that for this area of the glazing the influence of the A_x can be neglected.
The Owens relation is also recommended by ISO [26].

In figure 6 U-values are given calculated with the Owens relation as a function of the gap-width for the same glazings as in figure 2 for two set of conditions:

- hot plate conditions, out pane 5 °C, inner pane 15 °C;
- hot box conditions; temperatures of the outdoor and indoor environment -10 °C and +20 °C.

The hot plate conditions can be considered as an average winter situation of a moderate climate, the hot box conditions as design conditions for a moderate climate and average winter situation for colder climates.

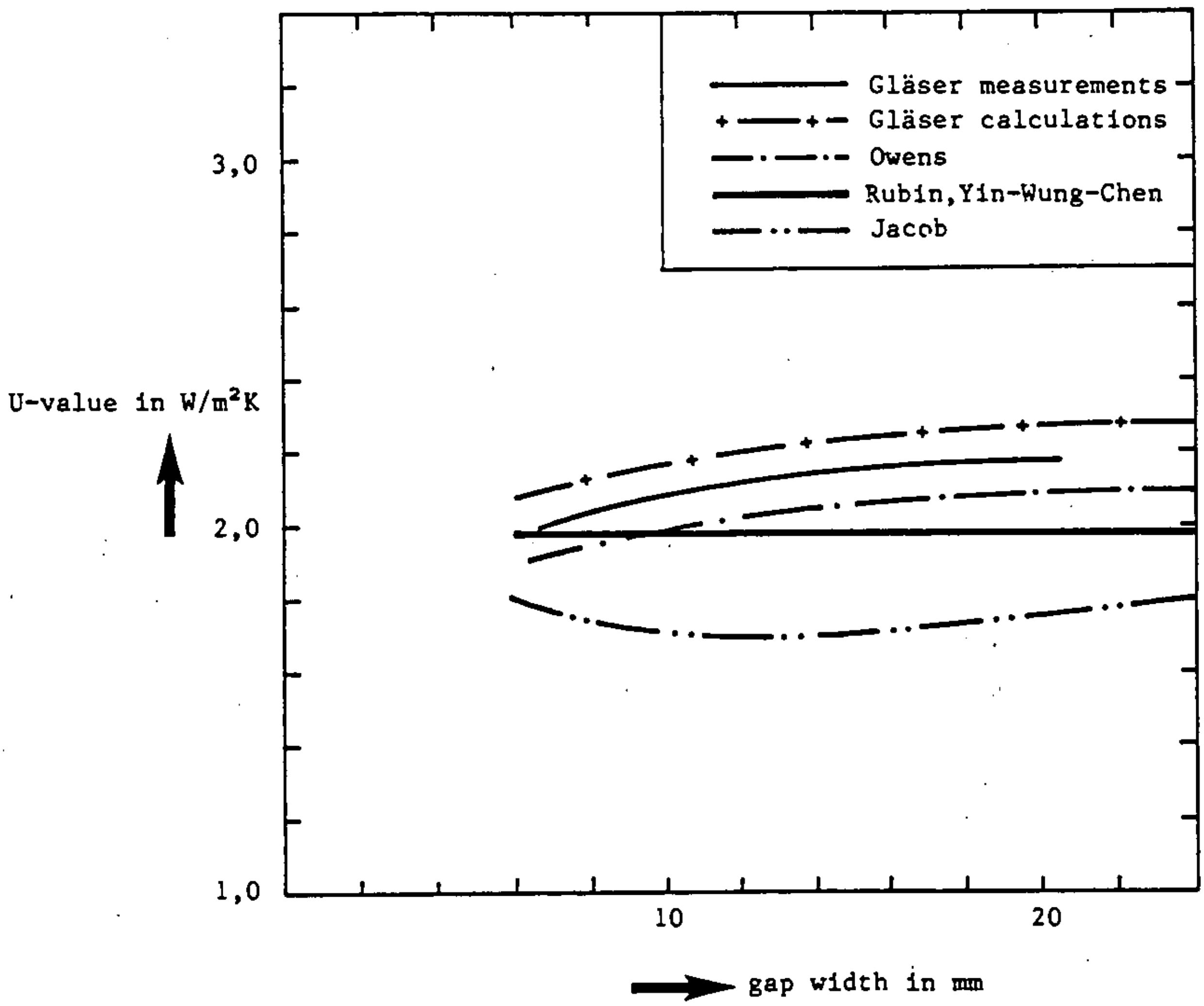

Figure 5: Comparison of measured and calculated U-values, hot plate conditions
outer pane 5 °C, 4 mm, height 0.77 m
inner pane 15 °C, 4 mm, height 0.77 m

$\varepsilon_{h1} = 0.84, \quad \varepsilon_{h2} = 0.065$

$h_e = 23\ W/m^2K, \quad h_i = 8\ W/m^2K$

SF_6
===

It can be seen that with a gap width of about 14 mm both sets of conditions result in an equal U-value. That confirms the statements of some researchers within the E.C. being that with ordinary normal double glazing, air filled gap, width 12 mm, they could not find a significant difference between the U-value measured with the hot box and with the hot plate method.

Figure 4 indicates that for colder climates, gap widths between about 12 mm and 24 mm give the lowest U-values.
For moderate climates the gap width should be about 20 mm to get the lowest U-value.

Owens derived [26] also Nu-Ra relations for horizontal and angled glazing from the measurements of Robertson, Powlitch and Dill [21], which are recommended by ISO [5] in the following way. When the direction of the heat flow is upward the heat transfer by convection is enhanced and the following relations can be taken:

horizontal gaps $Nu = 0.16\ Ra^{0.28}$
gaps at 45° $Nu = 0.10\ Ra^{0.31}$

When the direction of the heat flow is downward the convection can be considered as suppressed for practical cases and Nu = 1 can be taken.

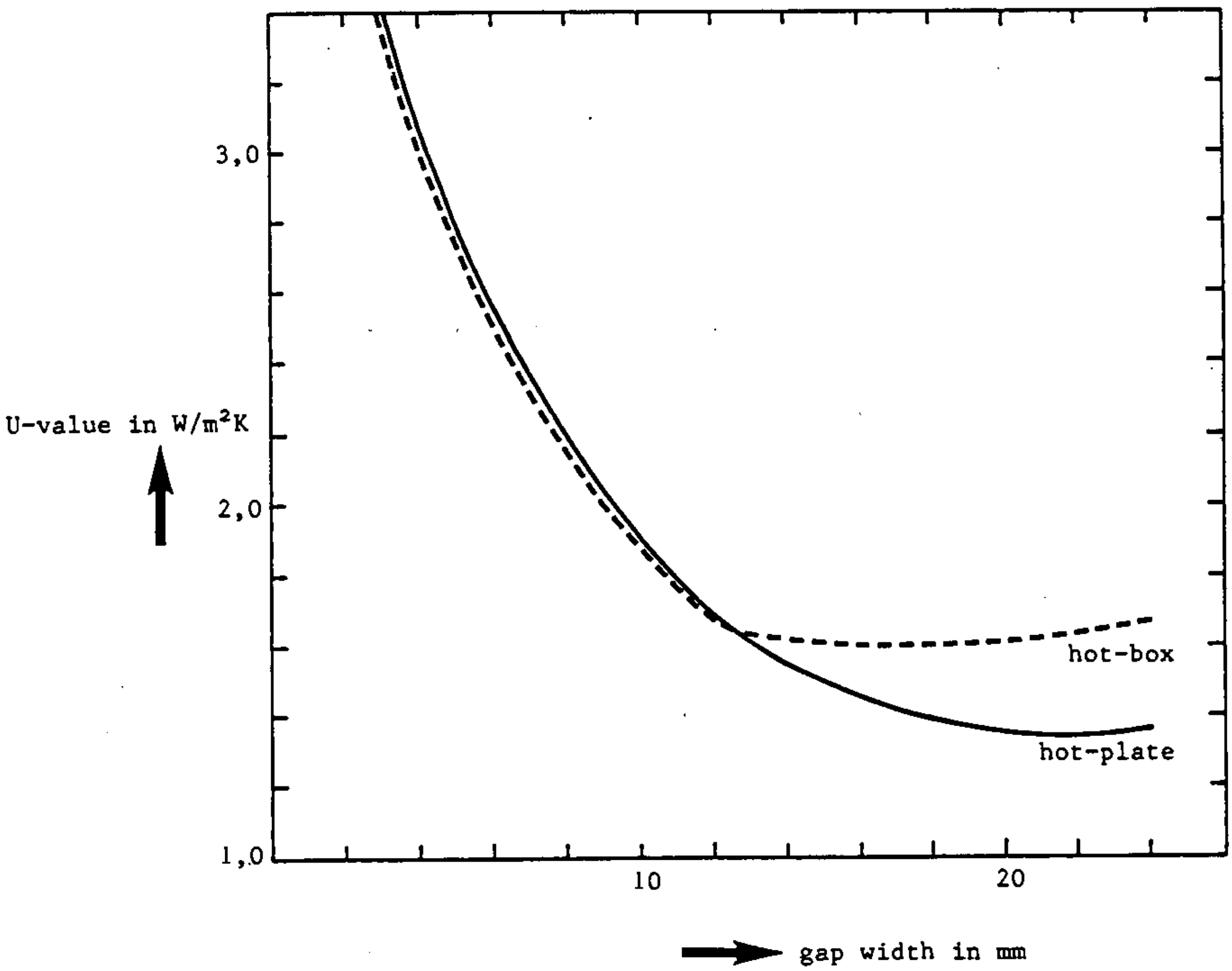

Figure 6: Calculated U-values ($\bar{Nu} = 0.035\ Ra^{0.38}$) as function of the gap width,
$\varepsilon_{h1} = 0.84$, $\varepsilon_{h2} = 0.065$, $h_e = 23\ W/m^2K$, $h_i = 8\ W/m^2K$, air.
Hot plate conditions: outer pane 5 °C, inner pane 15 °C.
Hot box conditions: temperature of the outdoor and indoor environment -10 °C and +20 °C, respectively.

3. CALCULATION OF THE PHYSICAL PROPERTIES OF GAS-MIXTURES

To calculate Raleigh numbers of gas-mixtures the effective thermal conductivity and the viscosity have to be determined.
Gläser [17] gives the following relations for the effective thermal conductivity.

$$\bar{\lambda} = \frac{\Sigma_i \; x_i \lambda_i \; M_i^{0.333}}{\Sigma_i \; x_i \; M_i^{0.333}} \tag{B1}$$

where x_i, M_i and λ_i are the molefraction, the molar mass and the thermal conductivity of the i_{th} component respectively.
In the same way the effective viscosity can be described by:

$$\bar{\mu} = \frac{\Sigma_i \; x_i \mu_i \; M_i^{0.333}}{\Sigma_i \; x_i \; M_i^{0.333}} \tag{B2}$$

Bird, Stewart and Lightfoot [22] also give semi-empirical approximations for λ and μ of mixtures.
Wilke [23] mentioned that these relations are sufficiently accurate for mixtures of non-polaric gasses at normal atmospheric pressures and temperatures above 100 K.

$$\bar{\mu} = \Sigma_{i=1}^{n} \frac{x_i \quad \eta_i}{\Sigma_{j=1}^{n} \; x_j \quad \phi_{ij}} \tag{B3}$$

$$\bar{\lambda} = \Sigma_{i=1}^{n} \frac{x_i \quad \lambda_i}{\Sigma_{j=1}^{n} \; x_j \quad \phi_{ij}} \tag{B4}$$

where:

$$\phi_{ij} = \frac{1}{\sqrt{8}} \left(1 + \frac{M_i}{M_j}\right)^{-0.50} \cdot \left| 1 + \left(\frac{\mu_i}{\mu_j}\right)^{0.50} \cdot \left(\frac{M_j}{M_i}\right)^{0.25} \right|^2 \tag{B5}$$

If there is a big difference in the molar masses of the components (e.g. air and SF_6) it is recommended to use the relations B3, B4 and B5.

4. PHYSICAL PROPERTIES OF GASES

For three gases commonly used in multiple glazings, the physical properties are given in table 2. These values are derived from [24].

Table 2: Physical properties of gases.

temperature in °C	ρ in kg/m^3	10^5 μ in kg/ms	10^2 λ in W/mK	Pr
Air M = 28.96 g/mole				
- 10 °C	1.326	1.661	2.336	0.715
0 °C	1.277	1.711	2.416	0.712
+ 10 °C	1.232	1.761	2.496	0.709
+ 20 °C	1.189	1.811	2.576	0.707
Argon M = 39.96 g/mol				
- 10 °C	1.829	2.038	1.584	0.668
0 °C	1.762	2.101	1.634	0.667
+ 10 °C	1.699	2.164	1.684	0.667
+ 20 °C	1.640	2.228	1.734	0.667
SF_6 M = 146.05 g/mol				
- 10 °C	6.844	1.383	1.119	0.822
0 °C	6.602	1.421	1.197	0.789
+ 10 °C	6.360	1.459	1.275	0.761
+ 20 °C	6.118	1.497	1.354	0.735

ρ = density

μ = dynamic viscosity

λ = heat conductivity

Pr = Prandtl number $c_p\mu/\lambda$

c_p = specific heat at constant pressure.

5. HEAT TRANSFER BY FREE CONVECTION ON THE INSIDE SURFACES OF GLAZINGS IN VERTICAL POSITION

Heat transfer by free convection can be described with the relation:

$$Nu = C\ (Gr\ Pr)^n \qquad (1)$$

where:

$Nu = h_c\ l/\lambda$;
h_c = convective heat transfer coefficient in W/m^2K;
l = length in m;
λ = thermal conductivity of the air in W/m^2K;
Gr = Grashofnumber.

$$Gr = \frac{g \cdot \beta \cdot \rho^2\ l^3}{\mu^2} \cdot \Delta\Theta$$

g = gravitational accelleration, 9.81 m/s^2;
β = coefficient of thermal expansion in K^{-1};
ρ = density in kg/m^3;
μ = dynamic viscosity in kg/m.s;
$\Delta\Theta$ = temperature difference between the surface and the fluid in K;
Pr = Prandtl number;
$Pr = C_p\ \mu/\lambda$;
C_p = specific heat at constant pressure in J/kgK.

The product GrPr is also called the Raleigh number.

In practical situations with glazings a laminair flow can be assumed, then $n = 1/4$ and $C = 0,555$ [27].

$$Nu = 0,555\ (Gr\ Pr)^{0.25} \qquad (2)$$

For still air at temperatures of about 20 °C and temperature differences between the surface of the glazing and the air up to about 10 °, relation (1) can be transferred to:

$$h_c = 1,42 \left(\frac{\Delta\theta}{H}\right)^{0,25} \ W/m^2K \qquad (3)$$

where h_c = convective heat transfer coefficient in W/m^2K
H = height in m.

This relation can be found in many handbooks and many researchers use it in computer calculations to calculate heat loads, etc.
An example: normal double glazing 2 x 6 mm, air space 12 mm, height 1 m, outside temperature -10 °C, room temperature 20 °C, k = 2,9 W/m^2K (h_e = 23 W/m^2K, h_i = 8 W/m^2K). Then the temperature of the inner pane will be 9 °C. According to relation (3) $h_c = 1,42\ (11)^{0,25}$ = 2,58 W/m^2K.
ASHRAE [6] gives for h_c with vertical glazings a relation independent of the height for glass temperatures of -10 °C up to 55 °C and temperature differences glass-air of 3 °C to 30 °C.

$$h_c = 1,77\ (\Delta\theta)^{0,25} \quad W/m^2K \qquad (4)$$

In the above mentioned example this means h_c = 3,22 W/m^2K, which results in a 3% higher U-value than with h_c = 2,58 W/m^2K.
In case of a glazing with U = 1,4 W/m^2K the relation (4) will cause a 6% higher U-value than relation (3).
ISO [5] assumes a value for free convection of h_c = 3,0 W/m^2K, independent of the height and independent of the temperature level and temperature difference glass-air.

VDI [29] recommends a relation for the free convection on vertical places that Churchill, Humbert and Chu [7] derived for the results of many authors:

$$\bar{Nu} = \left[0,825 + \frac{0,387\ Ra^{1/6}}{\left\{ 1 + \left(\frac{0,437}{Pr}\right)^{9/16} \right\}^{8/27}} \right]^2 \quad W/m^2K \qquad (5)$$

In the example this results in $h_c = 3,32\ W/m^2K$.

Caemmerer [31] used a relation for calculation of convective heat transfer at sunlit panes in a solar calorimeter box.

$$h_c = 3,48 + 0,09\ \Delta T\ W/m^2K \qquad (6)$$

However, Caemmerer does not mention what the relation was based upon.

Kollmar and Liese [28] use the relation

$$h_c = 1,97\ (\Delta T)^{0,25}\ W/m^2K, \qquad (7)$$

which leads in the example to $h_c = 3,59\ W/m^2K$.
The relation should be valid for vertical walls and radiative heating.

The conclusions that can be drawn are:
- the relations recommended by ASHRAE, ISO and VDI lead to a higher convective heat transfer than the relation found in handbooks and used by a number of researchers and Institutes;
- some authors give relations that result in a higher convective heat transfer than the relations of ASHRAE, ISO and VDI.

Despite the many uncertainties it is recommended that for detailed calculations to take relation (3) for situations where one can assume real still air (small rooms, small heights of glazing). For situations "still air" in rooms with normal sizes (no radiators, induction units, etc.) one can take relation (4).
Radiators etc. placed below the window increase the convective heat transfer.

6. REFERENCES

[1] Ito, Kimura, Oka; "A field experiment study on the convective heat transfer coefficient on exterior surface of a building", ASHRAE transactions, volume 78 (1972), pp. 184-192.

[2] Kimura; "Scientific basis of Air Conditioning Applied Science" Publishers Ltd, London.

[3] Rubin; "Calculating heat transfer through windows", Energy Research, volume 6 (1972), pp. 341-349.

[4] IEA, Air infiltration Centre, Technical Note AIC 13, January, 1984; "Wind pressure data requirements for air infiltration calculations".

[5] ISO, Draft proposal, ISO TC 160 W 62;
Thermal insulation of glazing; calculation rules for determining the steady state U-value of double or multiple glazing;
March 1985.

[6] ASHRAE, Handbook of Fundamentals 1981, chapter 27, Fenestration.

[7] ASHRAE Task group, Procedure for determining heating and cooling loads for computerising energy calculations. Algorithms for building heat transfer subroutines ASHRAE, New York 1975.

[8] Sharples S.
Full scale measurements of convective energy losses from exterior building surfaces; Building and Environment, Vol. 19, no. 1, pp 31-39, 1984.

[9] Eckert, E.R.G. and W.O. Carlson
Natural convection in an air layer enclosed between two vertical plates with different temperatures. Int. Journal of Heat and Mass Transfer, Volume 2, pp. 106-120.

[10] Mull, W. and H. Reiher
Der Wärmeschutz von Luftschichten, seine experimentelle Bestimmung. Beihefte zur Gesundheit-Ingenieur, Reihe 1, Heft 28, pp. 1-26 (1930).

[11] Jacob, M.
Free Heat Convection Through Enclosed Plane Gas Layers, Trans. Amer. Soc. Mech. Eng. 68 (1946), pp. 189-194.

[12] Graaf, J.G.A. de and E.F.M. van der Held
The relation between heat transfer and the convection phenomena in enclosed plane air layers; Applied Science Research A3 (1952), pp. 393-409.

[13] Jannot M. and C. Mazeas
Etude experimentale de la convection naturelle dans les cellules rectangulaires verticales; Journal Heat and Mass Transfer 16, pp. 81-100 (1973).

[14] Mynett J.A. and D. Duxbury
Fourth International Congress in heat transfer, NC 3-8, Versailles, (1970).

[15] Yin, S.H., T.Y. Wung and K. Chen
Natural convection in an air layer enclosed within rectangular cavities, International Journal of Heat and Mass Transfer, Volume 21, pp 307-315 (1978).

[16] Randall, K.R.
Natural convection heat transfer characteristics of plate enclosures. International Report, University of Wisconsin, Madison, USA (1978).

[17] Gläser, H.J.
Verbesserung der Wärmedämmerung bei Isoliergläsern; Glastechnische Berichte 50 (1977), no. 10, pp. 248-256.

[18] Linke, W.
Die Wärmeübertragung durch Thermopane Fenster; Kaltetechnik 8, pp. 378-384 (1956).

[19] Schinkel, W.M.M.
Natural convection in inclined air-filled enclosure; dissertation Delft University of Technology, 1980.

[20] Elsherbiny, S.M., G.D. Raithby and K.G.T. Hollands.
Heat transfer by natural convection across vertical and inclined air layers. Journal of Heat Transfer, Volume 104, pp. 96-102 (1982).

[21] Robinson, H.E., F.J. Powlitch, R.S. Dill.
Insulating value of air spaces,
Housing research paper no. 32, US, Housing and Home Financial Agency, Washington, 1954.

[22] Bird, R.B., W.E. Stewart and E.N. Lightfoot
Transport Phenomena, New York, Par. 1.4 and 8.3 (1960).

[23] Wilke, C.R.
Journal Chemistry and Physics 18, pp. 517-519 (1950).

[24] L'Air Liquide; Encyclopedie des gaz: Elseviers Scientific Publishing Company, Amsterdam, New York (1976).

[25] Keizer-Boogh, E.
Numerieke berekeningen van de k-waarde van dubbel glas, Technische Hogeschool Delft, (1984).

[26] Owens, P.G.
$\overline{Nu}$-Pa relations to describe the convective/conductive heat transfer in the gaps of multiple glazings, not published.

[27] Gröber, Erk und Grigull
Wärmeübertragung, Springer Verlag.

[28] Kollmar, A. and W. Liese
"Die Stralungsheizing"; 4e Aufl.; Verlag Oldenbourg, München.

[29] VDI, Wärmeatlas (1984), Fa 3, VDI-Verlag Düsseldorf.

[30] Churchill, S.W. and Humbert and Chu,
Laminair and turbulent free convection from a vertical plate, Int. J. Heat and Mass Transfer, 18 (1975), pp 1323-1329.

[31] Caemmerer, W.
Beitrag zum Problem des Sonnenschutzes von Fenstern; Gesundheits Ingenieur, 83 (1962), no. 12, pp 349-376.

[32] Robinson, H.E., F.J. Powlitch and R.S. Dill
The thermal insulating value of air spaces, National Bureau of Standards, Report 3030, Washington 1954.

3.2.3. Thermal bridges

P. Standaert
Engineering consultant
Heirweg 21, B-9990 MALDEGEM
BELGIUM

LIST OF SYMBOLS

λ	thermal conductivity	[W/mK]
θ	temperature	[°C]
b	width	[m]
h	surface coefficient of heat transfer	[W/m^2K]
l	length	[m]
q	heat flow density	[W/m^2]
A	area	[m^2]
Q	heat flow	[W]
R	thermal resistance	[m^2K/W]
T	absolute temperature	[K]
U	thermal transmittance	[W/m^2K]
U_m	mean thermal transmittance	[W/m^2K]
U_l	linear thermal transmittance	[W/mK]

Indices

c	characteristic
e	exterior
f	frame
g	glazing
i	interior
l	linear
m	mean
tb	thermal bridge
a	ambient
s	surface

1. THEORY

1.1. Definition

Thermal bridges are parts of the building envelope where, due to the two-dimensional or three-dimensional character of the heat conduction, either the inside surface temperatures are rather low, which can cause condensation, or the heat losses are rather high. The references, indicated by the word "rather", are the inside surface temperature and the heat loss supposing an one-dimensional heat conduction. (For some building envelope parts, e.g. complex window profiles, it is impossible to suppose such a simplified one-dimensional heat flow; in this way it is impossible to name these parts thermal bridges. Because this chapter principally deals with such elements, a more general title of it could be : "two-dimensional and three-dimensional heat flow".)

1.2. Numerical Methods for Two-dimensional and Three-dimensional Heat Transfer

To know the temperature field in and the heat flow through a certain object exposed to specified boundary conditions, a differential equation must be solved. For practical applications, such as encountered in building physics, no analytical solutions are available. Numerical methods, such as the finite element method or the finite difference method, start from a partition of the considered object; with some simplificating assumptions, the differential equation can be applied for each part, resulting in a system of linear equations. The solutions of this system are the approximative temperatures in the characteristic points of the partition. The more detailed the partition is, the better the approximation. So, to provide a good accuracy in the case of practical problems, a computer is needed to create and to solve the systems.

The following is a short review of the heat balance technique, a numerical method which can be seen either as a finite element technique or as a finite difference method [1]. Only the calculation of two-dimensional steady state heat transfer is treated, but the basic ideas are the same for three-dimensional problems. Because transient effects do'nt play an important role in the case of windows, they are beyond the scope of this chapter. For transient effects concerning thermal bridges, the reader is referred to [2,3].

Before calculating the temperature field in a certain object, the following data must be known :

- the geometry of the object.
- the thermal conductivities (λ) of the occurring materials. In this context it is assumed that the materials are isotropic and that λ is independent of temperature. Further, because only conduction is taken into account in the described method, equivalent thermal conductivities are to be derived for occurring air holes.
- the boundary conditions :
  - adiabatic boundary condition; this boundary condition occurs in practice at axes of symmetry and at cross-sections where the heat flow is one-dimensional (i.e. sufficiently away from a thermal bridge).
  - linear heat transfer from the surface to its environment (Neumann boundary condition). Though the heat transfer by radiation and convection is'nt a linear process, a linear relationship normally suffices in practice ($q = h (T_s - T_a)$)
  - known surface temperature (or known internal temperature) (Dirichlet boundary condition); this boundary condition occurs rarely in building physics.
  - known density of heat flow rate; e.g. solar radiation

Example 1 : figure 1 shows a horizontal section of a (half) concrete column in an insulated cavity wall. The mentioned data are given in this figure.

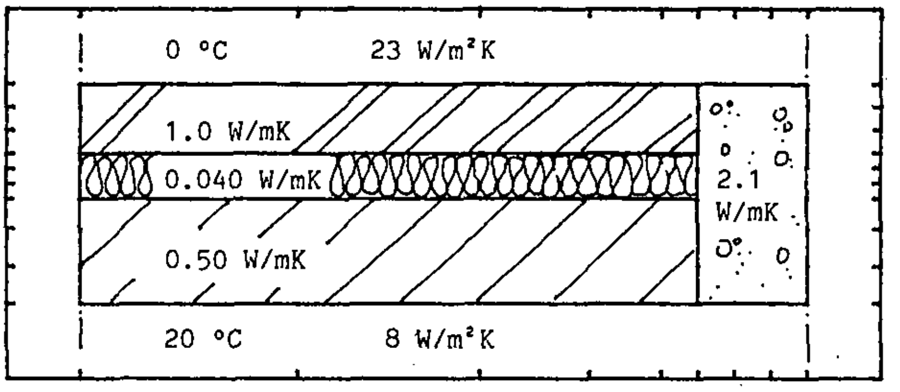

Figure 1: Horizontal section of a (half) concrete column in an insulated cavity wall.

The following steps can be distinguished in the heat balance technique :

- Partition of the object in triangles. The boundaries and materal limits must coincidence with sides of triangles. (Note that rectangular partitions occur in the further given applications; a rectangle can be divided in two rectangular triangles; it can be shown that the position of the dividing diagonal is arbitrary.)
- The only simplifying assumption in the heat balance technique is the linearity of the temperature field within a triangle. By this, the temperature in any point of the triangle area can be expressed as a linear function of the temperatures in the three angular points.
- Around each node a closed line is constructed in thought. This line bisects each of the adjacent sides. Outside the object this line coincidences with the boundary. Taking into account the assumption above and the law of Fourier ($\overline{q} = \lambda \text{ grad } T$), the line integral of the heat flow over this line can be calculated as a function of the adjacent node temperatures. The law of conservation of energy states that this line integral must be zero, which provides a linear equation.
- Executing this procedure for each of the n nodes with unknown temperature, a system of n linear equations with n unknown temperatures is formed. The solution of this system can be obtained using different

mathematical methods. Nevertheless, because of the fact that the left hand matrix of the system is a positive definite symmetric band matrix, some methods, advantageous for calculation speed and memory saving, can be applied; e.g. the Cholesky decomposition [4].

- Being known the node temperatures, and taking into account the assumed linearity of the temperature field within a triangle, the streamfunction value in each node can be derived.

The results can be visualized by a drawing of the isothermals and a drawing of the streamlines, which are derived from the temperatures and the streamfunction values in the nodes by linear interpolation. For the given example, the obtained drawings of isothermals and streamlines are represented in figure 2.

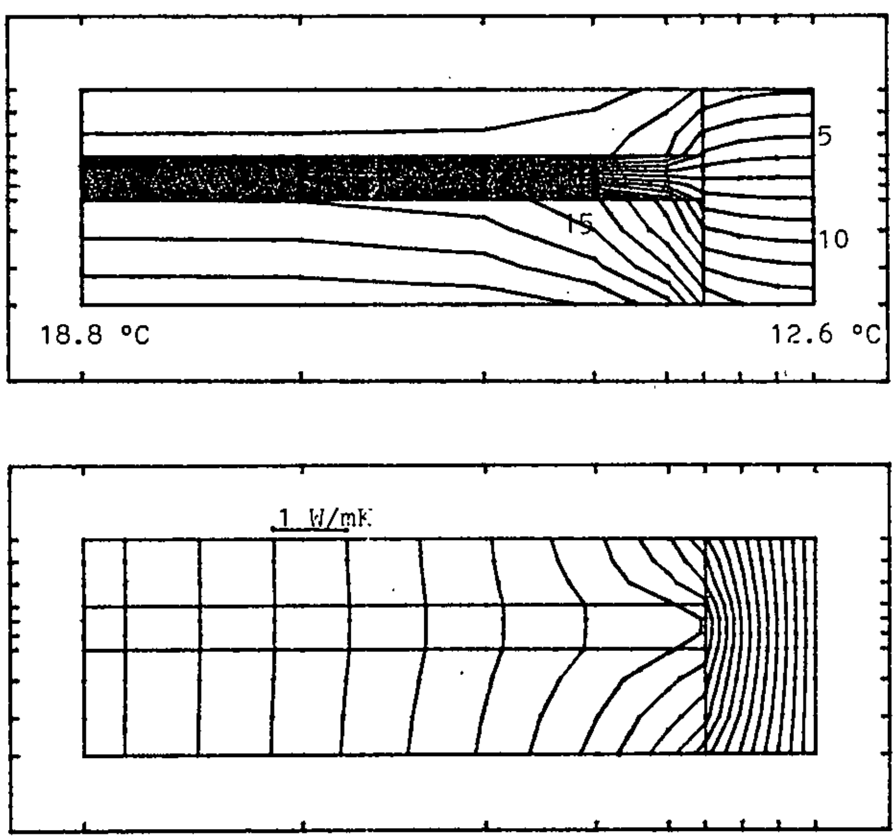

Figure 2: Isothermals (above) and Streamlines (under)

1.3. Evaluation of Thermal Bridges

1.3.1. Introduction

In fact the drawings of isothermals and streamlines suffice to evaluate thermal bridges in steady state :

- The minimal inside surface temperature (thermal bridge temperature) easily can be read from the isothermals plot. The dimensionless thermal bridge temperature, defined as the minimal inside surface temperature, divided by the difference between interior and exterior temperature, further can be determined by linear interpolation. In the example above e.g., the thermal bridge temperature is 12.6°C and the dimensionless thermal bridge temperature is 0.63. The dimensionless thermal bridge temperature characterizes the thermal bridge : from it, the minimal inside surface temperature can be calculated for any outside and inside temperature, to be compared with the dewpoint of the inside air when predicting the occurrence of surface condensation. Further considerations on condensation are given in chapter 3.4. of this book.
- From the streamlines plot, the amount of heat loss through the considered construction element of 1 m length (perpendicular to the section) can be derived by simply counting the number of streamlines (multiplied by the used increment). In the example above 20.5 W/m is obtained. Although with this explanation the evaluation can be considered as completed, there is a need to characterize the heat transfer through a thermal bridge in a more abstract way for two reasons: on the one hand we want to know the heat loss supplementary on the onedimensionally calculated one, on the other we want to include the heat loss through thermal bridges in global heat loss calculations. Two concepts are useful for this purpose: the mean thermal transmittance (U_m [W/m^2K]) and the linear thermal transmittance (U_l [W/mK]).

1.3.2. The mean thermal transmittance

The mean thermal transmittance U_m [W/m^2K] of a wall with one or more thermal bridges, is the total heat loss through this wall, assuming a unit temperature difference over it, divided by the characteristic area of the wall :

$$U_m = \frac{Q_{tb}}{A_c \cdot \Delta\theta_{ie}} \qquad [W/m^2K] \qquad (1)$$

In example 1, the total heat loss Q_{tb} amounts 20.5 W for a length of 1 m (perpendicular to the section), the assumed temperature difference $\Delta\theta_{ie}$ is 20°C and the characteristic area is 1 m^2 (the considered width of the wall is 1 m (0.85 m of cavity wall + 0.15 m of concrete column), and, as mentionned, the considered length is 1 m). Therefore the mean thermal transmittance U_m amounts 1.03 W/m^2K.

The U_m-value allows an easy integration of the thermal bridge effect in global heat loss calculations.

Remark: for complexly shaped building envelope parts a difficulty can arise to define the characteristic area of the considered part (e.g. in the case of corners, window edges, etc.). In theory the characteristic area may be chosen arbitrarily if the same area is used as in the global heat loss calculation. In practice it is convenient to choose the projected outside area as the characteristic surface.

1.3.3. <u>The linear thermal transmittance</u>

The linear thermal transmittance U_l [W/mK] of a thermal bridge is defined as the difference between the real heat losses through that thermal bridge and the onedimensionally calculated ones, assuming a unit temperature difference between the inside and the outside, and an unit length of that thermal bridge. By this, the U_l-value represents the thermal bridge effect itselfs.

$$U_l = \frac{Q_{tb}}{l_{tb} \cdot \Delta\theta_{ie}} - \sum_i (U_i \cdot b_i) \qquad [W/mK] \qquad (2)$$

In example 1 the first part of equation (2) amounts 20.5/(1x20) W/mK = 1.03 W/mK. Knowing the U-values of the two wall parts (U-cavity wall = 0.49 W/m^2K and U-column = 3.26 W/m^2K), the second part of equation (2), i.e. the one-dimensional heat loss, can be calculated : $0.49 \times 0.85 + 3.26 \times 0.15$ W/mK = 0.94 W/mK. The difference between these two parts amounts 0.08 W/mK, being the U_l-value of this thermal bridge.

The advantage of the U_l-value against the U_m-value is that for global heat loss calculations the normal one-dimensional heat loss calculation method remains valid, provided that a supplement is added, namely the product of the U_l-values of occurring thermal bridges and their respectively lengths. On the other hand, the way in which one-dimensional calculations are to be executed is not always determined unambiguously. In such cases the U_l-value is affected by the taken conventions. Therefore, in some cases as for complex building elements (e.g. window frames), the use of the U_m-value is preferred.

2. CASE STUDIES

2.1. Introduction

The scope of this chapter is to provide an insight in the complex matter of conductive heat transfer through windows. Successively the heat transfer through the glazing, through the window profile and through the window edge (i.e. the connection detail between the window frame and the wall) are treated, though these different elements can interfere as indicated further. No completeness concerning the heat transfer through all types of glazings, frames or edges is pursued. The given results have only an illustrative value. (If for example the U-value of a plastic window frame is given, it must be emphasized that other plastic frames will have other U-values.)

2.2. The Edge Effect in Double Glazing

A type of double glazing is shown in figure 3. Two panes of 4 mm each are separated by an air cavity of 12 mm. At the edge there is a hollow aluminium square profile protected by a rubber band. The data for a two-dimensional calculation are the following :

- geometry and assumed grid according figure 3.1.
- thermal conductivities : glass : 0.8 W/mK rubber : 0.2 W/mK
  aluminium : 230 W/mK air cavity : 0.07 W/mK.

  As mentioned, for the air cavity an equivalent thermal conductivity is obtained by dividing the thickness of the cavity by its thermal resistance (0.17 m^2K/W); this is a simplification.
- boundary conditions : θ_e = 0°C h_e = 23 W/m^2K θ_i = 20°C h_i = 8 W/m^2K
  adiabatic conditions at the left and right boundary.

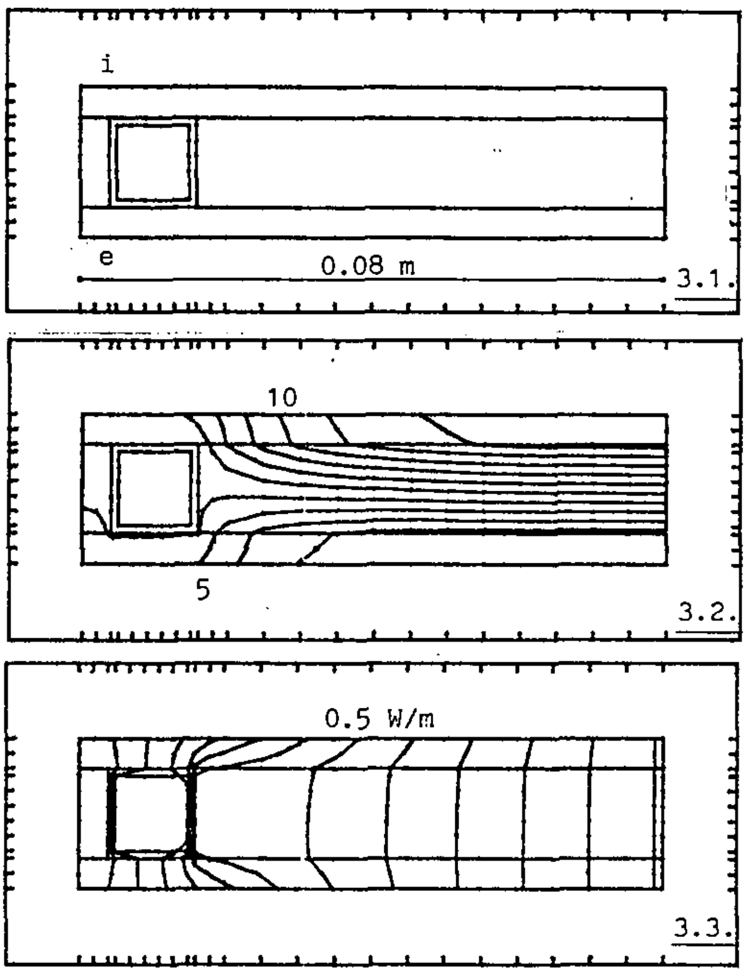

Figure 3: The edge effect in double glazing.

The results of the calculation are presented by an isothermals plot (figure 3.2.) and by a streamlines plot (figure 3.3.). From this last drawing it can be seen that the total heat loss amounts 6.06 W/m or 0.30 W/mK. So, the considered width being 0.08 m, the mean thermal transmittance amounts 3.79 W/m^2K. one-dimensional calculation neglects the edge effect : the U-value of the undisturbed glazing amounts 2.86 W/m^2K; so, for the shown part this would mean 0.23 W/mK. A simple substraction (0.30 - 0.23) gives the neglected supplement or the U_1-value: 0.07 W/mK.

For panes with different dimensions the error of an one-dimensional calculation can be easily derived using the U_1-value :

- 1 m x 1 m : 1-dim. : 2.86 W/K
  incl. edge eff. : (2.86 + 4x.07) W/K = 3.16 W/K (+10%)
- 1 m x .5 m : 1-dim. : 1.43 W/K
  incl. edge eff. : (1.43 + 3x.07) W/K = 1.65 W/K (+16%)
- .5 m x .5 m : 1-dim. : 0.71 W/K
  incl. edge eff. : (0.71 + 2x.07) W/K = 0.86 W/K (+21%)
- .25 m x .25 m : 1-dim. : 0.18 W/K
  incl. edge eff. : (0.18 + 1x.07) W/K = 0.25 W/K (+42%)

It may be concluded that for such a type of glazing, an important partition of the glazing area into small parts has a negative influence on the U-value and therefore must be avoided.

Concerning the calculation two remarks must be made. Firstly there is a three-dimensional heat flow in the corners of the glazing area; it can be shown by calculations that this three-dimensional effect is small compared with the two-dimensional one. Secondly, in practice the double glazing edge is normally covered by the window frame; this will have normally a positive influence on the described edge effect and therefore, the results above are too negative.

The question arises how the edge can be improved. From further calculations but also by some reasoning it can be shown that :

- the filling of the aluminium profile, with insulation or with aluminium itselfs (massive profile) has no influence on the edge effect.
- the replacement of the aluminium (λ = 230 W/mK) by another metal (with a lower thermal conductivity) has a negligible influence on the edge effect; (in the example above, a replacement by stainless steel (λ = 29 W/mK) will cause a drop of the heat loss from 6.06 W/m to only 5.99 W/m). Only a material with a λ-value comparable to the cavity-λ-value will eliminate the edge effect.

2.3. Heat Transfer through Window Frames

2.3.1. Wooden window frame

A wooden window frame with double glazing is shown in figure 4.1.. The data for a two-dimensional calculation are given in the same figure. Isothermals and streamlines are shown in figures 4.2. & 4.3.. To calculate an U_l-value with a practical meaning, equation (2) is applied considering the U-values and widths of window frame and glazing in the second part of it. Note that U_f is simply defined on the basis of width, without shape effect. We find:

U_l = 8.91 / (1 x 20) - (1.35 x 0.046 + 3.19 x 0.1) = 0.06 W/mK.

This U_l-value describes the thermal bridge effect arising from the glazing edge effect (main part) and from the shape of the profile (small part). The obtained U_l-value is lower than the U_l-value of the uncovered glazing edge, obtained above; this indeed shows the positive influence of the covering of the edge by the frame.

The knowledge of the obtained U_l-value is usefull when calculating the U_m-values of windows (glazing + frame). For that purpose the following equation must be applied :

$$U_m = U_g \times A_g + U_f \times A_f + U_l \times l_{edge} \tag{3}$$

Results of calculations for the same frame under the same boundary conditions are given in [6, page 105]; the highest difference for the obtained temperatures and fluxes is lower than 4%, showing the reliability of numerical methods.

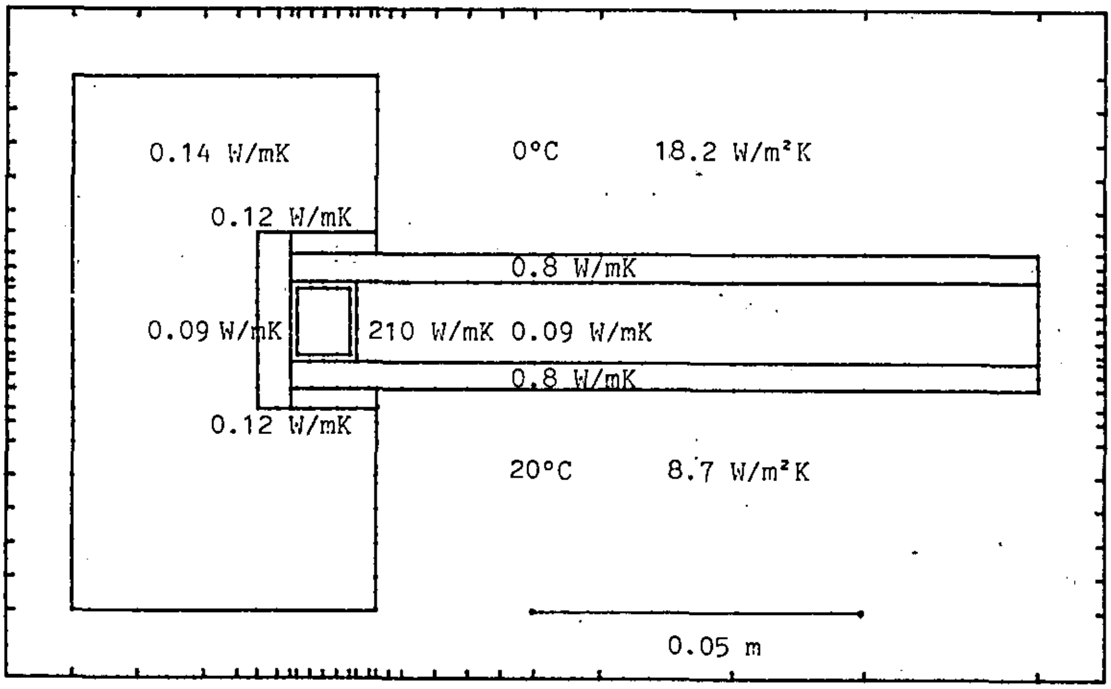

Figure 4.1.: Wooden window frame with double glazing : data

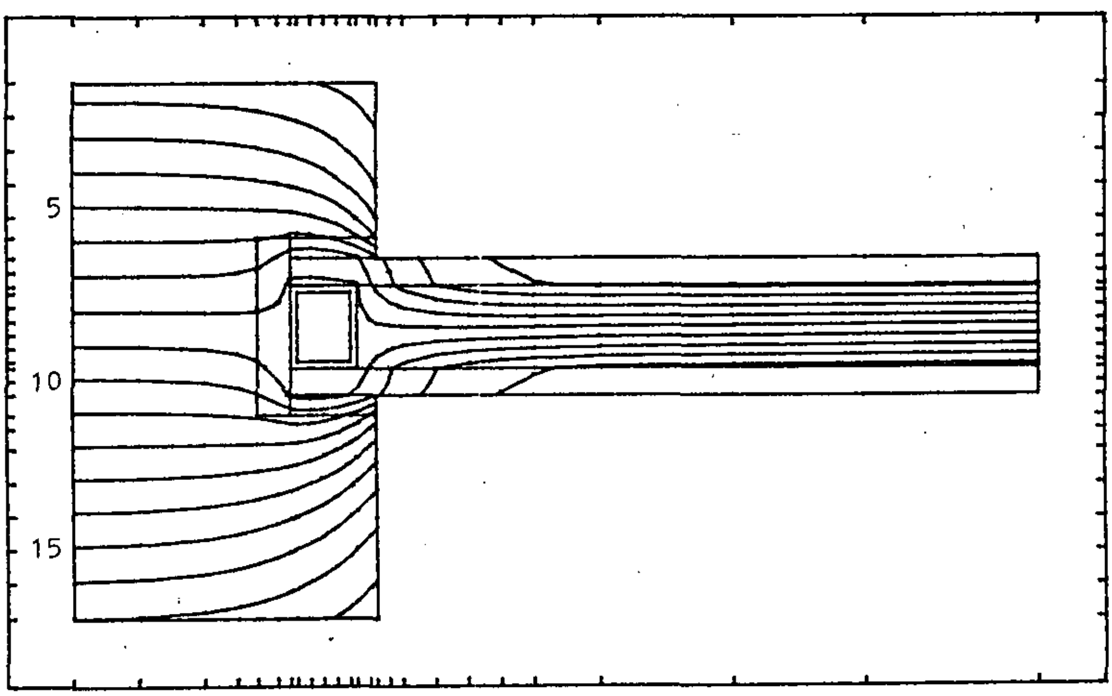

Figure 4.2.: Wooden window frame with double glazing : isothermals

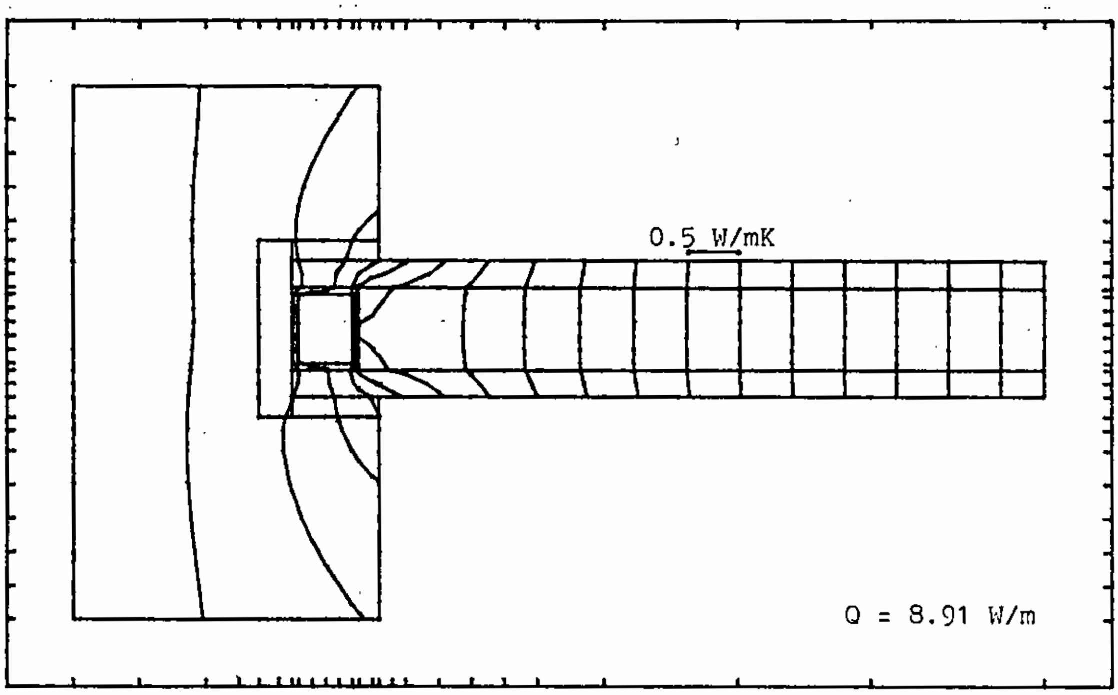

Figure 4.3.: Wooden window frame with double glazing : streamlines

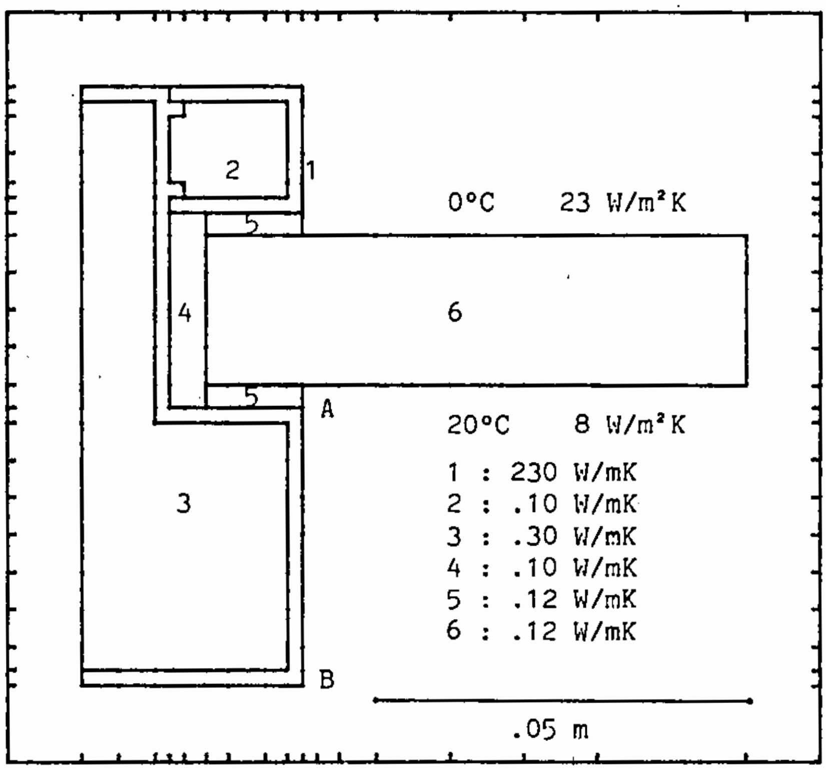

Figure 5.1.: Aluminium frame without thermal barrier : data

2.3.2. Aluminium window frame without thermal barrier

A half aluminium window frame without thermal barrier is shown in figure 5.1.. The double glazing is replaced by an homogeneous material with the same thickness and the same thermal resistance. The data for a two-dimensional calculation are given in the same figure. The obtained isothermals and streamlines are shown in figures 5.2. and 5.3.. The streamlines plot is unclear because all the streamlines go through the small, but extremely well conducting strip of aluminium. The total heat loss amounts 10.8 W/m of which 7.15 W/m goes through the aluminium frame.

The application of equation (2), as in the previous case study, has little sense : a good choice of the U-value of the frame is not obvious because of the expected important short-circuit effect. In this case it is better to calculate the mean thermal transmittance of the profile . Applying equation (1) (Q_{tb} = 7.15 W, A_c = 1 m x .04 m, $\Delta\theta_{ie}$ = 20°C), we find : U_{mf} = 11.9 W/m^{2}K. Because there is no important two-dimensional heat flow in the glazing, we do'nt need to calculate an U_m-value (or a U_l-value) for it. When calculating U_m-values of windows (glazing + frame), the following equation can now be applied :

$$U_m = U_g \times A_g + U_{mf} \times A_f \tag{4}$$

A comparison with formula (3) shows clearly that the U_{mf}-value contains both the one-dimensional and two-dimensional heat flow component. In some cases equation (3) and (4) may be combined (e.g. in this case study if there were a glazing edge effect).

The high value of U_{mf} proceeds from a cooling fin effect affected by the real area of the frame and not by the projected area. Suppose that the frame is 4 cm thicker at the inside (AB = 8 cm), then Q_{tb} = 9.02 W and U_{mf} = 15.0 W/m^{2}K. It is obvious that also the assumed values of the surface coefficients have an important effect on the calculated U_{mf}-values. It may be concluded from this case study, that the mean thermal transmittance of aluminium window frames without thermal barrier is mainly affected by the real area of the frame and by the value of the actual surface heat transfer coefficients.

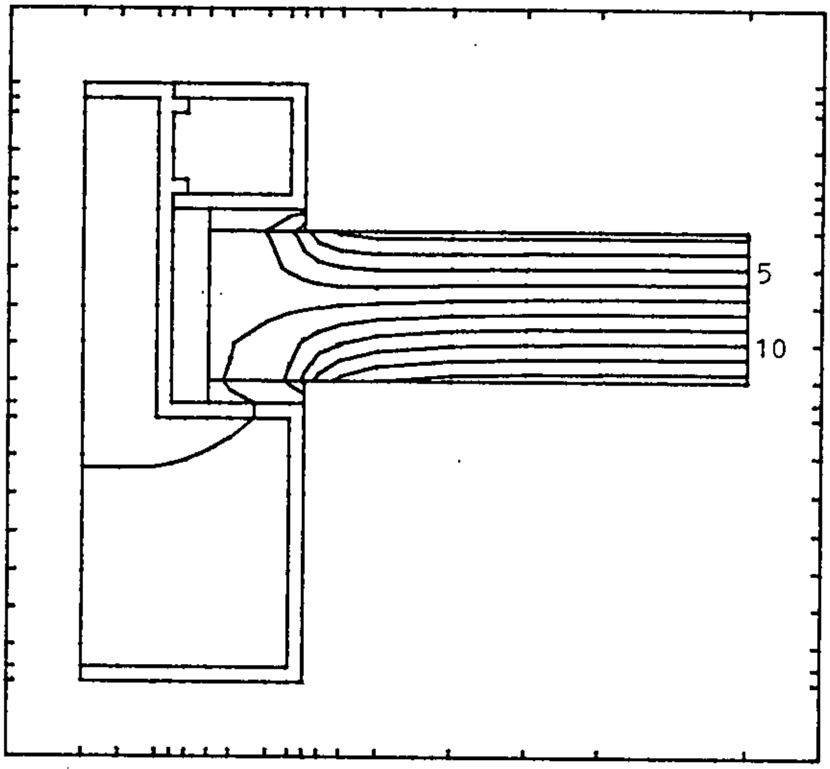

Figure 5.2.: Aluminium frame without thermal barrier : isothermals

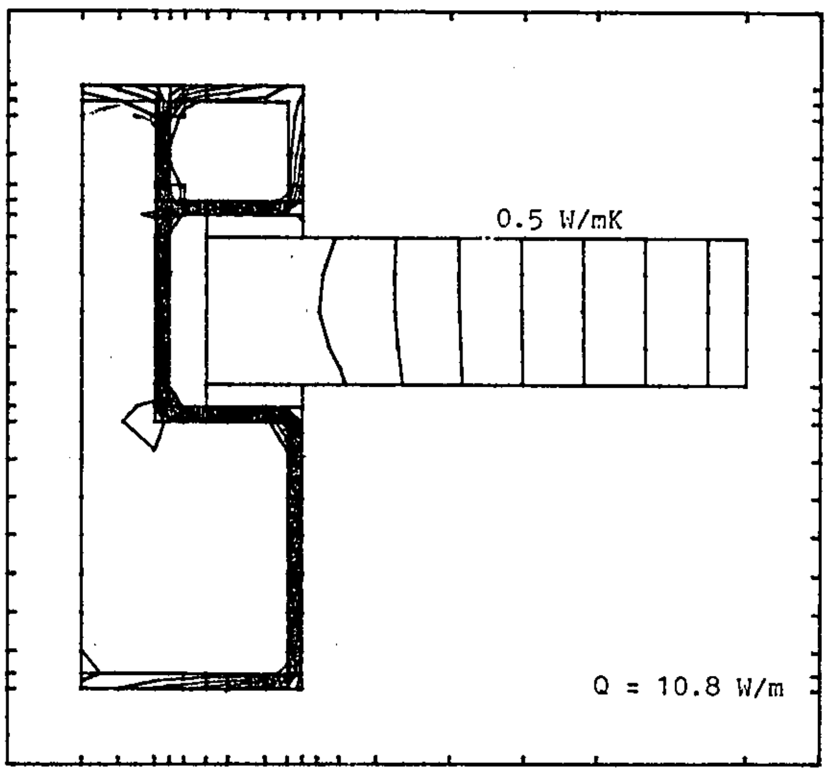

Figure 5.3.: Aluminium frame without thermal barrier : streamlines

2.3.3. Aluminium window frame with thermal barrier

An aluminium frame with thermal barrier is shown in figure 6.1.. In [11] this profile is presented as component in one out of four window examples from which the U-values from hot box tests are compared with calculated and tabulated values. The assumed geometry, again with a homogeneous glazing, and the assumed grid are shown in figure 6.2.. Following thermal conductivities and boundary conditions were assumed:

- λ : aluminium : 230 W/mK pvc : 0.20 W/mK rubber : 0.17 W/mK
  glazing : .15 W/mK cavities in aluminium : 0.10 W/mK
  S1 : 0.041 W/mK S2 : 0.11 W/mK S3, S4 : 0.081 W/mK.
  The λ-values of the cavities S1-S4 have been derived from a thermal resistance R = 0.37 m^2K/W (value for a cavity with on both sides an emissivity of 0.1).*)
- θ_e = 0°C h_e = 23 W/m^2K θ_i = 20°C h_i = 8 W/m^2K.

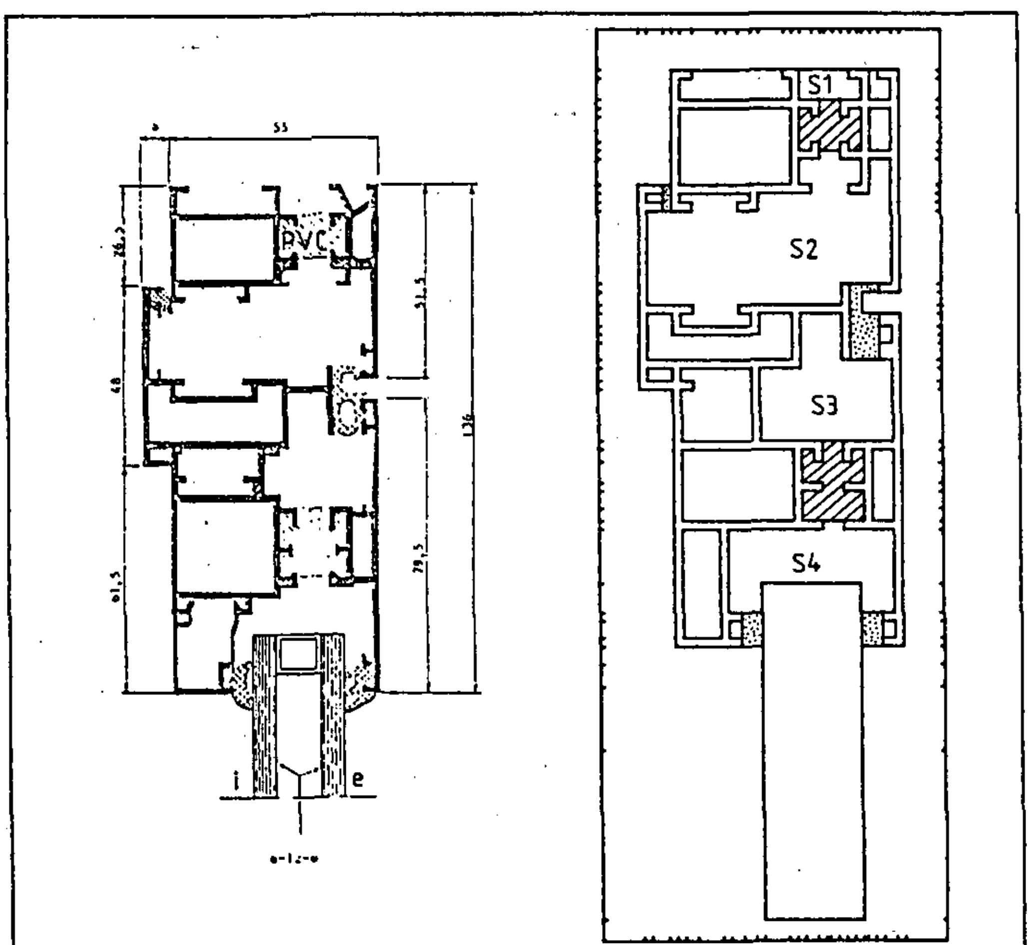

6.1. 6.2.

Figure 6.1. & 6.2.: Aluminium frame with thermal barrier : data

*) Emissivity e = 0.1 is a rough assumption only; for profiles with treated surfaces the emissivity will be higher.

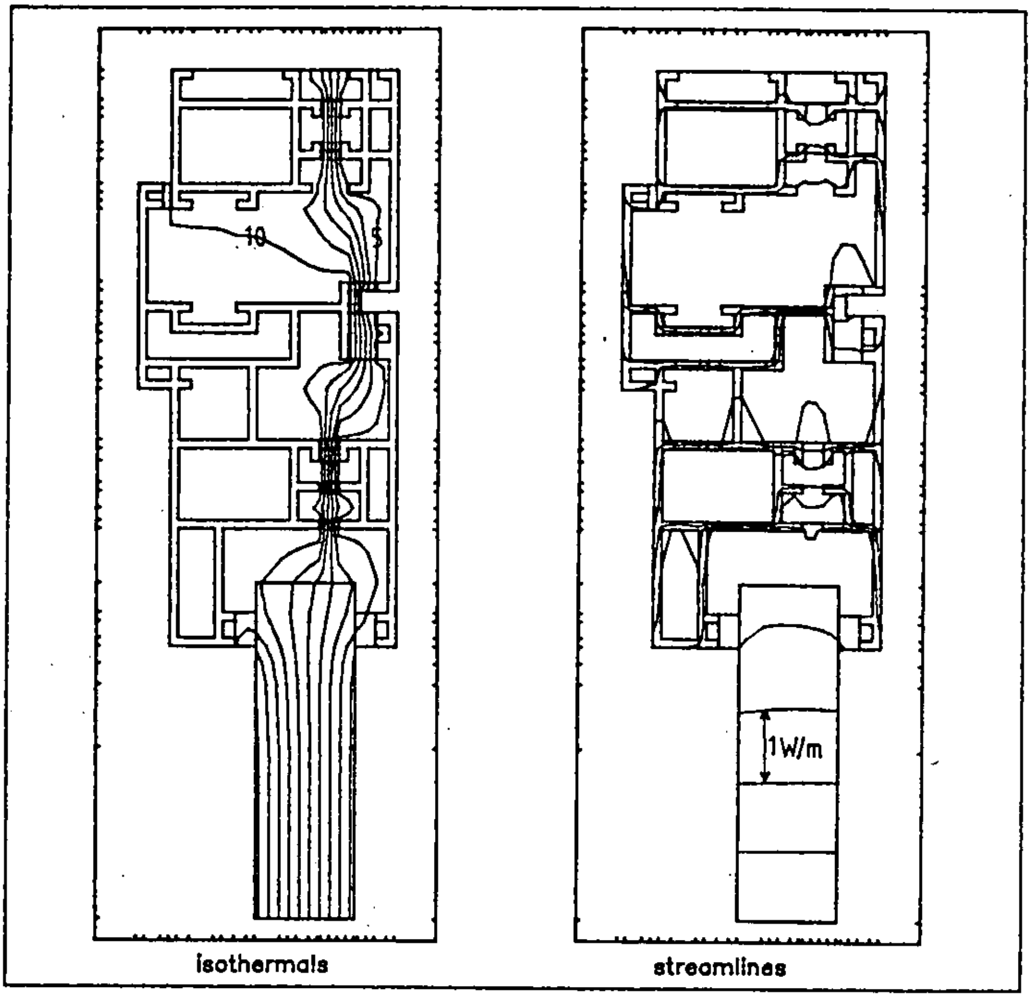

Figure 6.3. & 6.4.: Aluminium frame with thermal barrier : isothermals and streamlines

Figures 6.3. and 6.4. show the calculation results. The heat loss through the frame amounts 14.23 W/m; applying equation (1) we find : $U_{mf} = 5.2\ W/m^2K$. An analysis of the thermal breaks in detail will explain this rather high value.

In figure 7, different shapes of thermal breaks are shown. The left and right axes are supposed to be adiabatic. A temperature difference of 10°C is maintained from surface to surface. The calculated streamlines are presented. From this the mean thermal resistances can be deduced easily. The results show that the thermal resistance of thermal breaks is determined by :

- the shortest distance between the two aluminium parts;
- the contact area between the break and the aluminium (compare the number of streamlines through different thermal breaks in figure 6.4.);
- the λ-value of the break-material (not illustrated, but logical).

By this the U_{mf}-value of aluminium frames with thermal barrier mainly will be affected by the thermal quality of the thermal breaks. (Which however does not means that the the heat flow through the cavities is negligible)

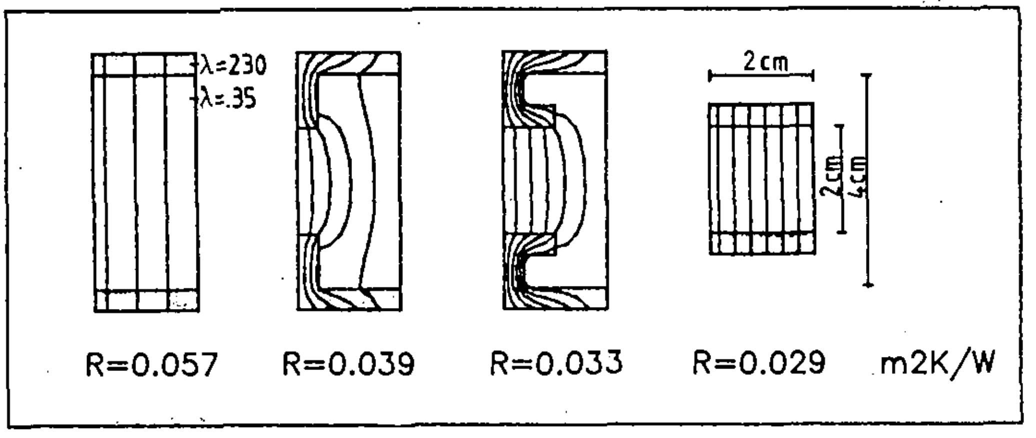

Figure 7.: Thermal resistance of thermal breaks

2.3.4. Plastic window frame with metal part

If plastic window frames contain no metal profiles, the expected mean thermal transmittance will be comparable with that of e.g. wooden frames, because of the comparable thermal conductivities.
If metal profiles are built in (to provide a higher strength) they can cause a short-circuit effect, by which the U_m-value will rise. This is illustrated in figure 8 : a steel section is setted in polyurethane foam. The calculated streamlines and the deduced thermal resistance show that the thermal resistance is substantially determined by the covering thickness of the plastic (and of course by the λ-value of the plastic); the effective thermal resistance is 0.37 m^2K/W, while the thermal resistance without the metal part should be 0.80 m^2K/W.
As an illustration, the analysis of a plastic frame with metal heart is given in figure 9. A U_{mf}-value of 2.14 W/m^2K can be derived. It must be emphasized that this rather low value results from the fact

that, firstly the covering thickness is rather high, and secondly the thermal conductivity of the plastic is rather low (0.05 W/mK). So, in no case the obtained U_{mf}-value may be generalized.

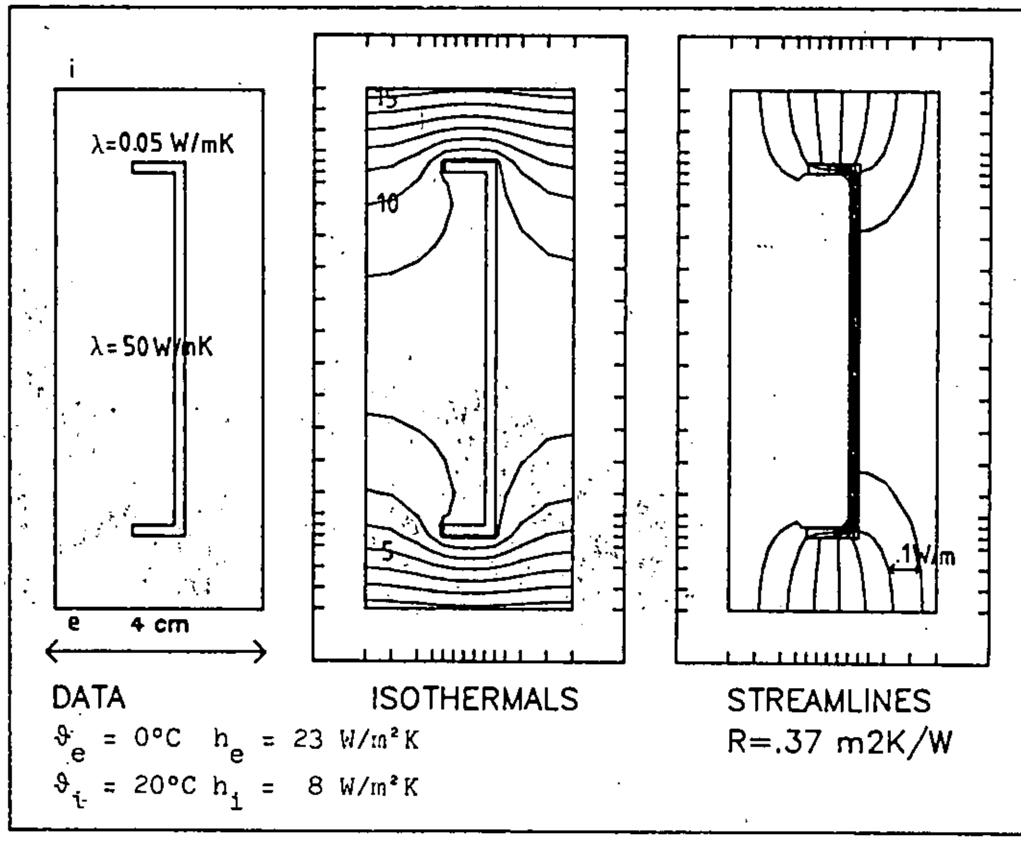

Figure 8.: Steel section in polyurethane frame

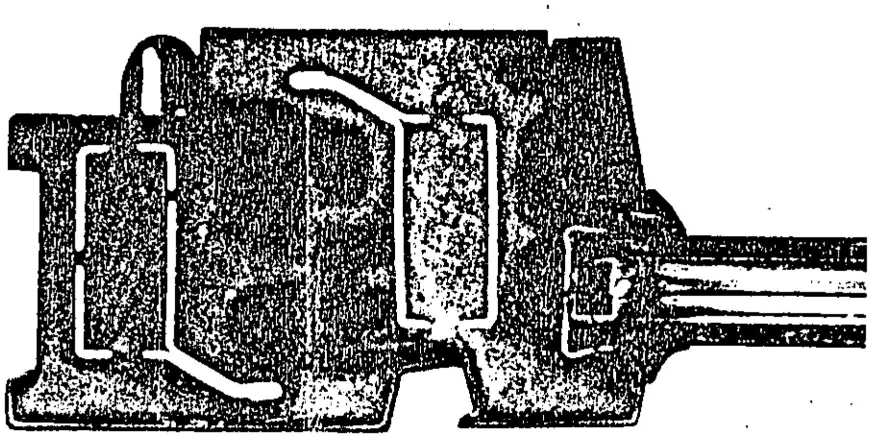

Figure 9.1.: Plastic window frame with metal heart

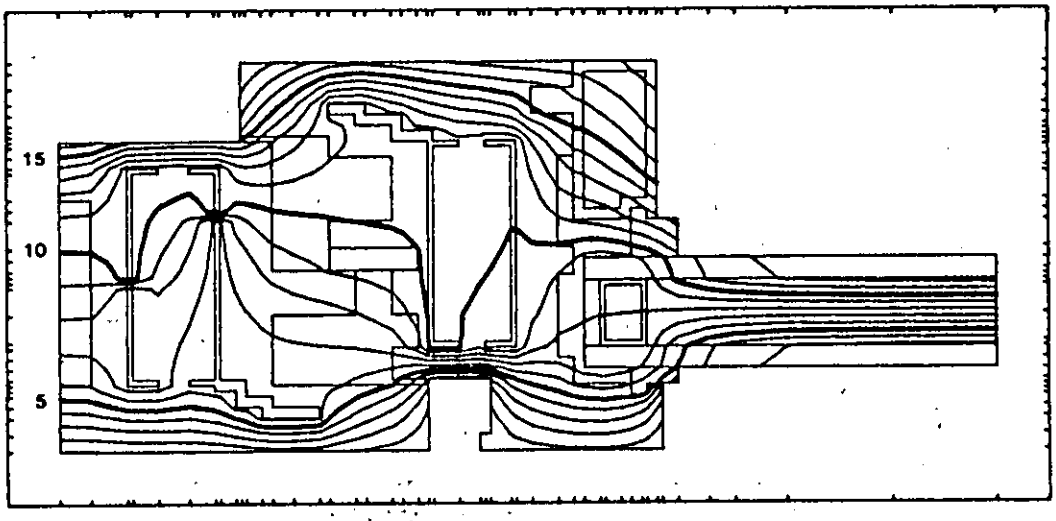

Figure 9.2.: Plastic window frame with metal heart : isothermals

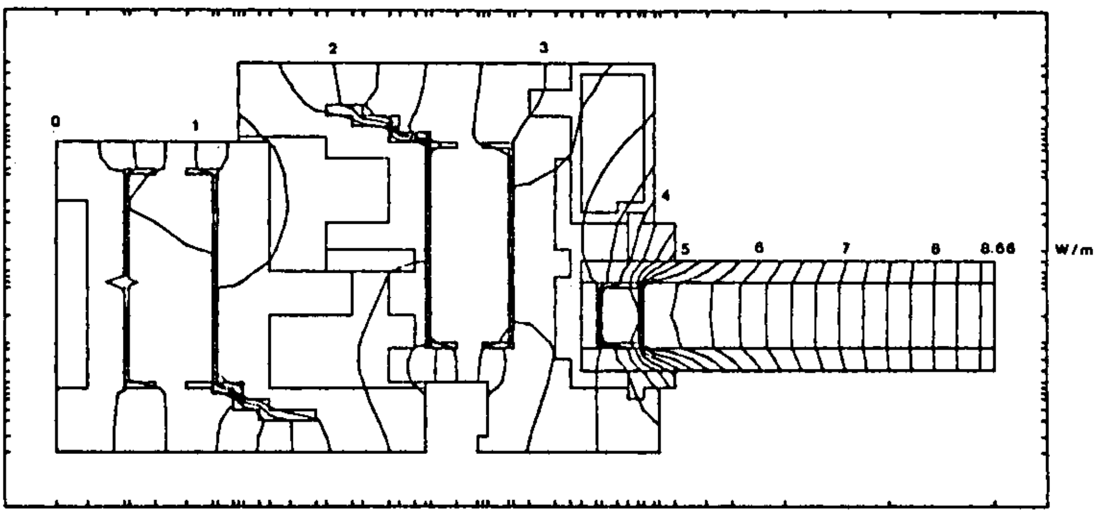

Figure 9.3.: Plastic window frame with metal heart : streamlines

2.4. Heat Transfer through Window Edges

At the connection between a window frame and a wall, important thermal bridges can occur. Figure 10 shows an axonometry of a wooden window frame (outside area .59 m x .54 m) with single glazing, placed in an insulated cavity wall (area 2.4 m x 2.0 m). The contacts between the inner and the outer leaf in the horizontal and the vertical sections near the window, mean a discontinuity in the thermal insulation. For the lintel, the results of a two-dimensional analysis are shown in figure 11. Without further calculation of U_l or U_m, it can be seen from the stream-lines plot that the thermal bridge effect is very important. The results of a three-dimensional analysis are presented by means of an inside axonometric vue of the isothermals on the surfaces of upper and under quadrant (figure 12). The calculated heat loss through the whole wall amounts 106.6 W, which is 35% higher than the one-dimensional result (78.9 W). A complete analysis of this case can be found in [7].

It is out of the scope of this text to discuss the enormeous amount of possible connections between windows and walls, but the case study above shows the opportunity of construction details without thermal bridges. For that purpose a basic rule is to provide the continuity of the thermal insulation. It is clear from the example above that the realization of this continuity, in the first instance has consequences on the wall construction, though it can result in some changes in profile technology. In general, the isolation of a window profile (assuming adiabatic sides), when studying the thermal characteristics of it (cfr. previous chapter), is an allowed supposition. In figure 11 for example, there is only a small heat exchange between the window frame and the wall. On this subject, a study of optimal connections is given in [8]. The position of the window (outside, middle, inside) is studied in [9]. Further considerations on surface heat transfer coefficients and on thermal bridges in general can be found in [10].

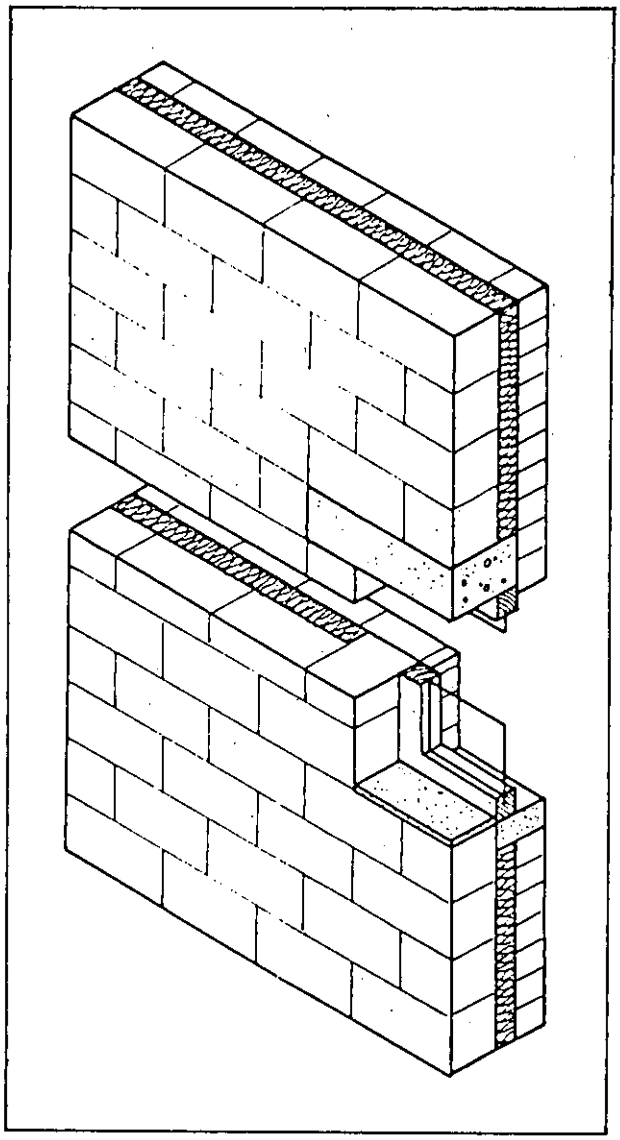

Figure 10.: Window in a cavity wall : axonometry

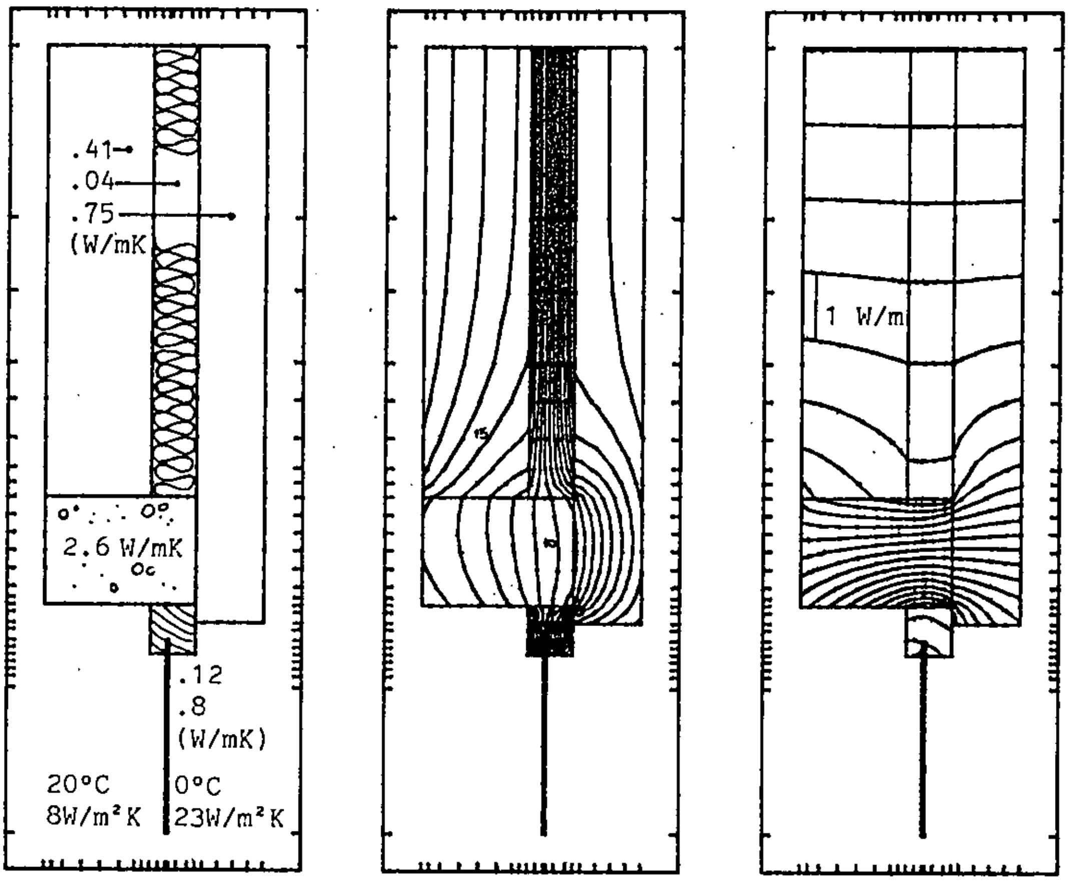

Figure 11.: lintel above a window in an insulated cavity wall : data, isothermals and streamlines

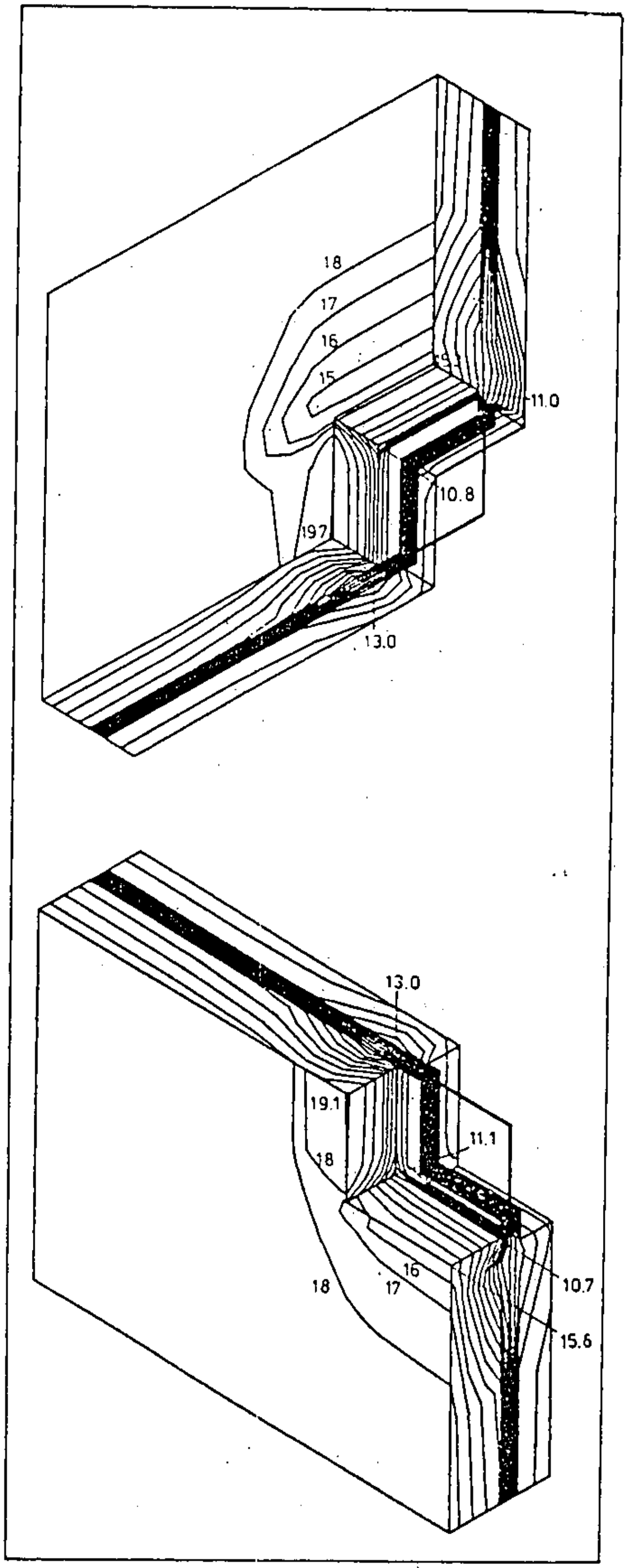

Figure 12.: Isothermals in upper and under quadrant

REFERENCES

[1] Oden, J.T., 'Finite-element analogue of Navier-Stokes equation', Journal of the Engineering Mechanics Division, Proceedings of ASCE, Vol. 96, No. EM4, August 1970

[2] Wolfseher, U., 'Rechnerische Ermittlung mehrdimensionaler Temperaturfelder unter stationären und instationären Bedingungen - Rechnsystem und bauphysikalische Anwendung', Doktorarbeit Universität - Gesamthochschule Essen, 1978

[3] Standaert, P., 'Thermal bridges : a two-dimensional and three-dimensional analysis', Proceedings of 'Thermal performance of the building envelope III, Clearwater Beach, dec. 1985', to be published by ASHRAE

[4] Martin, R.S. and Wilkinson, J.H., 'Symmetric decomposition of positive definite band matrices' in 'Linear Algebra', Ed. Wilkinson, J.H. and Reinsch, C., Springer Verlag, 1971

[5] Kasper, F.J., Müller, R., Rudolphi, R., Wagner, A., 'The thermal transmittance of windows', Bâtiment International / Building Research and Practice, Vol. 11, no. 5, 1983

[6] Jonsson, B., 'Heat transfer through windows', Swedish Council for Building Research, D13 : 1985

[7] Knapen, M. and Standaert,P., 'Experimental research on thermal bridges in different outer-wall systems', CIB-W40, Holzkirchen meeting, september 1985

[8] Kasper, F.J., Müller, R., Rudolphi, R., Wagner, A., 'Zum wärmeschutztechnischen Verhalten des Anschlussbereichs Fenster - Wand', Haustechnik, Bauphysik, Umwelttechnik 105, Heft 4, 1985

[9] Cziesielski, E., 'Thermal bridges at the joints between walls and window frames', Proceedings Windows in Building Design and Maintenance, Göteborg, Sweden, 13-15 june 1984

[10] Standaert, P., 'Twee- en driedimensionale warmteoverdracht : numerieke methoden, experimentele studie en bouwfysische toepassingen', doctoral dissertation, Katholieke Universiteit Leuven, 1984

[11] Dijk van, H.A.L.(ed.) 'Thermal transmission through windows. Selected examples to illustrate the need for a more standardized approach.' IEA Annex XII report, 1987.

3.3. Measurement techniques

3.3.1. Laboratory measurements of thermal radiation properties

K.Th. Knorr
TNO Institute of Applied Physics
P.O. Box 155
2600 AD DELFT
THE NETHERLANDS

LIST OF CONTENTS

LIST OF SYMBOLS

λ	Wavelength in μm
$\rho^{\perp}(\lambda)$	The near-normal specular spectral reflectance, being the specular reflected fraction of the radiation of wavelength λ, incidenting near to the normal axis.
$\rho\ (\lambda)$	The near normal spectral hemispherical reflectance being the in the hemisphere reflected fraction of radiation of wavelength λ, incidenting near to the normal axis.
$\varepsilon\ (\phi_e, \theta)$	The directional total emittance being the ratio of the total (all wavelengths) emitted radiant intensity in the direction ϕ_e of a surface at temperature θ (K) to the radiant intensity emitted by a black body at the same temperature and in the same direction ϕ_e.
$\varepsilon\ (T)$	The hemispherical total emittance being the ratio of the total (all wavelengths) emittance in the hemisphere by a surface at temperature θ (K) and the total emittance in the hemisphere of a black body at the same temperature.
σ	Stephan Bolzmann constant $5{,}67 \times 10^{-8}$ W/m^2K^4.
A	Area in m^2.
P_{el}	The net electric power for heating in W.
U_{sd}	The detector response for the reflected radiation by the sample and incidenting on the detector in mV.
U_{Au}	The detector response for reflected radiation from the reference sample (gold freshly evaporated on an optically smooth glass substrate) incidenting on the detector mV.

1. INTRODUCTION

In chapter 3.2.1 the infra-red properties of windows are described. One can use the various properties for different purposes:

- to identify the materials e.g. by means of the spectral absorption bands;
- to control the manufacturing process for instance by measuring the reflection and/or transmission at certain wave lengths;
- to qualify products such as coated glass;
- to calculate the heat balance of windows.

In this chapter the principles of a number of relevant measurement techniques are described for use in the laboratory. That means that a relatively high accuracy is required. The descriptions have mainly been taken from [1] in which more details about calibration accuracies can be found.

2. SPECTRAL MEASUREMENTS

Most of the spectral IR-measurement techniques have been derived from the spectrophotometric methods in the u.v. and visible region.

a. Transmission through infra-red absorbing materials

In figure 1 a typical i.r.-spectrophotometer is shown, used for the analysis of the transmission through i.r.-absorbing materials. It is a double beam meter with two gratings for the wave length region of 2.5 μm up to 40 μm.

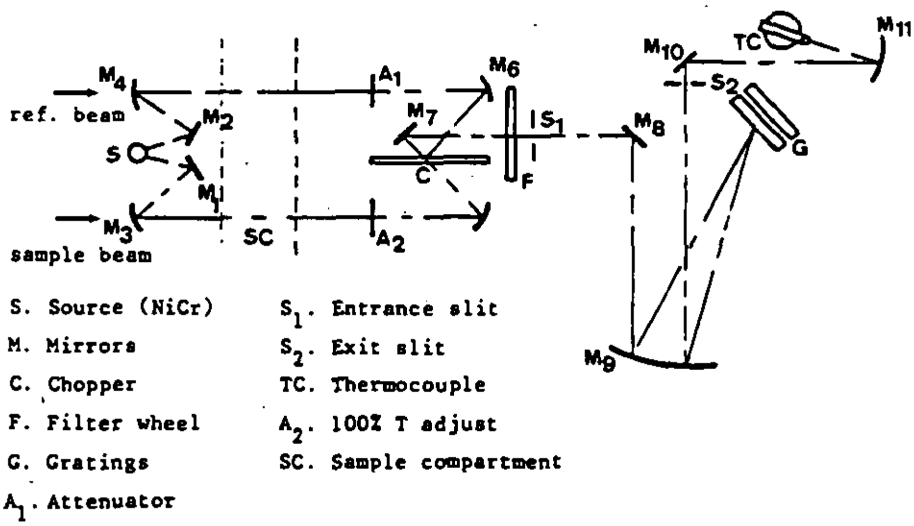

Figure 1: Optical diagram of a double beam infra-red spectrophotometer.

b. Spectral specular infra-red reflectance

To identify the types of coating and to measure the layer thickness, the spectral specular reflectance can be measured with an I.R.-spectrophotometer as mentioned under a. and a special attachment as shown in figure 2.

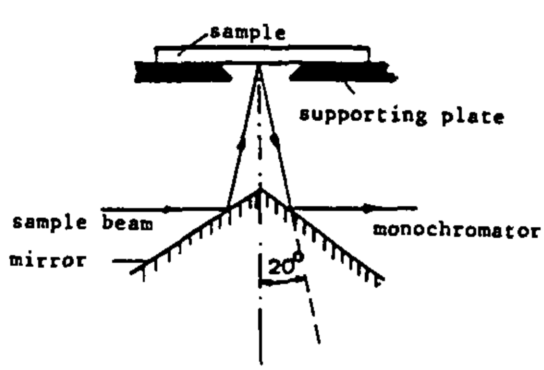

Figure 2: Specular reflecting unit for use with an infra-red spectrophotometer.

The angle of incidence is fixed at 20°. Only the specular component of the reflected beam comes into the monochromator and will be detected.
The principle of measurement is as follows: first a sample with gold freshly evaporated on an optically smooth glass substrate is laid on the supporting plate (figure 2). The scanning over the whole wave length range occurs automatically. Then the gold sample is replaced by the sample to be investigated, followed by a second scanning. By dividing the two detector responses from the recorder and multiplying by the average near-normal specular reflectance of gold (≈ 0.975), we obtain the near-normal specular reflectance of the sample for each wave length.

$$\rho_{\perp,s} = \frac{U_{ds}}{U_{Au}} \cdot 0.975$$

The temperature dependency of the infra-red reflectance of a selective surface is sometimes desired; therefore, the sample can be attached to a heating unit.

c. Near-normal hemispherical spectral reflectance

Especially for non-smooth surfaces it is of importance to measure the hemispherical spectral reflectance in the infra-red region. In figure 3 a schematic view of an apparatus for this purpose is given. The apparatus is based on the principle of an integrating sphere as also used in combination with spectrophotometer.

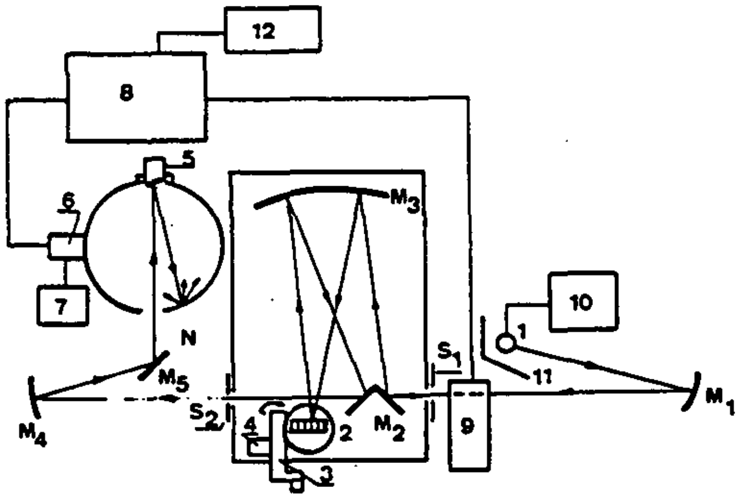

M. Mirror
S_1. Entrance slit
S_2. Exit slit
1. Globar source
2. Grating
3. Wavelength drum (wheel)
4. Wavelength dial
5. Sample holder with sample
6. Pyro-electric detector + preampl.
7. Voltage supply
8. lock-in amplifier
9. chopper, 20 Hz
10. Regulated power supply
11. Screen
12. Recorder or digital voltmeter

Figure 3: Schematic view of an integrating sphere reflectometer + spectrometer for the infrared region.

In this case a highly diffuse and highly reflecting inner surface of the sphere is obtained by a vacuum evaporated gold layer of about 0.1 μm thickness.

The inner diameter of the aluminium sphere is 0.10 m. There are three openings in the sphere, the entrance port, the detector port and the sample port.

The sample is positioned in such a way that the normal makes a fixed angle of 20° with the incident beam.

The sample holder contains a heating element, surrounded by a water cooled jacket. It is possible to heat the sample surfaces up to 400 °C. A freshly evaporated gold coating on a smooth glass substrate is measured first.

The average near-normal hemispherical reflectance of gold is assumed to be 0.075 ± 0.005. Then the gold sample is replaced by the sample under investigation and again the detector response is recorded.
Out of the equation:

$$\rho_{\perp}(\lambda) = \frac{U_{ds}}{U_{Au}} \cdot 0.975,$$

the near-normal hemispherical reflectance $\rho_{\perp}(\lambda)$ is calculated.
According to the Kirchhoff's law for opaque samples, the normal spectral emittance $(\varepsilon_{\perp}(\lambda)$ can be derived from $\rho_{\perp}(\lambda)$ with:

$$\varepsilon_{\perp}(\lambda) = 1 - \rho_{\perp}(\lambda)$$

d. Attenuated total reflectance method

This method has been developed as a means to identify multi-layer paints and plastic films with a weak absorptance in the IR-range [3], [4].
The most important component of the ATR-attachment is a hemi-cylindrical crystal or prism with a high refractive index. On the flat side the test sample is applied. Total reflection is occuring with an angle of incidence on the interface greater than the critical angle in the wave length region where the sample has no absorption, while in the absorption band regions the reflection is attenuated.

3. MEASURING TECHNIQUES FOR OVERALL PROPERTIES IN THE INFRA-RED WAVE LENGTH REGION

a. Measurement of the directional total emittance

a.1 For quick measurements of the total emittance at different emitting angles and at different temperatures $\varepsilon(\phi_e, T)$, Irving et al [2] designed a very suitable and relatively accurate apparatus. This method has the advantage that the hemiapherical total emittance $\varepsilon(T)$ can be obtained by the integration of the $\varepsilon(\phi_e, T)$ over all emitting angles.
A diagram of the equipment is shown in figure 4.

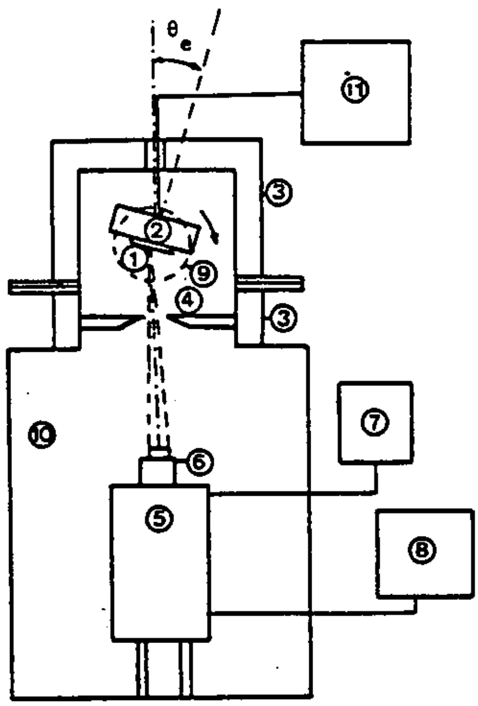

θ_e. Emitting angle
1. Sample
2. Heating unit (canthal wire 14 Ω) and Cromel-Alumel thermocouples
3. Water cooled jacket, 5°C.
4. Water cooled diaphragm, Ø 0.010 m
5. Bolometer + electronics
6. Detector head with Ge-lens
7. Voltage supply
8. Galvanometer
9. Rotating disc with knob and graduating disc, outside the jacket
10. Outer housing filled with dry air
11. Temperature controller and recorder

Figure 4: Schematic view of the equipment for measuring the directional total emittance.

The sample is attached with a heat transfer compound or screwed to a heating box, which ia turnable round an axis along the sample surface and through the centre. The angle is Θ_e adjustable from outside with a rotating disc from 15 ° - 75 °. The temperature of the upper surface of the heating box can be controlled from about 60 °C to 400 °C.

The heating box is surrounded by a black-painted cooled jacket, firstly, in order to reduce reflections from the wall to the sample and, secondly, to keep the ambient temperature constant. The jacket is cooled with water to 5 °C. Also, the upper part of the outer housing of the detector of the diaphragm are cooled to the same temperature.

To avoid condensation on the cooled wall, and to reduce CO_2 or water vapour absorption, dry air (dried with silicagel) is blown into the outer big box.

The detector box contains a bolometer, electronic chopper and amplifier. The output signal is a DC-current (0 - 2.10^{-2} A) and is led to a galvanometer. The detector head is exchangable; it contains in our situation a Ge-lens with a.r.-coating. With this lens only a spot of 4.10^{-3} m of the sample surface, in perpendicular position (figure 5), is "seen" by the detector surface.

The spectral sensitivity of the detector is from 2 µm to 20 µm.

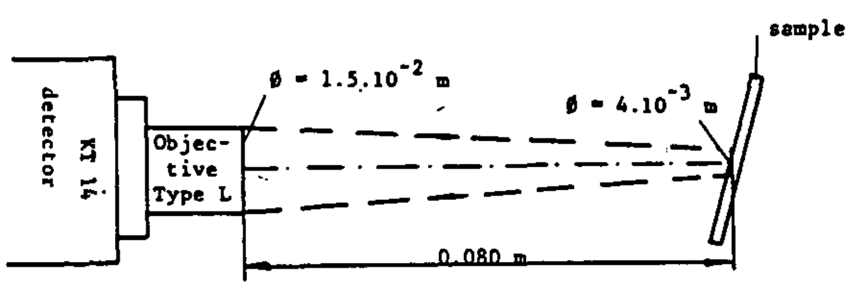

Figure 5: Envelope of the radiation beam from the sample surface reaching the detector head.

Equation:

If it is assumed that the inner wall of the cooling jacket with temperature T (K) is black, the total energy flux density G coming from the direction of the sample surface of temperature T_s(K) received by the detector surface is given by:

$$G = F\sigma \left[\varepsilon\ (\Theta_e . T_s)\ T_s^4 + \rho\ (\Theta_e . T_s)\ T_w^4 \right]$$

in which F is the view factor between the sample area and the detector area, σ is the Stephan-Boltzmann constant, $\varepsilon(\Theta_e,\ T_s)$ is the directional total emittance of the sample with Θ_e as the angle between the normal on the centre of the sample and the connecting line from the centre of the detector area to the centre of the sample, $\rho(\Theta_e,\ T_s)$ is the hemispherical directional total reflectance of the sample with temperature T_s, and T_w is the temperature of the cooled jacket. If the detector is calibrated with a black body radiator, then the energy flux density from the sample falling on the detector, as seen by the detector as coming from a black surface with temperature T_x, the emitted energy flux density is:

$$G' = F\ \sigma\ T_x^4$$

on the basis of this idea, G = G', so that

$$T_x^4 = \varepsilon(\Theta_e,\ T_s)T_s^4 + \rho(\Theta_e,\ T_s)T_w^4.$$

By taking

$\varepsilon(\Theta_e . T_s) = 1 - \rho(\Theta_e,\ T_s)$, we can write $\varepsilon\ (\Theta_e,\ T_s)$ as:

$$\varepsilon(\Theta_e,\ T_s) = \frac{T_x^4 - T_w^4}{T_s^4 - T_w^4} .$$

This will be the basic equation for the measurements if we assume that the detector response is (linearly) proportional to the intensity of the radiation received.

The detector has to be calibrated for instance with an oven in which the inner wall is controlled and is uniform all over the wall.

a.2 Lohrengel [5] describes an accurate method to measure the directional total emittance. Herewith the radiation from a heated sample is compared with the radiation from a well-defined black body at the same temperature. The detector, the sample and the black body are placed in vacuum, each of them surrounded by a black radiation shield. The surface temperature of the sample is measured indirectly using the heat conductivity of the sample.

b. Measurement of the hemispherical total emittance

Besides the possibility of calculating the hemispherical total emittance by integrating the measured directional total values over all emitting angles it can be desirable to have an apparatus to measure the hemispherical total emittance directly.
In figure 6 the principle of such an apparatus is given. The apparatus is based on a caloric method.

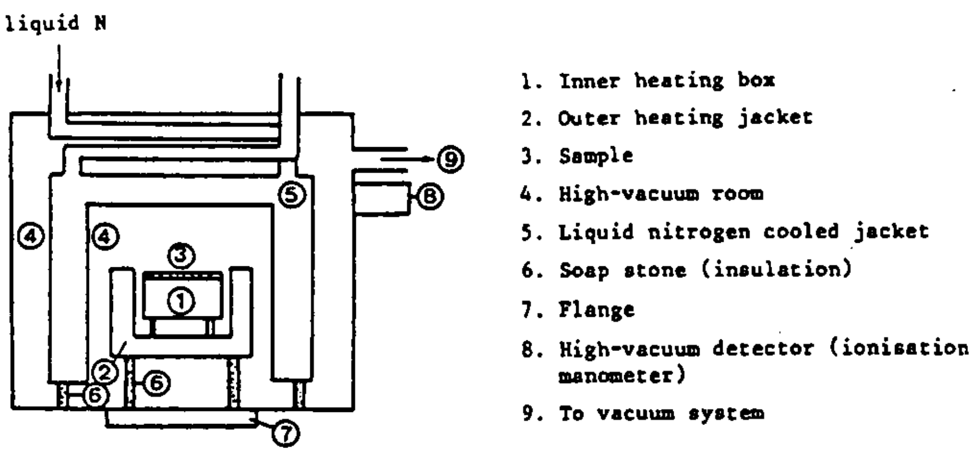

Figure 6: Diagram of the vacuum chamber with sample heater, heating jacket and cooling jacket.

The sample is attached by a heat transfer compound to the small inner heating box, which is electrically heated. The input power is measured. A second heating jacket partly surrounds the inner box and works as a shield in order to prevent radiation losses downwards and sideways. The two heating elements are fed separately.
Free convection is suppressed by evacuating the whole vacuum cylinder to about $1.33.10^{-3}$ Pa. The sample surface is, at the topside, directly surrounded by a jacket cooled with liquid nitrogen (T_W = 77.3 K), so that effective radiating can take place. The inner wall of the cooling jacket is coated with black copper oxide supplied by chemical immersion. The hemispherical total emittance of this coating, as measured with the directional apparatus is 0.67 at 80 °C.
The approximated equation to be used to determine the hemispherical total emittance of the sample with temperature T_S(K) is:

$$\varepsilon(T_s) \doteq \frac{P_{el}}{\sigma\, A_s(T_s^4 - T_w^4) - P_{el}\, \frac{A_s}{A_w}\,(1/\varepsilon_w - 1)}$$

in which P_{el} is the net electric power (W), A_S is the sample area (m^2), A_W is the area (m^2) of the inner wall of the cooling jacket as "seen" by the sample area, T_W is the temperature (K) of the cooled wall, ε_W is the hemispherical total emittance of the cooled wall and σ is the Stephan-Boltzman constant.
This equation is based on the radiant exchange between two gray bodies, if one body (here the sample) is enclosed by the other (here the cooled jacket) and if $A_S << A_W$ as is fulfilled in our case.

REFERENCES

[1] M. van der Leij, 'Spectral selective surfaces for the thermal conversion of solar energy', dissertation Technical University Delft, the Netherlands; Delft University Press, 1979.

[2] Irving, T.F. et al, Solar Energy, 2 (1958) 13.

[3] Karl Heinz Reichert, Anwendung der ATR-Methode zur infrarot spektroskopischen Untersuchung van Mehrschicht Anstrichfilmen; Farbe und Lack, nr. 1, 1966.

[4] Shimadzu Seisakusho Ltd, Koyoto Japan; Attenuated Total Reflectance Apparatus.

[5] J. Lohrengel; Temperatur- und Winkelabhängigkeit des Gesamte missiongrades slechter Wärmeleiter im Temperatur bereich von -60 °C bis 250 °C; dissertation Technical University, Aachen, 1969.

3.3.2. Test methods for steady-state thermal transmission

H. Erhorn
R. Stricker
M. Szerman

Fraunhofer Institute of Building Physics
Department of Heat and Climate
(Director: Prof.Dr.-Ing. habil K.A. Gertis)
Nobelstrasse 12
D-7000 STUTTGART 80
FEDERAL REPUBLIC OF GERMANY

LIST OF CONTENTS CTD

*) This chapter is based on a detailed contribution by H.A.L. van Dijk (TPD, the Netherlands).

LIST OF SYMBOLS

R	(areal) thermal resistance	$[m^2K/W]$
ϕ	heat flow rate	$[W]$
T	thermodynamic temperature	$[K]$
A	area	$[m^2]$
n	number of test specimen	$[-]$
q	(areal) density of heat flow rate	$[W/m^2]$
h	surface film coefficient	$[W/m^2K]$
U	(areal) thermal transmittance	$[W/m^2K]$

Subscripts

T	test specimen
W	window
S	surface
F	frame
G	glazing
h	hot side of specimen
c	cold side of specimen
i	interior
e	exterior
a	air
SK	sum of surface area of hot box walls ("skin")
en	environment
tot	total
pr	projected

1. INTRODUCTION

For the determination of thermal transmittance, U-value, several test methods may be applied which are based on different types of boundary conditions. The objective of this chapter is to compile how the countries participating in Annex XII handle the subject. Problem areas are listed to give a survey of the present state of the art. Additional information in relation to this area is available from chapter 3.3.3. and the Annex XII report: Thermal Transmission Through Windows; Selected Examples to Illustrate the Need for a More Standardized Approach [3].

2. DETERMINATION OF THERMAL TRANSMITTANCE (U-VALUE)

The thermal transmittance [U] can be determined directly by measuring the environmental temperatures on the hot [$T_{en,h}$] and cold [$T_{en,c}$] side of a test specimen in combination with the recorded heat flux passing through the specimen [q]. The measurements can only be effected in a hot box test apparatus.

Compiled to an equation:

$$U = q / (T_{en,h} - T_{en,c}) .$$

Applying the other method, the thermal resistance [R] is obtained at first by measuring the surface temperatures of the test specimen on the hot [$T_{T,S,h}$] and cold [$T_{T,S,c}$] side in combination with the recorded heat flux passing the specimen [q]. Therefore, both hot plate and hot box apparatus can be applied.

Compiled to an equation:

$$R = (T_{T,S,h} - T_{T,S,c}) / q$$

Based on measuring the thermal resistance [R], the determination of the thermal transmittance, U-value [U], will be accomplished by means of fixed surface coefficients [h_h, h_c] on the hot and cold surfaces of the test specimen.

Compiled to an equation:

$$U = 1 / (R + h_h^{-1} + h_c^{-1})$$

Standardized values of surface film coefficients are the same in Belgium (NBN B62-002) and the Netherlands (NEN 1068), inside/outside = 8/23 [$W/(m^2 \cdot K)$], whereas in Norway (NS 3031, 3 utg. Oct 86) and Germany (DIN 4108), inside/outside = 7.69/25 [$W/(m^2 \cdot K)$] is specified.
In the USA, surface film coefficients are not standardized (see p. 12). Measured values can be obtained by simultaneously recording surface and environmental temperatures on both sides of a test specimen. In the latter case, however, the results are considerably influenced by the configuration of the actual test apparatus. In this case, comparability of test results will only be possible if measurements have been carried out on the same test apparatus (see section 6.1 b: Problem Areas).

3. COMPILATION OF APPLIED TEST METHODS

Essentially, there are four measurement procedures in common practice concerning the testing of window systems, using two types of test apparatus, namely

- guarded hot plate
- guarded/calibrated hot box.

In Table 1, the various test procedures are compiled giving the possible combinations of measurement specification and test apparatus.

Table 1: Different Test Procedures

	apparatus	quantity measured	heat flux measured	temperatures measured
1 a.	hot plate	thermal resistance (parallel flat surfaces only)	heat input on hot side ("calorimetric")	hot and cold surfaces
1 b.	idem	idem	heat flux sensors	idem
2 a.	hot box	thermal resistance or U-value	heat input on hot side ("calorimetric") (either guarded or calibrated)	hot and cold surfaces or hot and cold ambient temperature
2 b.	idem	idem	heat flux sensors on surface	idem

The hot box method is used for testing both the complete window system and its individual components. Thermal resistance of glazing units normally will be determined by the guarded hot plate method.

4. PRINCIPLES OF MEASUREMENT AND DETERMINATION PROCEDURES

4.1 Guarded Hot Plate

a. Heat flux measured by way of heat input on hot side ("calorimetric")

The thermal resistance [R] of a plate-shaped test specimen will be determined by means of three parameters measured under constant conditions:

- A unidirectional constant heat flow [ϕ] passing a sample which is placed between a hot and a cold plate. A unidirectional constant heat flow is ensured by a guard section surrounding test specimen and hot plate separated by a narrow gap. The guard section consists of a ring heater and guard material to avoid, resp. to minimize, sideward heat losses.

- Temperature difference of the specimen average surface temperatures on hot and cold side [$T_{T,S,h} - T_{T,S,c}$].

- Metering area, i.e. surface area of the test specimen contacting the hot and cold plate [A].

Compiled to an equation:

$$R = n \cdot A\ (T_{T,S,h} - T_{T,S,c}) / \phi$$

Using: two specimen apparatus n = 2
one specimen apparatus n = 1

In Figure 1, a schematic drawing of a guarded two specimen hot plate apparatus is shown. The heat flow is measured by average power supplied to the central section of the heating unit (hot plate) [ϕ].

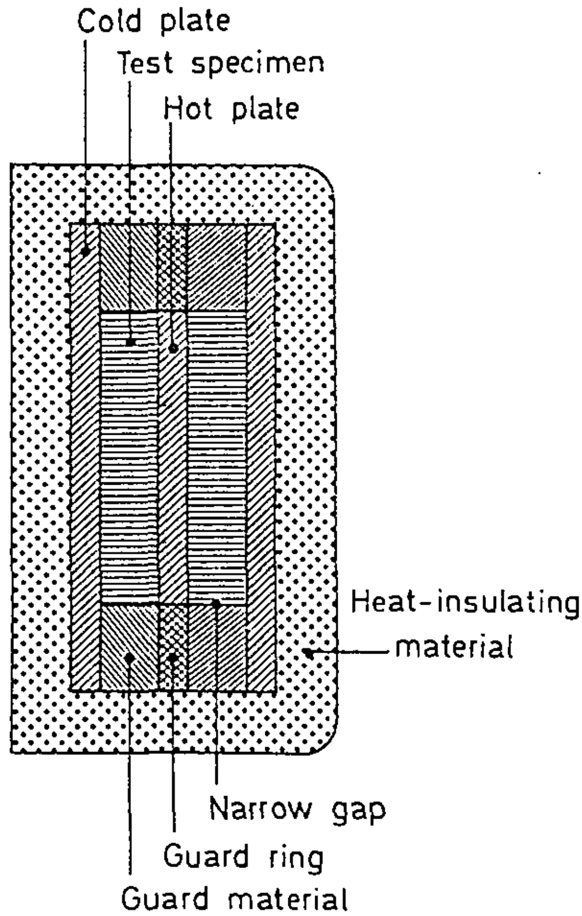

Figure 1: Schematic drawing of a guarded two specimen hot plate apparatus

b. Heat flux measured by way of heat flux sensors on surface

Two parameters have to be measured under constant conditions to be able to determine the thermal resistance [R] of a test specimen:

- The density of the unidirectional constant heat flow [q] passing a sample can be recorded directly by heat flux sensors which are placed on the test specimen in such a way that a representative heat transfer area is sized.
- Temperature difference of the specimen average surface temperatures on hot and cold side $[T_{T,S,h} - T_{T,S,c}]$.

  Compiled to an equation:

$$R = (T_{T,S,h} - T_{T,S,c}) / q$$

4.2 Guarded/Calibrated Hot Box

The determination of the areal thermal resistance [R] is based on the following conditions:

A constant quantity of heat passes a sample that is mounted in a partition wall between two rooms with different air, resp. environmental temperatures, the areal density of the heat flow rate [q] not being recorded directly, but by means of the heat supply into a hot box which is mounted to the hot side of the test specimen (see Figure 2). A heat source within the hot box ensures temperature control.

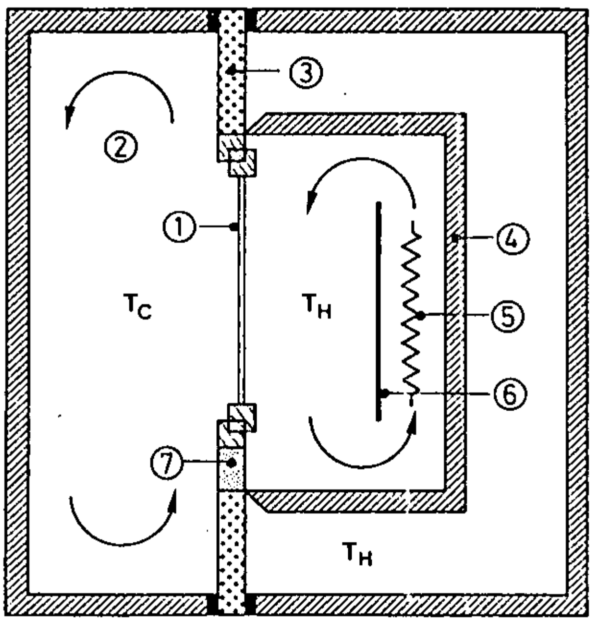

Figure 2: Schematic drawing of a measuring equipment on the basis of a guarded hot box

where: T_H air temperature within hot box and outside hot box walls
T_C air temperature on the cold side of test specimen

1 test specimen
2 cold box
3 thermal insulation
4 hot box
5 electric heating
6 screening device
7 mask (=insulating material, thermal resistance known)

Guarded Hot Box

Provided that the surface temperatures of both sides of the walls forming the hot box will be regulated in such a way that the heat transfer through the hot box walls is negligible, the heat quantity produced within the box [ϕ] is guaranteed to pass only areas of the test specimen [A] and the surrounding mask. After correction for the flow through the mask, the density of the heat flow rate through the test specimen [q] may then be obtained by way of

$$q = \phi/A$$

and the thermal resistance [R] by way of

$$R = (T_{T,S,h} - T_{T,S,c}) / q$$

or, if the environmental temperatures are recorded on both sides of the test specimen [$T_{en,h}$, $T_{en,c}$], the thermal transmittance [U] can be determined directly by

$$U = q / (T_{en,h} - T_{en,c})$$

Calibrated Hot Box

If the surface temperature differences of the hot box walls [$T_{SK,i} - T_{SK,e}$] are not negligible, it is necessary to subtract the skin losses [ϕ_{SK}] from the heat quantity produced in the hot box [ϕ] in order to get the net heat quantity passing a window system under test. A hot box skin loss coefficient [$q_{SK} \cdot A_{SK}$] can be derived when inserting a homogeneous test specimen with known thermal conductivity in place of a test window.

Compiled to equations:

$$\phi_{SK} = q_{SK} \cdot A_{SK} (T_{SK,i} - T_{SK,e})$$

$$q = (\phi - \phi_{SK}) / A$$

and again:

$$R = (T_{T,S,h} - T_{T,S,c}) / q$$

Hot Box Supplied with Heat Flux Sensors

Instead of measuring the heat supply into the hot box, the density of the heat flow [q] passing a test specimen may also be recorded directly by means of heat flux sensors which are placed on the specimen surface in representative heat transfer areas.
Again, considering the difference in the specimen average surface temperatures on the hot and cold side $[T_{T,S,h} - T_{T,S,c}]$, leads to the equation

$$R = (T_{T,S,h} - T_{T,S,c}) / q$$

In Figure 3, a schematic drawing of a measuring arrangement on the basis of heat flux sensors is presented.

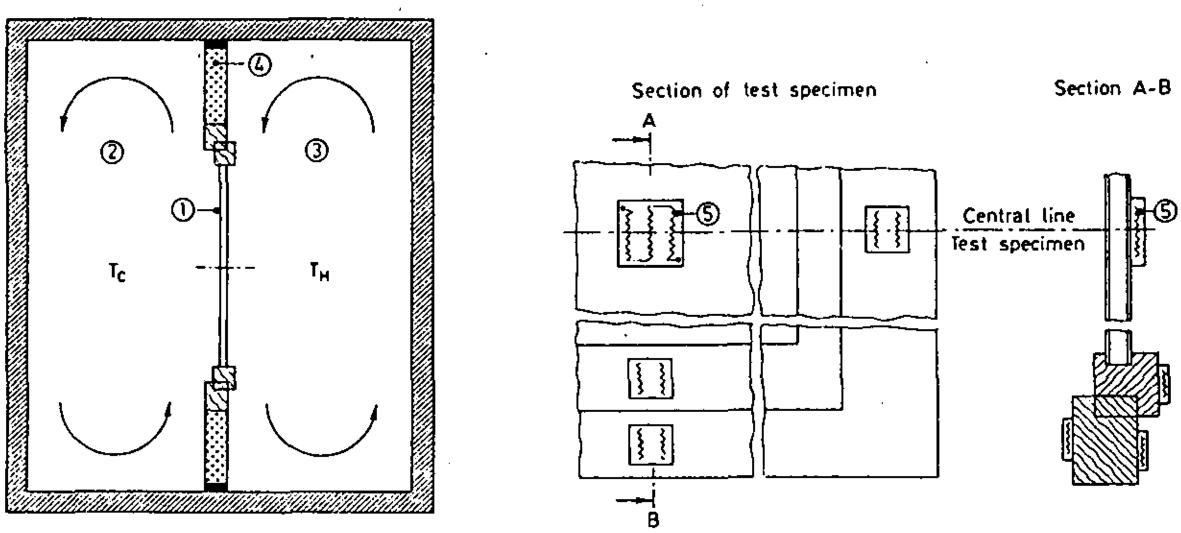

Figure 3: Schematic drawing of a measuring arrangement on the basis of heat flux sensors

where: T_H air temperature warm side
T_C air temperature cold side

1 test specimen
2 cold side
3 warm side
4 thermal insulation
5 heat flux sensors

5. TYPE AND STATUS OF TEST METHODS APPLIED WITHIN THE ANNEX XII PARTICIPATING COUNTRIES

A synopsis of the international application of the various test methods is compiled in Table 2.

Table 2: Test methods for window systems concerning steady-state heat transfer and status of test conditions

nations	Test methods for window systems					
	complete window system			glazing unit		frame
	hot box			hot plate, hot box		hot box
	guarded	calibrated	heat flux sensor	calori-metric	heat flux sensor	guarded
	Label of Standard					
B	NBN B 62-204	-	-	NBN B 62-201	-	-
D	DIN 52619 part 1	-	DIN 52619 part 1	DIN 52619 part 2	DIN 52619 part 2	DIN 52619 part 3
I	-	-	-	-	-	-
NL	I	-	-	-	I (1)	-
N	NS 3161	-	-	NS 3161 (hot box)	I (2)	-
CH	-	I	-	I (hot box)	-	-
UK	BSI 874 part 3	BSI 874 part 3, sect.3.1	-	BSI 874 part 3 (hot box)	-	-
USA	I	I	-	I	I	I

I: individually; not standardized

(1): two methods; one similar to ASTM-C 518-76 (hot plate with heat flux sensor), the other referring to ASTM-STP 855.

(2): determined as difference from measured U-value window and calculated glazing U-value according to [1].

The status of test conditions, i.e. whether standardized or individually chosen, is indicated as well as a survey is given specifying the various combinations of methods and test apparatus and what methods are used for testing window components (glazing unit, frame) or/and the complete window system. Such a survey cannot, however, account for special aspects of the specific situation within the individual Annex XII countries. Therefore, the state of the art will be pointed out country by country.

- Belgium

  In Belgium, glazing units and complete window systems are tested according to national standards, but not the frame as a single component.

  Label of National Standard and Type of Test Method

  Glazing Unit

  NBN B.62.201: Guarded Hot Plate

  Complete Window System:

  NBN B.62.204: Guarded Hot Box

- Federal Republic of Germany

  In Germany, a set of national standards is available for testing components and complete window systems, as well. There are two options for determining the areal thermal resistance of the complete window system:

  1) by means of a guarded hot box
  2) by means of heat flux sensors in a hot box arrangement.

  Label of National Standard and Type of Test Method

  Glazing Unit

  DIN 52 619, Part 2: Calorimetric Hot Plate or Heat Flux Sensor

  Frame

  DIN 52 619, Part 3: Guarded Hot Box

  Complete Window System:

  DIN 52 619, Part 1 (-A): Guarded Hot Box
  DIN 52 619, Part 1 (-B): Heat Flux Sensor

  Italy

  No standard

- Netherlands

Measurements are generally not standardized, complete window systems and frames are tested individually by the guarded hot box method. Test methods for glazing units are similar to US standards: ASTM-C 518-76; heat flux sensors in a hot plate apparatus referring to ASTM-STP 855: "Building applications of heat flux transducers, for guidelines on the application of heat flux sensors".

- Norway

In Norway, the hot plate method is usually not accepted. Hot box measurements of glazing unit and complete window system are standardized according to Scandinavian codes. U-values of frames are determined as the difference between U-values measured for the complete window system (by means of guarded hot box) and a U-value of the glazing unit calculated according to [1]. The thermal resistance of glazing units is measured in a guarded hot box, with the glazing unit being fixed in a wooden frame which has been calibrated as part of the boundary conditions by means of heat flux sensors.

Label of National Standard and Type of Test Method

Glazing Unit and Complete Window System:

NS 3161: Guarded Hot Box

This standard is in agreement with the Swedish code SS 024212 and the Danish code DS 1121. The Swedish code SS 024213 is also used, but only as a proposal.

- Switzerland

In Switzerland, there is no national standard for the determination of thermal transmittance. Hot plate measurements are not very common. Complete window systems are tested by means of a calibrated hot box according to [2].

- United Kingdom

In the U.K., standardized test methods are available for measuring the complete window system and the glazing unit as well.

Label of National Standard and Type of Test Method

Glazing Unit

BSI 874, Part 3: Guarded and Calibrated Hot Box

Complete Window System:

BSI 874, Part 3: Guarded and Calibrated Hot Box

- United States of America

There is no well-defined standard method for measuring window U-values currently in use in the U.S. Committee E-G of the ASTM has a draft standard under discussion. Although there are elements of controversy, one point generally agreed upon is that the measurement apparatus should be a hot box as described in ASTM C-236 (guarded) or ASTM C-976 (calibrated). Hot plate or heat flow meter measurements are not accepted for window or glazing units.

The commonly used reporting standard for U-value measurements includes use of the ASHRAE winter values of h_o = 34 W/m²K, h_i = 8.3 W/m²K for the heat transfer coefficients. (Summer U-values, which are used less frequently, assume h_o = 23 W/m²K.) The areas of controversy in measurement include the issues of

- whether laboratory tests should attempt to simulate some set of "realistic" exterior conditions
- how to determine the equivalent mean surface temperatures of a complex window system under test in order to correct the results to the ASHRAE conditions.

A standard procedure lacking, two approaches are in common practice:

- an apparatus using the baffle/fan arrangement of ASTM-C-236 and utilizing "natural convection", which may include small air flows tangential to the window in the direction of natural convection (used by National Wood Window & Door Mfgt. Assn. (NWWDA))
- use of the voluntary standard AAMA-1503 which specifies natural convection on the warm side and a 25 mph, normally incident wind on the cold side of the window together with a calibration procedure and prescribed surface temperature measurements (used by the American Architectural Mfgt. Assn. (AAMA)).

6. LIST OF PROBLEM AREAS ACCORDING TO VARIOUS STANDARDS

6.1 Concerning the Determination Procedure

a. Hot plate methods

- Only applicable to constructions with homogeneous plan-parallel flat surfaces.
- Only the resistance of the central part of the sample will be determined. The edges are either in the guard section or remain outside the scope of the heat flux sensor.

b. Hot box methods, general

- When directly determining only the U-value (for glazing, frame or complete window) without determining thermal resistance and actual surface film coefficients, it is not possible to transfer the results to other conditions or to compare them to results obtained by different determination procedures (neither tests nor calculations). This is e.g. the case with Belgian standard NBN B62-204.
- The definition of "average" surface temperatures for derivation of the thermal resistance is a problem area. In fact: for e.g. a frame with different surface temperatures at the same side the term "thermal resistance" is only properly defined in combination with a definition of the positions where "the" surface temperatures are measured.
  Any definition in this respect would do, but in order to be able to connect the surface film coefficients in a proper way, the surface temperature should be averaged in a specified way, namely over the total (front plus side a.s.) area of the frame.
  It is this total area on which the heat transport via the heat transfer coefficients takes place; see also problem area 6.1.c.
  The same applies for the thermal resistance of a complete window. The surface temperature should be averaged on the total areas rather than on the projected areas of the glass and frame parts .
  In German standard DIN 52 619, Part 1(A), for instance, the mean temperatures are weighted according to the projected areas.

- For the transformation from thermal resistance to U-value and vice versa, values for the surface coefficients of heat transfer are used: Measured values when the measured U-value is involved (see above) or standard values to derive a "standard U-value" from measured thermal resistance.

  For obvious reasons, thermal resistance and U-value are defined on the projected area of the window or window component. However, as mentioned above, the surface film coefficients transport the heat over the total surface area (see also chapter 3.2.3, Thermal Bridges). If - either standard or actual - surface film coefficients are assumed to be applied only to the projected area (e.g. DIN 52 619, Part 1(A), (B) and Part 3), then "cooling fin" kind of effects are overlooked, particularly in case of metal frames.

  This means that the film coefficients have to be multiplied by a factor: $a = A_{tot}/A_{pr}$, the ratio of total over projected area.
  Actually, neither radiation nor convection will be exactly proportional to the total area, due to dead corners, concavities etc., but do still provide the best approximation of the real situation.

  Hence, instead of defining

$$U = \frac{1}{R + h_i^{-1} + h_e^{-1}}$$

  the definition should be:

$$U = \frac{1}{R + (a_i\ h_i)^{-1} + (a_e\ h_e)^{-1}}$$

  where:

  $a_i = A_{tot\ i}/A_{pr}$

  $A_{tot\ i}$: total area on hot side;

  A_{pr} : projected area (arbitrarily defined from inside or outside);

  a_e : idem, on cold side.

It is self-evident that in special cases specific solutions may be required. For a harmonica-shaped surface e.g. it is clear that the IR-radiative heat transfer coefficient should not be increased according to the total surface, because in that case radiation exchange usually does not differ from that of a flat plate; the convective heat transfer, however, is indeed increased by approximately A_{tot}/A_{pr}.

- If the resistances of glazing and frame are measured separately, a possible thermal bridge through the pane edge and the frame will not be considered. On the other hand, if the thermal resistances of frame and glazing are derived from a test on a complete window, these values cannot always be used in combination with different components, e.g. a different glazing in the same frame.

  Mostly, the resistance of the glazing is presented as the value for the center part of the glazing and the edge effect is then considered as an inseparable part of the frame resistance. It is also possible to present "the edge effect" as a linear thermal bridge (e.g. negative linear R_l-value per m profile length, in W/mK). Both approaches are completely exchangeable, and in both approaches it is the combination of frame and glazing which determines the effect. See also chapter 3.2.3 "Thermal Bridges".

- If the thermal transmittance of a window system including a temporary insulation device (e.g. roller blinds) is determined by means of averaging the U-values of frame and glazing unit (incl. temporary insulation), then the heat flows simultaneously passing the blind housing will be neglected. Moreover, the determination should consider both day and night conditions.

c. Guarded or calibrated hot box methods

- With the determination of only one combined thermal resistance for the complete window (e.g. DIN 52 619, Part 1(A)) it is not possible to transfer test results to windows with different glazing/frame area ratios or to windows with different combinations of components.

- Like the determination of separate resistances for frame and glazing in a single test, also the derivation of a U-value from a measured combined resistance for a complete window can only be carried out on the basis of the assumption that the heat transfer coefficients of glazing and frame are the same (with - if applicable - a correction for $a = A_{tot}/A_{pr}$, the ratio of total over projected area; see problem area 6.1.b).

If this assumption is valid, the measured heat flow through the window $[\phi_W]$ can be separated into the heat flow through the glazing $[\phi_G]$ and the frame $[\phi_F]$ by:

$$\phi_F = \frac{A_F \cdot a_{F,i} \, (T_{a,i} - \overline{T}_{Fs,i})}{A_F \cdot a_{F,i} \, (T_{a,i} - \overline{T}_{Fs,i}) + A_G \, (T_{a,i} - \overline{T}_{Gs,i})} \cdot \phi_W$$

where $\overline{T}_{Fs,i}$ is the mean temperature over the total frame area on the hot side.

$$\phi_G = \phi_W - \phi_F$$

Based on the surface to surface temperature differences for frame and glazing, the thermal resistances for both components can be derived separately.

NB: It should be noted that these resistances should not be considered as parallel resistances from which the resistance for the complete window can be directly derived by weighting the areas. In general, the surface temperature will be different, so that only the U-values of frame and glazing can be directly combined.

In case the assumption of equal surface coefficients of heat transfer seems not valid, the thermal resistance of frame or glazed part should be measured separately. The partial heat flow (ϕ_F or ϕ_G) may then be derived from the temperature difference across the surface of the component with known resistance.

The resistance of the glazing, for instance, can either be derived by calculation (see chapter 3.2.2), by a separate hot plate or hot box test or by applying heat flux sensor(s) to the glass during the guarded or calibrated hot box test proper (see problem area 6.3.d).

d. Hot box tests using heat flux sensors

- The use of heat flux meters allows the thermal resistance of glazing and frame to be measured directly in a single test without assuming equal transfer coefficients. The heat flux sensors measure the local heat fluxes (heat flow densities) into or from the surface; for the derivation of the heat flow it is necessary to estimate the area over which the measured heat flux is valid. For a flat and homogeneous surface the definition of "representative" areas may be a problem; for complex surfaces (e.g. frames with front and side surfaces) this is even more the case.
  The thermal resistance can be derived by multiplication of the projected area and the temperature difference between hot and cold surfaces and division by the total heat flow:

  $$R = \frac{A_{pr} \cdot (T_{T,s,h} - T_{T,s,c})}{\sum_j \cdot dA_j \cdot q_j}$$

  where dA_j : parts of the surface with heat flux q_j

  $$\sum_j \cdot dA_j = A_{tot}$$

  In e.g. German standard DIN 52 619, Part 1(B), however, the thermal resistance is defined as:

  $$R_{DIN} = \frac{(T_{T,s,h} - T_{T,s,c})}{q}$$

  where q is "the" heat flux through representative areas.

  Even if the heat flux q is taken as the weighted mean value over the total surface, the German definition over-estimates the thermal resistance of a frame with a factor A_{tot}/A_{pr}.

  In fact, every heat transport through surfaces that are not in the same plane as the window is neglected.

6.2 Concerning Ambient Conditions

a. General, both for hot plate and hot box methods

- The harmonization of "standard" values for the surface coefficient heat transfer for the derivation of thermal transmittance from measured thermal resistance is a problem area. This subject is discussed in chapter 3.2 (Thermal Transmission). Particularly concerning the convective heat transfer coefficient on the room side, there are two possibilities: either a fixed value or a function of temperature difference. A fixed value can be defended by arguing that in practice the free convection near the window is governed by the convective patterns in the whole room rather than by the difference between air and window surface temperature.

  On the other hand it is a well-known fact that free convection near the window may indeed be strongly reduced as the window surface temperature is increased; if that is so, then - like for the convection inside a cavity (chapter 3.2.2) - the temperature effect should be taken into account, e.g. with the equation presented in section 5 of chapter 3.2.2.

  If an extra layer is added to a window, then the actual extra resistance induced by the addition of this layer might be increased even more when a reduction in convective heat transfer could or should be taken into account.

b. Hot plate methods

- Both the temperature difference and, to a lesser extent, the temperature level may have an influence on the value of thermal resistance. Example:

Table 3: Listing of results of thermal resistances determined by using selected equations from chapters 3.2.1 and 3.2.2. The results show the effect of temperature level in combination with different types of double glazing units.

Selected temperature levels of surface temperatures on hot and cold side of the test specimen				double glazing			
				clear glass, uncoated, air-filled		idem, with low-emissivity coating and 100 % argon-filled	
$T_{s,i}$ (°C)	$T_{s,e}$ (°C)	$\bar{T}$ (°C)	ΔT (K)	cavity width (mm) 12	24	cavity width (mm) 12	24
				thermal resistance (m^2K/W)			
15 25	5 15	10 20	10 10	0.180 0.167	0.201 0.188	0.531 0.506	0.657 0.648
effect of temperature level (% per 10 K)				7	6	5	1
15 20	5 0	10 10	10 20	0.180 0.180	0.201 0.186	0.531 0.531	0.657 0.548
effect of temperature difference (% per 10 K)				0	8	0	20

NB: In case there is a significant temperature effect it should be realized that equal surface temperatures for two samples with different resistances in fact correspond with different environmental temperatures, if standard surface film coefficients are assumed.

- The effect of a possible low-emissivity coating on one of the outer surfaces on the IR-radiative film coefficient will not be detected.
- Obviously, the orientation of the sample (from horizontal to vertical) will influence the free convection in the cavity of a multi-glazing system.
- The relatively small scale of the sample in a hot plate apparatus might have some effect on both the radiative and convective heat transfer within a multiple glazing unit.
- The resistance of the sample is measured under isothermal surface conditions. In practice, the heat flux will cause a temperature gradient over the height. This will have some effect on the onset of convection in the cavity in a multiple glazing system, thus on the thermal resistance.

c. Hot box methods, general

- When the thermal resistances of frame and/or glazing are the prime quantities measured in a hot box, neither the deviation of the actual surface coefficients of heat transfer from the ("standard") situation in practice nor difficulties in the correct determination of the actual coefficients (see problem area 6.2.b) seem to be relevant problem areas.

  However, even then it is important that the ambient conditions are as realistic as possible because the thermal resistances may well be influenced by the conditions at the surface.
  The surface film coefficients are subject to all variations also to be met in practice:

  convection: forced: wind speed, direction;
  free: dimensions of room (e.g. hot box), height of sample, temperature difference air/window surface.
  radiation: emissivity and temperature of room (hot and cold box) surfaces.

For instance, some laboratories use hot boxes with increased convection to compensate for the low emissivity of the walls. Probably, the effect of this deviation from "standard" ambient conditions will differ from one window type to another.

The direction of forced convection (simulation of wind) on the cold side of the window is also likely to affect the test result due to its influence on the local heat transfer coefficients: a perpendicular air flow may cause high velocities in the center and low velocities in the edge zone of the sample; an air flow parallel to the window may cause dead corners which, moreover, depend on the orientation (horizontal, vertical) of flow.

- A special problem area is caused by low emissivity of outer surfaces. The standard surface film coefficients are not valid and there is no measure to define how the actual surface coefficients of heat transfer differ from standard conditions. In e.g. German standard DIN 52 619 the low-emissivity situation is avoided by prescribing a black surface paint in this case, thus preventing the low-emissivity effect.

- A somewhat similar problem is posed by <u>products with internal circulation of ambient air</u>, e.g. through or around curtains, screens, etc. Standard surface film coefficients are not applicable, and again there is no measure to define how the actual heat transfer coefficients differ from standard conditions.
  The best solution is to ensure that the ambient conditions with the product being replaced by a conventional window (or calibration panel) are as close to standard conditions as possible. Based on the difference in thermal transmission with and without such components, the extra thermal resistance induced by the component can be directly derived. Then, in the extra resistance, surface effects (change in heat transfer coefficients) are included.

- The <u>actual surface coefficients of heat transfer</u> may remain unknown if the thermal transmittances of frame and/or glazing are measured directly. Nevertheless, even then it is obvious that information concerning the actual surface film coefficients is very valuable in the process of analysing the test results (and again, see problem area 6.1 b).

In this respect, the problem of the definition of the <u>environmental temperature</u> emerges.

The convective heat transfer coefficient should be derived from the difference between (mean) window surface and (mean) room <u>air</u> temperature; the radiative coefficient should be derived using the temperature difference between window and room wall <u>surfaces</u>. Usually, however, the difference between ambient surface and ambient air temperature will be small.

In some cases, instead of air and/or surface temperatures, an environmental temperature is measured, being a somehow weighted mean value for air and <u>all</u> surrounding surfaces, including the (colder) test sample itself. In NBN B62-204, e.g. the ambient temperature in the hot box is measured with a black globe at a distance of 0.75 m from the window.

6.3 Concerning Test Conditions

a. Hot plate methods

- If the heat flux is determined with a <u>heat flux sensor</u> precautions should be taken to avoid that the heat flux sensor influences the heat flow through the sample, e.g. by applying a guard ring with correct dimensions and thermal conductivity.
- If the heat flux is determined by the input of electric power, a <u>guard zone</u> should be applied around the metered zone, with equal surface conditions to prevent lateral heat fluxes.

b. Hot box methods, general

- Temperature sensors applied on the window surfaces should have the same emissivity as the surface to which they are applied and should not in any other way disturb the heat flow through the surface.

c. Guarded or calibrated hot box methods

- The test sample is placed either directly in the opening between the hot and cold room or in the opening of an insulated mask, if the sample dimensions are smaller than the dimensions of the hot box allow. Thirdly, it is also possible to place the hot box of a guaroed hot box against the glazing. In the first two cases there will be a heat flow around the sample edge through the wall or mask. The calibrated but also guarded box should be calibrated for this heat loss by replacing the test sample by an insulation sheet with known thermal resistance.

  The connection of this insulation sheet to the walls or the mask should be of the same dimensions (thickness and position) as the test sample in order to avoid differences in lateral heat flows there.
  Only in case of a guarded hot box placed against a homogeneous flat surface of the sample, like against the glazing, it may be assumed that there are no lateral heat flows at the edge of the measured part of the sample; in this case, calibration will not be necessary.

d. Hot box tests using heat flux sensors

- The heat flux sensors should have the same emissivity as the surface to which they are applied and should not in any other way disturb the heat flow through the surface.
  Often, these conditions are difficult to fulfil, even on homogeneous flat surfaces, and certainly on the more complex frame surfaces.

6.4 Conclusions

- The U-value from a hot box test should never be presented without indicating also the actual heat transfer coefficients.

- The resistances of frame and glazig should be determined as separate values. The edge effect of the glazig may be contained in the resistance of the frame or be considered separately as a linear thermal bridge. Only with separate values for frame and glazing, the results can be transferred properly to other - e.g. standard - conditions and other window dimensions. For components like curtains, screens, etc. for which standard heat transfer values are not applicable, the results should be presented as extra resistance, added to a window without such components, measured under "standard" conditions.

- Deviations in the U-value of a window component or complete window system caused by the determination procedure are of equal or maybe greater importance than deviations caused by ambient conditions.

- Deviations caused by the determination procedure can be easily avoided by an international agreement on a procedure which takes the relevant problem areas into account.

- Deviations caused by ambient conditions can be avoided to a large extent by ensuring that the conditions are as closely as possible equal to standard conditions in practice. International agreement on standard conditions is strongly recommended. If a detailed record is made of the actual test conditions, a transformation to other (standard) conditions will in most cases be possible, with the understanding that the resistance of the window proper may also change with the ambient conditions, in a way known only for specific cases (see chapter 3.2.2).

- Deviations caused by test conditions can be avoided by selecting the most appropriate test method (e.g. avoiding disturbance of the heat flux by heat flux sensors on a complex surface) and accurate measurement techniques (e.g. calibration).

7. AN INTERNATIONAL AGREEMENT: ISO ACTIVITIES CONCERNING STANDARDIZATION

This section will not discuss the activities of the International Organization for Standardization (ISO) but explain the agreements concerning principles of test methods and measurement.

The actually existing ISO drafts are not specified for window systems. The ISO working group TC 160/WG2 is preparing a first draft proposal concerning the guarded hot plate apparatus.

In 1986, a joint working group was formed by members of the Technical Committees TC 59/160/162/163 in order to prepare draft proposals concerning hot box and heat flux sensor test methods specially designed for window systems.

Although not directly applicable to window systems, the draft proposal ISO DP 8990 (13th draft) "Calibrated and Guarded Hot Box" has been selected as an example to demonstrate the collaborative efforts of the participating countries to establish mutually accepted standards granting national independence in testing procedures and ensuring sufficient compatibility of test results.

Test method according to DP 8990

For testing purposes, the application of both calibrated and guarded hot box methods is considered suitable. It is recommended that calibrations be carried out for the guarded hot box, too. The performance of the apparatus shall be checked by means of specimens of known thermal resistance. These checks shall be repeated at intervals to detect a possible drift in calibration.

Measurements according to DP 8990

Two alternatives are proposed:

1. The thermal resistance is determined by measuring surface temperatures, heat flow rate and metering area. The thermal transmittance, U-value, will be calculated by means of surface coefficients fixed within relevant building codes.
2. The thermal transmittance, U-value, is determined directly by means of environmental temperature difference between cold and hot side and measured average density of heat flow. The environmental temperatures are calculated from air and wall surface temperatures of the hot box.

Alternative 2. is to be used for test specimens with thermal bridges or special geometry. Within this alternative, the surface temperatures of the test specimens will be measured, too, to be able to determine the actual surface film coefficients under test. In this way, comparability with alternative 1. is ensured.

Besides the agreements concerning the determination of thermal transmittance by test methods (although not yet for windows), a first step has been taken concerning determination of thermal transmittance of glazings by calculation methods, providing unified boundary conditions. For calculating thermal transmittance of double or multiple glazing, a proposed ISO standard has been elaborated, its 4th revision now being circulated ("Calculation Rules for Determining the Steady-State 'U-value', Thermal Transmittance, of Double or Multiple Glazing", TC 160, W 62, 1986).

REFERENCES

[1] Heiersted, R.S.: K-values of Wooden Windows

Norwegian Building Research Institute, Report of Feb. 21, 1984
(In Norwegian)

[2] Frank, Th.; Gay, J.B. et al.

Fenster und Fenstersysteme, Stand der Forschung und Entwicklung
EMPA/EPFL Switzerland, May 1984

[3] Thermal Transmission Through Windows. Selected Examples to Illustrate the Need for a More Standardized Approach.
IEA-Annex XII, Windows and Fenestration, Report Step 2 (1987)

3.3.3. Field measurements of thermal transmission

Th. Frank
T.W. Püntener
EMPA Section Building Physics
CH-8600 DUBENDORF
SWITZERLAND

J.B. Gay
C. Roulet
EPFL - GRES
CH-1015 LAUSANNE
SWITZERLAND

LIST OF SYMBOLS

α	Solar absorptance	
ε	Surface emittance	
Λ	Areal thermal conductance	W/m^2K
σ	Stephan-Bolzman constant $5.67 \cdot 10^{-8}$	W/m^2K^4
I	Radiation intensity	W/m^2
T	Thermodynamic temperature	K
U	Areal thermal transmittance	W/m^2K
h	Surface coefficient of heat transfer	W/m^2K
q	Areal density of heat flow rate	W/m^2
t	Celsius temperature	C

Subscripts

L	Longwave (3 - 50 µm)
R	Radiation
S	Solar-Radiation (0.3 - 2.5 µm)
c	Convection
i	interior
e	exterior
r	Radiation
s	surface

1. SURFACE FILM COEFFICIENTS

The net sensible heat flux balance at the exterior surface of a building can be expressed as follows :

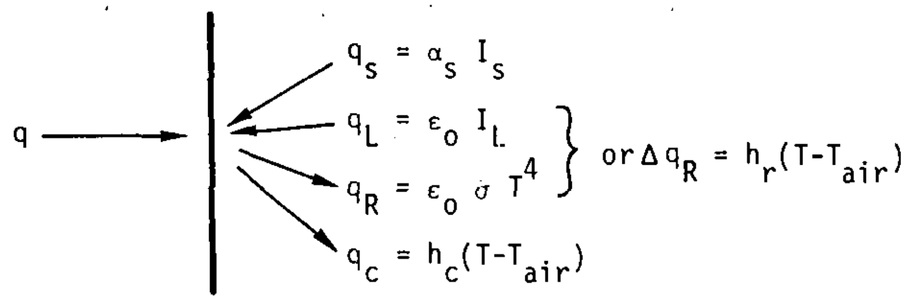

Fig.1 : Heat fluxes at the exterior building surface

q	:	Net heat flux from or into the surface (W/m^2)
q_s	:	Absorbed shortwave radiation (solar) (W/m^2)
		α_s solar absorptance
		I_s global solar irradiance incident upon the suface (W/m^2)
q_L	:	Absorbed longwave radiation (atmosphere and ground) (W/m^2)
		ε_o longwave emittance of the surface
		I_L longwave irradiance incident upon the surface (W/m^2)
q_R	:	Emitted longwave radiation (W/m^2)
		σ Stefan-Bolzmann constant $5.67 \cdot 1o^{-8} (W/m^2K^4)$
		T surface temperature (K)
q_c	:	Convective heat transfer (W/m^2)
		h_c convective heat transfer coefficient (W/m^2K)
		T_{air} Ambient air temperature (K)
Δq_R	:	Radiative heat loss of the surface (W/m^2)
		h_r radiative heat transfer coefficient (W/m^2K)

Heat flux balance : $$q + \alpha_s I_s + \varepsilon_o I_L = \varepsilon_o \sigma T^4 + h_c(T - T_{air}) \qquad (1)$$

According to the heat flux balance equation (1) different measurement methods have been used to determine the radiative and convective heat transfer coefficients at the exterior building surface.

Ito and Oka [Lit.3,4] ,Sharples [Lit.7,9] ,Chapman [Lit.8] and Sturrock [Lit.5] used two heated panel elements with slightly different surface temperatures in order to determine the convection heat transfer coefficients.By measuring the net heat flux q into the surface and the surface temperature T for both panels (index A and B),the convective heat transfer coefficient h_c becomes :

$$h_c = \frac{q_A - q_B - \varepsilon_0 \sigma \left(T_A^{\ 4} - T_B^{\ 4}\right)}{(T_A - T_B)} \qquad (2)$$

where q_A, q_B, T_A and T_B are measured data.

Figure 2 shows the results of the experimental study performed by Sharples [Lit.7] .The building used in his work was the 18 storey Arts Tower at Sheffield University,U.K. The measurements were made in the north facade on different floors (6th,14th and 18th).Surface wind speeds v_s were measured 1 m from the building surface.

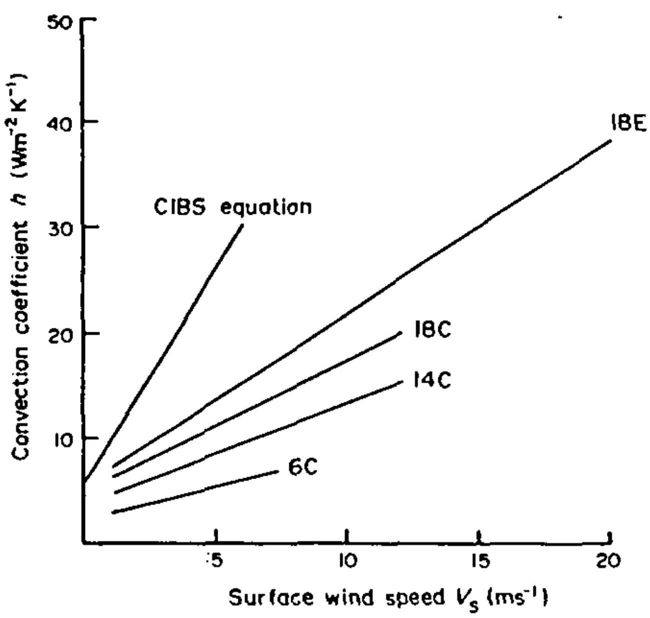

Fig.2 : Linear regression between convection coefficient h_c and surface wind speed v_s for windward conditions at different levels of the building [Lit.7] .

The method of the measurement according to equation (2) shows two critical points,which have to be treated very carefully :

a) Exact measurement of the heat flows q_A and q_B.

b) The temperature difference of the two panels (T_A - T_B) has to be chosen in a reasonable range in order to get small errors and the same temperature dependency of h_c.

The measurements of Sharples have been restricted to nocturnal observations in order to eliminated any influence of solar effects.

Field measurements including shortwave and longwave radiation measurements have been performed in Switzerland [Lit.10,11] on two test cells (5 x 3 x 3 m) with different ir-properties of the surfaces,one with a high (0.92) and the other with a low (0.07) surface emissivity. According to equation (1) the following relationship for h_c is given:

$$h_c = \frac{q + \alpha_s I_s + \varepsilon_0 (I_L - \sigma T^4)}{(T - T_{air})} \tag{3}$$

$$h_r = \frac{\varepsilon_0 \, (I_L - \sigma \, T^4)}{(T - T_{air})} \tag{4}$$

where q, I_s, I_L, T and T_{air} are measured data.

The most critical points of this method are the proper measurement of the longwave and shortwave radiation as well as the heat flux q. The comparison of two sufaces with identical solar absorptivity α_s and different emissivities ε_0 allowed the study of the influence of ir-radiation heat loss to the sky and the environment.For well insulated building surfaces an undercooling below the ambient air temperature has often been observed. Therefore a definition of a radiative heat transfer coefficient h_r is not always possible.Since the longwave radiation exchange takes place between the surface and the environment (sky and ground) ,it would be better to consider a ir-radiation loss ΔIR instead of a radiation film coefficient.

Fig.3 illustrates the measured convective film coefficient at the north facade of the EMPA test cell facility [Lit.10] ,which may be representative for small one storey buildings.

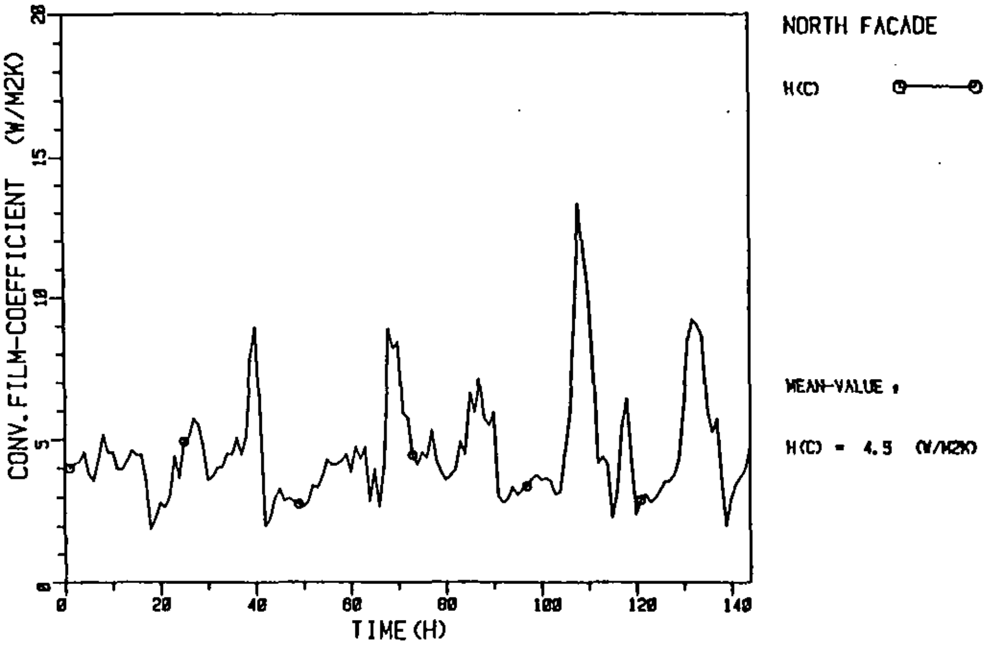

Fig.3 : Measured convective film coefficients from the EMPA test cell facility (mean value over the whole north facade area of 15 m^2) [Lit.10].

Conclusions

Different field studies on the subject of convective heat transfer at the exterior building envelope [Lit.1 - 9] showed the difficulty to find good correlation models.One main reason may be the lack of good air flow models,which allow the determination of surface wind velocities around the whole building envelope.

Some investigations also demonstrated,that for wind sheltered building elements,very low convective film coefficients ($h_c < 5$ W/m^2K) may be observed.This fact should be taken into account in more detail when cooling loads problems and thermal comfort situations in summer time are considered.

2. AREAL THERMAL CONDUCTANCE

Measurement and interpretation

The areal thermal conductance of a building element,surface to surface is defined as :

$$\Lambda = \frac{q}{(T_{si} - T_{se})}$$

where the following notations are used :

q areal density of heat flow rate (W/m^2)

T_{si} internal surface temperature of the building element (K)

T_{se} external surface temperature (K)

The areal thermal transmittance of the element,environment to environment, is the U-value.It can be deduced from the thermal conductance and the surface film coefficients by :

$$\frac{1}{U} = \frac{1}{h_i} + \frac{1}{\Lambda} + \frac{1}{h_e}$$

The thermal conductance can be obtained by measuring the heat flow rate with a heat flow meter (HFM) as well as the surface temperatures on both sides of the element under steady state conditions.

However, since the steady state is never really encountered on site, such a simple measurement is not possible.Several measurements have to be taken periodically during a suitable period of time.These measurements can then be interpreted by different methods:

a) The classical method, which is already widely used [Lit.12] and even standardized [Lit.13].It assumes that the thermal conductance can be obtained by dividing the mean density of heat flow rate by the mean temperature difference.If the index j enumerates the individual measurements, then :

$$\Lambda = \frac{\sum_j q_j}{\sum_j (T_{sij} - T_{sej})}$$

b) The dynamic interpretation method, which takes into account the thermal variations by the use of the heat equation [Lit.14] .The building element is represented in the model by its thermal conductance and several time constants.These unknown parameters are obtained by fitting values of the heat flow rate computed from the temperature measurements to the measured ones.With this approach, a set of linear equations must be solved.

The results of both interpretation methods are equal to the real value if the following conditions are met [Lit.15] :

- The heat content of the element is the same at the end and at the beginning of the measurement.This is easily achieved on window panes.
- The solar radiation has an influence on the heat flow rate of the building element.Therefore only night measurements should be interpreted.
- The HFM is well calibrated and does not modify significantly the heat flow rate through the panes or this effect has to be taken into account.

Corrections on the measured values

The HFM, which is a thin thermally resistive plate with sensors arranged in such a way that the electrical signal given is directly related to the heat flow rate through the plate, adds a thermally resistant layer to the measured element.If this layer were infinitely large and thin, the correction would be negligible or easy determined if the thermal resistance of the HFM was known.If the indoor surface temperature was taken under the HFM,this correction is zero.
But the HFM has a given thickness and a finite surface area.The heat flow lines are modified in the region where the HFM is installed,according to figure 4.This lowers the heat flow through the HFM and a correction must be made .

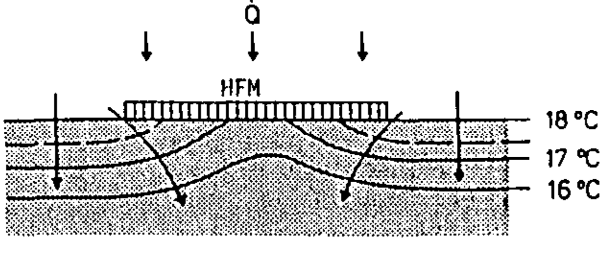

Figure 4 : Deviation of the heat flow lines by the additional local thermal resistance of the HFM.

If q' is the measured heat flow rate and q the one through the element without an HFM, the error e can be defined as :

$$e = \frac{q' - q}{q}$$

This error depends on the following factors,by decreasing order of importance :

- Surface resistance over the HFM
- Diameter of the active part of the HFM
- Total diameter of the HFM (including guard ring)
- Thermal resistance of the HFM
- Thermal conductivity of the layer below the HFM
- Thickness of the first layer below the HFM
- Thickness of the HFM and the guard ring

The error e grows with the thermal conductivity of the first layer of material situated just under the HFM (for window panes,it's glass) and the thermal resistance of the HFM; and is lowered if the HFM is large and thin.This error can be computed by solving the heat equation by the finite element method and a correction factor can be obtained. Figure 5 to 8 give the results for a single and a double glazed window [Lit.19] :

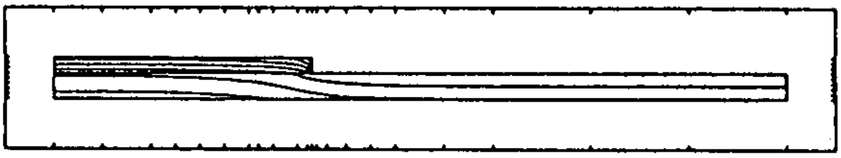

Figure 5 : Configuration A "HFM on a single glazed window " [Lit.19]

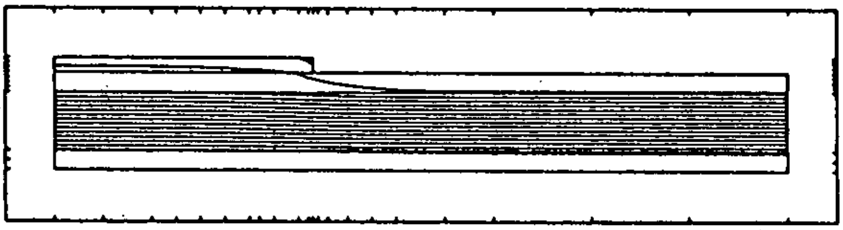

Figure 6 : Configuration B "HFM on a double glazed window " [Lit.19]

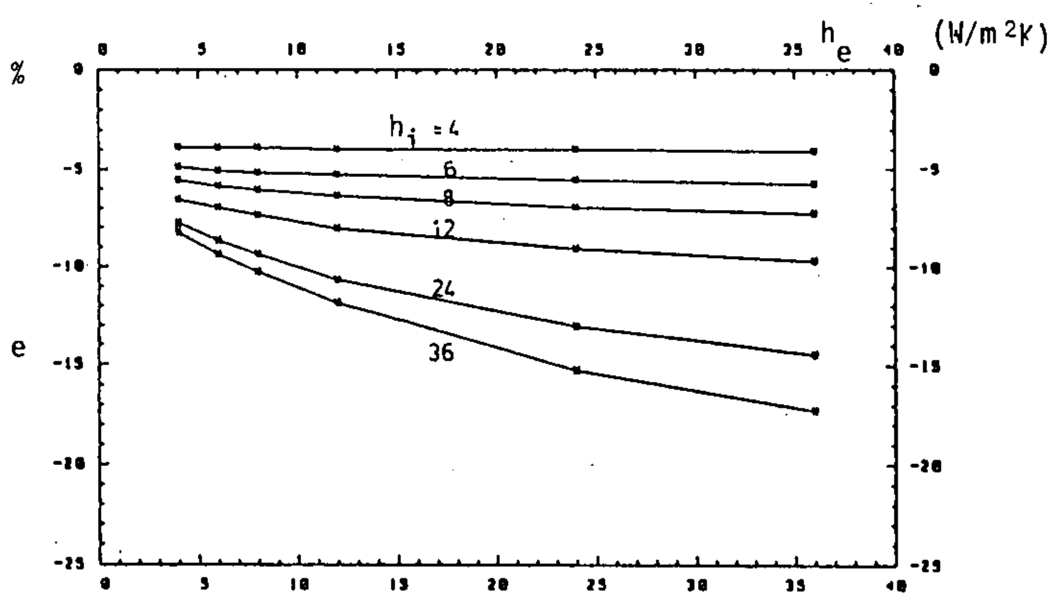

Figure 7 : Correction-factor e for HFM-configuration A (single pane) in function of the surface film coefficients h_e and h_i .
λ_{glas} = 0.8 W/mK , λ_{HFM} = 0.25 W/mK [Lit.19]

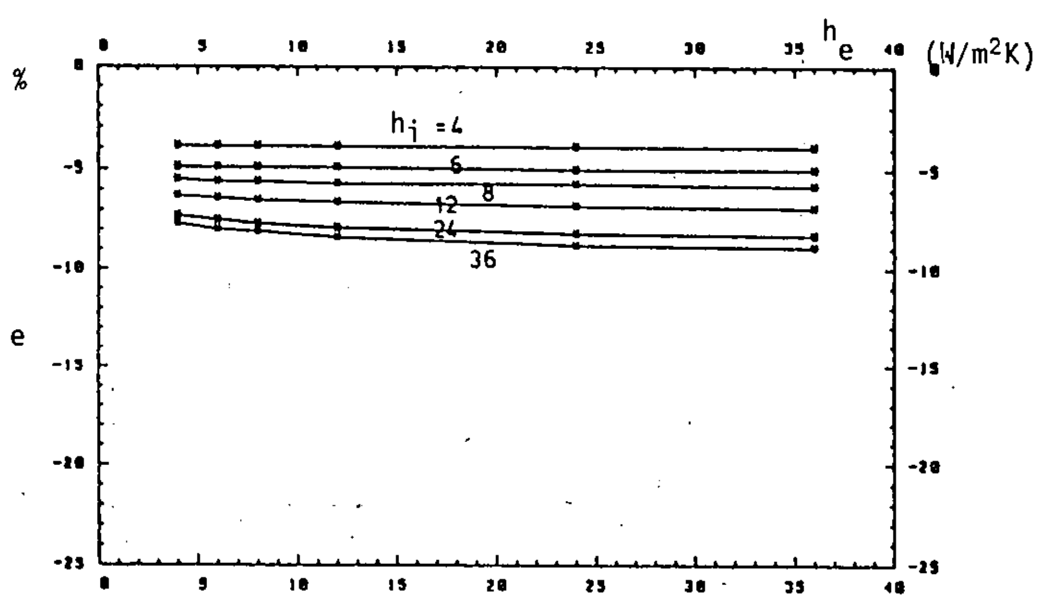

Figure 8 : Correction-factor e for HFM-configuration B (double pane) in function of the surface film coefficients h_e and h_i .
λ_{glas} = 0.8 W/mK , λ_{HFM} = 0.25 W/mK [Lit.19]

Flanders [Lit.17] claims, that the largest factor affecting the accuracy is the convection mode changing over the HFM.The HFM may sense turbulent convection while the measured element experiences laminar flow.Very flat and smooth edged HFMs may partially prevent this phenomenon.Burch et al. [Lit.18] advise not to use the HFM without special precautions on glass surfaces.

For all these reasons and advices,HFM have to be used with care.A guard ring,made of a material of same thickness and same thermal resistance as the HFM , may prevent most of these perturbations.

Conclusions

It has been found,[Lit.15 ,19 and 20],that :

- HFM measurements on insulating window panes can be made within a accuracy of 10 %.
- For very light elements like windows,both classical and dynamical interpretation methods give good results if the element is not submitted to direct or diffuse solar radiation.One night is generally long enough to get reliable results.
- Uncontrollable statistical errors caused by slight changes in thermal contact or convection around the HFM account for about 5 % of the measured value.
- A guard ring has to be used and /or correction factors taking into account the perturbation of the heat flow lines caused by the HFM itself have to be computed.

References

[1] K.Gerhart Modellversuche über die Verteilung des konvektiven Wärmeüberganges an Gebäudefassaden. Kälte-Klimatisierung 5,1967

[2] F.B.Rowley et al Effects of air velocity on surface coefficients. ASHRAE Trans. 36,1930

[3] N.Ito et al A Field experiment study on the convective heat transfer coefficient on exterior surface of a building. ASHRAE Trans.,1972

[4] M.Oka et al The unit to measure convective heat transfer coefficients on the exterior surface and its performance. Trans. of Arch.Inst.of Japan,1967

[5] N.S.Sturrock Localised boundary layer heat transfer from external building surface. Ph.D.Thesis University of Liverpool,1971

[6] R.J.Cole et al The convective heat exchange at the external surface of buildings. Building and Environment 12,1977

[7] S.Sharples Full scale measurement of convective energy losses from exterior building surfaces. Building and Environment 19,1984

[8] F.J.Chapman Model studies of convective heat transfer from buildings. Ph.D.Thesis University of Leeds,1979

[9] S.Sharples Forced convective heat transfer from building facades. Ph.D.Thesis University of Sheffield,1982

[10] T.Frank et al Measurement report : Test cells "Maugwil" EMPA Report 1982

[11] C.Zürcher et al The influence of thermal and solar radiation on the energy consumption of buildings. Infrared Physics 22,1982

[12] B.R.Anderson Site testing thermal performance: a CIB survey Building Research and Practice 12,1984

[13] NT Build 215 Thermal resistance . Nordtest Standard 1982

[14] S.Ahvenainen et al Thermal conductance of wall structures
LVI-tekniikan laboratorio,Report 54
Espoo (Finland) 1980

[15] C.Roulet et al Investigation on the on site measurement of the thermal transmittance of building elements.
GRES Report 85-01-09 , EPFL 1985

In situ U-value measurement : Reliable results in shorter time by dynamic interpretation of the measured data.
ASHRAE-DOE-8TECC third conference on thermal performance of the exterior envelopes of buildings,Clearwater Beach Florida, 1985

[16] P.Suter et al Mesure de flux de chaleur.
Wärmeschutzforschung im Hochbau
Seminar EMPA 1984

[17] S.N.Flanders Heat flow sensors on walls - what can we learn?
ASTM workshop - personal communications

[18] D.M.Burch et al Measurement methods for evaluating of thermal integrity of building envelopes.
U.S.National Bureau of Standards
Washington, NBSIR 82-2605 , 1982

[19] P.Standaert Two- and three-dimensional heat transfer : Numerical methods and experimental studies.
Ph.D. Thesis University of Leuven , 1984

[20] C.Roulet Errors caused by the HFM.
Internal working document for ISO
TC 163/SC1 , 1986

3.4. Condensation

A.F. Nielsen
Norwegian Building Research Institute
Division Trondheim
N-7034 TRONDHEIM NTH
NORWAY

LIST OF SYMBOLS

T_i is indoor temperature

T_e is outdoor temperature

U is U-value of the construction

h_i is surface coefficient of heat transfer W/m^2C

q is condensation heat flow (W/m^2)

r is condensation heat (J/kg)

B is mass flow surface resistance $(kg/m^2\ s)$

c_A is moisture content in the air (kg/m^3)

c_o is saturation moisture content at the surface (kg/m^3)

Introduction.

This chapter is concentrated on the condensation problems on glass and windows. It does not describe the moisture balance for the building or condenstion in structures. The humidity indoor depend on the moisture load, room size and ventilation rate. The user behaviour has large influence on the moisture load and the ventilation rate. The problems of moisture is explained more in detail in (1) or (2).

Several international committees is working on problems in connection with moisture.

CIB W-40 Heat and Moisture Transfer in Buildings.

This group held its last meeting in Holzkirchen, Germany in September 1985. One of the topics was surface condensation.

RILEM TC 35-PMB Methods of predicting moisture conditions in Building Materials and Components. This group held a work-shop in Lund, Sweden in June 1986.

IEA held a meeting in September 1985 in Leuven, Belgia on Condensation and Energy problems.(3)

It has later been decided to start a new IEA annex on Condensation and Energy Problems. This task will work on all aspects of moisture and condensation.

3.4 Condensation.

1. Theory

Surface condensation will occur if the surface temperature T_s is lower than the *saturation temperature (dew point)* T_a of the surrounding air. The condensation will normally create a water film on the surface. If the surface temperature is below 0 ^oC then the condensation will be in the form of rime or ice.

For a one-dimensional heat flow is the surface temperature T_s under stationary conditions:

$$T_s = T_i - \frac{U}{h_i} (T_i - T_e)$$

where T_i is indoor temperature
T_e is outdoor temperature
U is U-value of the construction
h_i is surface coefficient of heat transfer W/m^2K

If surface condensation shall be avoided then T_s shall be higher than T_a. From the formula it is seen that the surface heat transfer coefficient determine the surface temperature and therefore the condensation risk. The internal surface heat transfer coefficient contains both radiation and convection parts as described earlier (chapter 3.2.1 and 3.2.2). Chapter 3.2.3 gives examples of calculated surface temperatures on profiles and glazing.

In most heat transfer calculations a fixed internal surface resistance is used. But in some cases condensation can change the heat balance, because the condensation releases heat.

In addition to radiation and convection heat flow, there will be condensation heat flow.

$$q = r \cdot B_p (c_A - c_o)$$

q is condensation heat flow (W/m^2)

r is condensation heat (J/kg)

B is mass flow surface resistance (kg/m^2 s)

c_A is moisture content in the air (kg/m^3)

c_o is saturation moisture content at the surface (kg/m^3)

Normally it is better to use double panes than single panes. But the energy saving can be less than expected or zero. This happens when the room has extra high moisture content, and the outdoor temperature is low. Then condensation will occour and the heat released from condensation will increase the glass temperature. If we can not accept condensation and use double panes, then we have to ventilate the excess moisture out. This will cost energy. The energy balance will show that the energy savings from double panes will be less than expected from a calculation without taking moisture into account. Problems of this type can happen in stables and some high humidity industrial buildings.

2. Condensation on the glass surface

Figure 1 gives curves of condensation for different types of glazing. The values has been calculated with a fixed internal surface resistance of 0,13 m^2K/W. The curves are applicable to the central part of the window where there is no effect from the thermalbridge of the spacers.

Internalshutter or add-on panes gives an extra heat resistance. When in place the temperature on the surface of the glass will decrease. Then the risk of condensation will be increased especially if the air can flow around the shutter. Figure 2 to 4 gives curves for the surface temperature on the glazing for different shutter heat resistance. If the shutter is air- and water vapour tight there will be no problem with condensation.

The theoretical calçulations should be used with caution. In practice condensation will first occur near the spacer. Condensation at night can in most cases dry-out during the day if the sun comes up. In most buildings with occupants some kinds of curtains are used especially in the nighttime. This is the same as using a non-airtight shutter and will increase condensation.

In many cases will the radiator below the window send hot air up between the glass and curtain. This will prevent the condensation, but the energy consumption will correspondingly increase.
The use of separate woodframes for the inner and outer glass will eliminate the problems with lower temperature near the frame. But then there will be more problems with airtightness and possible condensation between the glasses.

3. Condensation on the frame

If the frame material has a high thermal conductivity (as with metals), then condensation can occur first on the frame. It will be especially severe if the thermalbridge is not broken with some better insulating material. If more than one layer of glazing is used, then massive metal frames should never be used. Calculations of the U-value and the surface temperature for all metal frames should be made before deciding which window frame is best for the application. See examples in chapter 3.2.3.

The metal spacer along the edge between each pane of the sealed unit acts as a severe thermal bridge, causing a temperature short-cut between the inner and outer pane. The edge zone of about 60 mm has a steep temperature gradient. The problem of condensation on the glass near the frame for sealed units can be partially avoided if the sash profile covers the temperature gradient from the cut edge of the inner pane. The metal spacers is then placed below the edge of the frame and the surface temperature will be higher. Further information is found in (4).

4. Condensation on the wall

In some cases condensation can occur on the wall near the window frame. This will happen when the thermal insulation of the wall is too low, probably because of a thermal bridges (examples is found in chapter 3.2.3 figure 11). Use of better insulating windows will have no effect on this problem.

References

(1) L.E. Nevander and B. Elmarson: Moisture handbook. Theory, dimensioning, construction (in swedish).
Svensk Byggtjänst, Stockholm 1981.

(2) H. Erhorn and K. Gerlis: Minimum Insulation or/and minimum Air change rate.
Fraunhofer Institut für Bauphysik 1986.

(3) IEA News, Issue 3, dec. 1985

(4) R. S. Heiersted. Improving condensation resistance on the inner pane of sealed units by increasing the glazing rebate. Congress Windows in building Design and Maintenance, Göteborg 1984 (p605-610).

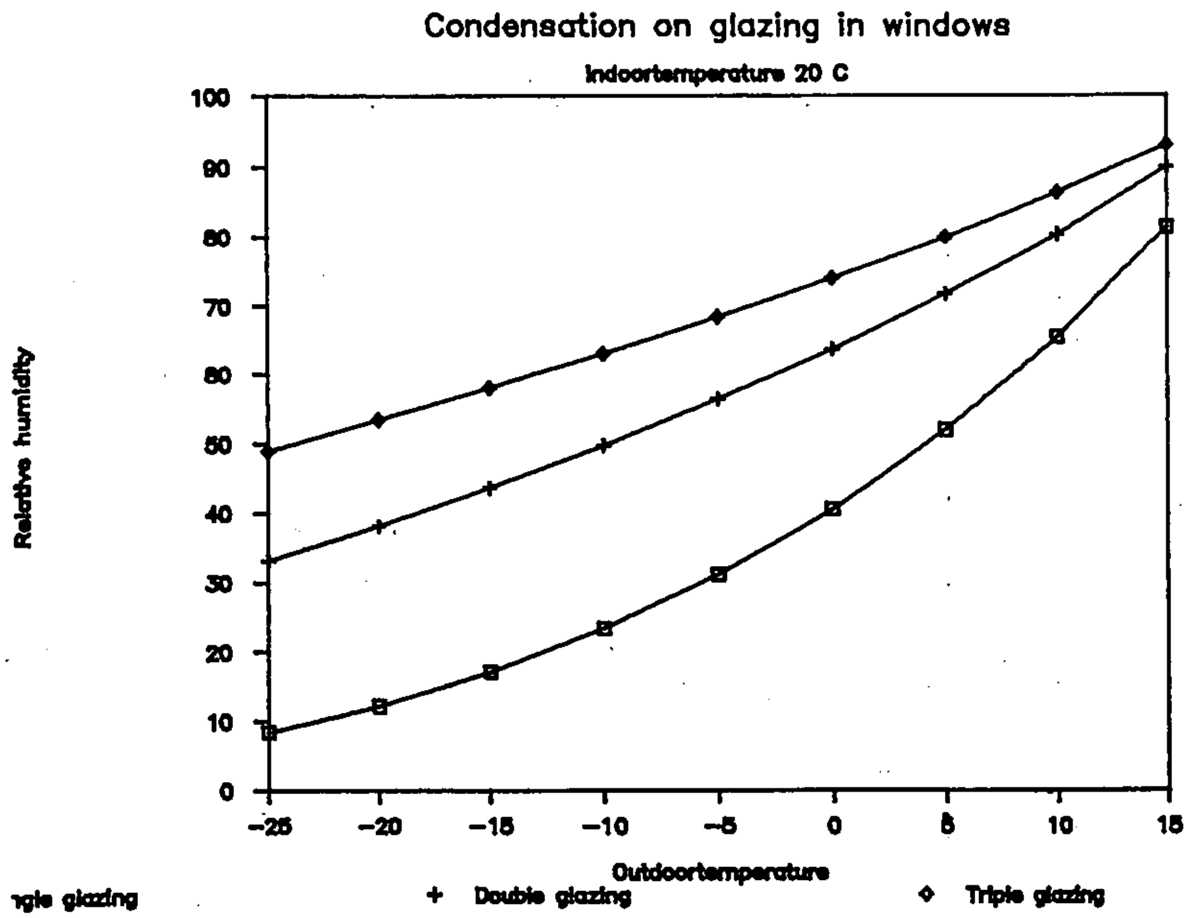

Fig. 1. Condensation on central part of glazing.

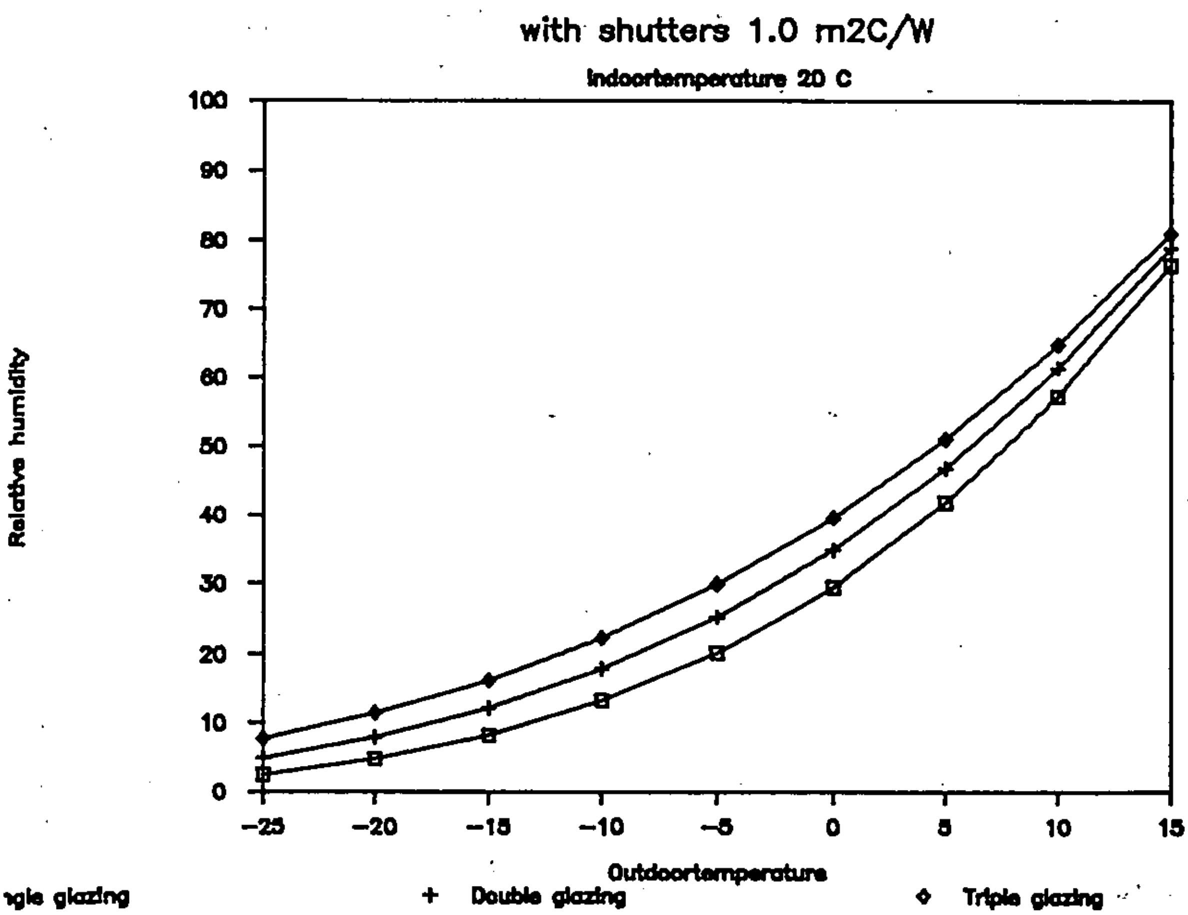

Fig. 2. Condensation on glazing with internal shutters.

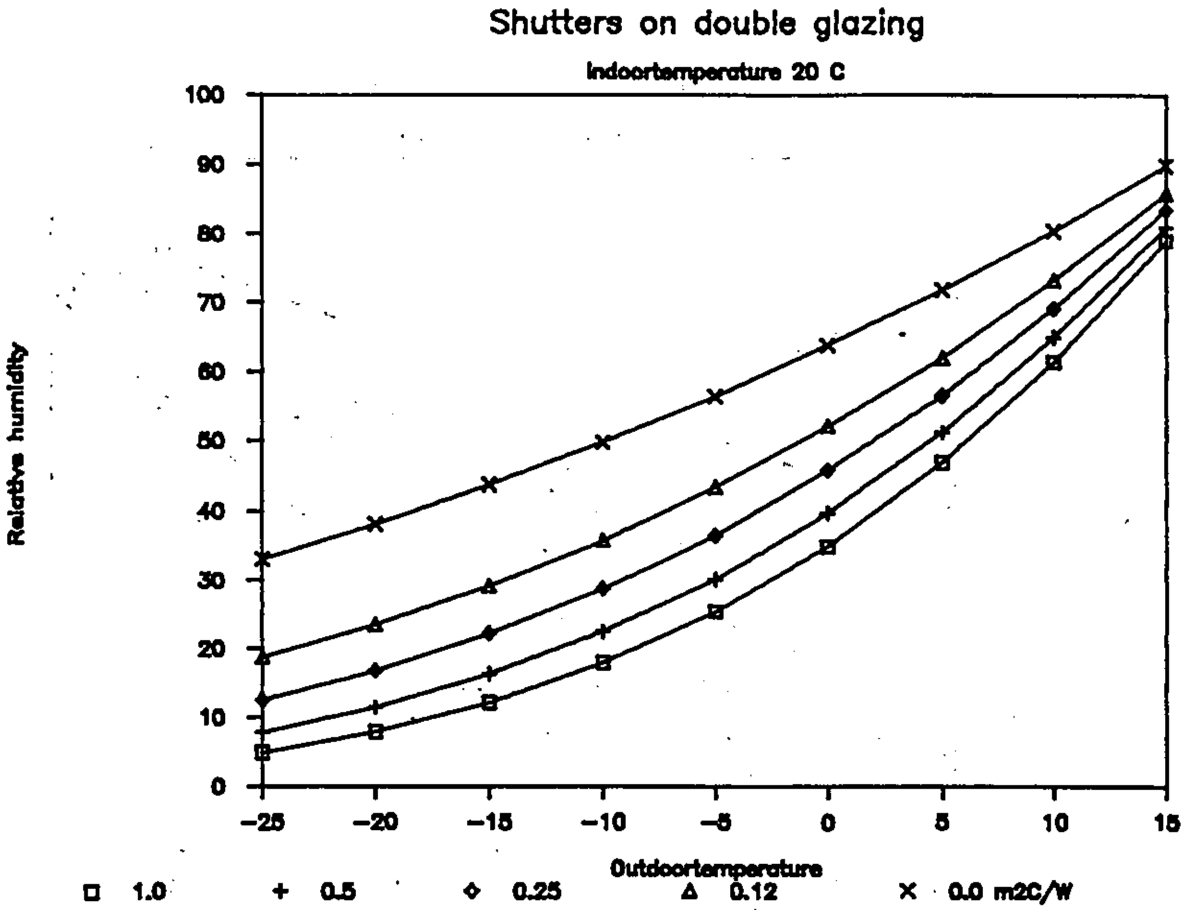

Fig. 3. Condensation on double glazing for different internal shutters or curtains.

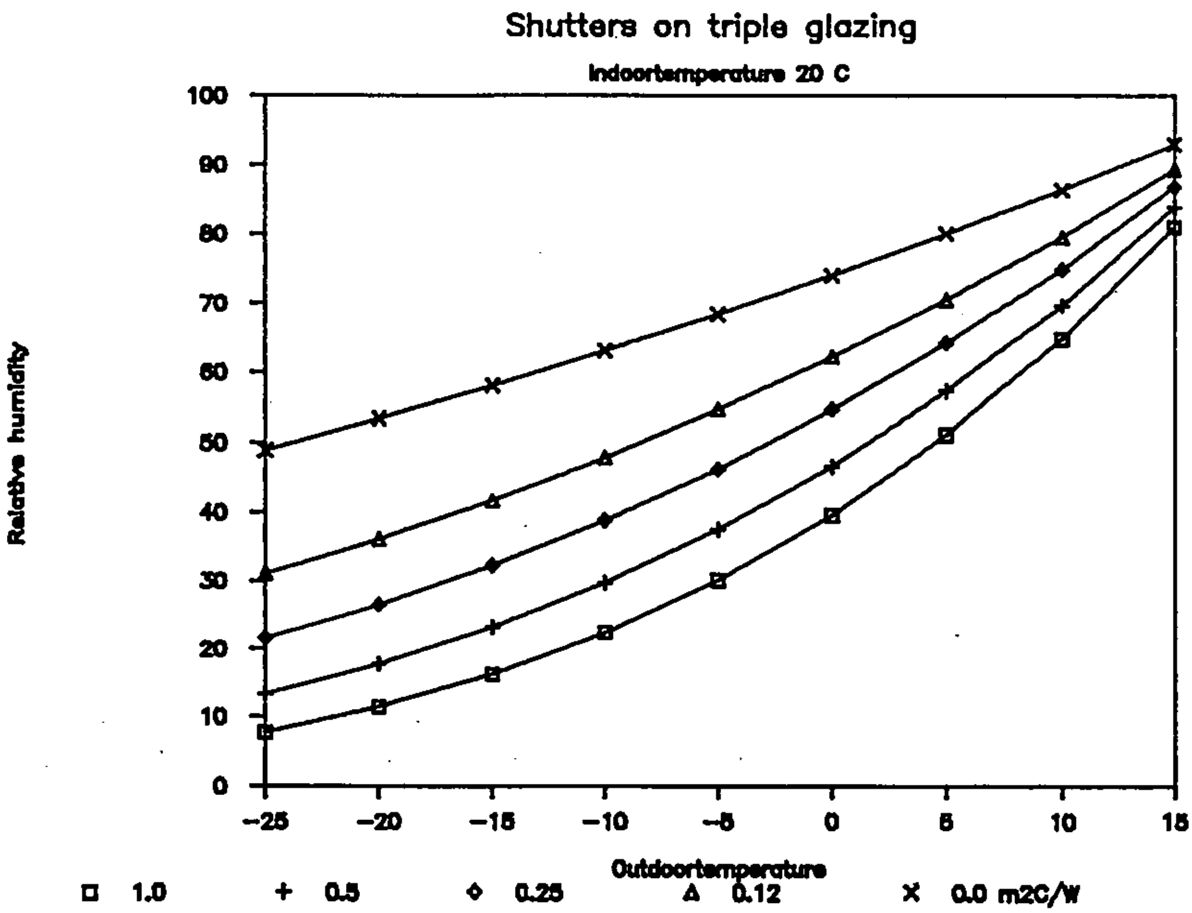

Fig. 4. Condensation on triple glazing for different internal shutters or curtains

3.5. Influence of infrared radiation barriers

H. Erhorn
R. Stricker
M. Szerman

Fraunhofer Institute of Building Physics
Department of Heat and Climate
(Director: Prof.Dr.-Ing. habil K.A. Gertis)
Nobelstrasse 12
D-7000 STUTTGART 80
FEDERAL REPUBLIC OF GERMANY

LIST OF SYMBOLS

σ	Stefan-Boltzmann constant 5.67	$[W/m^2K^4]$
$C_{1,2}$	radiation factor between two surfaces	
	$C_{1,2} = \dfrac{\sigma}{1/\varepsilon_1 + 1/\varepsilon_2 - 1}$	$[W/m^2K^4]$
Λ	thermal conductance	$[W/m^2K]$
ε	total hemispherical emissivity	[-]
h	surface coefficient of heat transfer	$[W/m^2K]$
U	(areal) thermal transmittance	$[W/m^2K]$
g	total solar energy transmission coefficient	[-]
τ	direct solar transmittance	[-]
α	solar absorptance	
ρ	solar reflectance	

Subscripts

t	total
eq	equivalent
l	light
1,2	surfaces
r	radiation
w	window
f	frame
g	glazing
a	ambient
i	inside

1. INTRODUCTION

Heat transfer at surfaces of building components consists of a convective and a radiative share. In chapters 3.2.1 and 3.2.2 detailed theoretical descriptions of both heat transfer mechanisms have been extensively dealt with. In this chapter, effects caused by a reduction of the radiative heat transfer due to IR-coated surfaces on the thermal insulation of building components (windows in particular) will be quantified. Furthermore, it will be shown that a decrease in the U-value due to IR-reflecting layers does not necessarily improve the energy balance of a window during the heating period.

2. FIELDS OF USE OF THERMAL RADIATION BARRIERS

IR-coated surfaces are especially efficient in building components with poor heat insulation [1]. Therefore, such coatings will mainly be found in connection with window systems, where in most cases the glass surface is coated. Usually, the surfaces in gaps of multiple glazings are preferred as here the coatings are protected from mechanical damages and pollution [2]. Another possibility to improve the heat insulation of glazing units is to install IR-treated transparent foils in the gap of the glazings [3].

With increasing frequency, IR-reflecting surfaces are also used on temporary insulation devices, both exterior [1], [4] (shutters, sunblinds etc.) and interior ones [1], [5] (curtains, darkblinds etc.).

Occasionally, low-ε-coatings are also applied to opaque building components. For interior surfaces, specially treated wallpapers [6] or reflective foils to be installed behind heating surfaces [7] are offered. For exposed surfaces, special paints [8] or coated facade elements [9], [10] are available.

3. COMPARISON OF OPAQUE AND TRANSPARENT BUILDING ELEMENTS

In the following, heat transmission phenomena in transparent and opaque areas are compared in order to improve knowledge of IR-coating induced effects on all characteristic values of building physics pertinent to window systems. In Figure 1, the heat flows in a wall are compared to those in a double glazing unit, for winter conditions at night.

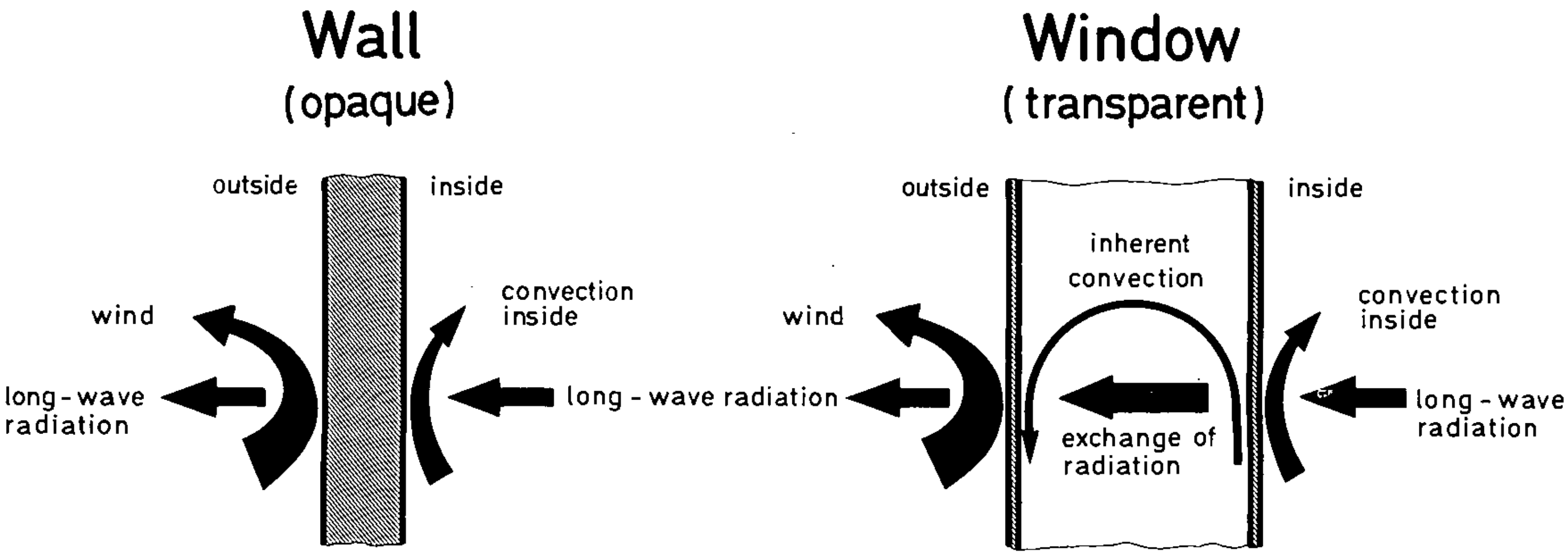

Fig. 1: Schematic presentation of heat transfer mechanisms in exterior building components, exemplified for a wall and a window

In walls, indoor air heat is usually transferred from the room by way of convection and by radiation of the warm surfaces enclosing the room to the interior surface of the outer wall. From here it is transferred via thermal conduction to the exterior surface and from there by convection to the outdoor air and by way of radiation to the terrestrial surroundings or into the atmosphere.

In a window, heat transmission through sealed insulating glazing leads to the same phenomena as far as the interior is concerned. As window glazing is almost not transparent in the wavelength range of infrared radiation (compare Figure 2) here, as well, energy radiated from the surfaces enclosing the room is absorbed and transmitted by thermal conduction through

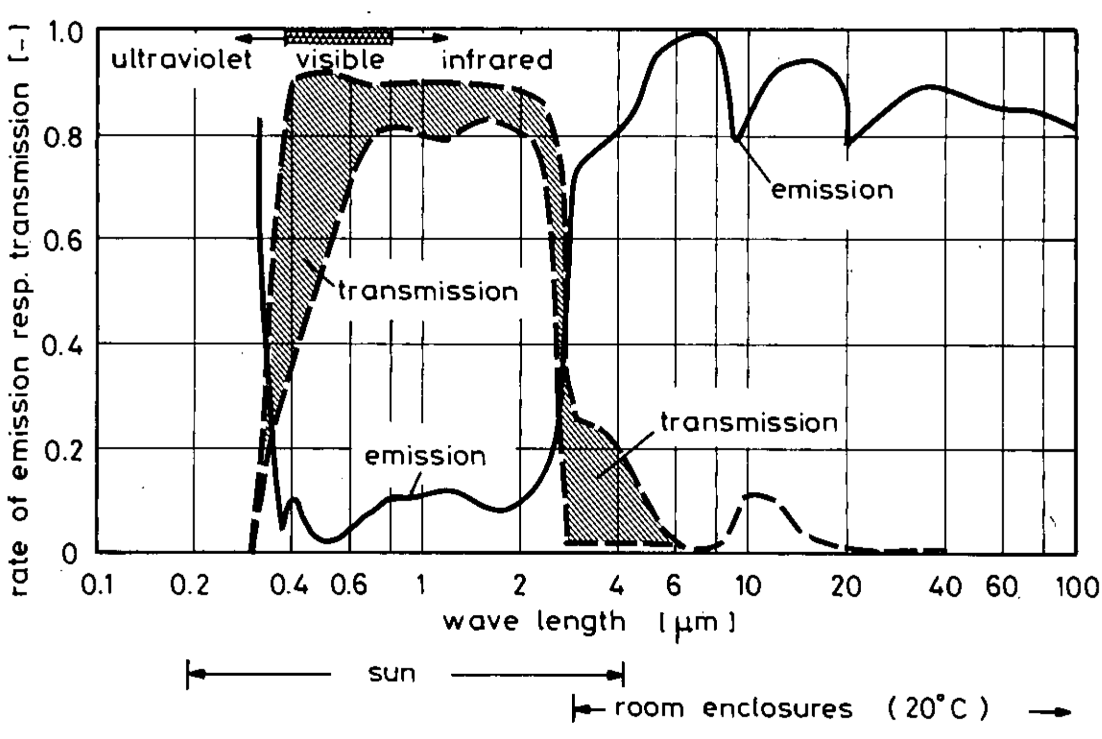

Fig. 2: Spectral emittance and transmittance of a commercial window pane within the short-wave and long-wave radiation ranges: also shown are the wavebands of the spectra for solar radiation and for a heat-reflective building surface of 20°C, acc. to [2]. In the hatched fields certain scatterings are shown that are caused by the composition of the glass melt. The transmissivity is strongly influenced by the content of ferric oxide and by the degree of oxidation which can vary during the process of glass production.

the interior pane to the air gap between the glazings. From here, heat is transferred to the exterior pane by radiation and free convection and, for a very little part, by thermal conduction in the air. From the pane, heat is again transmitted by thermal conduction, and on the exterior surface heat is emitted by convection and radiation as was the case with the opaque wall. If a temporary insulation is applied to the window, transmission phenomena are the same as in the air gaps of the sealed insulating glazing. Depending on tightness, the convective heat emission is additionally influenced by infiltration of air across the temporary insulation. Evidently, glazing units provide a much larger field of application for infrared-effective coatings since, here, a much greater quantity of heat flows is transmitted by thermal radiation than is the case in opaque walls.

In comparing solar radiation transmission mechanisms in opaque and transparent building elements, it becomes quite clear that a component's energy balance may also deteriorate due to infrared-reflective coatings.

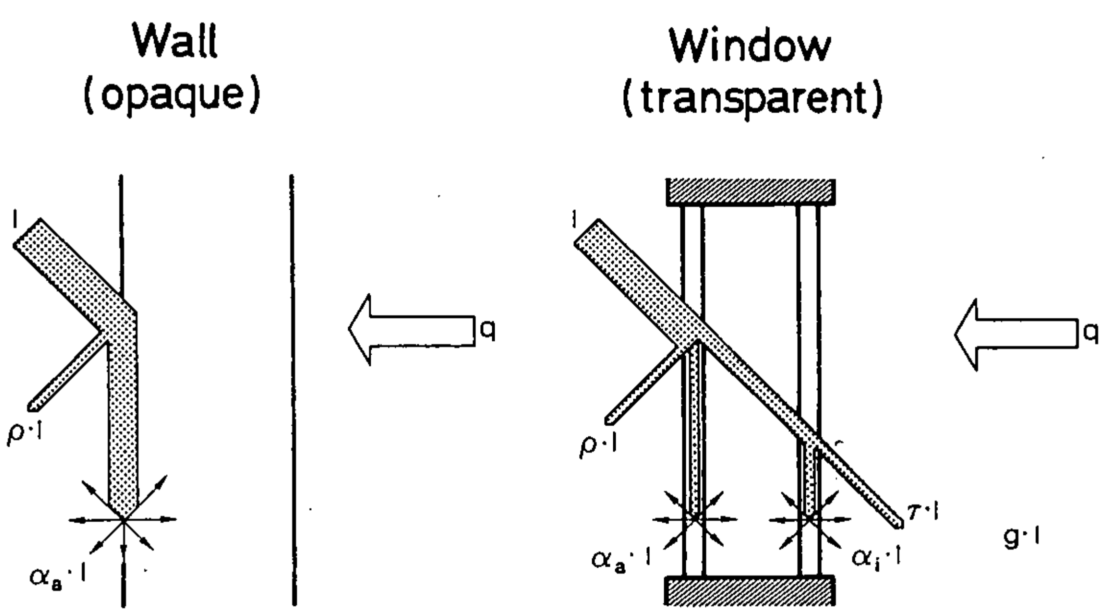

Wall	Window
$q = U \cdot \left(T_{AIR,i} - T_{AIR,a} - \frac{\alpha_a \cdot I}{h_a} \right)$	$q = U \cdot \left(T_{AIR,i} - T_{AIR,a} - \frac{\alpha_a \cdot I + \alpha_i \cdot I}{h_a} - \frac{\alpha_i \cdot I}{\Lambda} \right) - \tau \cdot I$
total solar energy transmission coefficient g:	total solar energy transmission coefficient g:
$q = U \cdot (T_{AIR,i} - T_{AIR,a}) - g \cdot I$	$q = U \cdot (T_{AIR,i} - T_{AIR,a}) - g \cdot I$
$g = U \cdot \frac{\alpha_a}{h_a}$	$g = \tau + U \cdot \left(\frac{\alpha_a + \alpha_i}{h_a} + \alpha_i \cdot \frac{1}{\Lambda} \right)$
e.g.: $U = 0.5$ W/m²K; $\alpha_a = 0.7$; $h_a = 25$ W/m²	e.g.: $U = 2.6$ W/m²K; $\tau = 0.70$; $\alpha_a = 0.09$; $\alpha_i = 0.06$; $h_a = 25$ W/m²K; $\frac{1}{\Lambda} = 0.215$ m²K/W
$g = 0.01$	$g = 0.75$

Fig. 3: Schematic presentation of heat transfer mechanisms in an exterior wall and a window system caused by solar radiation with determination of the total solar energy transmission coefficient acc. to [11].

In Figure 3, the processes of heat transmission of solar radiation in a wall and in a sealed insulating pane of glass are illustrated. By means of the actual total energy transmission coefficient the range of solar gains is explained. Since in opaque areas solar radiation is absorbed at the exterior surface and can only be transferred into the room via thermal conduction, the useable solar radiation is exclusively dependent on the insulation level and on the shortwave absorption abilities of the building components. In transparent areas, on the other hand, solar energy is transmitted directly into the room according to their respective transmittance. Additionally, a low heat flow will pass into the room by absorption at the glass surfaces as is the case with the exterior wall. In consequence, the decisive factor for solar gains in glazing systems is the direct solar transmittance. Having selected the wrong material for low-ε coatings, i.e. one with a low solar transmittance, it is quite possible that the total solar energy transmission coefficient and thus the solar gains will be strongly reduced.

4. INFLUENCE OF INFRARED RADIATION BARRIERS ON THE WINDOW U-VALUE

a. Glazings

In [2] calculations regarding the resistance of stable air layers with various widths of gaps and treatment of the surfaces were carried out. Table 1 shows the boundary conditions used here. In Figure 4 the thermal

Table 1: Material values and boundary conditions underlying the calculations.

Parameter		Units and range of values
Air temperatures:	indoor outdoor	20 °C – 10 °C
Thermal resistances:	internal external	0.13 m^2K/W 0.04 m^2K/W
Radiation factor between glazing surfaces in the air space		0.0...5.67 W/m^2K^4
Width of space between glazing surfaces		0.0...0.12 m
Height of glazing		1m
Material value for air in the space		according to [12]
Thermal resistence of pane of glass		0.01 m^2K/W

resistance of an air gap is described in dependence on the width of gaps for various compositions of surfaces (infrared emissivity). The curves are limited by the broken straight line to pure thermal conduction (no radiation, no free convection). It can be seen that the maximum of the specific thermal resistance with conventional glass surfaces is achieved ($C_{1,2}$ = 5...5.67 W/m^2K^4) with widths of gaps of approximately 2 cm to 3 cm and is about 0.17 m^2 K/W. The influence of free convection becomes especially evident with infrared reflective surfaces, i.e. with such surfaces that

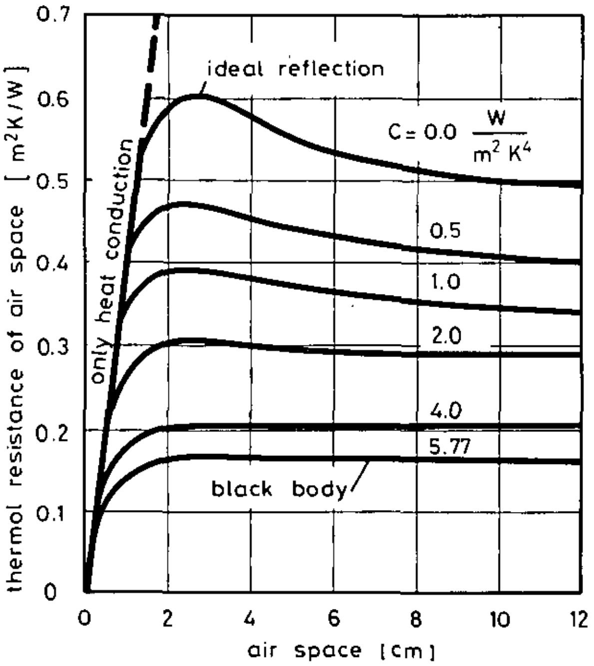

Fig. 4: Thermal resistance of stable vertical air layer according to width of air space and different radiation factors C, acc. to [2]. Black body indicates that the emittance ε of both surfaces is 1.0. Ideal reflection indicates that the emittance of at least one surface equals zero.

have a small radiation factor. A specific width of gaps being exceeded, free convection can set in (see chapter 3.2.2). The maximum with an ideal mirror ($C_{1,2}$ = 0) can be achieved with $1/\Lambda \approx 0{,}6$ m^2K/W. [13] and [14], too, come to similar conclusions. The free convection being relatively important in heat transfer is the reason for the fact that the thermal resistance decreases with increasing widths of gaps. This has a particularly drastic effect for small radiation shares.

By inserting one or more foils at equal distances into the air space of multiple glazings the heat insulation is increased. In Table 2, the (areal) thermal transmittance for some types of double glazing units is indicated in dependence on the number of foils fitted into the gap of double glazings and on the composition of the foils (emittance). As is to be seen from Table 2, the heat losses of the glazing surfaces can be reduced by the foils.

With several foils in the air gap the thermal conductivity of the glass plays a secondary part. In the investigations by [15] measurements on double glazings with coatings and foils have been made. The results are presented in Figure 5. A good correspondence with [2] can be observed.

Table 2: (Areal) thermal transmittance for various double glazings with no, one, or more foils in the air gaps of double glazings, installed behind each other at regular intervals, for two different emittances of the foil surfaces [2].

Type of glazing	Sketch	Heat transfer coefficients (W/m^2K)*						
		Without foil	n foils each in the air space of the double glazing					
		n = 0	n = 1		n = 2		n = 3	
			ε=0,85	ε=0,2	ε=0,85	ε=0,2	ε=0,85	ε=0,2
Double glazing with 70 mm distance between panes	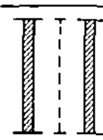	2,8	1,9	1,0	1,4	0,7	1,2	0,5
Double glazing consisting of single glazing and in-sulation glazing (air space between panes 10 to 16 mm)with 70 mm distance between the panes	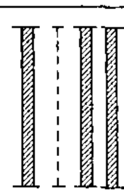	2,0	1,5	0,9	1,2	0,6	1,0	0,5
Double glazing consisting of two insulation glazing units (air space between panes 10 to 16 mm) with 70 mm distance between the panes	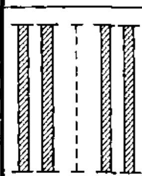 70	1,4	1,2	0,8	1,0	0,5	0,9	0,4

* Heat transfer coefficients represent lower limit values.

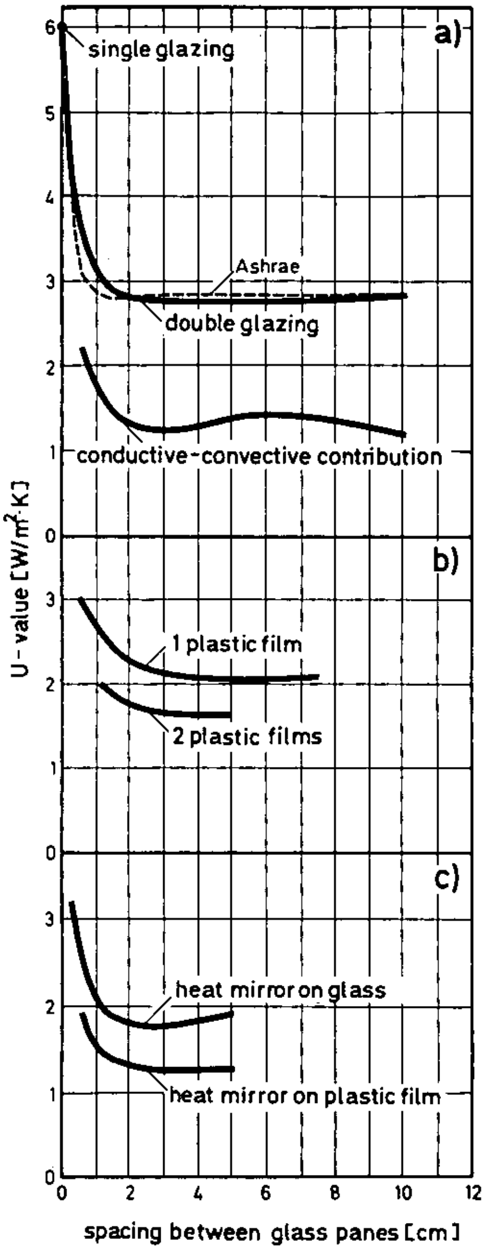

Fig. 5: Sample thermal transmittance according to [15].
Glass spacing for the prototype windows.

a) Ordinary double glazing and double glazing with aluminum foil on the inside of both glass panes.

b) Double glazing with one or two plastic films.

c) Double glazings with heat mirror coating on plastic film, where the plastic film is mounted on the surface of one glass pane or suspended between panes.

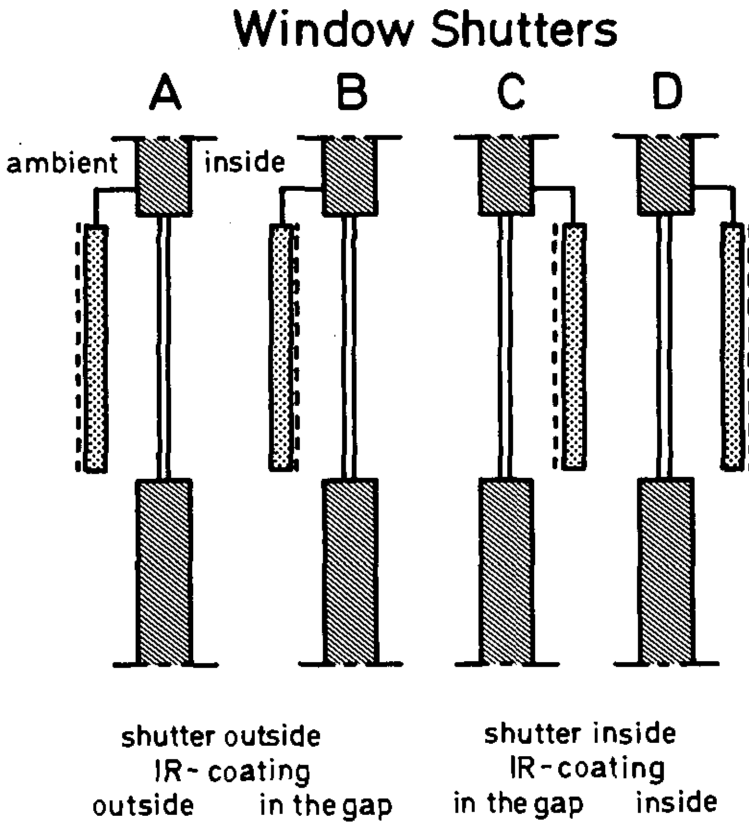

Fig. 6: Schematic presentation of the arrangement of low-ε-coatings for window systems with temporary insulation

A: IR-coating on the exterior surface of the outdoor shutter

B: IR-coating on the inner surface of the outdoor shutter

C: IR-coating on the exterior surface of the indoor shutter

D: IR-coating on the inner surface of the indoor shutter

Due to whether the gap between the temporary insulation and the window is airtight or not, the efficiency of the shutter is quite varied, because of the different ratio of convective and radiative heat transfer.

Moreover, the distance between the window and the shutter has an influence on the heat transfer.

b. Temporary insulation

To improve the insulation effect of the additional thermal insulation devices described in chapter 3.6, occasionally low-ε coatings are used as well. In [1] calculations regarding the decrease in the U-value of window systems were carried out. In Figure 6 the several investigated arrangements of IR-coatings are illustrated. The infrared effective layer is once installed at the exterior surface and then on the gap facing surface. The degree of air tightness of the cover is gradually varied between "tight" and "not tight"; in the case of "tight" a tight (stable) air layer according to DIN 4108 corresponds to it and in the case of "not tight" a gap with a surface to air coefficient of h_t = 8 or rather 12 W/m^2K. The infrared effectiveness of window covers must always be seen in connection with the insulation value and the degree of tightness of the cover.

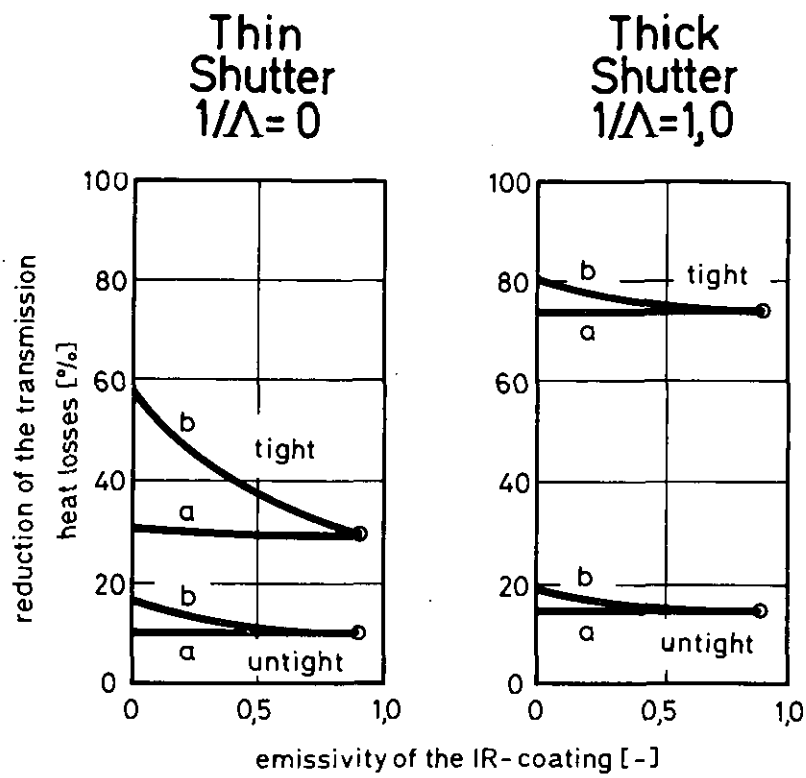

Fig. 7: Reduction in percent in the transmission heat losses of a double glazing window system with an outdoor, tightly resp. untightly placed shutter according to the emissivity of the shutter and the arrangement of the IR-coating, acc. to [1]

a: IR-coating on the exterior surface of the shutter

b: IR-coating on the gap-facing surface of the shutter

The attainable reduction in transmission heat losses for a sealed double glazing window system is presented in Figure 7. The figure shows what can be achieved in that case by infrared treatment with two insulating values and degrees of tightness.

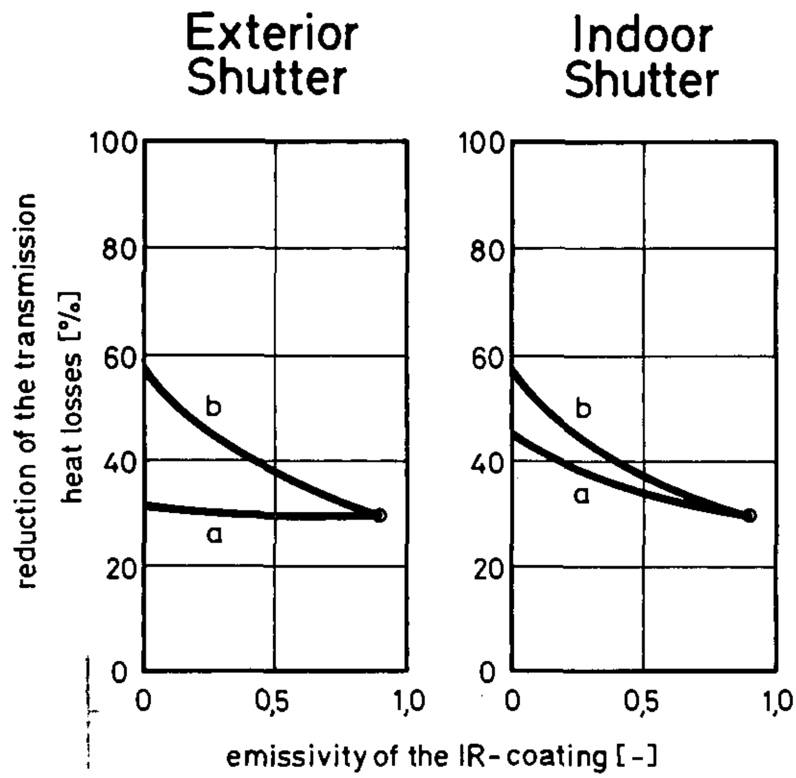

Fig. 8: Reduction in percent in the transmission heat losses related to the IR-coating of the shutter, comparing exterior resp. indoor shutters, acc. to [1]. The graphs are related to a very thin, tight shutter ($1/\Lambda \approx 0$)

a: IR-coating on the exterior resp. indoor surface of the shutter

b: IR-coating on the gap-facing surface of the shutter

Conclusions:

- The cover has to be installed in an airtight way to become effective.

- In the case of an airtight installation the increase in the insulation value of the cover is considerably more effective than an infrared treatment (comparison of the left and right diagram in Figure 7). This is also confirmed by other investigations, [16] to [18].

- An infrared treatment on the exterior surface is almost always ineffective (horizontal course of all a-curves).

Similar results can be obtained for covers installed inside (Figure 8) as well.

In [4] the calculations by [1] were verified by measurements. The results are compiled in Table 3. A good correspondence can be observed. In [5] measurements on curtains and blinds with low-ε coatings were carried out. The measurements were performed in connection with a sealed double glazing window system (U_W = 3.0 W/m^2K). The results are presented in Figure 9. Here, as well, a good correspondence with the calculations by [1] could be observed.

Table 3: Calculated [1] and (measured) [4] relative U-values for a U-value of the window of 2.5 W/m^2K.

Remarks	Relative U value in %. Shutter without heat resistance.		
Outside	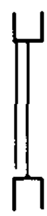		
	not reflect	reflective	reflective
not sealed	90 (82)	90 (85)	82
sealed edges	70	70	42
Inside			
	not reflect	reflective	reflective
sealed edges	70 (76)	55	42 (49)

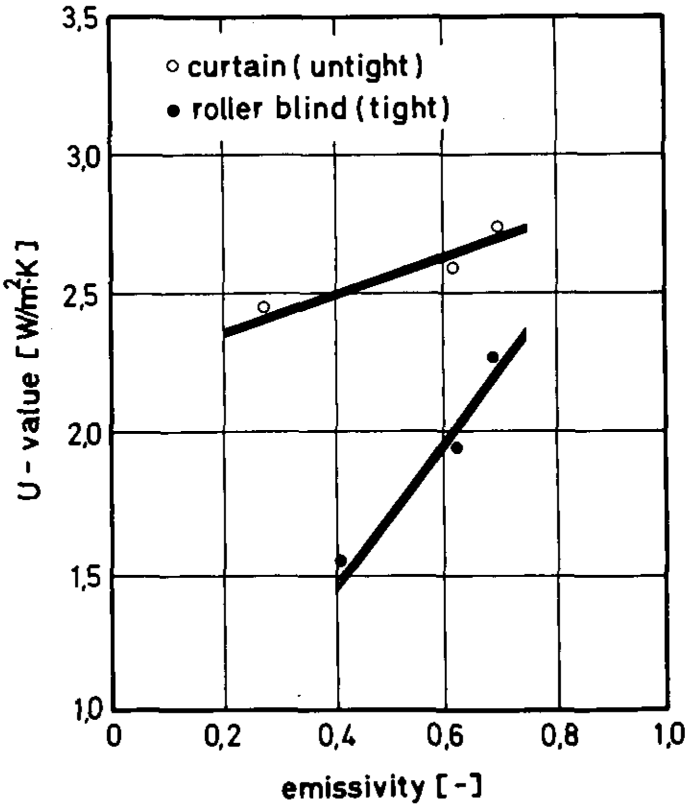

Fig. 9: Measured U-values (window and shutter) as function of the emissivity of the shutter, acc. to (5).

5. INFLUENCE OF INFRARED RADIATION BARRIERS ON OTHER RELEVANT WINDOW CHARACTERISTICS

In selecting the coatings, care has to be taken that the other window relevant values such as light transmittance and solar energy transmittance do not significantly decrease due to improvement of the U-value.
In Figure 10 the total solar energy transmission coefficients are indicated in dependence on the U-value for clear glass and IR-coated glasses and windows with integrated foils acc. to [19] through [22].
It can be observed that solar transmittance decreases as thermal insulation is improved. In the following, two different examples will serve to illustrate, by means of the equivalent U-value, according to [23] how the energy losses adjust during a heating period under average German conditions, with south orientation.

Example 1: Double glazing, according to [19] with IR-coating, wooden frame (25 %) $U_W = 1.8\ W/m^2K$ ($U_{frame} = 1.5$, $U_{glazing} = 1.9$); $g = 0.66$; $\tau_L = 0.63$

Example 2: window, according to [22], with IR-coated foils $U_W = 0.7\ W/m^2K$; $g = 0.34$; $\tau_L = 0.56$

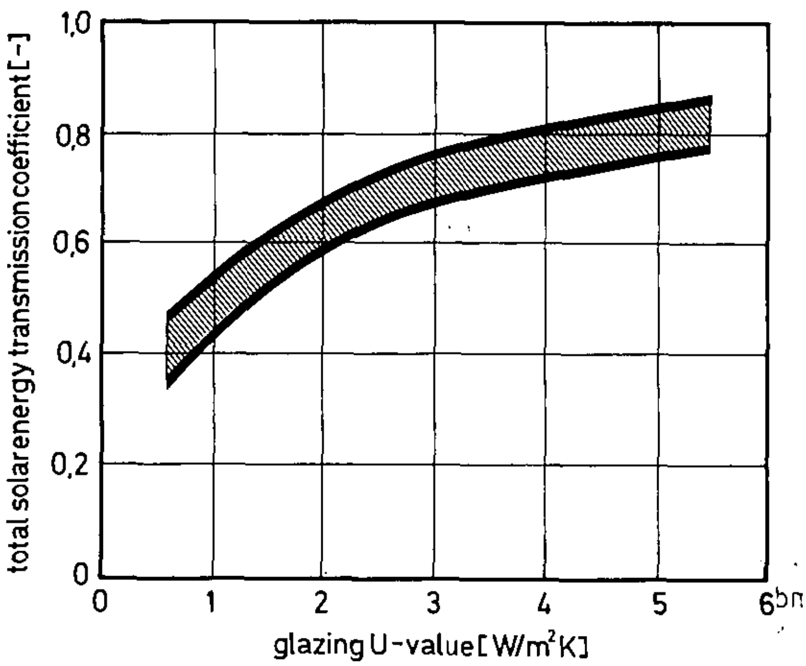

Fig. 10: Total solar energy transmission coefficient as function of the U-value of untreated resp. IR-coated glazings and glazing units with integrated foils. The drawn range only comprises glazings with a high total energy transmission coefficient related to the respective U-value [19 through 22]. Other glazings, e.g. with gold coating, have a far lower total solar energy transmission coefficient.

According to [23] the following is valid for the equivalent U-value describing the average energy losses of a building component during the heating period in view of the solar radiation, of transparent areas with south orientation under average German conditions:
$U_{eq} = U_W - g \cdot 2.4\ [W/m^2K]$

Consequently, the examples lead to the following results:

example 1: $U_{eq} = 0.2\ W/m^2K$
example 2: $U_{eq} = -0.1\ W/m^2K$

Although the exemplary constructions differ from each other by about 1.1 W/m^2K regarding their U-values, they only differ by about 0.3 W/m^2K regarding their energetic behaviour. When comparing the low-ε coated double glazing unit [18] with a commonly used untreated unit (U_W = 2.6 W/m^2K, U_g = 3.0 W/m^2K; g = 0.75; τ_L = 0.8), then Δ Ueq differs much less from Δ Uw (ΔU_W = 0.8, ΔU_{eq} = 0.6). The conclusion is that the total solar energy transmission coefficient will be significantly reduced only for glazing units with multiple IR-coatings and that the energy balance will thus be influenced more unfavourably.

Regarding the daylighting in rooms, construction 2 which is insulated more efficiently has significant disadvantages. This would lead to an increased internal heat load due to artificial lighting. Here, the best values are rendered by the uncoated panes. For more detailed information in this respect please refer to chapter 5.

6. CONCLUSIONS

In part, IR-coatings may considerably contribute to improving the thermal insulating values of window constructions. In evaluating the performance of a complete window system, however, along with the U-values other relevant values have to be considered, too. It is only by comparison of all significant parameters that the intended optimization will be ensured in each individual case.

REFERENCES

[1] Gertis, K.; Erhorn, H.:
Infrarotwirksame Schichten zur Energieeinsparung bei Gebäuden?
GI 103 (1982), H.1, p. 20 - 24 and 33 - 34

[2] Erhorn, H.:
Möglichkeiten zur Verbesserung des Wärmeschutzes von Mehrfachverglasungen. Fenster und Fassade 10 (1983), H.4, p. 105 - 110.

[3] Erhorn, H.:
Halten die Folienrollos, was ihre Entwickler versprechen?
Arcus 2 (1984), H.3, p. 101 - 102.

[4] Knoll, B.; Dubbeld, M.:
Insulation and Climate Effect of Reflective Material on the Parapet and Obstruction of the Convection. Commission of the European Communities. Delft (1984), EUR 9225 EN, P. 27 - 35.

[5] König, N.; Gertis, K.; Snatzke, C.; Völkel, D.:
Temporärer Wärmeschutz von Fensterflächen durch textile Vorhänge und Rollos. Report BW 174/85 of the Fraunhofer Institute of Building Physics, Stuttgart (1985).

[6] Erhorn, H.:
Wie effektiv sind wärmestrahlende Innenraumauskleidungen wirklich?
Bauphysik 5 (1983), H.3, p. 97 - 98.

[7] Erhorn, H. und Gertis, K.:
Wie lassen sich die Wärmeverluste in Brüstungen hinter Heizkörpern wirksam reduzieren? GI 104 (1983), H.5, p. 237 - 238 and 247 - 253.

[8] de Jong, J. et al.:
Energy Saving by Infrared Reflective Finishing.
Report TNO-TH, Nr.: 600.256, Delft (1977).

[9] Zürcher, C.:
Physical Background for Energy Saving by Reduction of the Heat Radiation from Building Envelopes. CIB-Symposium on Energy Conservation in the Built Environment, Copenhagen, Denmark (1979).

[10] Frank, T.; Sagelsdorff, R.:
Reduction of Energy Consumption of Buildings by Application of Spectrally Selective Surfaces. CIB-Symposium on Energy Conservation in the Built Environment, Copenhagen, Denmark (1979).

[11] Hauser, G.:
Fenster und Heizwärmeverbrauch. TAB 15 (1984), H.6, p. 429 - 433.

[12] Gröber, H.; Erk, S.; Grigull, E.:
Die Grundgesetze der Wärmeübertragung.
3rd ed., Springer-Verlag, Berlin (1963).

[13] Gertis, K.:
Belüftete Wandkonstruktionen. Thermodynamische, feuchtigkeitstechnische und strömungsmechanische Vorgänge in Kanälen und Spalten von Außenwänden. Wärme- und Feuchtigkeitshaushalt belüfteter Wandkonstruktionen. Berichte aus der Bauforschung, H.72, Verlag W. Ernst & Sohn 1972.

[14] Gösele, K.; Schüle, W.:
Schall, Wärme, Feuchte. Grundlagen, Erfahrungen und praktische Hinweise für den Hochbau. 7th ed., Bauverlag GmbH, Wiesbaden/Berlin 1983.

[15] Klems, J.H.:
A Calibrated Hotbox for Testing Window Systems. Report LBL 9803 of Lawrence Berkeley Laboratorium, Berkeley (1979).

[16] Künzel, H.; Snatzke, C.:
Das Fenster und seine Wärmebilanz bei Berücksichtigung der Sonneneinstrahlung und zusätzlicher Schutzmaßnahmen.
KI 5 (1977), H.5, p. 191 - 192.

[17] Geiger, W. und Furter, R.:
Praktische Bewertung von Sonnenschutzvorrichtungen mit Hilfe kalorimetrischer Messungen.
Schweiz. BI. Heiz. und Lüftung 45 (1978), H.3, p. 78 - 108.

[18] Without author:
Wärmehaushalt von Gebäuden. p. 51 - 52. From: Schäden erforschen - Schäden vermeiden. Broschüre der fünf europäischen Materialprüfungsanstalten. BAM Berlin (1981).

[19] Pilkington Glass Ltd. (Editor):
Transmission Properties of Windows. St. Helens (1985), United Kingdom

[20] Vegla GmbH (Ed.):
Vegla-Spectrum 1 (1984). Aachen.

[21] Heiersted, R.S.; Nielsen, A.F.:
Coated Glazing and Energy Consumption in Residential Buildings - Measurements and Calculations. Proceedings CIB 83.

[22] Keller, B.; Francelet, P.X.; Roulet, C.A.:
Der Einfluß von hochisolierenden Fenster- und Fassadensystemen auf Raumklima und Energiebedarf. NEFF-Projekt 225, Fa. Geilinger, Winterthur (1985).

[23] Gertis, K.:
Passive Solarenergienutzung - Umsetzung von Forschungserkenntnissen in den praktischen Gebäudeentwurf. Bauphysik 5 (1983), H.6, p. 183 - 194.

3.6. Influence of night protection

A.F. Nielsen
Norwegian Building Research Institute
Division Trondheim
N-7034 TRONDHEIM NTH
NORWAY

LIST OF CONTENTS I

1. Theory

Windows have a higher U-value than the rest of the building envelope. One way of minimizing the heat loss through the window is to use movable insulation. This insulation could be used in periods, when there is no solar gain. In practice the insulation will be used in night periods.

A window with movable insulation will have 2 different U-values, one in the day and another lower one in the night.

In the day:

$$U = \frac{1}{R_i + R_w + R_e}$$

where R_i and R_e is the heat surface resistances
R_w is the surface to surface heat resistance of the window.

In the night:

$$U = \frac{1}{R_i + R_w + R_s + R_e}$$

where R_s is the heat resistance of the night protection including the air layer of the window pane and shutter.

The calculations of the heat resistance should be done as described in earlier chapters taking into account the heat transfer coefficients, the thermal resistance of materials and air cavities. If the construction is complicated it is necessary to make measurements on the construction. This is done in a hot box, where the temperatures and surface air flows can be simulated. Measured and calculated values are given in section 3.3.2. For a more realistic measurement the effect of the shutters can be measured in the field as the difference in total heat loss from the building with shutters open and closed. This has been found to be in good agreement with calculations for the Danish low-energy houses (1).

2. Types of night protections.

The movable insulation can be placed inside, outside or between the window panes. These possibilities have different advantages and disadvantages as described in the next section.

2.1 External insulation.

The most common form is external shutters. In most cases they are of a non-transparent material and must be removed during the day. That is done by using sidehung or horizontal sliding shutters, see examples in (1). Figure 1 shows different external shutter types. External shutters are best used with inside openable windows. Then it is possible to close the shutter from the inside and to escape in case of fire. Other window types could also be used, but in most cases it is necessary to open and close the shutters from the outside. External rollerblinds can also be used, but will never be as good as rigid shutters.

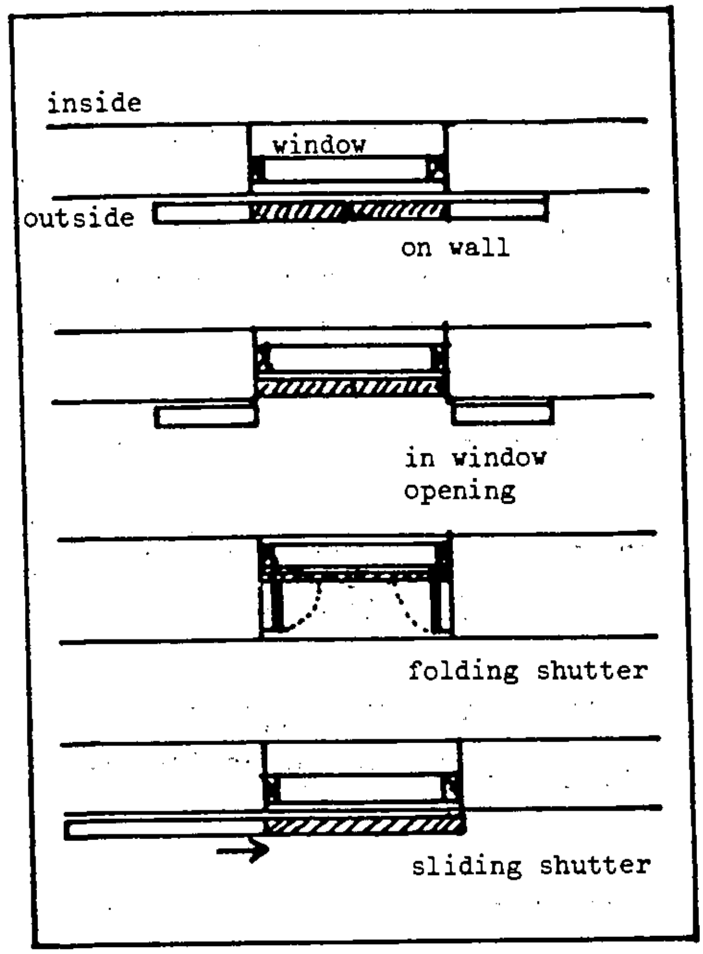

Figure 1. External shutters (2)

2.2 Insulation between the panes.

This type on construction can only be used on fixed windows. The insulation can be placed permanently between the panes as blinds or moved in and out as sliding shutters (figure 2). The shutters could be stored under the window. With three or more panes it is practical to divide the panes in groups placed in separate frames. The insulation is then placed between the frames as foils, on rollers.

Instead of rigid insulation or roller blinds a compressible insulation material can be used. In the day it is compressed below the frame and in the night is pulled up to fill the window. In United States (3) and Denmark (4) test on insulation consisting of polystyrene beads of 5 - 10 mm diameter has been made. The balls are blown in between the panes in the evening and blown out to a storage in the morning.

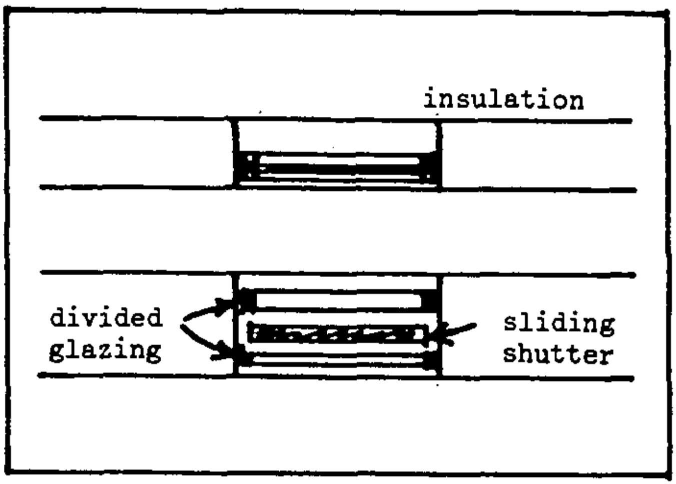

Figure 2. Insulation between the panes (2)

2.3 Internal insulation.

Figure 3 shows internal insulation in the form of shutters or blinds. Internal blinds has been used for many years as a protection against looking into the rooms. They will in many cases also give a lower U-value.

3. Considerations - critical points.

3.1 External insulation.

This method has a few critical points.These are:

The shutter material shall be resistant to the climate, i.e. rain, wind and solar radiation.

The shutter shall be airtight as airflow between the shutter and window pane will give a higher U-value than expected.

If the shutter is placed on the outside of the wall, and not in the window recess, thermal bridge problems can be expected.

In the day shall the shutters be placed so that the solar transmission area of the window is affected as little as possible.

These points show that in windy periode outside roller blinds will give small reductions in heat loss as they are not airtight. The airtightness of the shutter should be measured in the same way as the window in the laboratory with airtesting equipment.

3.2 Insulation between the panes.

The critical points are:

The edge of the insulation shall be fairly airtight against the window frame or there will be extra heat loss from airflow around the insulation.

The insulation material shall always be taken away in the day-time as the construction can operate as a solar collector without any air flow. High temperatures in the glazing can be expected when exposed to direct sun and sealed window panes can crack.

In some cases condensation on the outer glass can occur, if the inner pane and insulation are not airtight.

3.3 Internal shutters.

The critical points are:

Condensation on the inner pane will occour if the shutter is not airtight because the pane temperature decreases and warm humid room air can reach the pane. It is difficult to get an effective seal around the insulated layer. Condensation will also occur when the shutters are taken away in the morning.

Cracks in sealed panes will easyily occur on sunny days caused by the solar collector effect if the insulation is not taken away during the day.

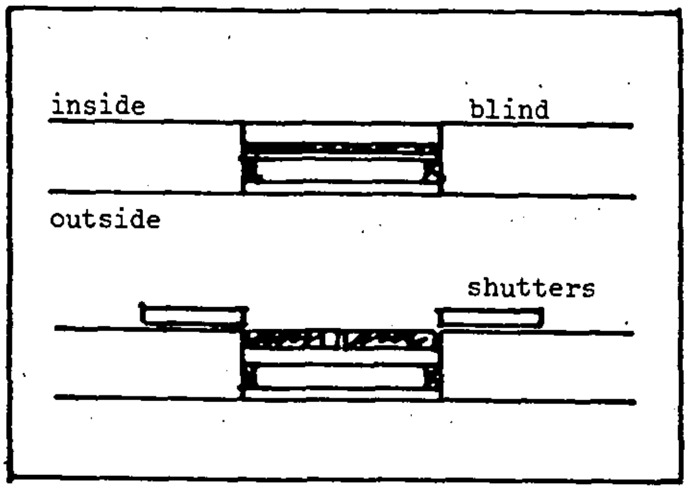

Figure 3. Internal insulation (2)

3.4 General considerations.

Thermal bridge effect has to be taken into account in the construction.

In many buildings the windows are also fire-escape openings and use of shutters may affect the escape time from a room.

Shutters can assist in protecting against burglary.

Night shutters can be used against overheating in the summer, but that will have effect on the energy consumption for light.

In very cold periods with little solar radiation, the shutters can be used both night and day.

It is important that the shutters are easy to handle otherwise they will not be used.

4. Condensation

Condensation occurs on the surface with the lowest temperature in the room if the dew point temperature is higher. Normally the window panes have the lowest temperature, and the condensation occurs there. On winterdays in cold and moderate climate condensation on single glazing will occur. Condensation can be prevented by using windows with more panes. The inside surface temperature will be higher, but the thermal bridge effect from the spacer will still allow the possibility of condensation near the frame. Use of inside insulation will worsen the problem as the temperature difference between the pane and inside air increases. Figure 4 gives the outdoor temperature where condensation will occur for different glass types with indoor temperature of 20°C and variable relative humidity. Examples of cases with internal shutters are found in section 3.4.

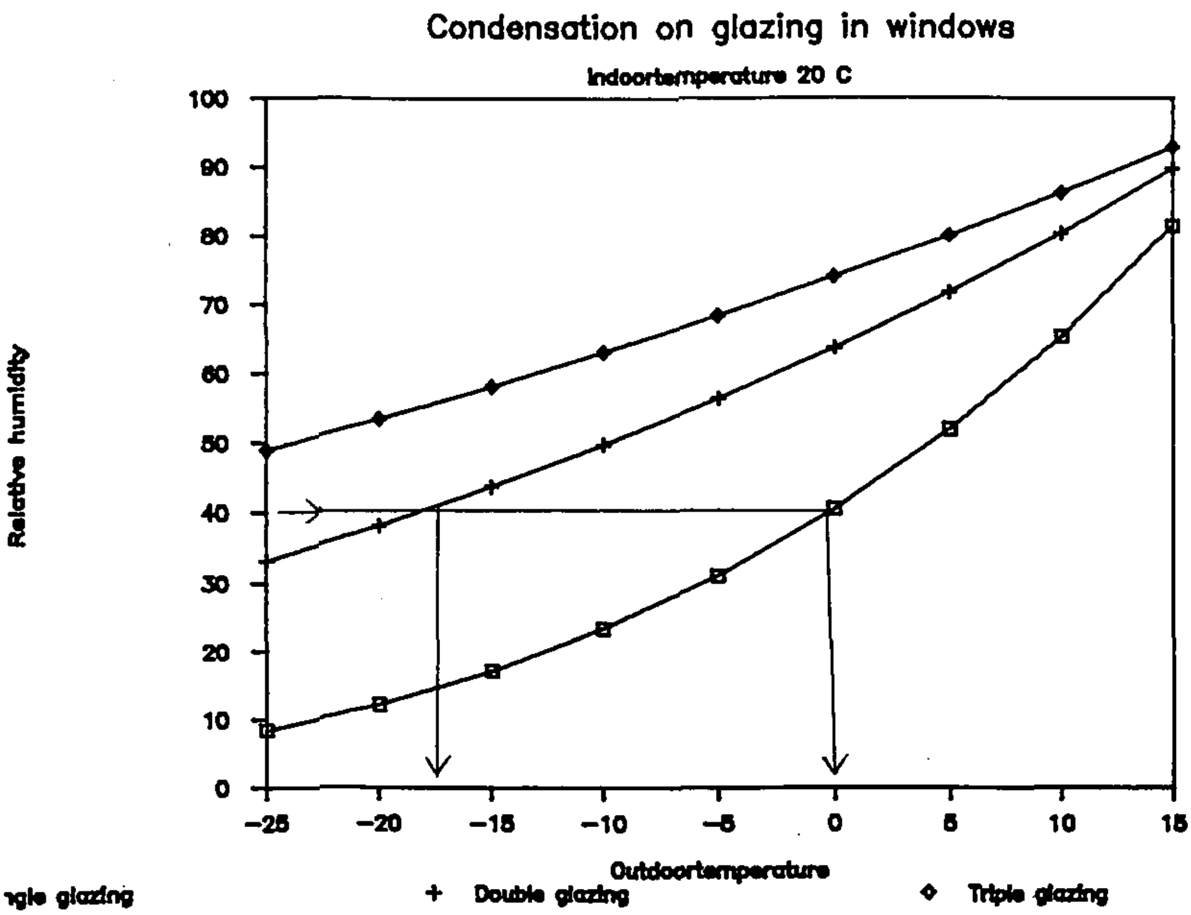

Figure 4. Condensation on the central part of glazings with different relative humidity. If the relative humidity is 40 % then single glazing will show condensation for outdoor temperatures below 0 °C. Double glazing for temperatures below -18 °C. Triple glazing for temperatures below -30 °C. For double and triple sealed unit condensation near the edge will occur at higher temperature because of the thermal bridge. In the central part the dishing effect (contraction of the glazing from pressure difference between air in and outside the sealed unit) can also give condensation at higher outdoor temperature than given in the diagram.

For internal insulation it is important to know the change in inside surface temperature when the shutters are closed and open (5). Figure 5 shows, that the temperature decreases slowly when shutters are closed and the temperature increases rapidly when the shutters are removed. Condensation due to inflow of room air when the shutters are taken away is only a short-term problem.

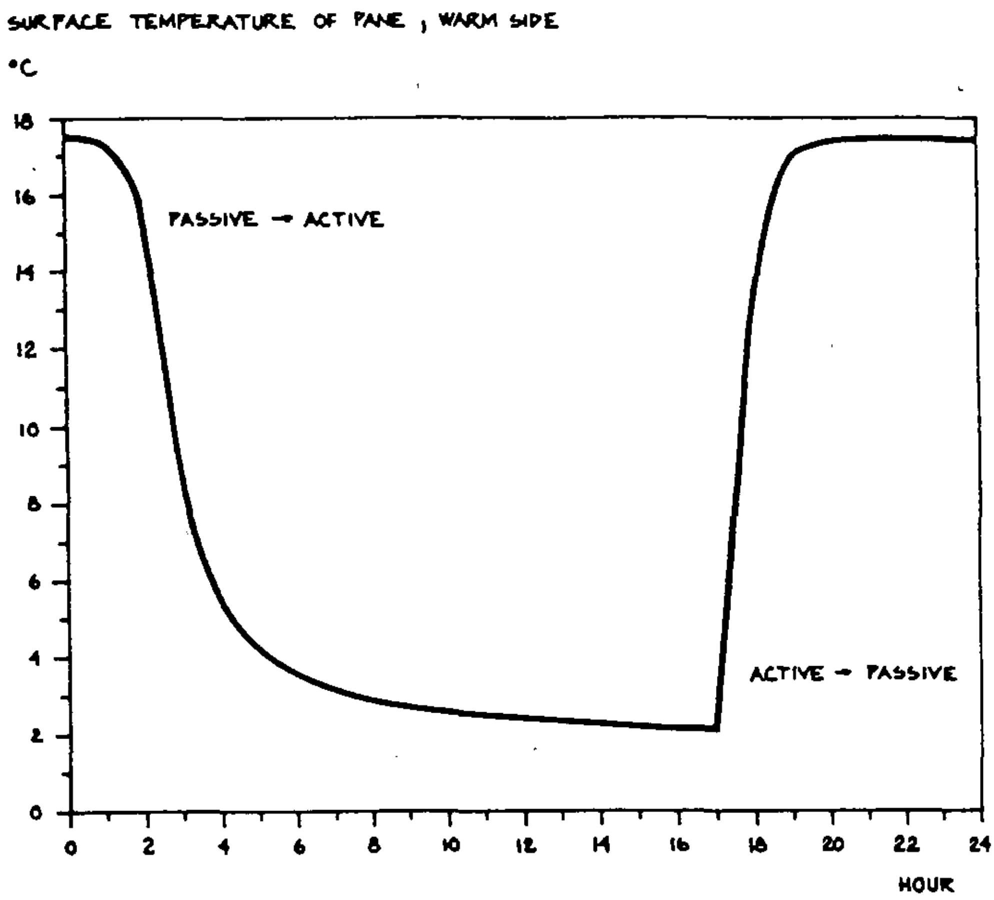

Figure 5. Shutter system with 30 mm PIR foam on double panes. Hot box measurements cold side 0°C, warm side 20 °C. Measured inside pane temperature when the internal shutter was closed at 0 hours and open at 17 hours. The surface temperature increases 11° in 1 hour.

5. Air tightness.

External shutters are exposed to the wind forces, and the insulating efficiency depends on the air tightness of the joints. Tests have been made on the Danish low-energy houses (1) with the tracer gas decay method with pressurization and depressurization. The results are shown in table 1. The cases a, b and c are:

a) all windows closed and all shutters open
b) all windows closed and all shutters closed
c) all windows behind the shutters open and all shutters closed

House type		D	E	F.
Infiltration measurement	a)	0,08	0.10	0.08
(air change pr. hour)	b)	0.08	0.08	0.05
	c)	0.10	0.08	0.06
Depressurization 50 Pa	a)	1.61	1.24	0.64
(air change pr hour)	b)	1.57	1.19	0.53
	c)	2.22	1.23	0.72

Table 1

These tests were done on the whole building, but laboratory measurements can also be made with test equipment used on windows as described in chapter 6. Measurements of airtightness of the shutters are best done during development in the laboratory, but the ageing effects shall be taken into account.

6. U-values

In table 2 and 3 calculated U-values for 2 types of shuttersystems has been presented. In practise the U-values will be higher than calculated because of thermal bridges and non-airtight constructions. Table 4 gives measured values that can be expected to be more reliable.

Further measurements is found in (8) - (11). In this literature is given more information on the construction. Information on a hot-box type, where it is possible to test non-airtight shutters is found in (11). In (9) and (10) is found measurements with different types of windowsills. The difference in energydemand can be approx. 20%.

Panes in window	1	2
no shutters	5,9 W/m²K	3,0 W/m²K
10 mm mineralwool	1,7 "	1,35 "
20 mm "	1.2 "	1,0 "
50 mm "	0,63 "	0,57 "
100 mm " (not practical)	0,35 "	0,33 "

Table 2. Calculated U-values for external shutters. Heat conductivity of mineralwool 0,04 W/mK and heat resistance of airpace between shutter and glass 0,16 m^2K/W.

no	3,0 W/m²K
30 mm	1,3 "
50mm	0,86 "
100 mm	0,46 "

Table 3. Calculated U-values for shuttersystems with polystyrenebeads (assumed heat conductivity 0,05 W/mK) between the glasses in fixed windows.

U-values	Window W/m²K U	Window +shutter W/m²K U	Shutter m²K/W R	Ref.:
Al. Rollershutter ext.	2,6	1,8	0,17	6
PVC Rollershutter ext.	2,6	1,5	0,28	6
Double PVC Rollersh. ext.	2,6	1,3	0,38	6
Jalousie Al. ext.	2,6	1,8	0,17	6
Wood 20 mm shutter ext.	2,6	1,3	0,38	6
Wood + min.wool 50 mm ext.	2,6	1,0	0,61	6
Beadwall 60 mm	2,8	0,7	1,07	6
Shutter 50 mm min.wool ext.	2,5	0,62	1,21	1
Shutter 35 mm EPS ext.	1,71	0,67	0,91	1
Shutter 75 mm min.wool ext.	2,43	0,43	1,91	1
30 mm PIR internal	2,5	0,68	1,07	5
1 foil internal	2,5	1,84	0,14	7
2 foils internal	2,5	1,3	0,37	7
1 woven textile internal	2,5	2,05	0,09	7
1 foil between glasses	2,3	1,1	0,47	4
2 foils between glasses	2,3	0,75	0,90	4
4 foils between glasses	2,3	0,6	1,23	4

Table 4. Measured U-values and heat resistance for the shutters from hot-box measurements.

7. Utilization

The energy savings from shutters depends on the construction, the climate, and how the shutters are used. In most cases they are used between sunset and sunrise. As the night temperature is lower than the mean outdoor temperature the savings will be larger than that calculated with the normal U-values, dayly mean temperature difference and the time used. Use of night time set back of indoor temperature will give less savings.

A good estimate that with good quality external shutters with 40 mm inculation is the same savings as an extra layer of glass in the windows. In Norway the savings will be 10 -15% if the shutters is used 12 hours pr. day from October to March.

Use of season shutters - shutters closed all the winter - will change both the heat loss and solar gain. The savings depends highly on window orientation and U-value. Calculations from Norway indicate that for south facing double windows will energy savings first accur when the U-value of window and shutter is below 1,4 W/m^{2}K. For north facing window below 2,3 W/m^{2}K. The energy savings from season shutters will be lower than night shutters with the same U-value. But season shutters can be better insulated.

There are many theoretical calculations of saving e.g. (2), (5), (6), (7). In practice the user behaviour is very important and the ease of handling. Results from Danish low-energy houses (1) indicate that the shutters are used most nights in the winter and sometimes also during the day in cold periods.

References:

1) Saxhof, B: External insulating shutters in energy conservation houses. Thermal Insulation Laboratory, Technical University of Denmark, report no. 129, 1982.

2) Esbensen, T and Skjoldborg, C: Heatinsulated Windowshutters. Danish Building Research Institute, report 138, 1982 (in Danish)

3) Harrison, O: Beadwalls.
Solar Energy pp 317-19, vol.17, 1975

4) Vest Hansen, T: Highinsulated windowconstructions with mobile nightinsulation (in danish). Thermal Insulation Laboratory, report no. 45, 1977.

5) Byberg, M.R. et al: Insulated shutters.
Thermal Insulation Laboratory, report no. 144, 1983.

6) Frank, Schmid: Temporarer Warmeschutz von Fenstern.
Insitut für Fensterteknik, Rosenheim

7) Dubbeld, M.: Energy saving by using rolling shutters, reflective layer and edge seals and the effect of the window rill. TNO, 1984, EEC-report EUR9225EN

8) Belgian Building Research Institute:
Termische isolatie van Rolluiken, Brussel 1981, Belgium

9) Belgian Building Research Institute:
Experimentele bepaling van de k-waarde van vensters, Brussel 1979

10) Van Veen, G.: Energiebesparing met gordijnen Bouwwereld - 78 (1982) nr 20 blz 50-51 TNO, The Netherlands

11) Nielsen, Tommy: Skodder og persienners lufttæthed, et måleudstyr.
Teknologisk institut, Danmark, 1984

4. SOLAR PROPERTIES OF WINDOWS

4.1. Introduction

H.A.L. van Dijk
TNO Institute of Applied Physics
P.O. Box 155
2600 AD DELFT
The Netherlands

Solar radiation falling on the window consists in general of direct radiation from the sun, diffuse radiation from the sky plus radiation reflected from the ground and surrounding objects (including frame!).
It is obvious that the amount of solar radiation on a window depends on climatic conditions, solar height (thus: latitude and time), orientation and slope of the window.
The solar radiation which reaches the window, is partly reflected, partly absorbed and partly transmitted directly. See figure 1.

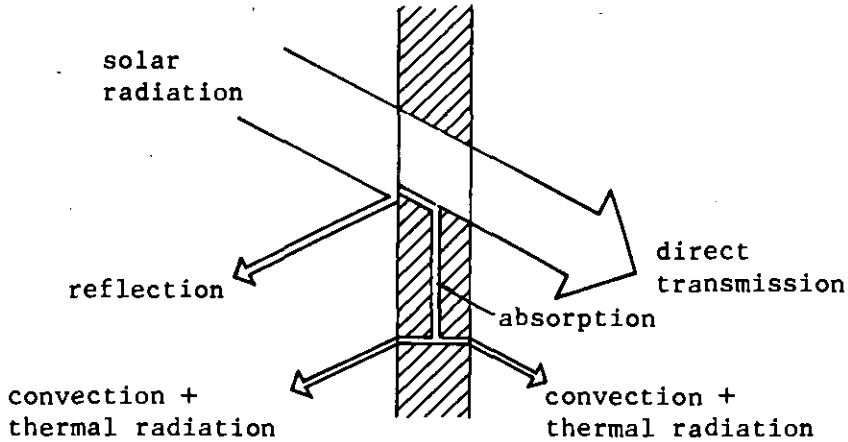

Figure 1: Illustration of the transmission of solar energy through a window.

The direct or primary solar transmission has already been defined as the solar radiation which is transmitted directly through the window and enters the room as short wave radiation.

The secondary solar transmission is the part of the absorbed solar heat which enters the room by convection and thermal radiation.
An important quantity to describe the solar transmission through the window is the total solar energy transmission coefficient (also called 'solar factor'); the ratio between total (direct plus secondary) solar heat penetrating through the window and the given incident solar radiation.

The absorptivity and reflectivity of the window panes or other components depend on wavelength and angle of incidence. The spectrum of the solar radiation ranges from UV and visible to the near infra-red. The dependence on wavelength and angle may also have an effect on the appearance or colour; the dependence on the angle of incidence needs special attention because of the solar height and azimuth and the distribution between direct and diffuse solar radiation.
Moreover, because clear glass is for about 80% transparant for solar radiation one can expect the application of glass types which have a higher absorptance or reflectance for solar radiation.

Concerning the secondary transmission, the network in figure 2 illustrates that - like for the (dark) heat transmission - the heat transfer coefficients play an important role. It is clear that since the temperature differences have a large influence on the heat transfer coefficients, one should be careful in selecting the values. In case of heat absorbed by the inner venetian blinds from figure 2, for instance, the increased temperature of the blind slats will cause an enhanced convective heat flow.

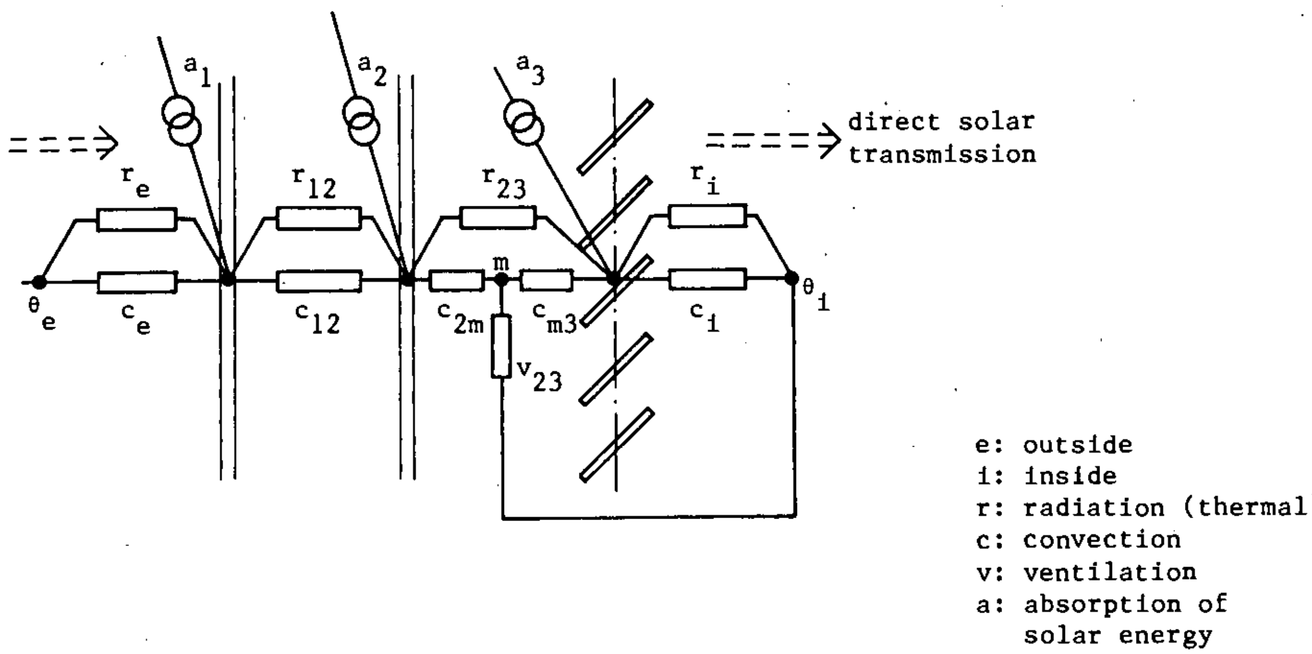

Figure 2: Network representation including solar radiation; example for double glazing with internal blinds.

Obviously, the properties of the window components themselves play a major role, such as:

- the optical properties of the panes and other components;
- the geometry and position of shading devices (e.g. slats).

With known coefficients and properties the solar transmittance, thermal transmittance and the window temperatures can be calculated by solving a network like shown in figure 2. However, only for simple window constructions, like for combinations of parallel airtight panes and sheets coefficients and properties can be predicted with sufficient accuracy.

For more complex windows measurements under realistic indoor and outdoor conditions will often be needed. Only for some special cases computer models are available, e.g. to determine the direct solar transmittance through venetian blinds.

In this chapter 4 the solar transmission properties of windows are introduced.
In section 4.2. a presentation is given on the incident solar radiation and the influence of atmospheric conditions, incidence angle and external shadings.
In section 4.3. the solar properties of windows are presented with an extensive discussion and illustration of the complications mentioned above.
Section 4.4. deals with measurement techniques: laboratory measurements of the solar optical properties (4.4.1.) and field measurements of solar transmission and overall performance (4.4.2.).
Particularly when evaluating the results from the various field test methods the problem areas discussed in section 4.3. are to be taken into account.
Section 4.5. presents a survey of current definitions on solar properties in the countries participating in the project and graphs and tables with actual data from calculations and tests.

4.2. Solar radiation

P. Brunello
Istituto di Fisica Tecnica e Tecnologie Industriali
Università di Udine
ITALY

R. Zecchin
Istituto di Fisica tecnica
Università di Padova
ITALY

LIST OF CONTENTS I

List of symbols

l	:	latitude	(deg)
h	:	hour angle	(deg)
d	:	declination	(deg)
ϑ	:	angle of incidence	(deg)
Θ	:	angle of incidence	(deg)
β	:	solar altitude	(deg)
φ	:	solar azimuth	(deg)
ψ	:	surface azimuth	(deg)
χ	:	tilt angle	(deg)
I	:	solar radiation	(W/m^2)
n	:	day of the year	(–)
M	:	air mass	(–)
A	:	apparent solar irradiation	(W/m^2)
B	:	atmospheric extinction coefficient	(–)
C	:	diffuse radiation factor	(–)
f	:	hourly sunlit fraction	(–)
F	:	mean effective sunlit fraction	(–)
F'	:	angle factor	(–)
ρ	:	reflectivity	(–)
Q	:	monthly solar radiation	(J/m^2)
E	:	quantity of energy	(J)

Subscripts

c	:	solar constants
n	:	normal
λ	:	spectral
D	:	direct
d	:	diffuse
s	:	solar
g	:	ground
t	:	total
h	:	horizontal
r	:	reflected
f	:	of the fin

1. Solar geometry

The sun and its planets with their satellites make up together the "solar system". The sun is of paramount importance because of the energy coming from it which reaches the earth and makes life possible. The solar energy is transferred in the form of thermal radiation, i.e. of electromagnetic waves, and its relationship with the atmosphere, ground and objects is governed by the nature and properties of these waves. Table 1 summarizes some magnitudes concerning the relationship between Sun and Earth.

TABLE 1 – MAGNITUDES CONCERNING SUN AND EARTH

SUN
- mean diameter: 1390×10^3 km
- surface temperature: ~5760 K

EARTH
- mean diameter: 12.7×10^3 km
- surface temperature : ~300 K

EARTH–SUN
- mean distance: 1.5×10^8 km
- tilt of earth's axis on orbit plane: 23.5 deg.

The basic angles for determining the position of the sun with respect to a given point P on the earth surface are (see Fig. 1):

- latitude (l): angular distance of the point P north or south of the equator.
- hour angle (h): angle in the equatorial plane between the projection of OP and the projection of a line from the centre of the sun to the centre of the earth.
- sun's declination (d): angular distance of the sun's rays north (or south) of the equator.

The sun's declination changes through the year as shown in Table 2. The values given in Table 2 are approximated, as the calendar year does not coincide with a complete revolution about the sun; exact values can be obtained from the "Ephemeris Tables" but for the purposes of building energy calculations the values reported here can be considered satisfactory. Alternatively the following empirical equation can be used to calculate the angle d as a function of n, day from start of the year:

$$d = 23.45 \sin (0.986 (284+n)) \qquad (1)$$

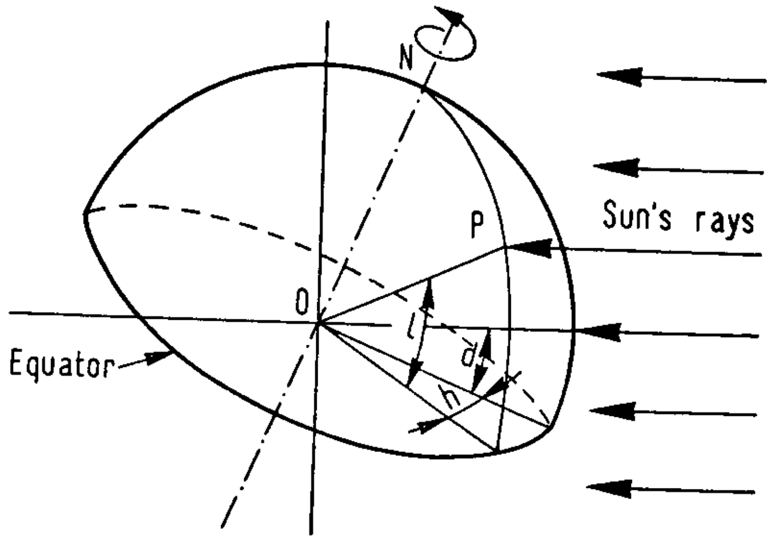

Fig. 1 - Latitude, hour angle, and sun's declination

Solar radiation, together with the other climatic parameters (temperature, wind velocity, etc.) are subject to variations as the time passes. In order to avoid misunderstandings in calculations, measurements and comparisons, it is essential to know what the correct meaning attributed to the word "time" is. The following different definitions can be in fact set up.

Universal Time (UT): the time, expressed in hours, (from 0 to 24), reckoned at the Greenwich meridian (zero longitude);

Local Civil time (LCT): the time reckoned at a given longitude: LCT is more (less) advanced than UT by four minutes for each degree difference in longitude east (west) of Greenwich.
Local Solar time (LST): the time measured by the apparent diurnal motion of the sun.

Standard Time (ST): the time used for clocks setting throughout a zone covering about 15 of longitude: *it is the LCT of a selected meridian near the centre of the zone.*

TABLE 2 – PARAMETERS RELATED TO SOLAR RADIATION

	I_n W/m^2	EOT min.	d deg	A W/m^2	B –	C –
Jan	1395.6	–11.2	–20.00	1229.4	0.142	0.058
Feb	1384.2	–13.9	–10.80	1213.7	0.144	0.060
Mar	1363.4	– 7.5	0.00	1185.3	0.156	0.071
Apr	1340.7	+ 1.1	+11.60	1134.9	0.180	0.097
May	1320.5	+ 3.3	+20.00	1103.3	0.196	0.121
Jun	1309.8	– 1.4	+23.45	1087.6	0.205	0.134
Jul	1311.1	– 6.2	+20.60	1084.4	0.207	0.136
Aug	1324.1	– 2.4	+12.30	1106.5	0.201	0.122
Sep	1344.5	+ 7.5	0.00	1150.6	0.177	0.092
Oct	1366.9	+15.4	–10.50	1191.6	0.160	0.073
Nov	1387.7	+13.8	–19.80	1220.0	0.149	0.063
Dec	1398.4	+ 1.60	–23.45	1232.6	0.142	0.057

Data refers to the twenty–first day of each month

I_n : extraterrestrial solar radiation
EOT : equation of time
d : sun's declination
A : apparent solar radiation at unit air mass
B : atmospheric extinction coefficient
C : diffuse radiation factor

Daylight Saving Time (DST): time one hour in advance of LST, adopted in many countries during the summer.

Equation of time (EOT): the difference between LST and LCT at a given locality, due to variation of earth's orbital velocity, obliquity of earth's orbit etc.

$$LST = LCT + EOT \tag{2}$$

Values of EOT during the year, are given in Table 2. EOT can also be evaluated, expressed in minutes for a give day n from start of the year, by means of the following equation [8]:

$$EOT = -.0002 + .4197\cos(x) - 3.2265\cos(2x) - .0903\cos(3x) - 7.351\sin(x) - 9.3912\sin(2x) - .3361\sin(3x) \tag{3}$$

where:

$$x = 2\pi\, n/366 \tag{3'}$$

The knowledge of the Local Standard Time and of the time, in minutes, elapsed from local solar noon allow for calculating the hour angle (h), expressed in deg:

$$h = 0.25 \times (\text{No. of min. from local solar noon}) \tag{4}$$

For any applications the knowledge of the angle of incidence (ϑ) of the solar beam with respect to a given surface, is necessary; such angle is defined as the angle between the solar beam and a line normal to the given surface.

To determine the angle of incidence the sun position can be most conveniently expressed by means of the following angles (see Fig. 2):

– solar altitude (β): the angle between the sun rays and the horizontal plane;

– solar azimuth (φ): the angle, measured from South, between a vertical plane containing the sun and the Nort–South direction.

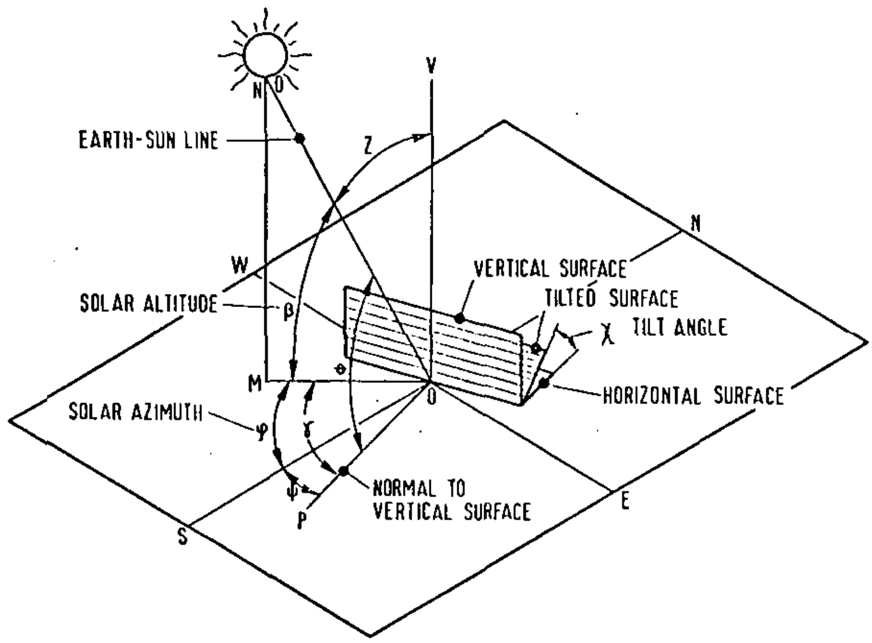

Fig. 2: Solar angles for tilted and horizontal surfaces

The following equations relate the previously mentioned angles (l, h and d) to the angles β and φ:

$$\sin(\beta) = \cos(l)\cos(d)\cos(h) + \sin(l)\sin(d) \tag{5}$$

$$\sin(\varphi) = \cos(d)\sin(h) / \cos(\beta) \tag{5'}$$

As for the surface, its position can be expressed by the following angles (see Fig. 2):

- surface azimuth (ψ): the angle, measured from South, between the vertical plane normal to the surface and the North–South direction;

- tilt angle (χ): the angle between the surface and the horizontal plane.

For any surface the incidence angle ϑ is related to β, φ, ψ and χ as follows:

$$\cos(\vartheta) = \cos(\beta)\sin(\chi)\cos(\varphi - \psi) + \sin(\beta)\cos(\chi) \tag{6}$$

It should be remembered that the surface is in shade if the surface-solar azimuth (φ−ψ) is greater than 90 deg.

2. Solar radiation

The solar constant (I_c) is the solar radiation incident per unit time and unit area upon a surface normal to the sun's rays at the outer limit of the atmosphere when the earth is at its mean distance from the sun; its value is 1353 W/m^2 (4871 kJ/m^2 h, 1164 kcal/m^2 h, 444.7 Btu/ft^2 h) with a probable error of +/– 2%.

Because of the variation of the distance between earth and sun, the solar radiation reaching the outer limit of the atmosphere changes during the year and can be evaluated, at the n–th day, by means of the following equation (values of I_n are given also in Tab. 2):

$$I_n = I_c \left(1 + 0.033 \cos (360\ n/365)\right) \tag{7}$$

The spectral distribution of the solar radiation at the outer limit of the atmosphere (also called "extraterrestrial solar radiation") is shown in Fig. 3, and is quite close to the one of the blackbody at the temperature of 6000 K.

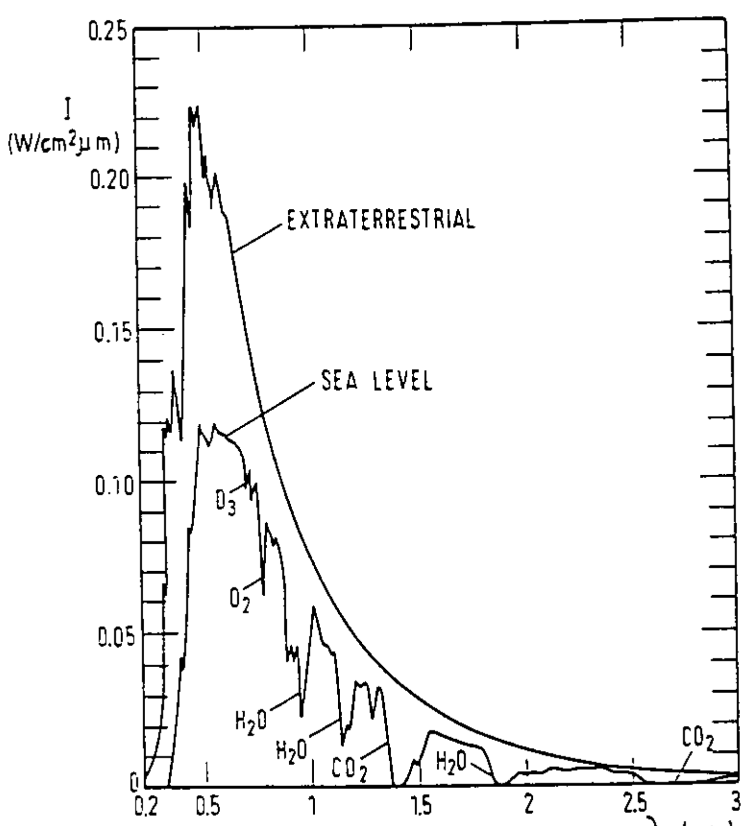

Fig. 3: Spectral distribution of solar radiation

Ultraviolet radiation includes the wavelength range from 0.2 to 0.4 μm; visible radiation covers the range between 0.4 and 0.7 μm; the infrared radiation occurs at higher wavelengths.

Part of the solar radiation crossing the atmosphere is scattered by gas molecules (air and H_2O) and dust particles; moreover part of the radiation is absorbed mainly by O_3 and H_2O). Some of the solar radiation intercepted by the atmosphere reaches anyway the earth's surface in the form of "diffuse solar radiation", while the part of the solar beam directly reaching the the earth's surface forms the "direct solar radiation". In Fig. 3 the spectral distribution of solar radiation at sea level, is given; the most relevant absorption effects are shown as well.

The longer the path of solar radiation through the atmosphere, the more relevant are the above described phenomena. In solar radiation calculations, the unit depth of the atmosphere is taken as ists thickness along the vertical (zenith direction); the ratio of the length of a given path of the sun's rays to this unit thickness is called "air mass" (M) and can be approximated by the following equation.

$$M = 1/\cos(90 - \beta) \qquad (8)$$

It follows that the direct solar radiation on a plane normal to the solar beam on a clear day (I_{Dn}), at ground level is well represented by [1]:

$$I_{Dn} = A/\left(\exp\left(B/\sin(\beta)\right)\right) \qquad (9)$$

where A is the apparent solar irradiation at M = 1, and B is the atmospheric extinction coefficient. A and B are given in Table 2.

The knowledge of I_{Dn} and of the incidence angle (ϑ) allows for the evaluation of the direct solar radiation falling on any surface:

$$I_D = I_{Dn} \cos(\vartheta) \qquad (10)$$

As far as the diffuse component is concerned a simplified general relation for the diffuse solar radiation (I_d), for a clear sky, falling on any surface is given approximately by [1]:

$$I_d = C\, I_{Dn}\, F' \tag{11}$$

where C is the diffuse radiation factor given in Table 2 and F' is the angle factor between the surface and the sky:

$$F' = \left(1 + \cos(\sigma)\right)/2 \tag{11'}$$

An extra amount of radiant energy (called "albedo") can reach a tilted surface due to the solar radiation reflected from the ground (I_g):

$$I_g = I_{Dn}\left(C + \sin(\beta)\right)\rho_g\left(1 - F'\right) \tag{12}$$

where ρ_g is the reflectivity of the ground surface (average values are 0.1 for bitumen, 0.2 for grass, 0.3 for concrete, 0.8 for snow).

The sum of direct, diffuse and albedo components is called usually total solar radiation (I_t):

$$I_t = I_D + I_d + I_g \tag{13}$$

As a result of the actual weather conditions involving a strongly variable cloud cover, the distribution of direct and diffuse components of solar radiation, is quite different from the above described clear sky distribution.

Whenever the actual pattern of solar radiation availability is relevant, data based on long term weather recording should be used. These data are usually available as hourly or monthly values and are mostly collected in form of total solar radiation. When necessary the related direct and diffuse component can be derived by using empirical correlation, as e.g. those due to Liu and Jordan [2].

A more detailed treatment on solar radiation and related topics can be found e.g. in references [1], [3], [4].

3. Shadows by overhangs and vertical fins

It is of great importance, for the energy balance of a building and for thermal load calculations, to determine with accuracy whether and how much the glass surface of a window is shaded by the projections close to it and by buildings around it. This shading reduces the solar heat gain through the window because the shaded portion is not reached by the direct component of the solar radiation, and also the diffuse and ground reflected components are partially intercepted. For a certain time span of the day, however, adjacent shading surfaces can also behave as solar reflectors, thus increasing the amount of solar radiation reaching the window.

The problem is therefore quite complex and a correct account for these effects is usually worthwhile. Shadows can be projected by mountains, buildings, trees, parts of the building considered, or even by the reveals around the windows. From a general point of view one can resort to a mathematical approach based on the solar geometry relationships previously dealt with or in special cases, when the architectural aspect is relevant, even the use of light projection on a model of the building. Here below, the case of the reveal around a window (Fig. 4), which is the most common case, will be considered in some details.

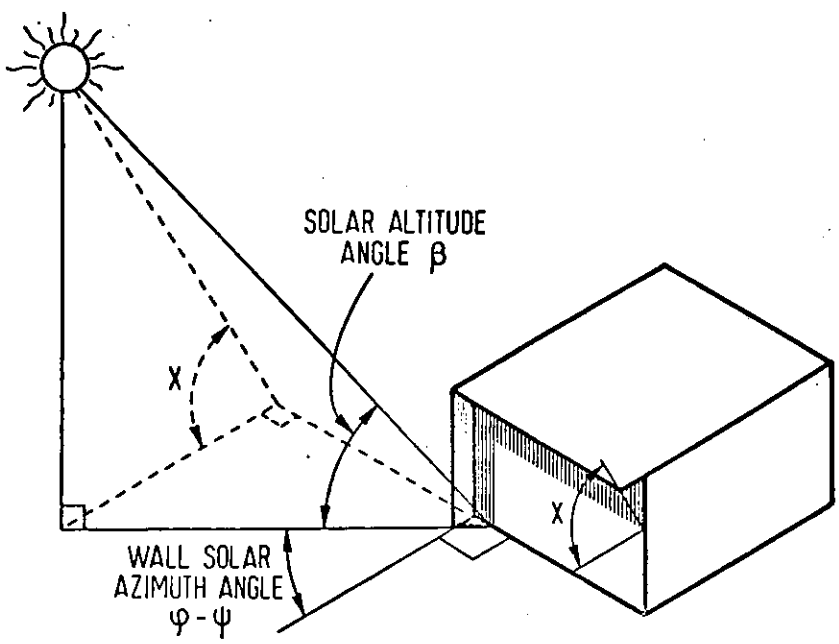

Fig. 4: Solar angles for shade calculations

The location of the sun is defined by the solar azimuth angle (φ) and the solar altitude angle (β). The

location of the sun with respect to the particular wall, with a given azimuth angle ψ, is defined by the wall solar azimuth angle $(\varphi - \psi)$ and the solar altitude angle (Fig. 4).
The shading of a window by a vertical projection alongside the window is the tangent of the wall solar azimuth angle $(\varphi - \psi)$, multiplied by the depth of the projection.

The shading of a window by a horizontal projection above it is the tangent of angle x (a resultant of the combined effects of the altitude angle and the wall solar azimuth angle (B), multiplied by the depth of the projection; it can be easily shown that:

$$\tan(x) = \tan(\beta) / \cos(\varphi - \psi) \qquad (14)$$

Many charts have been developed for quick calculation of shadows; the one proposed by Carrier Co. is reported here [5]: the upper part of the chart shown in Fig. 5 determines the tangent of the wall solar azimuth angle and the bottom part determines tan (x).

For more complex cases and whenever repetitive calculations are involved, the use of computers is becoming more and more common; in this respect the procedure presented in [6] by Tseng–Yao Sun is suggested; the related FORTRAN Subroutine is very efficient for computer simulation of the thermal behaviour of buildings involving an hour–by–hour solution to the energy balance.

Recently, however, some correlation methods based on monthly average climatic data have been developed for energy consumption calculations and are gaining the favour of the users because of their accuracy and simplicity. Consequently, the need arises for determining on a monthly basis suitable mean effective values of the sunlit fraction of a given surface.

In [7] these mean values have been calculated as a function of orientation and relative position of the receiving and shading surfaces, for latitudes around 45 deg and two basic configurations, overhangs and side fins, attached to the window; this approach is discussed here below.

To allow for more detailed calculations, separate coefficients have been derived for the different components of solar radiation (direct, diffuse, reflected by the ground and by the shading surfaces themselves). In fact, an overall coefficient (which obviously can be easily derived by summing up the above mentioned partial coefficients) could not take into account the variation of each component according to different climates, ground characteristics and shading surfaces' reflectivities.

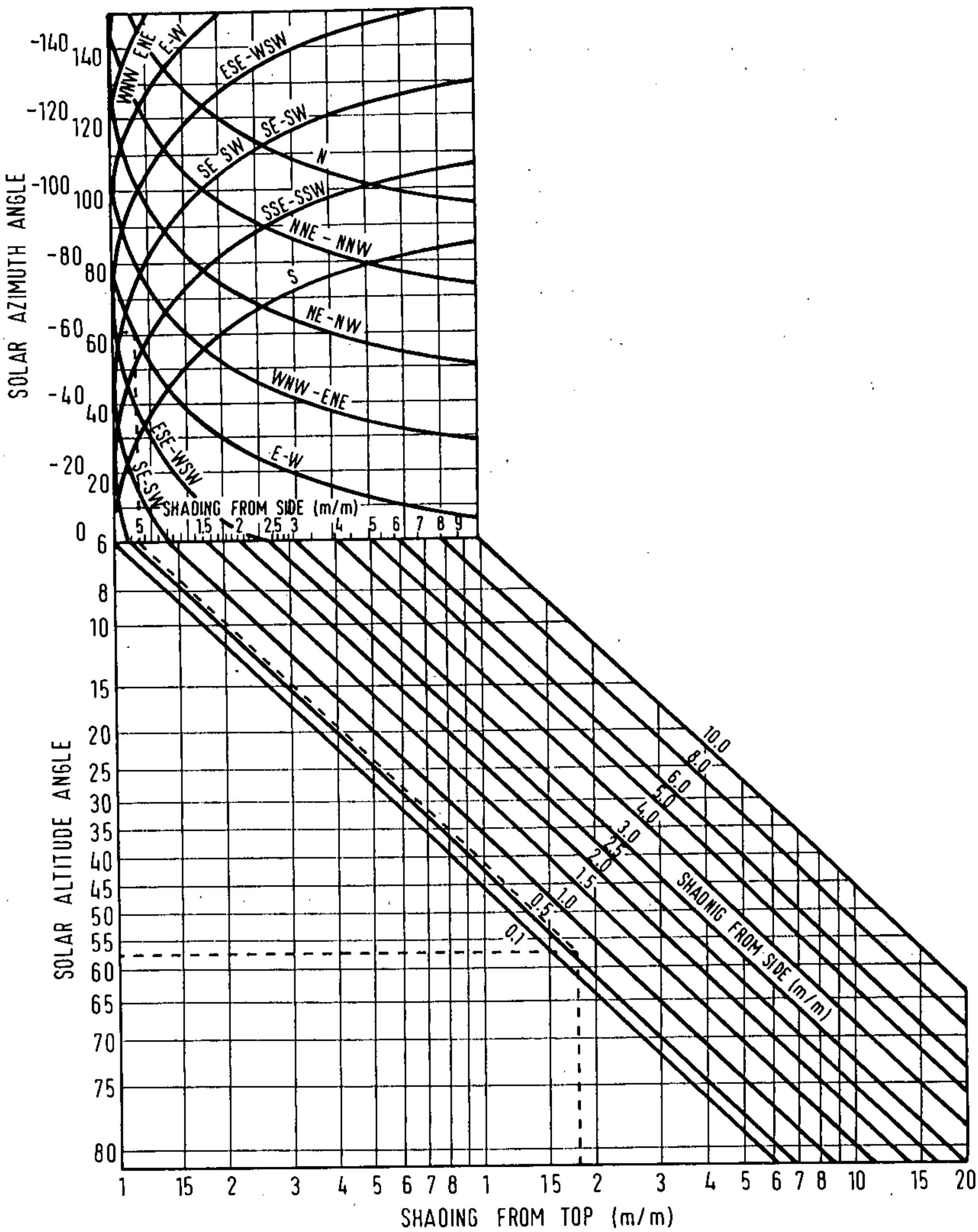

Fig. 5: Chart for shade calculations, according to [5]

a) The coefficients for direct solar radiation

For a given geometry, if $(f_D)_k$ is the sunlit fraction at the k–th hour, the mean effective value F_D can be defined as:

$$F_D = \sum_{i}^{24}{}_k (f_D\, I_D)_k \,/ \sum_k (I_D)_k \tag{15}$$

where $(I_D)_k$ is the direct solar radiation on the window at each hour. Therefore, if Q_D is the monthly direct solar component per unit area for the considered orientation, the related quantity of energy E_D collected by the window with surface S will be:

$$E_D = F_D\, Q_D\, S \tag{16}$$

b) The coefficients for diffuse solar radiation

Even though sky radiation is not isotropic, for the purpose of evaluating the monthly irradiated fraction of a window this hypothesis is acceptable. Thus, by choosing a certain number N of source points uniformly distributed in the sky facing the window and being $(f_d)_j$ the irradiated ratio corresponding to each of them, the mean reduction factor, F_d, will be:

$$F_d = \sum_{1}^{N}{}_j (f_d)/N \tag{17}$$

Obviously, F_d does not change with the month nor with the orientation of the window. If Q_d is the monthly sky component per unit area on the given orientation, the related quantity of diffuse energy collected will be:

$$E_d = F_d\, Q_d\, S \tag{18}$$

c) The coefficients for albedo

The solar radiation reflected by the ground onto a vertical surface is sometimes significant and can be reduced by side fins intercepting the view of part of the ground. The average effect can be calculated by considering a certain number N of directions uniformly distributed on the hemispace in front of the windows at zero height and suitably averaging the resulting irradiated fractions (f_g) of the window:

$$F_g = \sum_{1}^{N}{}_j (f_g \cos(\theta))/N \tag{19}$$

where θ is the incidence angle of each direction. F_g does not vary with month or orientation. The monthly albedo Q_g per unit area on a vertical surface is usually approximated as:

$$Q_g = \rho_g\, Q_{th}/2 \tag{20}$$

where Q_{th} is the monthly total radiation per unit area on a horizontal surface and ρ_g is the ground reflectivity. Therefore, the related quantity of energy E_g collected by the window will be expressed as:

$$E_g = F_g\, \rho_g\, (Q_{th}/2)\, S \tag{21}$$

d) The coefficients for radiation reflected by side fins

The fraction $(f_r)_k$, of the global solar radiation incident on the side fin surface which is reflected onto the window at the k–th hour can be suitably calculated for the different months, orientations and geometries. The average effective value F_r is expressed as:

$$F_r = \sum_{1}^{24}{}_k (f_r I_t)_k / \sum_{1}^{24}{}_k (I_t)_k \tag{22}$$

where I_t is the hourly global solar radiation on the side fin.

For calculating the fractions f_r, a reflectivity of the fin ρ_f=0.35 has been assumed. For different values ρ'_f the effective coefficient simply becomes:

$$F'_r = F_r\, \rho'_f /0.35 \tag{23}$$

If Q_t is the monthly global radiation per unit area on the inner surface of the considered fin, whose surface is S_f, the energy E_r collected by the window will be:

$$E_r = F_r\,Q_t\,S_f \tag{24}$$

The above mentioned reduction factors F_D, F_d, F_g, and F_r have been derived for two basic geometries (with side fins and overhang, respectively), shown in Fig. 6.
Each of them is given in correlation form as follows:

$$F = c_1 + c_2\,X + c_3\,X^2 + c_4\,Y + c_5\,Y^2 + c_6\,XY \tag{25}$$

where X and Y are dimensionless geometrical parameters defined as:

$$X = a/b \qquad\qquad Y = c/b \tag{26}$$

whith a, b, c, shown in fig. 5. The c's coefficients for some months well representing the different periods of the year, are given in Tabs. 3, 4, 5 and 6 at different orientations. Equation (25) has been validated for $1<X<5$ and $0.6<Y<5$. If $Y>5$ for side fins, or $X>5$ for overhangs, it can be assumed that the shade fraction (1-F) of the window varies inversely with Y and X respectively.

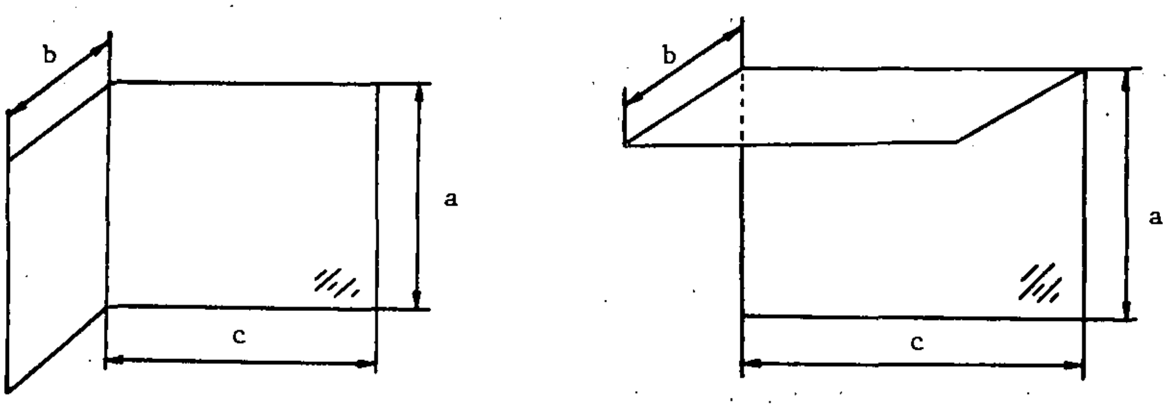

Fig. 6: Geometrical parameters for a window with side fins or overhangs

It is important to observe that the location (right and left) of the side fins with respect to the window, as shown in Fig. 6, must be taken into account and appears on the tables just after the orientation symbol.

TABLE 3 — COEFFICIENTS FOR DIRECT RADIATION - SIDE FINS

DECEMBER

S	SW/r - SE/1	W/r - E/1	NW/r - NE/1
.6583575E+0	.9817492E+0	.1000000E+1	.1000000E+1
-.2266422E-1	.0000000E+0	.0000000E+0	.0000000E+0
.2441688E-2	.0000000E+0	.0000000E+0	.0000000E+0
.1840062E+0	.1204265E-1	.0000000E+0	.0000000E+0
-.2412011E-1	-.1675707E-2	.0000000E+0	.0000000E+0
.1653661E-2	.0000000E+0	.0000000E+0	.0000000E+0

N	NE/r - NW/1	E/r - W/1	SE/r - SW/1
.0000000E+0	.2563688E-1	-.1527464E-1	.3273833E+0
.0000000E+0	-.2303274E-1	-.8372018E-1	-.7367104E-1
.0000000E+0	.3662576E-2	.9975188E-2	.8367244E-2
.0000000E+0	.2914308E-1	.3015773E+0	.3188503E+0
.0000000E+0	-.4046922E-3	-.2512756E-1	-.3889975E-1
.0000000E+0	-.4627896E-2	-.1637155E-2	.2192373E-2

MARCH , SEPTEMBER

S	SW/r - SE/1	W/r - E/1	NW/r - NE/1
.7217833E+1	.7276053E+0	.1000000E+1	.1000000E+1
-.7438363E-1	-.1963830E-1	.0000000E+0	.0000000E+0
.7970220E-2	.1786600E-2	.0000000E+0	.0000000E+0
.1440666E+0	.1595515E+0	.0000000E+0	.0000000E+0
-.1764336E-1	-.2179747E-1	.0000000E+0	.0000000E+0
.3439377E-2	.1859242E-2	.0000000E+0	.0000000E+0

N	NE/r - NW/1	E/r - W/1	SE/r - SW/1
.0000000E+0	.1235256E+0	.3229005E+0	.7838658E+0
.0000000E+0	-.1191721E+0	-.1318897E+0	-.7838658E-1
.0000000E+0	.1484863E-1	.1400496E-1	.7811745E-1
.0000000E+0	.1911236E+0	.4084612E+0	.1488189E+0
.0000000E+0	-.6382186E-2	-.5370123E-1	-.1985924E-1
.0000000E+0	-.5412668E-2	.6281510E-2	.4240694E-2

JUNE

S	SW/r - SE/1	W/r - E/1	NW/r - NE/1
.8562810E+0	.5517147E+0	.8205751E+0	.1000000E+1
-.1021012E+0	-.1306157E+0	-.1158203E-1	.0000000E+0
.8545905E-2	.1329032E-1	.1181140E-2	.0000000E+0
.1267566E+0	.2449733E+0	.1066600E+0	.0000000E+0
-.1735129E-1	-.3068576E-1	-.1464583E-1	.0000000E+0
.6143565E-2	.7932172E-2	.8763518E-3	.0000000E+0

N	NE/r - NW/1	E/r - W/1	SE/r - SW/1
.1584781E+0	.2109747E+0	.8978539E+0	.9696248E+0
-.1079525E+0	-.1619418E+0	-.7058647E-1	-.3034492E-1
.1679404E-1	.1679404E-1	.6352358E-2	.1846154E-2
.9186073E-1	.4818090E+0	.1056831E+0	.3722388E-1
.8956682E-2	-.6328511E-1	-.1588301E-1	-.5817287E-2
-.1069628E-1	.7807618E-2	.5786315E-2	.3211286E-2

TABLE 4 — COEFFICIENTS FOR RADIATION REFLECTED BY SIDE FINS

DECEMBER

S	SW/r - SE/1	W/r - E/1	NW/r - NE/1
.6812917E-1	.8282978E-1	.5792674E-1	.8914035E-2
.1205531E-1	.1627286E-1	.9326912E-2	.1992773E-2
-.1250620E-2	-.1985112E-2	-.1022332E-2	-.1389578E-3
-.3551842E-1	-.4354403E-1	-.2789582E-1	-.5361893E-3
.4308545E-2	-.5389217E-2	.3378578E-2	-.2559981E-3
-.3166266E-3	-.4861942E-3	-.6197477E-3	-.2881153E-3

N	NE/r - NW/1	E/r - W/1	SE/r - SW/1
.2656610E-1	.3902614E-1	.3902614E-1	.4596127E-1
.3725063E-3	.6522808E-2	.6522808E-2	.2299117E-2
-.7942729E-4	-.7543423E-3	-.7543423E-3	-.9925561E-4
-.1164338E-1	-.2002920E-1	-.2002920E-1	-.1963661E-1
.1090774E-2	.2629227E-2	.2629227E-2	.2476543E-2
.4861360E-3	-.3736494E-3	-.3736494E-3	-.3676468E-3

MARCH , SEPTEMBER

S	SW/r - SE/1	W/r - E/1	NW/r - NE/1
.6996718E-1	.4941154E-1	.5535686E-1	.4572193E-1
.9629758E-2	.7687849E-2	.5623383E-2	.6229408E-2
-.8833747E-3	-.6650127E-3	-.3176182E-3	-.5856082E-3
-.3484270E-1	-.2447213E-1	-.2692943E-1	-.2309202E-1
.4201334E-2	.3120874E-2	.3456015E-2	.3065358E-2
-.2761104E-3	-.6992797E-3	-.6797718E-3	-.6077430E-3

N	NE/r - NW/1	E/r - W/1	SE/r - SW/1
.2656722E-1	.2701147E-1	.3510731E-1	.4941154E-1
.3712407E-3	.8769605E-2	.8893620E-2	.7687849E-2
-.7913244E-4	-.1041876E-2	-.1062035E-2	-.6650127E-3
-.1164280E-1	-.1574753E-1	-.1979720E-1	-.2447213E-1
.1091049E-2	.19333540-2	.2654969E-2	.3120874E-2
.4856093E-3	-.1534122E-3	-.4726890E-3	-.6992797E-3

JUNE

S	SW/r - SE/1	W/r - E/1	NW/r - NE/1
.5294620E-1	.3204721E-1	.4499137E-1	.5490587E-1
.5793816E-2	.7273187E-2	.7246659E-2	.8693293E-2
-.5260548E-3	-.7940448E-3	-.7344913E-3	-.9131517E-3
-.2623012E-1	-.1788570E-1	-.2216627E-1	-.2674258E-1
.3355026E-2	.2446770E-2	.2805464E-2	.3277588E-2
-.4636855E-3	-.4306721E-3	-.5042016E-3	-.5852338E-3

N	NE/r - NW/1	E/r - W/1	SE/r - SW/1
.2842331E-1	.2822006E-1	.4596127E-1	.5792674E-1
.2123589E-2	.4947459E-2	.2299117E-2	.9326912E-2
-.2779017E-3	-.5260516E-3	-.9925561E-4	-.1022332E-2
-.1514948E-1	-.1692768E-1	-.1963661E-1	-.2789582E-1
.1725048E-2	.2264314E-2	.2476543E-2	.3378578E-2
.4140955E-3	-.1350872E-4	-.3676468E-3	-.6197477E-3

TABLE 5 — COEFFICIENTS FOR DIRECT RADIATION - OVERHANGS

DECEMBER

S	SW - SE	W - E	NW - NE
.6865997E+0	.7045241E+0	.8896798E+0	.9743633E+0
.1570513E+0	.1641611E+0	.9480339E-1	.2303263E-1
-.1959305E-1	-.2124070E-1	-.1357816E-1	-.3662530E-2
-.6647628E-1	-.9953736E-1	-.1359779E+0	-.2914322E-1
.7177373E-2	.9418348E-2	.9945637E-2	.4047292E-3
.4444780E-2	.8052224E-2	.1381003E-1	.4627852E-2

MARCH , SEPTEMBER

S	SW - SE	W - E	NW - NE
.3946133E+0	.2793407E+0	.5793743E+0	.8342525E+0
.3425205E+0	.3384076E+0	.2351007E+0	.1377892E+0
-.4428783E-1	-.4079404E-1	-.2944913E-1	-.1975185E-1
-.2405340E+0	-.1213074E+0	-.1735935E+0	-.1797894E+0
.2388837E-1	.1282408E-1	.1842390E-1	.1212161E-1
.1858643E-1	.6838236E-2	.1019958E-1	.1776111E-1

JUNE

S	SW - SE	W - E	NW - NE
.3898929E+0	.2993838E+0	.1475811E+0	.6112601E+0
.1997252E+0	.2519035E+0	.3496385E+0	.2276654E+0
-.1290323E-1	-.2497271E-1	-.3937469E-1	-.2793052E-1
-.3196495E+0	-.2049561E+0	-.7794288E-1	-.2180556E+0
.4027730E-1	.2344580E-1	.9696432E-2	.2443956E-1
-.1006901E-2	.9284214E-2	.1186975E-2	.1021759E-1

TABLE 6 — COEFFICIENTS FOR DIFFUSE RADIATION AND ALBEDO

SIDE FINS		OVERHANGS	
DIFFUSE RAD.	ALBEDO	DIFFUSE RAD.	ALBEDO
.8064304E+0	.5260172E+0	.7093850E+0	.1000000E+1
-.3791048E-1	.3647472E-8	.1259059E+0	.0000000E+0
.3870970E-2	-.2313656E-9	-.1388585E-1	.0000000E+0
.9156904E-1	.1228718E+0	-.1046224E+0	.0000000E+0
-.1086153E-1	-.1242198E-1	.1104618E-1	.0000000E+0
.1277012E-2	-.7988831E-9	.3960083E-2	.0000000E+0

By example the direct radiation coefficient, F_D, for a window facing east with a side fin on the left, can be calculated, for the month of June, as:

$$F_D = .8978539 - .07058647\,X + .006352358\,X^2 + .1056831\,Y - .01588301\,Y^2 + .005786315\,XY$$

Therefore, for example, given a window with a=1.5 m, b=0.30 m, and c=1m it results:

$$X = 5 \qquad Y = 3.33 \qquad F_D = 0.975$$

If side fins and overhangs as herewith described are present at the same time, there is no shadow overlapping, and the shaded fractions (1–F) can be summed up (caution should be paid only for reflected radiation as the amount of energy on the inner surface of each fin could be affected by the other shading components).

REFERENCES

[1] "ASHRAE Handbook, 1977 Fundamentals", Chapter 26, ASHRAE, New York, 1977.

[2] Liu, B.Y., and Jordan, R.C., "The Interrelationship and Characteristic Distribution of Direct, Diffuse and Total Radiation", Solar Energy, 4, 1960.

[3] Threlkeld J.L. "Thermal Environmental Engineering", Prentice Hall Inc., 1970.

[4] Duffie, J.A. and Beckman, W.A. "Solar Energy Thermal Processes", J. Wiley & Sons, 1974.

[5] "Handbook of Air Conditioning System Design", Carrier Air Conditioning Company, McGraw-Hill, 1965.

[6] Sun, T.Y. "Shadow Area Equations for Window Overhangs and Side Fins and their Applications in Computer Calculations" ASHRAE Semiannual meeting, Columbus (OH), 1968.

[7] Brunello, P., Lissia, G. and Zecchin, R. "Monthly Effective Shaded fractions of Windows for Energy Calculations" Solar '85, Rayleigh (NC), 1985.

[8] Kusuda, T. "NBSLD, the Computer Program for Heating, and Cooling Loads in Buildings" NBS-BSS 69, Washington D.C., 1976.

4.3. Solar properties of Fenestration

P. Brunello
Istituto di Fisica Tecnica e Tecnologie Industriali
Università di Udine
ITALY

R. Zecchin
Istituto di Fisica tecnica
Università di Padova
ITALY

List of symbols

ϑ	:	incidence angle	(deg)
I	:	radiation flux	(W/m^2)
k	:	extinction coefficient	(m^{-1})
ρ	:	reflectance	(–)
α	:	absorptance	(–)
τ	:	transmittance	(–)
λ	:	electromagnetic radiation wavelength	(μm)
q	:	heat flux	(W/m^2)
t	:	temperature	(C)
U	:	overall heat transfer coefficient	(W/m^2K)
h	:	surface heat transfer coefficient	(W/m^2K)
C'	:	characteristic parameter	(–)
C	:	characteristic parameter (mean value)	(–)

Subscripts

L	:	referring to thickness L
b	:	backward
a	:	absorbed
t	:	transmitted
s	:	of shading
r	:	short wave radiation
c	:	convection
i	:	infrared
p	:	conduction
m	:	mean
e	:	effective

1. Optical properties of glazing materials

Fenestration, term used for any light transmitting opening in a building envelope, usually includes glazing materials and shading devices.

Glazing materials commonly used are glass or plastic sheets and other materials having good light transmittance. The shading devices, applied for both glass protection and privacy, are draperies, venetian blinds and roller shades.

The optical properties of window glazing materials have been measured extensively only for the so-called clear glass, even though some of the most widely used optical data originates before plate glass was almost completely replaced with glass produced by the modern float process. For other glazing materials the available data are contradictory and incomplete.

The optical properties of glass to be considered are the index of refraction and the absorptivity. Both characteristics are functions of the wavelength of the incident radiation. Ordinary glass transmits the shorter wavelength (0.2 to 3 μm) with relative ease, whereas it is entirely opaque to the longer wavelenghts range. Only the performance within the former range needs to be considered, therefore, with respect to absorption and index of refraction. For all practical purposes both of these properties can be considered to remain constant throughout the wavelength range of the solar spectrum.

The index of refraction is a measure of the degree to which a radiant ray is bent toward the perpendicular to the surface of a substance of high density, through which it has to pass, from a substance of lesser density such as air. The index of refraction is defined by Snell's law, as the ratio of the sine of the angle of incidence, ϑ_1, to the sine of the angle of the refracted ray, ϑ_2, (Fig. 1):

$$n = \sin(\vartheta_1) / \sin(\vartheta_2) \qquad (1)$$

A value of $n = 1.526$ is a common assumption for glass.

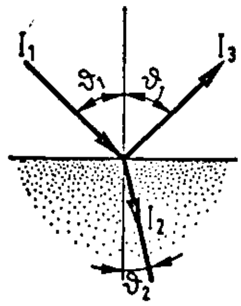

Fig. 1 - The phenomenon of refraction and reflection

Reflection of radiant waves from either surface of the transparent substance is closely related to this property, and can be expressed by suitable relationships derived by Fresnel; e.g. for nonpolarized radiation:

$$\frac{I_1}{I_3} = \frac{1}{2} \cdot \left[\frac{\sin^2(\vartheta_2-\vartheta_1)}{\sin^2(\vartheta_2+\vartheta_1)} + \frac{\tan^2(\vartheta_2-\vartheta_1)}{\tan^2(\vartheta_2+\vartheta_1)} \right] \tag{2}$$

where I_1 is the incident radiation and I_3 the backward reflected component.

The remaining part I_2, forward transmitted inside the glazing material, is affected by the absorption characteristics of the glass, dependent upon its chemical constituents. E.g. ferric and ferrous oxides are two compounds used to increase the absorption of glass for solar radiation. The former is strongly absorbent in the ultra-violet portion and various degrees of absorption are obtained by controlling the quantities of these two compounds. The thickness of the glass sheet is also a factor in reducing the energy of the ray inside the glass.

Such effects can be described by Bourger's law, providing the ratio between the intensity of the radiation I_L after a lenght L and the initial one I_2.

$$I_L / I_2 = e^{-kL} \tag{3}$$

where k is the extinction coefficient of the considered material.

When reaching the opposite surface of the glazing material, the ray is partially transmitted (thus exiting the glass pane) and partially reflected again into the glass (thus generating multiple reflection–absorption phenomena as shown in Fig. 2).

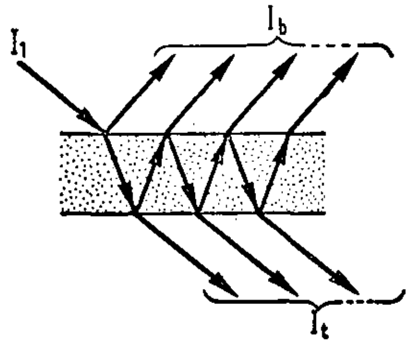

Fig. 2 - Multiple reflection and refraction inside a glass pane

By suitably summing up these multiple effects, overall reflectance ρ, absorptance α and transmittance τ can be defined for the considered glass pane:

$$\rho = I_b / I_1 \tag{4}$$
$$\alpha = I_a / I_1 \tag{5}$$
$$\tau = I_t / I_1 \tag{6}$$

where I_b, I_a and I_t are the total radiations reflected outside, absorbed and transmitted through the glass sheet.

The glass manufacturer can control such properties of his product over wide range by resorting to two basic techniques: the addition of suitable chemicals (mainly oxides, as above mentioned) to the mass of the glass, or the addition of coatings or films on the surface of the glass.

The first way allows for the control of the absorptance and therefore of the transmittance with minor effect on reflectance; the second one can be used either for reflection and absorption purpose, although the use for reflectance control is more common practice.

It must be stressed that, when a heat-absorbing coating is applied to a clear glass, the resulting increase in temperature may be great enough under severe conditions to cause excessive expansion, and cracking is likely to occur if adequate provision has not been made for this contingency.

Moreover, it should be noted that absorbing glasses do not reject the absorbed heat completely: part of it is transmitted by convection and infrared radiation, as shown in § 3.

As far as surface treatments are concerned, during the past years many techniques, which can materially increase the reflectance for solar radiation, have become available. These include durable ceramic coatings with reflectances up to 0.25, adhesive metalized films with reflectances from 0.22 to 0.45, and vacuum-deposited metallic films with relatively high reflectance for longwave as well as solar radiation. The latter are, in general, not sufficiently durable for use where they must be washed and so they are finding their place in laminated glass, which retains the high reflectance but protects the film, and in insulating windows (double glazing).
Ceramic coatings are both durable (in some cases they are harder than the base glass) and have low longwave emittance. The metallic coatings which produce the high solar reflectances mentioned proviously also have low longwave emittances, but when they are used in laminated glass, they do not alter the glass emittance.

Organic coatings instead, used for increasing the absorptance, have a slightly higher longwave emittance than the 0.84 now recommended for use with glass, but the effect on the surface coefficients is too small to be considered.

Emittance values down to 0.2 and 0.1 for hard and soft coatings respectively have been so far achieved. A reduction in the emittance of the glass surface can cause a marked reduction in the inner surface coefficient and therefore exerts a strong influence upon both the window U-value and the inward-flowing fraction of the absorbed radiation.
The optical properties τ, and α of some glass sheets available on the market are shown as a function of wavelength (Fig. 3) and of the angle of incidence (Fig. 4).

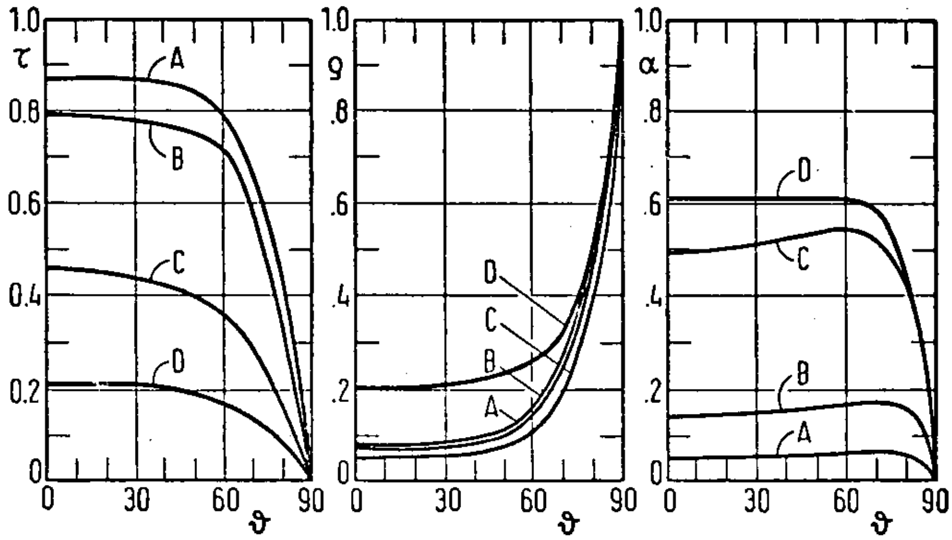

Fig. 3 - Optical properties of some glasses as a function of incidence angle [1], [2]:

A: common window glass (3 mm)

B: soda-lime glass (6 mm)

C: green heat absorbing plate (6 mm)

D: solar reflecting glass 35/22

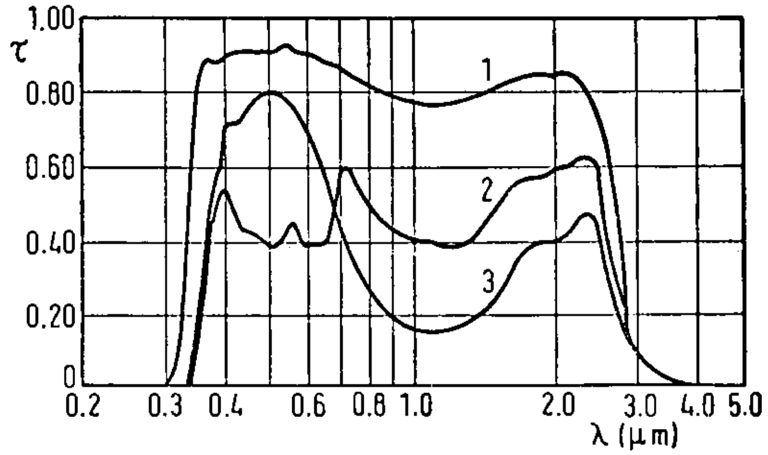

Fig. 4 : Spectral transmittance for typical architectural glass [1]:

1: common window glass (3 mm)

2: gray heat-absorbing plate (6 mm)

3: green heat-absorbing plate (6 mm)

2. Optical properties of shading devices

Fenestration in residential and commercial buildings is often combined with shading devices, namely draperies, venetian blinds, rolling shutters etc. A choice of shading devices involves several considerations related to the different tasks which such elements have to perform.

Shading devices are sometimes depended upon to give a certain degree of privacy. When draperies are closed, two major factors determine the degree of privacy: closeness of weave and on which side the major illumination is with respect to the side on which privacy is desired.

As far as comfort conditions are concerned, radiant energy protection and brightness control shall be considered.

Thermal comfort depends on several factors including not only the temperature of air but also the temperatures of surrounding surfaces. A relatively cold surface nearby, such as a bare glass in winter, can have a strong effect on a person's comfort: as well as sources of heat as warm glass or direct sun radiation. Shading devices must therefore be suitably placed on the interior or the exterior of the window in order to avoid common mistakes as, for example, interior absorbing curtains which are easily overheated by the sun if no additional external devices are present.

Light colored shading devices possessing the greatest total surface area usually provide the best protection as they reflect back outdoors a portion of the entering radiation, and the air conditioning system, if present, is able to pick up by convection the heat they have absorbed, thereby keeping their surfaces relatively cool. This results in minimum re-radiation.

Eye comfort is essential in most occupied spaces. Direct sunlight should not strike the eye, neither should bright glare or light from "too bright" surfaces. Thus, indoor shading devices transmitting light to indoors should be of an off-white color so that when exposed to full sunlight the surface is not too bright.

When two indoor shading devices are used, the one on the indoor side (away from the window) should be the darker, and usually the more open of the two so that it can be used as a brightness control for the other shading device: or, when used alone it can provide brightness reduction for the outdoor view.

Similarly to glasses, the relevant solar optical propeties of shading devices are the reflectance, absortpance and transmittance of the material in respect to solar radiation. However, three basic types of shading devices must be separately considered.

A relatively thin layer of material, such as a sheet of paper, having radiation impinging upon it, may be described in terms of reflectance and transmittance, with the remainder to make up unity being attributed to absorptance, as for a sheet of glass.

A fabric instead, must be regarded as a grid that is a layer or sheet with parts of the area missing. The reflectance of the fabric is, therefore, the reflectance of the surface itself times the fraction of the surface that is present, meaning the total area minus the openings. The transmittance of the fabric is the transmittance of the sheet times the area which is present, plus the fraction of the surface that is absent.

Yarn is made up of many fibers, twisted and plied. A woyen fabric is, therefore, not exactly like a thin layer or sheet because radiation is believed to be reflected from fiber to fiber and thence through the fabric or through the openings between yarns, even if the fibers are themselves opaque to the radiation involved. The radiation comes out of the other side in diffuse form. Also, if the fibers are transparent, diffraction, reflection, multiple absorption and considerable reflection back toward the source take place.

Data for draperies of different closeness can be found, for example in [3] as shown in Fig. 5.

Such effects are significant even in the case of venetian blinds, where the single sheets of metal are completely separated from each other and can be tilted at occupant's choice.

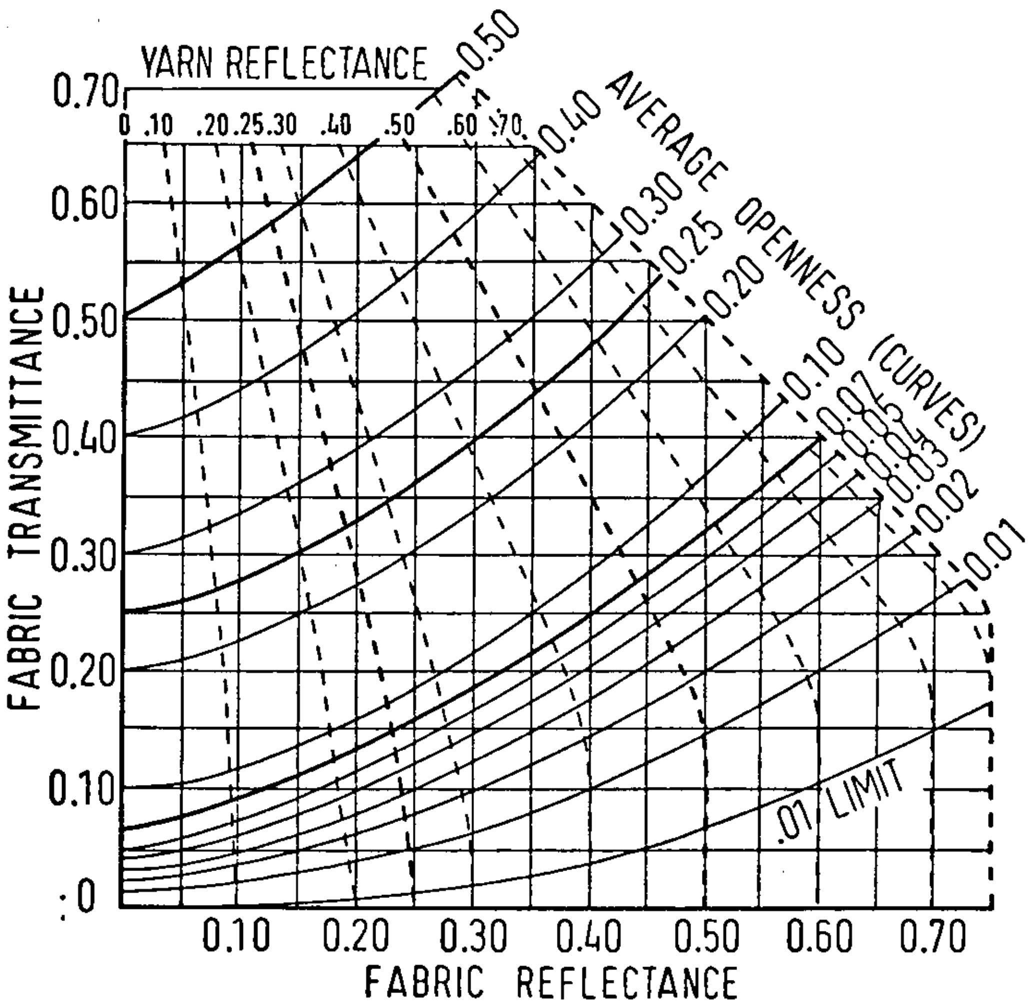

Fig. 5 - Transmittance and reflectance of fabrics [1]

3. Characteristic parameters of solar performance

The phenomena taking place in a fenestration affected by the sun, can be suitably modelized in order to define bulk thermo-optical properties of the window considered [6].

For a window subject to solar radiation, multiple reflections on the surfaces can be observed, depending on the angle of incidence, and accompanied by the absorption of a certain quantity of energy through glasses and screens: if their optical properties are known, as a function of the angle of incidence, it is possible to calculate both solar energy directly transmitted into the building and the various quantities absorbed by each element affecting the windows thermal balance (Fig. 6). This balance can be spread into some thermal sub-balances (Fig. 7).

a) For every j-th surface of glass pane or screen the following equation can be written

$$[\, q_c + q_i + q_p + q_a \,]_j = 0 \qquad (7)$$

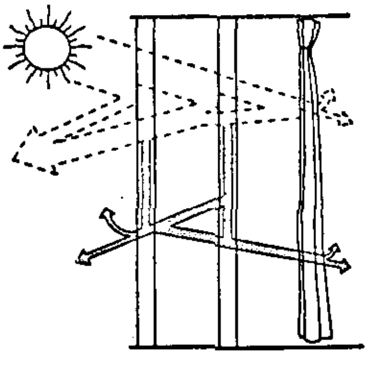

Fig. 6 - Heat fluxes in a window subjet to solar radiation

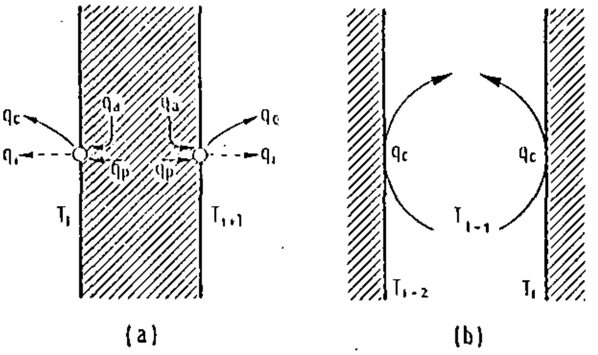

Fig. 7 - Thermal balances on the surfaces of the window's elements

where:

q_c : convection heat flow rate

q_i : mutual radiation (infrared) heat flow rate

q_p : conduction heat flow rate

q_a : absorbed solar heat gain.

b) For the air inside the h-th air gap, the following balance can be applied:

$$[\Sigma q_c]_h = 0 \tag{8}$$

Σq_c being the sum of all convective heat fluxes exchanged by the air with the surfaces delimiting the gap considered.

Once every heat flux has been expressed according to the principles of heat transfer, a system of algebraic equations can be set up, whose unknows are the temperatures of the various elements composing the window.

By solving such thermal balance the unknown temperatures can be obtained; hence it is possible to evaluate the various thermal fluxes transmitted by the examined window at any hour of the day, due to the solar radiation and to the temperature difference between internal and external air; moreover, it is possible to distinguish the solar heat gain passing directly through the window from the one that, being absorbed, warms it up and is partially released by convection and infrared radiation to the room: the distribution between these different heat fluxes, as will be seen later, is quite different from one type of window to another.

According to ASHRAE [1] the heat flux q exchanged through a window subject to the air temperature difference Δt, and to solar radiation, can be expressed with reasonable approximation by superimposing these two effects as the algebraic sum of a part (q_1) due to the mere difference of temperature, and of another part due only to the solar radiation (q_2):

$$q = q_1 + q_2 \tag{9}$$

The component q_1 can be determined by means of the overall heat transfer coefficient U:

$$q_1 = U\ \Delta t \qquad (10)$$

The thermal flux q_2 is constituted, as already mentioned, by the radiation directly transmitted, mainly in the visible and near infrared field (q_r), and, as a consequence of the overheating due to the absorbed radiation, by the heat fluxes exchanged by radiation in the far infrared (q_i) and by convection (q_c). Consequently:

$$q_2 = q_r + q_i + q_c \qquad (11)$$

Such flux can be expressed by means of the so called "shading coefficient" C'_s introduced by ASHRAE, defined as the ratio between the heat flux q_2 through the window considered (evaluated *with nil air temperature difference*), and the corresponding heat flux q^*_2 for the single strength clear glass taken as a reference:

$$C'_s = q_2 / q^*_2 \qquad (12)$$

It is to be noted that, within this definition, q_2 and q^*_2 refer to the effects of total (direct plus diffuse) solar radiation, thus assuming a conventional propotion of direct to diffuse.

The usefulness of this parameter lies in the fact that usually it shows little variation over a wide range of the angle of incidence of the sun rays (this assumption shall be discussed later on). So, knowing the hourly values of q^*_2, as a function of latitude, of the time of the year and of the window's orientation (data available in tables, [1]) it is possible to evaluate, the corresponding values of the heat flux transmitted by any window by means of C_s mean value of C'_s, over the sunshine period.

It is nevertheless clear that it is not possible in this way to evaluate the various solar heat gains separately, and particularly to distinguish between the short wave radiation q_r and the components q_i and q_c, which are very significant with absorbing glasses.

Whenever the knowledge of the coefficient C'_s only is not sufficient, it is convenient to introduce three similar coefficients C'_r, C'_i, C'_c, defined as follows:

$$C'_r = q_r / q^*_2 \qquad C'_i = q_i / q^*_2 \qquad C'_c = q_c / q^*_2 \qquad (13)$$

together with their related mean values C_r, C_i, C_c, and C_s

Consequently, also:

$$C_s = C_r + C_i + C_c \tag{14}$$

The knowledge of the various heat flux components released to the room consents to the considered window being better described. Moreover, proper transfer functions can be applied to every heat flux when the room's thermal load has to be calculated under unsteady state conditions [1].

All these parameters can be evaluated while performing the above described detailed calculations and once known, they allow the thermal flux q and its various constituents to be easily determined according to the above seen equations.

Since the heat fluxes which take place in the considered physical system (the window components connected to a room) are non-linear functions of temperature levels and temperature differences, the following assumptions have been used in the calculations.

As the temperature differences between the inner surfaces are relatively small, the mutual radiation heat exchanges have been linearized although assuming a radiation coefficient dependent on the third power of the mean temperature of the surfaces. For the evoluation of the radiation heat exchanges on the inner surface of the window system in order to establish a reference condition, the surface temperature of the inner ambient has been assumed equal to the inner air temperature.

While the external surface heat transfer coefficient in supposed to be constant and equal to 23 W/m^2K, for the inner surfaces and the air gaps, instead, the heat transfer coefficients have been considered temperature dependent according to [4], [9], [10] and [11] to improve the accuracy of the calculations.

As a result of the above assumptions the U and C coefficients are temperature dependent; nevertheless calculation tests specifically performed for this purpose have shown a weak dependence of them on temperature and temperature differences within the range of interest of building physics. Thus the superimposition of effects as per eq. (9) can provide a satisfactory approximation for practical applications.

The thermal and optical parameters of several types of windows have been calculated with reference to the most common combinations of glasses and screens found in buildings. Specifically, the elements in Table 1 have been considered; to roughly qualify the various types of glass and screens, the values of τ and ρ at normal incidence are given.

The screens are indentified by capital letters, the gaps (air or Argon filled) with small letters and the glass types with numbers.

For the vertical blinds and venetian blinds, it should be observed that their optical properties have been approximated because, strictly speaking, the portion of direct radiation crossing them may be relevant and depends greatly on the incidence angle, especially when they are partially open; the cases herewith considered refer to a tilt angle of the strips adjusted to fully intercept the direct sun rays.

Whenever a coated glass (glass types 3, 4, 5 and 6 on Table 2) has been considered, the treated surface has been placed on the internal surface for single glazings and inside the gap in the cases of double glazing.

Some commonly used combinations of such elements (identified by a graphic sketch and by an alphanumerical sequence adopting the classification of Table 1) are shown in Table 2 together with their coefficients C_r , C_i, C_c, C_s: for each case the U-value (expressed in $W/m^2 K$) is also given.

The gaps between two glasses have been considered always close; when the gaps are bounded by one of the screens previously mentioned, however, both extreme hypothesis of air-tight and completely open air gaps have been considered; this last case is modelized by assuming the air temperature to be the same on both sides of the screen; the choice of a suitable intermediate value of the characteristic parameters therefore is left to the designer's experience.

The calculation of the U-values has been performed with reference to an internal temperature of 20°C and to an external temperature of 0°C.

As far as the C coefficients are concerned, they have been evaluated at 20°C for a South facing orientation and with nil temperature difference across the window. The solar radiation pattern corresponds to January 21 at 45 N latitude; calculation tests have shown that the influence of the latitude is small at least in the range of the european latitudes, while more significant is the influence of the time of the year; this fact is strictly connected to the more general problem of the influence of the angle of incidence on the coefficients of shading. A practical approach for taking into account this influence has been provided [8]. In Fig. 8, the calculated values of the shading coefficient C'_s and of its three components C'_r, C'_i and C'_c as functions of the angle of incidence ϑ of the solar radiation, is shown for some of the considered types of glazing.

Table 1 — WINDOW ELEMENT CHARACTERISTICS

CODES	ELEMENTS DESCRIPTION	τ	ρ
1 :	REFERENCE SODA-LIME GLASS 3 mm [2]	0.88	0.08
2 :	SODA-LIME GLASS 6 mm [2]	0.78	0.07
3:	THERMOSIV [7]	0.51	0.15
4:	ARGENTO 32 [7]	0.30	0.13
5 :	SOLAR REFLECTING GLASS 35-22 [2]	0.22	0.19
6 :	SOLAR REFLECTING GLASS 24-28 [2]	0.28	0.19
7 :	GREEN HEAT-ABSORBING GLASS 6 mm [2]	0.47	0.04
A :	LIGHT VENETIAN BLINDS [1]	0.05	0.55
B :	DARK VENETIAN BLINDS [1]	0.05	0.35
C :	OPEN WEAVE SHADE [1]	0.60	0.30
D :	SEMI-OPEN WEAVE SHADE [1]	0.30	0.25
E :	CLOSED WEAVE SHADE [1]	0.07	0.08
F :	LIGHT VERTICAL BLINDS [5]	0.34	0.59
G :	DARK VERTICAL BLINDS [5]	0.34	0.33
a :	AIR GAP 9 mm		
b :	AIR GAP 12 mm		
c :	AIR GAP 100 mm		
d :	AIR GAP 200 mm		
e :	ARGON GAP 12 mm		

Table 2 — CHARACTERISTIC PARAMETERS FOR DIFFERENT TYPES OF WINDOWS

Sect.1	CODE	AIR PERVIOUS SCREEN					AIR TIGHT SCREEN				
		Cr	Cc	Ci	Cs	U	Cr	Cc	Ci	Cs	U
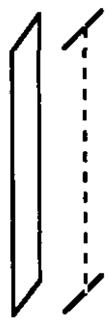	1 d A	.05	.22	.13	.40	4.81	.05	.10	.18	.33	2.72
	1 d B	.05	.32	.18	.55	"	.05	.15	.25	.45	"
	1 d C	.60	.05	.04	.69	4.81	.60	.03	.05	.68	2.78
	1 d D	.30	.21	.16	.67	"	.30	.14	.18	.62	"
	1 d E	.07	.41	.27	.75	"	.07	.27	.31	.65	"
	1 d F	.35	.04	.04	.43	"	.35	.02	.04	.41	"
	1 d G	.34	.16	.12	.62	"	.34	.10	.14	.58	"
	1	.97	.01	.02	1.00	6.33					

Sect.2	CODE	AIR PERVIOUS SCREEN					AIR TIGHT SCREEN				
		Cr	Cc	Ci	Cs	U	Cr	Cc	Ci	Cs	U
	2 d A	.04	.22	.13	.39	4.73	.04	.09	.18	.31	2.70
	2 d B	.04	.30	.17	.51	"	.04	.14	.24	.42	"
	2 d C	.52	.07	.05	.64	4.72	.52	.04	.06	.62	2.76
	2 d D	.26	.21	.14	.61	"	.26	.13	.17	.56	"
	2 d E	.06	.38	.24	.68	"	.06	.24	.29	.59	"
	2 d F	.30	.07	.04	.41	"	.30	.03	.05	.38	"
	2 d G	.29	.17	.11	.57	"	.29	.10	.13	.52	"
	2	.84	.02	.04	.90	6.19					

Sect.3	CODE	AIR PERVIOUS SCREEN					AIR TIGHT SCREEN				
		Cr	Cc	Ci	Cs	U	Cr	Cc	Ci	Cs	U
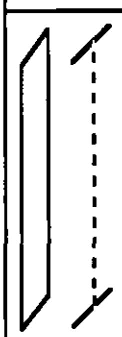	4 d A	.02	.19	.09	.30	4.51	.02	.05	.14	.21	2.52
	4 d B	.02	.22	.11	.35	"	.02	.04	.18	.24	"
	4 d C	.21	.13	.05	.39	4.50	.21	.05	.07	.33	2.54
	4 d D	.11	.19	.09	.39	"	.11	.08	.12	.31	"
	4 d E	.02	.25	.13	.40	"	.02	.13	.17	.32	"
	4 d F	.13	.14	.05	.32	"	.13	.05	.07	.25	"
	4 d G	.12	.17	.08	.37	"	.12	.07	.10	.29	"
	4	.34	.08	.09	.51	5.76					

Sect.4	CODE	AIR PERVIOUS SCREEN					AIR TIGHT SCREEN				
		Cr	Cc	Ci	Cs	U	Cr	Cc	Ci	Cs	U
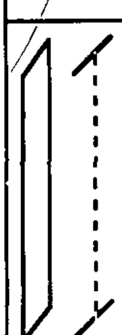	5 d A	.01	.16	.06	.23	3.53	.01	.05	.10	.16	1.69
	5 d B	.01	.18	.08	.27	"	.01	.05	.12	.18	"
	5 d C	.15	.11	.03	.29	3.53	.15	.03	.05	.23	1.63
	5 d D	.07	.16	.06	.29	"	.07	.06	.09	.22	"
	5 d E	.02	.20	.10	.32	"	.02	.09	.13	.24	"
	5 d F	.09	.12	.03	.24	"	.09	.03	.05	.17	"
	5 d G	.08	.14	.05	.27	"	.08	.05	.08	.21	"
	5	.23	.10	.03	.36	4.32					

Table 2 — *Cont.*

Sect.5

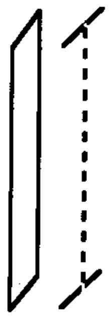

CODE	Cr	Cc	Ci	Cs	U	Cr	Cc	Ci	Cs	U
	AIR PERVIOUS SCREEN					AIR TIGHT SCREEN				
6 d A	.02	.17	.07	.26	3.53	.02	.05	.11	.18	1.69
6 d B	.02	.19	.09	.30	"	.02	.05	.15	.22	"
6 d C	.19	.11	.03	.33	3.53	.19	.03	.05	.27	1.63
6 d D	.09	.16	.07	.32	"	.09	.07	.10	.26	"
6 d E	.02	.22	.12	.36	"	.02	.11	.15	.28	"
6 d F	.11	.11	.03	.25	"	.11	.03	.05	.19	"
6 d G	.11	.14	.06	.31	"	.11	.05	.08	.24	"
6	.29	.09	.03	.41	4.32					

Sect.6

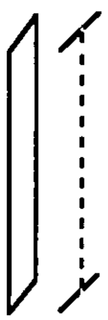

CODE	Cr	Cc	Ci	Cs	U	Cr	Cc	Ci	Cs	U
	AIR PERVIOUS SCREEN					AIR TIGHT SCREEN				
7 d A	.02	.23	.10	.35	4.73	.02	.06	.17	.25	2.70
7 d B	.02	.27	.13	.42	"	.02	.07	.20	.29	"
7 d C	.30	.13	.06	.49	4.72	.30	.05	.08	.43	2.76
7 d D	.15	.21	.11	.47	"	.15	.10	.14	.39	"
7 d E	.03	.29	.17	.49	"	.03	.17	.21	.41	"
7 d F	.17	.13	.06	.36	"	.17	.05	.08	.30	"
7 d G	.17	.18	.10	.45	"	.17	.09	.12	.38	"
7	.49	.07	.10	.66	6.19					

Sect.7

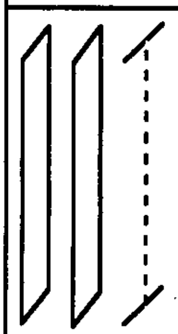

CODE	Cr	Cc	Ci	Cs	U	Cr	Cc	Ci	Cs	U
	AIR PERVIOUS SCREEN					AIR TIGHT SCREEN				
1 b 1 d A	.04	.25	.15	.44	2.57	.04	.08	.24	.36	1.93
1 b 1d B	.04	.33	.20	.57	"	.04	.13	.31	.48	"
1 b 1d C	.52	.09	.05	.66	2.55	.52	.05	.07	.64	1.91
1 b 1d D	.26	.25	.15	.66	"	.26	.16	.20	.62	"
1 b 1d E	.06	.44	.25	.75	"	.06	.28	.33	.67	"
1 b 1d F	.31	.09	.05	.45	"	.21	.04	.07	.42	"
1 b 1d G	.30	.20	.12	.62	"	.30	.12	.16	.58	"
1 b 1	.84	.02	.04	.90	3.01					

Sect.8

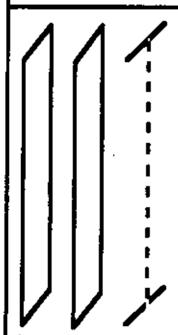

CODE	Cr	Cc	Ci	Cs	U	Cr	Cc	Ci	Cs	U
	AIR PERVIOUS SCREEN					AIR TIGHT SCREEN				
1 d 1 d A	.04	.25	.15	.44	2.36	.04	.08	.24	.36	1.74
1 d 1 d B	.04	.34	.20	.58	"	.04	.13	.32	.49	"
1 d 1 d C	.52	.09	.05	.66	2.36	.52	.05	.07	.64	1.76
1 d 1 d D	.26	.26	.15	.67	"	.26	.16	.20	.62	"
1 d 1 d E	.06	.44	.25	.75	"	.06	.29	.33	.68	"
1 d 1 d F	.31	.09	.05	.45	"	.31	.04	.07	.42	"
1 d 1 d G	.30	.20	.12	.62	"	.30	.12	.16	.58	"
1 d 1	.84	.02	.04	.90	2.76					

Table 2 — *Cont.*

Sect.9

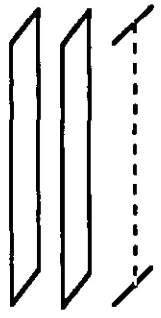

CODE	AIR PERVIOUS SCREEN					AIR TIGHT SCREEN				
	Cr	Cc	Ci	Cs	U	Cr	Cc	Ci	Cs	U
2 b 2 dA	.03	.27	.13	.43	2.52	.03	.09	.23	.35	1.83
2 b 2 d B	.03	.33	.17	.53	"	.03	.06	.32	.41	"
2 b 2 d C	.38	.14	.06	.58	2.52	.38	.07	.10	.55	1.86
2 b 2 d D	.19	.26	.14	.59	"	.19	.15	.19	.53	"
2 b 2 d E	.04	.39	.21	.64	"	.04	.24	.28	.56	"
2 b 2 d F	.22	.15	.06	.43	"	.22	.07	.10	.39	"
2 b 2 d G	.22	.22	.11	.55	"	.22	.12	.16	.50	"
2 b 2	.62	.06	.09	.77	2.95					

Sect.10

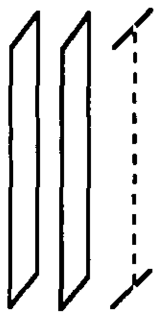

CODE	AIR PERVIOUS SCREEN					AIR TIGHT SCREEN				
	Cr	Cc	Ci	Cs	U	Cr	Cc	Ci	Cs	U
3 b 2 d A	.03	.22	.11	.36	1.66	.03	.09	.20	.32	1.34
3 b 2 d B	.03	.26	.13	.42	"	.03	.09	.24	.36	"
3 b 2 d C	.27	.12	.06	.45	1.66	.27	.06	.09	.42	1.35
3 b 2 d D	.13	.21	.11	.45	"	.13	.12	.16	.41	"
3 b 2 d E	.03	.30	.16	.49	"	.03	.18	.23	.44	"
3 b 2 d F	.16	.14	.06	.36	"	.16	.07	.10	.33	"
3 b 2 d G	.15	.18	.09	.42	"	.15	.10	.14	.39	"
3 b 2	.43	.05	.07	.55	1.85					

Sect.11

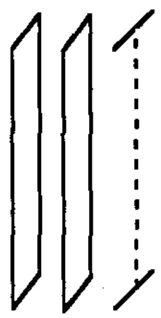

CODE	AIR PERVIOUS SCREEN					AIR TIGHT SCREEN				
	Cr	Cc	Ci	Cs	U	Cr	Cc	Ci	Cs	U
2 b 3 d A	.03	.28	.13	.42	1.66	.03	.11	.23	.37	1.34
2 b 3 d B	.03	.31	.15	.49	"	.03	.12	.27	.42	"
2 b 3 d C	.28	.17	.07	.52	1.66	.28	.08	.12	.48	1.35
2 b 3 d D	.14	.26	.12	.52	"	.14	.15	.19	.47	"
2 b 3 d E	.03	.35	.17	.55	"	.03	.21	.25	.49	"
2 b 3 d F	.17	.19	.07	.43	"	.17	.09	.13	.39	"
2 b 3 d G	.16	.24	.11	.51	"	.16	.13	.17	.46	"
2 b 3	.43	.08	.11	.62	1.85					

Sect.12

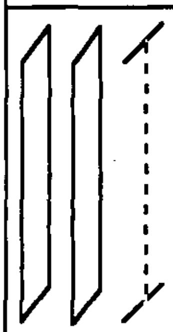

CODE	AIR PERVIOUS SCREEN					AIR TIGHT SCREEN				
	Cr	Cc	Ci	Cs	U	Cr	Cc	Ci	Cs	U
4 b 2 d A	.01	.17	.08	.26	2.39	.01	.06	.13	.20	1.76
4 b 2 d B	.01	.19	.09	.29	"	.01	.06	.16	.23	"
4 b 2 d C	.16	.11	.05	.32	2.38	.16	.05	.08	.29	1.78
4 b 2 d D	.08	.16	.08	.32	"	.08	.08	.11	.27	"
4 b 2 d E	.02	.21	.11	.34	"	.02	.11	.15	.28	"
4 b 2 d F	.09	.12	.05	.26	"	.09	.05	.08	.22	"
4 b 2 d G	.09	.14	.07	.30	"	.09	.07	.10	.26	"
4 b 2	.26	.05	.08	.39	2.77					

Table 2 — *Cont.*

Sect.13

CODE	AIR PERVIOUS SCREEN Cr	Cc	Ci	Cs	U	AIR TIGHT SCREEN Cr	Cc	Ci	Cs	U
5 b 2 d A	.01	.13	.06	.20	1.78	.01	.05	.11	.17	1.42
5 b 2 d B	.01	.14	.07	.22	"	.01	.05	.12	.18	"
5 b 2 d C	.11	.08	.04	.23	1.78	.11	.04	.06	.21	1.43
5 b 2 d D	.05	.12	.06	.23	"	.05	.06	.09	.20	"
5 b 2 d E	.01	.15	.08	.24	"	.01	.08	.12	.21	"
5 b 2 d F	.06	.09	.04	.19	"	.06	.04	.07	.17	"
5 b 2 d G	.06	.11	.05	.22	"	.06	.05	.08	.19	"
5 b 2	.17	.04	.07	.28	2.00					

Sect.14

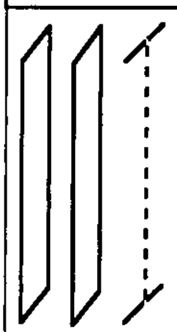

CODE	AIR PERVIOUS SCREEN Cr	Cc	Ci	Cs	U	AIR TIGHT SCREEN Cr	Cc	Ci	Cs	U
6 b 2 d A	.01	.14	.07	.22	1.78	.01	.05	.12	.18	1.42
6 b 2 d B	.01	.16	.08	.25	"	.01	.06	.14	.21	"
6 b 2 d C	.14	.09	.04	.27	1.78	.14	.04	.07	.25	1.43
6 b 2 d D	.07	.13	.07	.27	"	.07	.07	.10	.24	"
6 b 2 d E	.02	.18	.10	.30	"	.02	.10	.14	.26	"
6 b 2 d F	.08	.10	.04	.22	"	.08	.05	.07	.20	"
6 b 2 d G	.08	.12	.06	.26	"	.08	.06	.09	.23	"
6 b 2	.22	.04	.07	.33	2.00					

Sect.15

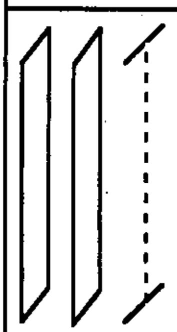

CODE	AIR PERVIOUS SCREEN Cr	Cc	Ci	Cs	U	AIR TIGHT SCREEN Cr	Cc	Ci	Cs	U
7 b 2 d A	.02	.21	.10	.33	2.52	.02	.07	.16	.25	1.83
7 b 2 d B	.02	.24	.12	.38	"	.02	.08	.20	.30	"
7 b 2 d C	.22	.13	.06	.41	2.52	.22	.06	.09	.37	1.86
7 b 2 d D	.11	.20	.10	.41	"	.11	.10	.14	.35	"
7 b 2 d E	.03	.27	.14	.44	"	.03	.15	.19	.37	"
7 b 2 d F	.13	.14	.06	.33	"	.13	.06	.09	.28	"
7 b 2 d G	.13	.18	.08	.39	"	.13	.09	.12	.34	"
7 b 2	.36	.06	.09	.51	2.95					

Sect.16

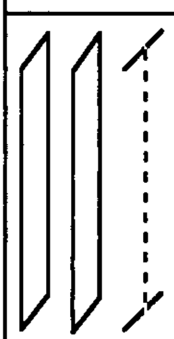

CODE	AIR PERVIOUS SCREEN Cr	Cc	Ci	Cs	U	AIR TIGHT SCREEN Cr	Cc	Ci	Cs	U
2 b 7 d A	.02	.34	.13	.49	2.52	.02	.12	.24	.38	1.83
2 b 7 d B	.02	.36	.15	.53	"	.02	.13	.26	.41	"
2 b 7 d C	.22	.25	.09	.56	2.52	.22	.11	.15	.48	1.86
2 b 7 d D	.11	.32	.13	.56	"	.11	.16	.20	.47	"
2 b 7 d E	.03	.39	.17	.59	"	.03	.21	.25	.49	"
2 b 7 d F	.13	.28	.09	.50	"	.13	.12	.16	.41	"
2 b 7 d G	.13	.31	.12	.56	"	.13	.15	.18	.46	"
2 b 7	.36	.14	.18	.68	2.95					

Table 2 — *Cont.*

Sect.17		AIR PERVIOUS SCREEN					AIR TIGHT SCREEN				
	CODE	Cr	Cc	Ci	Cs	U	Cr	Cc	Ci	Cs	U
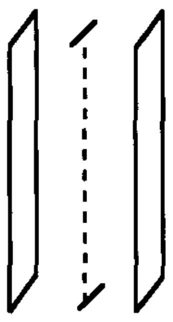	2 c A c 2	.03	.08	.11	.22	2.00	.03	.08	.11	.22	1.77
	2 c B c 2	.03	.11	.15	.29	"	.03	.11	.15	.29	"
	2 d 2	.62	.06	.09	.77	2.70					

Sect.18		AIR PERVIOUS SCREEN					AIR TIGHT SCREEN				
	CODE	Cr	Cc	Ci	Cs	U	Cr	Cc	Ci	Cs	U
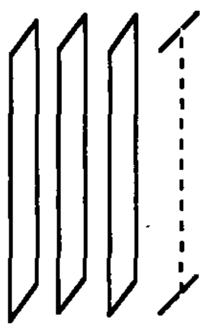	2a2a2dA	.02	.29	.13	.44	1.85	.02	.11	.23	.36	1.46
	2a2a2dB	.02	.32	.15	.49	"	.02	.12	.27	.41	"
	2a2a2dC	.29	.18	.07	.54	1.85	.29	.09	.12	.50	1.47
	2a2a2dD	.14	.27	.13	.54	"	.14	.15	.19	.48	"
	2a2a2dE	.03	.36	.18	.57	"	.03	.22	.26	.51	"
	2a2a2dF	.17	.20	.07	.44	"	.17	.09	.13	.39	"
	2a2a2dG	.16	.24	.11	.51	"	.16	.13	.17	.46	"
	2a2a2	.46	.08	.11	.65	2.09					

Sect.19		AIR PERVIOUS SCREEN					AIR TIGHT SCREEN				
	CODE	Cr	Cc	Ci	Cs	U	Cr	Cc	Ci	Cs	U
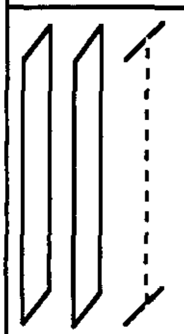	2e3dA	.03	.26	.15	.44	1.36	.03	.09	.27	.39	1.15
	2e3dB	.03	.28	.18	.49	"	.03	.09	.31	.43	"
	2e3dC	.28	.16	.08	.52	1.37	.28	.09	.12	.49	1.18
	2e3dD	.14	.25	.13	.52	"	.14	.15	.19	.48	"
	2e3dE	.03	.34	.19	.56	"	.03	.22	.26	.51	"
	2e3dF	.17	.18	.08	.43	"	.17	.10	.13	.40	"
	2e3dG	.16	.23	.12	.51	"	.16	.14	.17	.47	"
	2e3	.43	.08	.11	.62	1.55					

Sect.20		AIR PERVIOUS SCREEN					AIR TIGHT SCREEN				
	CODE	Cr	Cc	Ci	Cs	U	Cr	Cc	Ci	Cs	U
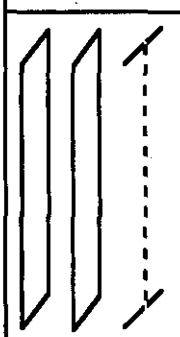	5e2dA	.01	.11	.07	.19	1.50	.01	.04	.11	.16	1.24
	5e2dB	.01	.12	.08	.21	"	.01	.04	.13	.18	"
	5e2dC	.11	.07	.04	.22	1.50	.11	.04	.06	.21	1.27
	5e2dD	.05	.10	.06	.21	"	.05	.06	.09	.20	"
	5e2dE	.01	.14	.09	.24	"	.01	.08	.12	.21	"
	5e2de	.06	.08	.04	.18	"	.06	.04	.06	.17	"
	5e2dG	.06	.10	.06	.22	"	.06	.05	.08	.20	"
	5e2	.17	.04	.06	.27	1.72					

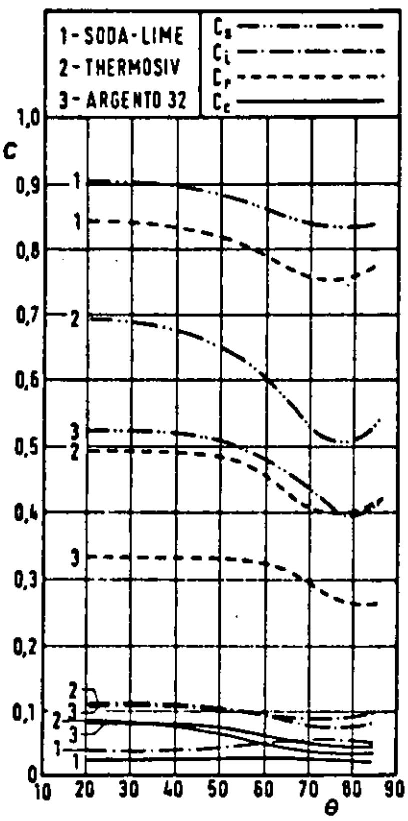

Fig. 8 - Characteristic parameters vs the angle of incidence

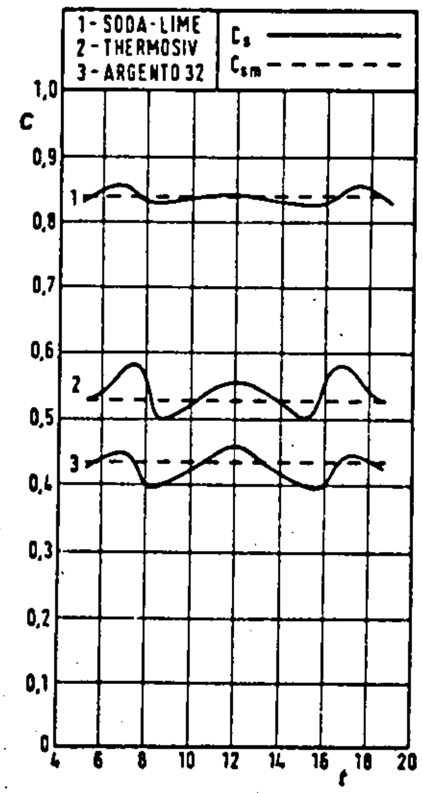

Fig. 9 - Hourly pattern of C'_S and the average C_S

It appears that the dependence of the coefficients on the angle can be relevant. Although obviously the relative importance of the solar heat gain for high incidence angle is lower than for near-normal incidence, the application of a constant value, as usually done, relies only on the evaluation of a correctly weighed average over a suitable period. As a sample, in fig. 9 the houly pattern of the shading coefficient for three different glass types is shown, along with the weighed mean value C_S which ensures the correct evaluation of the total daily solar energy gain, while the use of this last average coefficient for hourly calculations of the solar heat gain produces an error which nevertheless is not very significant.

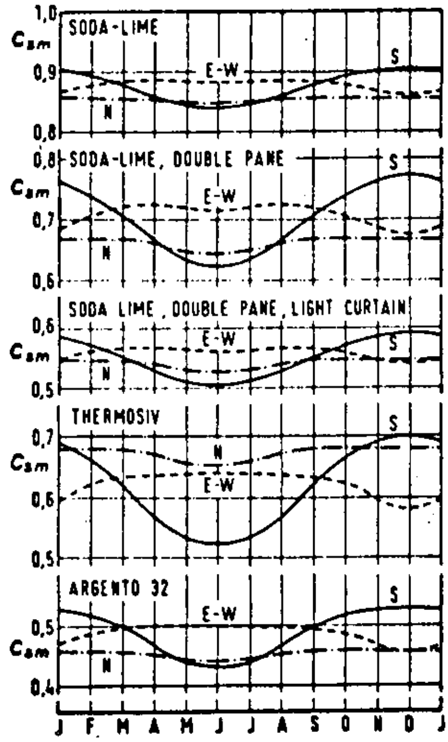

Fig. 10 - Yearly patterns of C_S

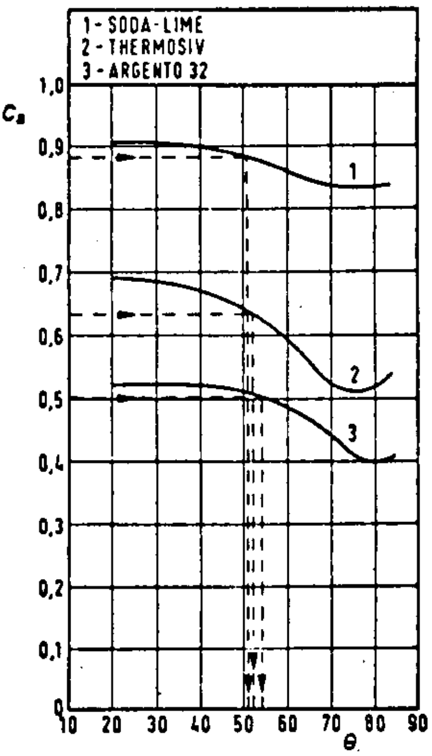

Fig. 11 - Procedure for evaluating the effective angle of incidence

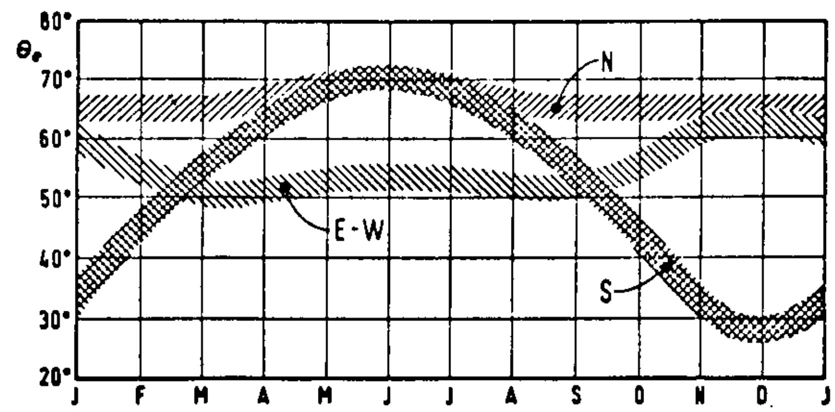

Fig. 12 - Yearly patterns of the effective angle of incidence

On the other hand, since the solar pattern changes significantly as a function of the time of the year and of the window azimuth, the analysis of the variations of C_S with these two variables can be much more remarkable as shown in fig. 10 for various combinations of glasses and curtains.

For practical applications it would be interesting to take into account the variablility of the window parameters with the minimum amount of effort and information. By observing the plots of C'_S as function of the angle of incidence, it can be shown (see fig. 11) that the angle of incidence corresponding to the mean value (C_S) of the shading coefficient C'_S at given orientation, latitude and time of the year, is almost independent on the type of glass among those here considered; such value can be called "effective angle of incidence" (ϑ).

A further investigation has shown that the effective angle of incidence varies with the orientation and the time of the year as shown in fig. 12 for many types of glass.

Consequently the possiblity of defining an "effective angle of incidence" as above discussed, allows for an easy calculation of C_S under any condition, if the thermal-optical properties of the window are described not by a unique value of shading coefficient as is usual at present, but by the pilot of C'_S vs. ϑ (possibily in polynomial form for numerical applications).

REFERENCES

[1] "ASHRAE Handbook, 1977 Fundamentals", ASHRAE, New York, 1977.

[2] Yellott, J.I. "Selective Reflectance: a New Approach for Solar Heat Control", ASHRAE N. Y. 1967.

[3] Keys, M. W. "Analysis and rating of Drapery Materials used for Indoor Shading", ASHRAE Transactions, vol. 73, 1967.

[4] Jakob, H. " Heat Transfer", Wiley & Sons, New York 1957.

[5] "VERTIKA: Sun control effectiveness of vertical blinds", Vertical Blinds Ltd., 1972.

[6] Brunello, P. and Zecchin, R. "Characteristics parameters of window", I.I.R. Commission E1-E2, Jerusalem, 1982.

[7] SIV - Società Italiana Vetro, Technical Bulletins, San Salvo.

[8] Brunello, P. and Zecchin, R. "Analysis of solar properties of window", Windows in Building design and maintenance, Goteborg, 1984.

[9] Marinelli, V. "Sullo scambio termico convettivo nelle intercapedini verticali", Condizionamento dell'aria, 6, 1978.

[10] Eckert, E.R.G. and Carlson, W.O. "Natural Convection in Air Layer enclosed between two vertical plates with different temperatures" International Journal of Heat and Mass transfer, Vol. 2, 1961.

[11] Min, C., Schutrum, L. and Parmelee, G. "Natural Convection and Radiation in a panel-heated room" Heating Piping and Air Conditioning, 5, 1956.

4.4. Measurement techniques

4.4.1. Laboratory Measurements of Solar Optical Properties

P. Brunello
Istituto di Fisica Tecnica e Tecnologie Industriali
Università di Udine
ITALY

R. Zecchin
Istituto di Fisica tecnica
Università di Padova
ITALY

LIST OF SYMBOLS

I	:	irradiance	(W/m^2)
τ	:	transmittance	(-)
ρ	:	reflectance	(-)
α	:	absorptance	(-)
ϑ	:	incidence angle	(deg)
λ	:	wavelength	(μm)

Subscripts:

λ	:	spectral
ϑ	:	directional
s	:	solar

1. Introduction

Many experimental techniques have been developed over the past years for determining the solar-optical properties of the window components. In this pragraph a synthetic review of some standard procedures will be briefly described.

2. Transmittance

Solar transmittance is usually determined starting from the spectral transmittance over the solar range (0.2 to 3.0 μm) measured by means of a spectrophotometer.

The optical layout and the block diagram of a spectrophotometer are shown in Fig.1 and Fig. 2 respectively.

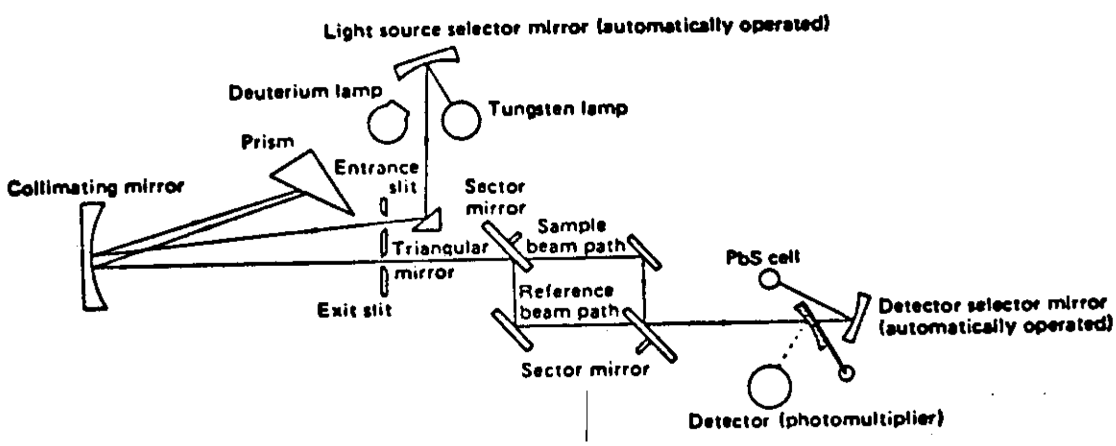

Fig. 1 - Optical layout of a spectrophotometer [1]

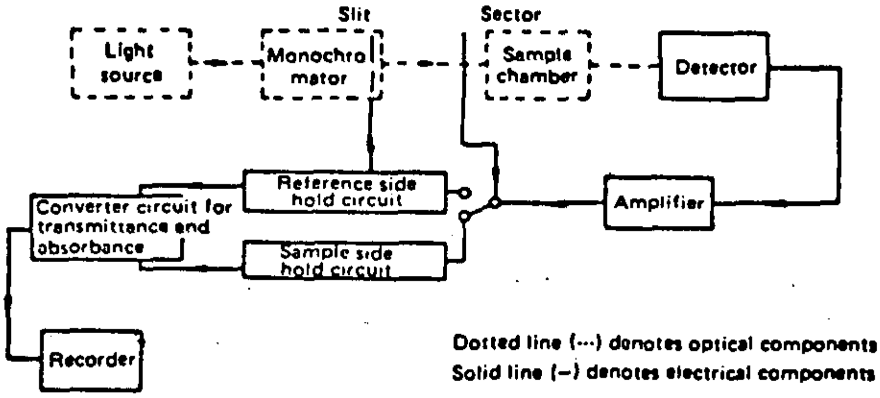

Fig. 2 - Block diagram of a spectrophotometer [1]

The basic concept on which the system operates is to measure by means of a suitable detector, the heat flux emitted by a monocromatic lamp with and without the sample to be tested, placed in between (Fig. 3). The ratio between the two signals gives the monocromatic transmittance, $\tau_{\lambda\vartheta}$:

$$\tau_{\lambda\vartheta} = [(I_\lambda)''/(I_\lambda)']_\vartheta \tag{1}$$

where $(I_\lambda)'$ and $(I_\lambda)''$ are the measured signals without the sample and with the sample at ϑ incidence, respectively.

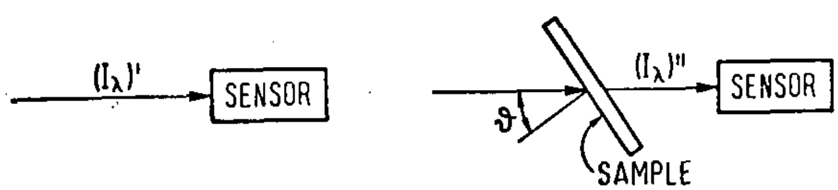

Fig. 3 - Readings for the evaluation of spectral transmittance

By suitably changing the source, the spectral distribution of $\tau_{\lambda\vartheta}$ can be easily found.
The ratio between the integral (over the solar range Λ) of the spectral transmittance multiplied by the standard solar spectral intensity and the integral of the solar spectral intensity itself gives then the solar transmittance for the considered angle of incidence ϑ:

$$\tau_{\vartheta} = \int_{\Lambda} (i_{\lambda})_s \tau_{\lambda\vartheta} \int_{\Lambda} (I_{\lambda})_s d_{\lambda} \tag{2}$$

By suitably adjusting the sample, the measurements can be performed at different angles of incidence. Nevertheless manufacturers usually provide only normal incidence properties, valuable in classifying and identifying glasses, but not sufficient for a complete evaluation of their performance, as the incidence angle of solar radiation on actual windows rarely approaches normal incidence.

Transmittance of window glass for the visible portion of the solar spectrum (between 0.4 and 0.7 μm, can be determined from the spectral transmittance, or it can be measured by means of a filtered light source and a photocell.

An alternative simplified procedure has been proposed in [2] for making quick determinations of the solar-optical properties of glass, as shown in Fig. 4. This instrument consists of a normal incidence pyroheliometer attached to a tilting mount; between the sun and the pyroheliometer is placed a rotatable sample-holder which can vary the angle of incidence between the solar ray and the sample from 0 to 80 deg. A reading of solar radiation intensity with no glass in the holder, divided by an immediately subsequent reading with the glass in place at the desired incident angle, gives the transmittance at that particular angle. the entire range of incident angles can be covered in a few minutes during the middle of a clear day, when there is little variation in the intensity of the direct solar beam.

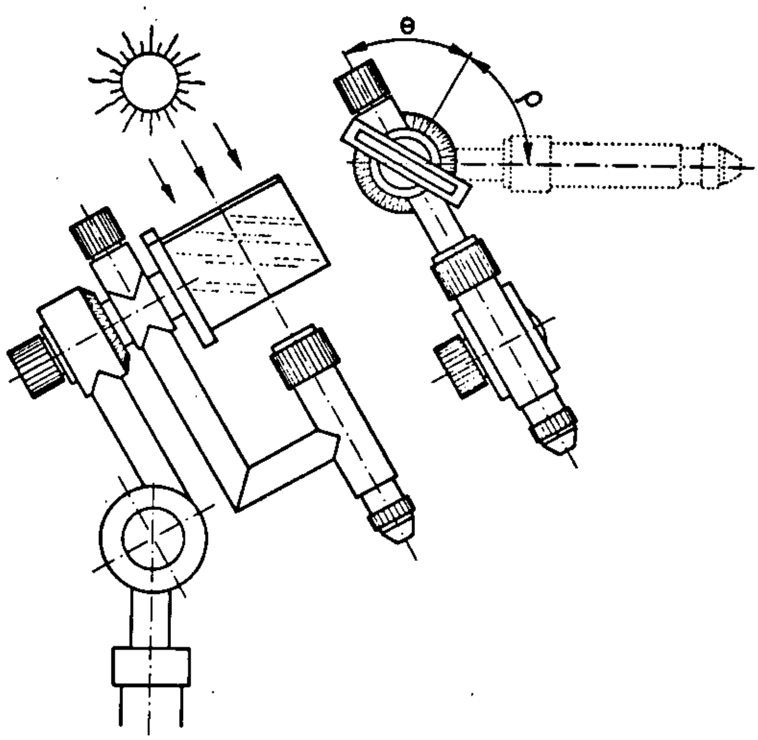

Fig. 4 - Apparatus for the evaluation of solar directional properties, according to [1]

3. Reflectance

A suitable device assembly of deflecting mirrors added to a spectrophotometer allows for measuring also the reflectance of a given surface.

The device consists of three mirrors deflecting the incident rays emitted by the source and readdressing it to the detector again: in this case, however, the evaluation of the intensities $(I_\lambda)'$ and $(I_\lambda)''$ without and with the sample surface requires certain rearrangements of the deflecting mirrors (see Fig. 5).

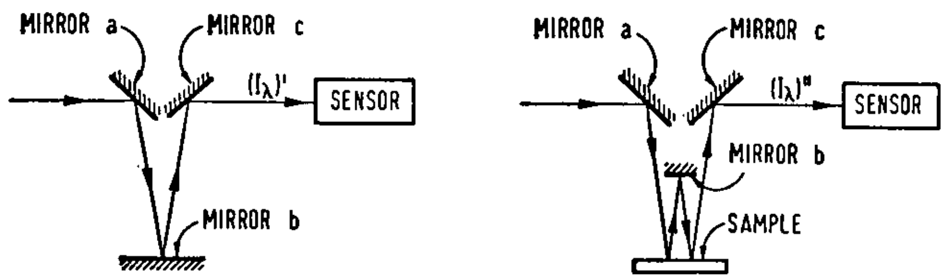

Fig. 5 - Readings for the evaluation of spectral reflectance

It is important to mention that the ratio between the two measurements provides ρ^2 and not ρ, because of the two reflections on the surface to be tested

$$\rho^2{}_\vartheta = [(I_\lambda)''/(I_\lambda)']_\vartheta \qquad (3)$$

The abovedescribed device does not allow for evaluating ϑ incidence angles below $\vartheta \cong 6$ deg; even measurements at high incidence angles may become inaccurate because of the spread of the reflected components due to the thickness of the glass sheet (see Fig. 6).

In this case the rays can fall onto a wider area of the sensor, whose sensitivity is not uniform on its surface.

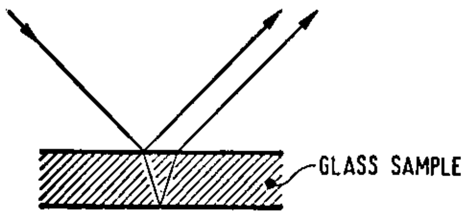

Fig. 6 - Spread effect due to sample thickness

For accurate measurement of the reflectance at normal incidence, a suitable optical apparatus is usually applied (Fig. 7).

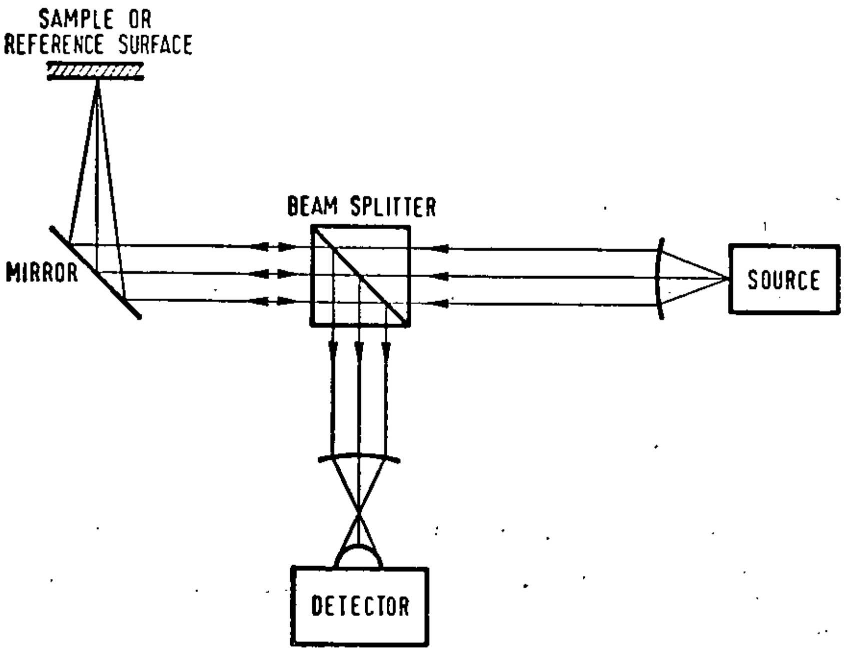

Fig. 7 - Apparatus for the evaluation of spectral reflectance

In this case, however, the measurements require a reference surface whose reflectivity is known.

As already seen for transmittance, also the solar reflectance can be calculated by suitably integrating the spectral reflectance.

A direct mean of measuring the solar reflectance is the previously described instrument proposed in [2], since the pyroheliometer can be mounted on an arm which enables it to rotate around the glass sample without disturbing the incident angle setting. The reflected energy is measured by simply rotating the pyroheliometer to the angle of rejection and reading the intensity of the reflected beam.

4. Absorptance

When the transmittance and reflectance are known, absorptance is found by

$$\alpha_{\lambda\vartheta} = 1 - (\tau_{\lambda\vartheta}+\rho_{\lambda\vartheta}) \qquad (4)$$

When the spectral values of transmittance and reflectance are available, the spectral absorptance can be found and the total normal absorptance can then be found by the same integration process as is used for the other two properties.
Absorptance can also be found from calorimetric measurements; in this case it is more convenient to determine the reflectance as:

$$\rho_{\lambda\vartheta} = 1 - (\alpha_{\lambda\vartheta}+\tau_{\lambda\vartheta}) \qquad (5)$$

thus bypassing the problems described in § 2.

REFERENCES

[1] Perkin-Elmer Corp., Analytical Instruments, Technical Bulletins, Norwalk, Ct.

[2] Yellott, J.I., "Selective Reflectance: a New Approach for Solar Heat Control", ASHRAE Transaction, Vol. 70, ASHRAE NY, 1967.

4.4.2. Field measurements of solar energy transmission

J.H. Klems
Windows and Lighting Program
Applied Science Division
Lawrence Berkeley Laboratory
University of California
Berkeley, CA 94720
USA

LIST OF CONTENTS I

1. SOLAR CALORIMETERS

Measurement of solar energy transmission through window systems has historically been closely linked with a single piece of experimental apparatus, the ASHRAE solar calorimeter [1]. This device, a diagram of which is shown in figure 1, was used at the ASHRAE Research Laboratory in Cleveland, Ohio, between 1948 and 1961 to study a series of fenestration systems in order to predict air conditioning peak loads [2-18]. This data was used to arrive at the concept of shading coefficient and to calculate many of the values for this quantity found in ASHRAE Fundamentals. The calorimeter was subsequently moved to the University of Florida, where work continued [19-20]. It is still used (primarily for commercial testing).

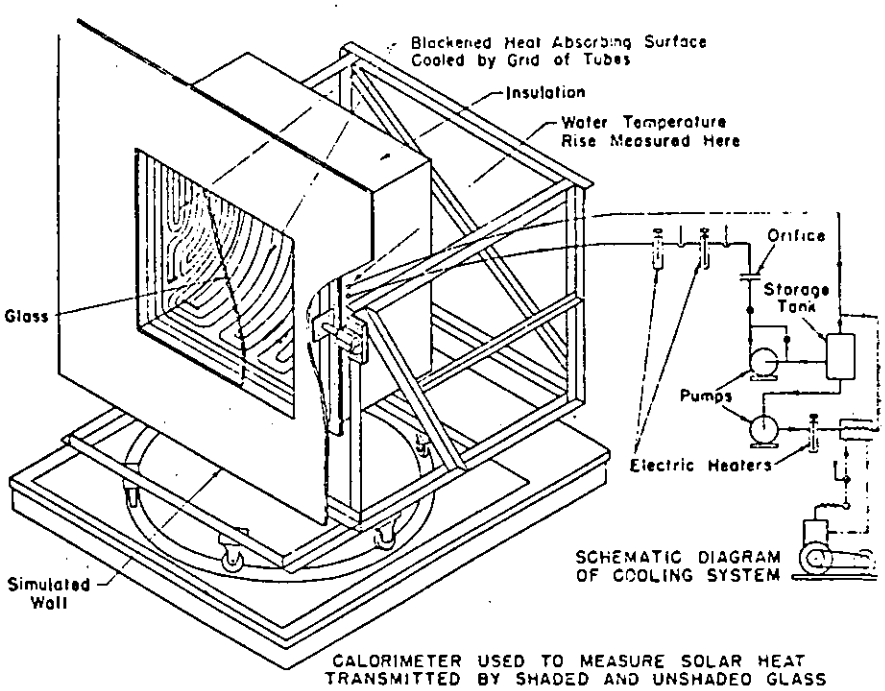

Figure 1: Schematic arrangement of ASHRAE solar calorimeter and cooling system [1].

A cross secton of the calorimeter is shown in figure 2 [20]. The sample opening is 1.22 m (4 ft) square. Temperature control is provided by the fluid circulating in the cylindrical walls, with natural convective heat transfer between the window system and the collector. Similar calorimeters (see figure 3) have been built at the University of Arizona [21].

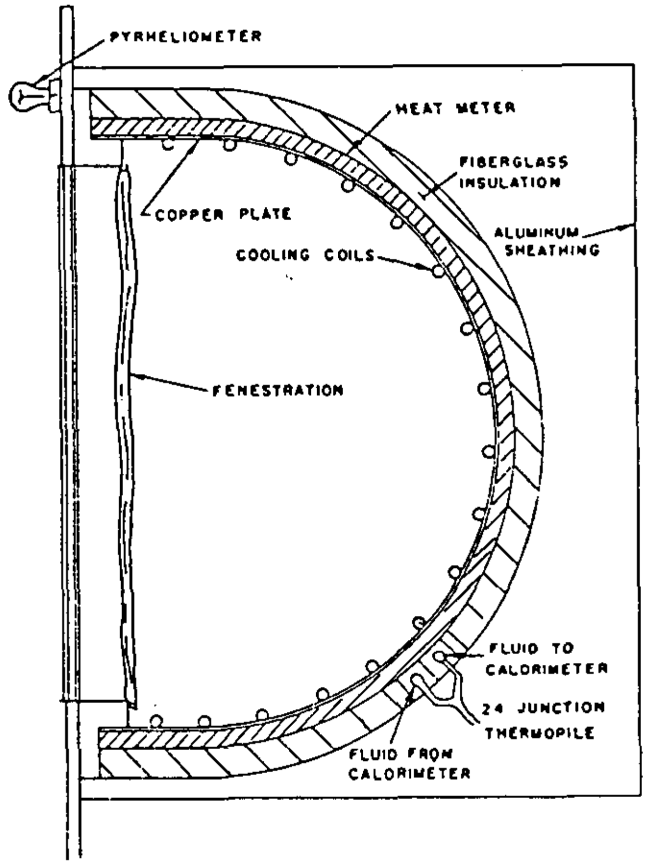

Figure 2: Cross section of ASHRAE solar calorimeter [20].

While originally the calorimeter was used to measure both nighttime U-values and daytime heat gain, after the development of the shading coefficient concept it was used for a direct measurement of the shading coefficient by holding the inside air temperature equal to the outdoor temperature. Because the heat extraction is through the absorber, if a window system transfers an appreciable part of the incident solar energy to the interior air it is necessary to hold the absorber temperature below air temperature in order to achieve equal indoor and outdoor air temperature. In turn the radiative coupling between the window and the room is altered. It is therefore not possible to measure the solar gain under the same conditions that would be experienced in actual use, and for complex shading systems it is not at all clear what experimental corrections one should make to account for this. In practice, measured internal and external heat transfer coefficients are converted to standard values using a method described by Yellott [22] for simple, plane-parallel glazing systems (*i.e.*, systems which present parallel glass surfaces to the indoor and outdoor environments), with no correction whatever being made when the window system is more complex (*e.g.*, drapes, blinds, shutters).

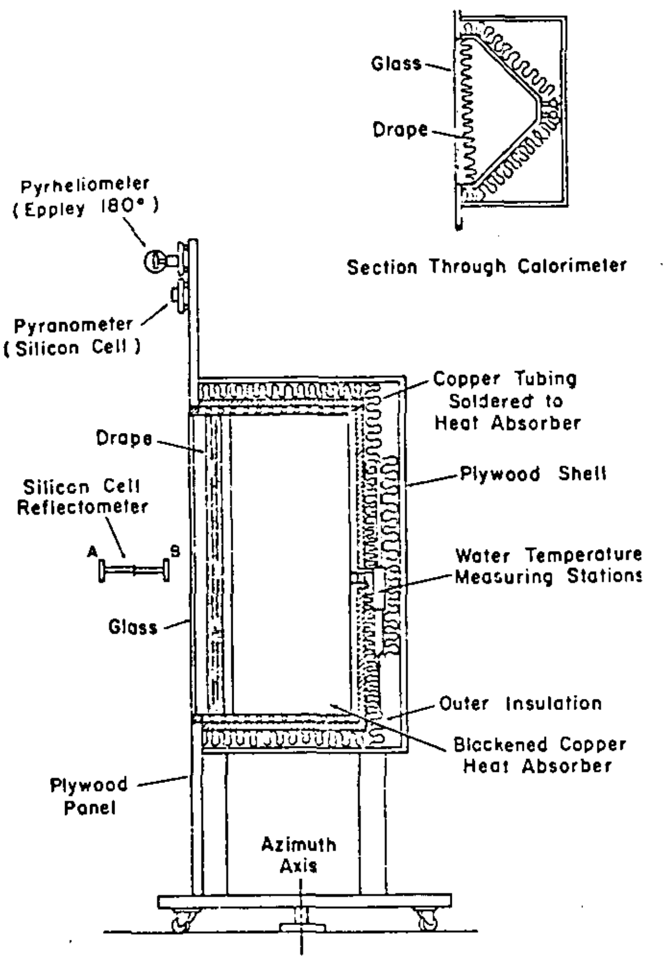

Figure 3: Schematic cross-section of Yelott solar calorimeter [21].

2. LARGER FIELD-TEST FACILITIES

Because the original calorimeter methodology was developed for studying peak loads, and because correction from measurement to actual conditions is uncertain for complex fenestrations, more recent work has moved toward measurements at full scale. A metering calorimeter has been introduced into the Passive Solar Test Facility at the National Bureau of Standards [23] (see figure 4). As can be seen from figure 5, this calorimeter has an interior which is designed to be very similar to that of a guarded hot box as described in ASTM Standard C-236. The calorimeter has an aperture of 2.09 m (high) by 1.26 m, and sets inside a room of the Passive Solar Test Facility, which acts as the guard for the calorimeter. Since the exterior wall against which the metering calorimeter mounts has an opening of 1.54 m (high) by 1.22 m, the latter is the effective sample opening. This facility is

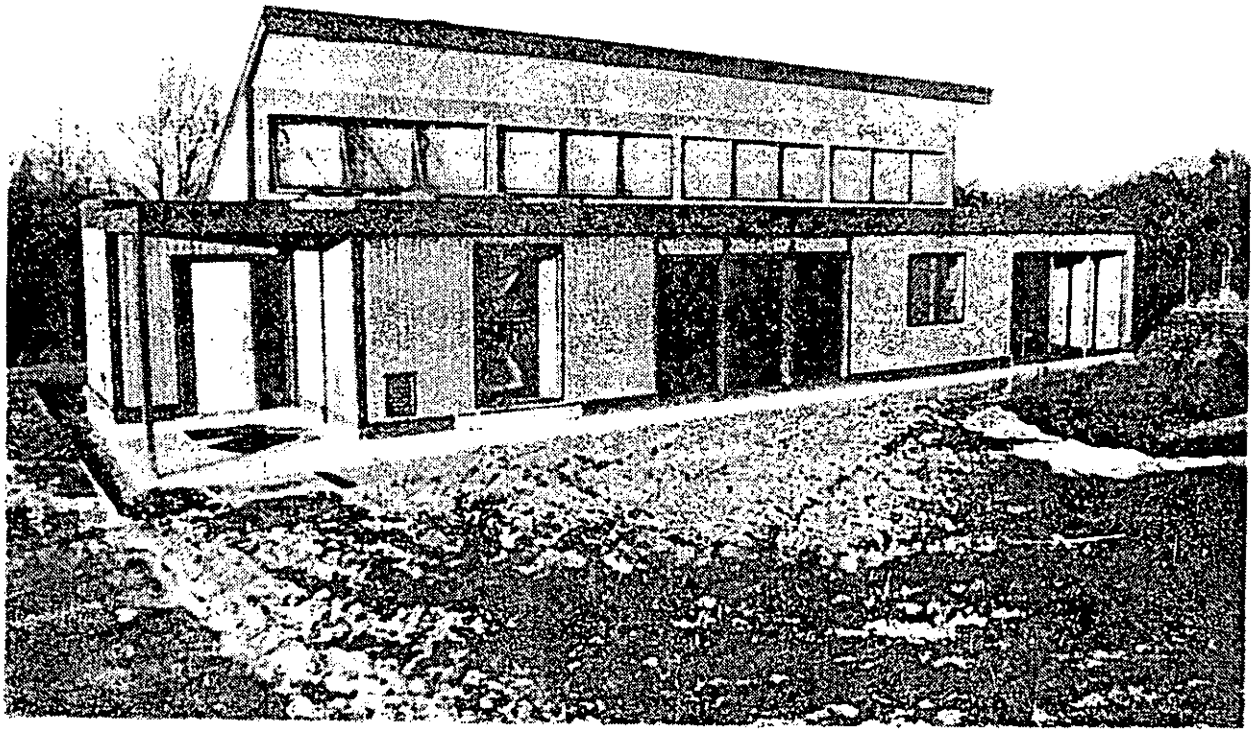

Figure 4a: Photograph of NBS/DOE passive solar test building [23].

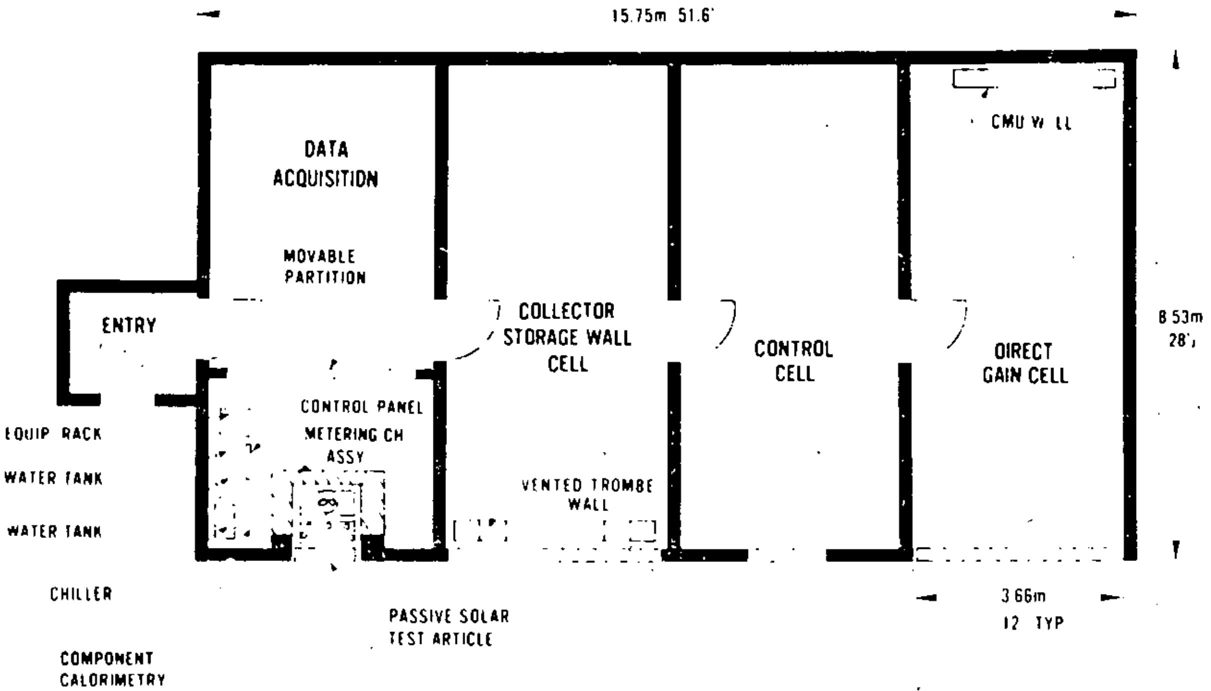

Figure 4b: Floor plan of passive solar test building showing location of metering calorimeter.

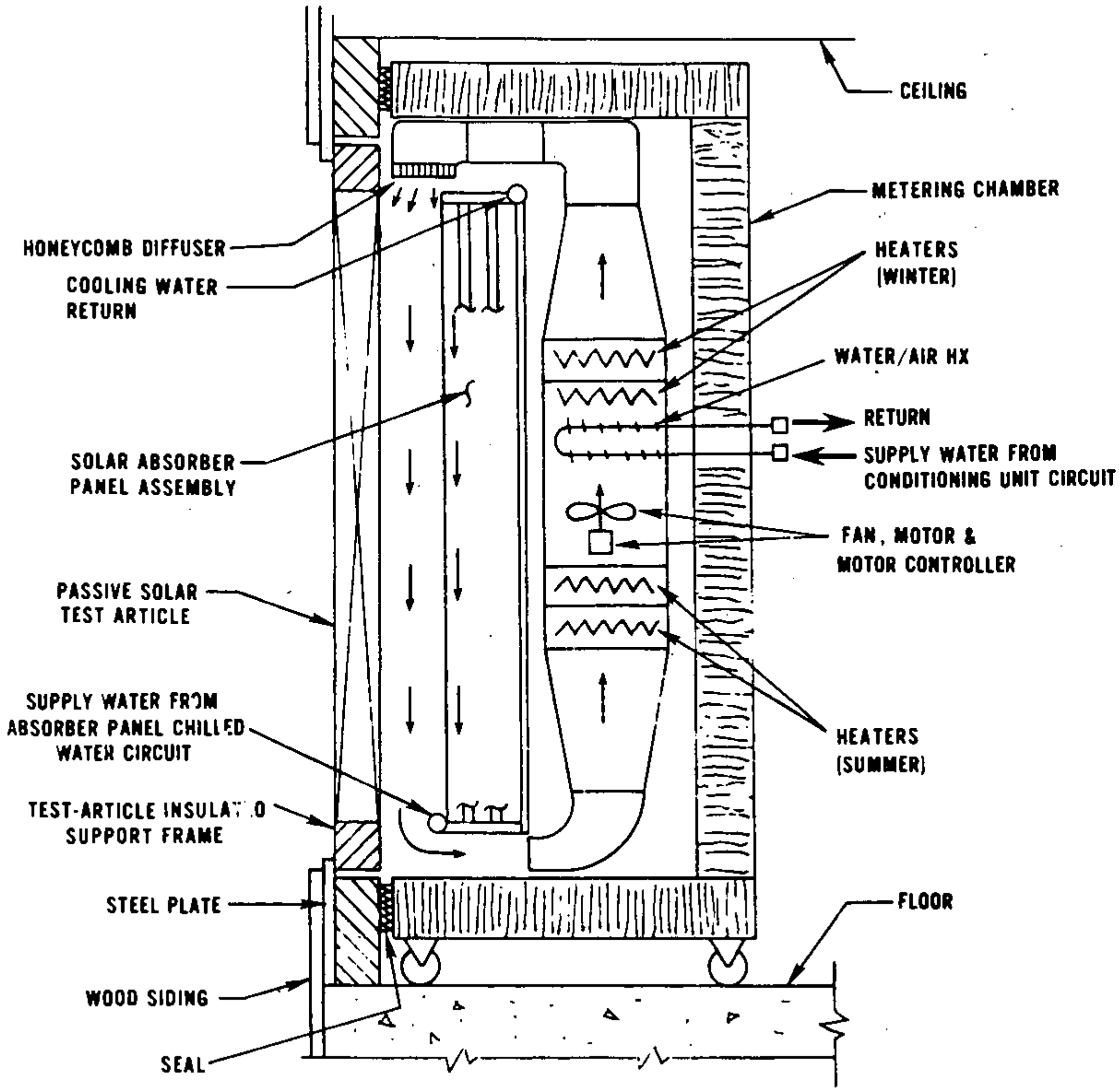

Figure 5: Schematic drawing of NBS metering calorimeter.

designed to measure net heat flow, *i.e.*, the combined effects of U-value and shading coefficient under actual weather conditions with south-facing orientation. Obviously, the interior conditions are artificial and are designed for test purposes (specifically, separating radiative and conductive effects) rather than realistic representation of an interior environment. Reference 23 contains all of the data which has so far been published from this facility, which is currently inactive.

A room-sized calorimeter for testing windows also exists at the Owens-Corning Research Laboratory (Granville, Ohio, USA). This is, however, a proprietary facility and data from it, while occasionally released, is not generally publically available. The facility is used in developing new products.

A large experimental building, the LESO, has been built at the Ecole Polytechnique Fédérale de Lausanne, Switzerland. Shown in figure 6, this facility consists of nine south-facing, thermally isolated, occupied offices [24]. Heat and light

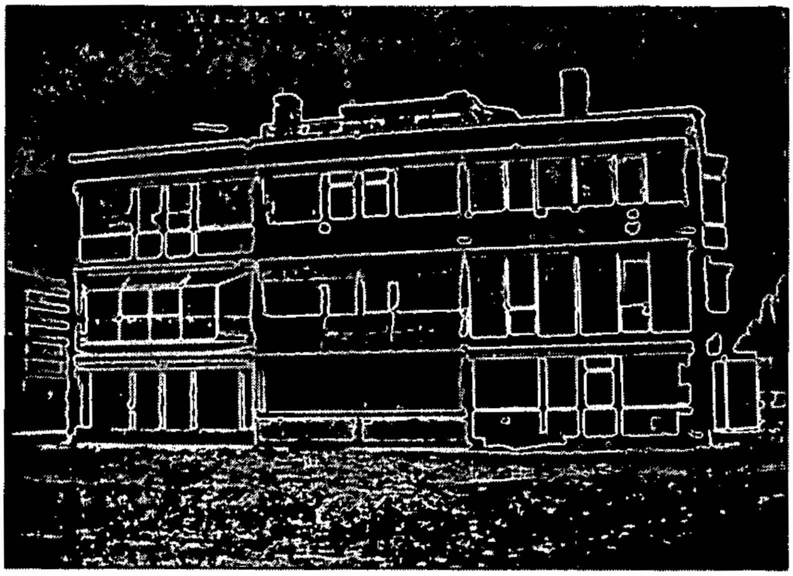

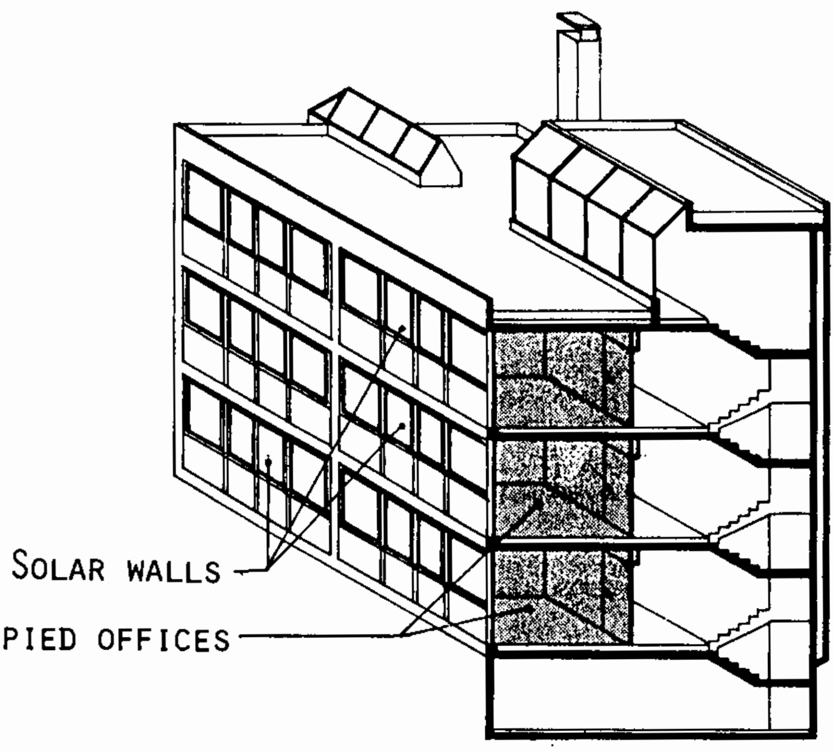

Figure 6: The LESO facility at the Ecole Polytechnique Fédérale, Lausanne (Switzerland), Latitude 46 °5, Altitude 410 m.

inputs to each office, air exchange rates and human occupancy are measured; entering solar energy is calculated from the solar flux incident on the building. This facility is oriented toward the measurement of seasonal performance of large (2.80 m x 7.20 m) wall sections which are passive solar systems; in this respect it is similar to the 3 non-calorimeter rooms of the NBS Passive Solar Facility described above. However, the LESO is unique in its use of well-controlled, occupied spaces as test modules and in its emphasis on comfort and occupancy effects along with average thermal performance. The large number of identical test rooms is also a significant advantage, allowing the simultaneous study of up to nine different configurations.

The typical LESO measurement period is a full year. During this time measurements of the average heating energy with the facade shaded are used to infer the facade heat loss coefficient, for which ±10% accuracy is claimed. Weekly-averaged heat inputs and incident solar fluxes are used to determine the average useful solar fraction, and relevant air and surface temperatures are integrated to evaluate comfort performance. Additional information is inferred by modeling the system with a detailed simulation code. Occupancy-associated performance fluctuations of up to 35% have been observed for solar systems. These are interpreted as primarily due to occupant behavior. The error sources to be dealt with in using measurements of this type to determine fenestration net performance have to some extent been discussed in the literature [25].

The PASSYS Project, a sizable program to deploy standardized calorimeters among a number of European countries, is currently being undertaken by the Commission of the European Communities [26]. The planned calorimeter [27], shown in conceptual form in figures 7 and 8, appears to have a sample opening of approximately 2.5-m square. It consists of a heavily-insulated shell, electric heating and a liquid-based cooling system. Since no provision is made for determining the amount of solar energy stored in the calorimeter envelope, it can be inferred that the intent is at least initially to measure long-term average or pseudo-steady-state performance. A discussion of some of the measurement issues in this generic type of facility has appeared in the literature [28,29].

The PASSYS Project plans to erect initially two and later up to six of these calorimeters at a chosen location in each of the participating countries. The first are to be in operation during 1987. The first year of the three-year project will be devoted to determining the method by which subsequent measurements will be made. As this research progresses it is obvious that instrumentation and design of the calorimeters may change from the plans contained in figures 7 and 8. A second goal of the research is to validate the detailed simulation program ESP and to develop simplified design tools.

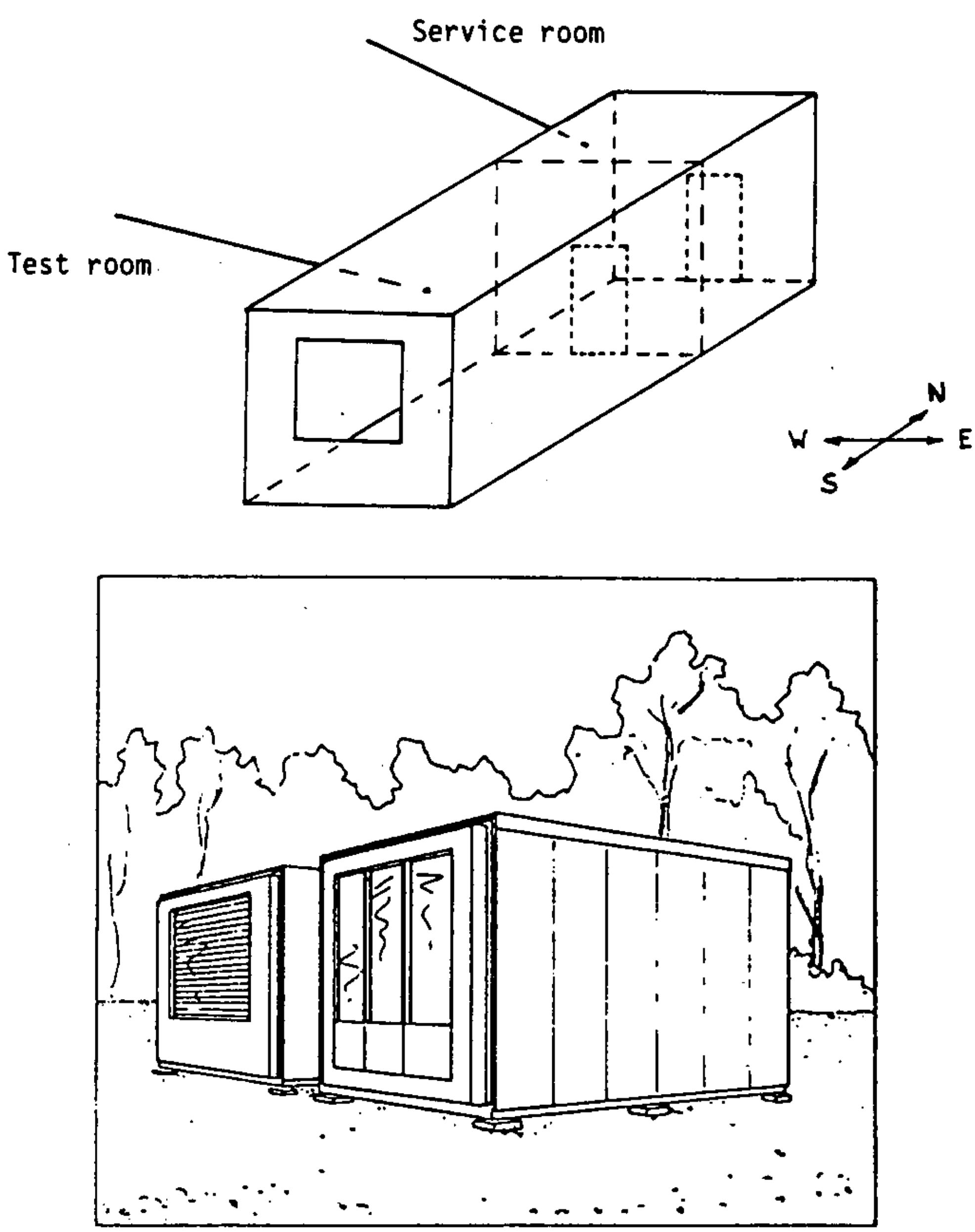

Figure 7: The PASSYS Facility.

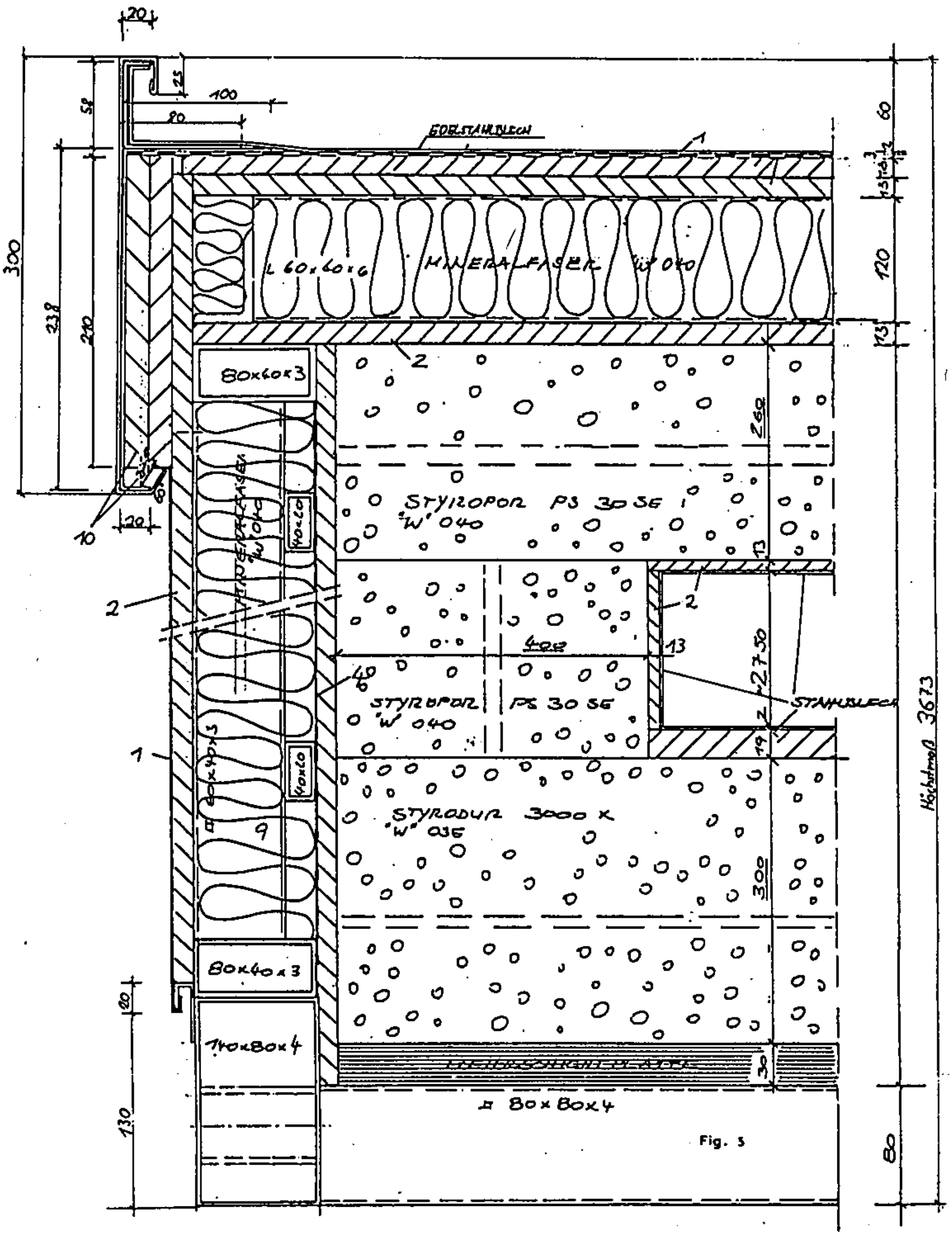

Figure 8: Details of the PASSYS Facility.

A common feature of all of the existing room-sized facilities so far discussed is that they make measurements which are averaged over one or more diurnal cycles. The diurnal average will include in the measurement the thermal storage effects of the measurement facility, and these effects significantly affect the fraction of the incident solar energy which will be termed useful. It is therefore not possible to generalize the measured results to other types of buildings and facilities without employing some form of detailed numerical model of the test facility. But the algorithms and assumptions contained in such a model are precisely those which are most critical to determining fenestration performance and which are therefore most in need of a detailed empirical test. To make such a test it is necessary to measure the overall energy flows through the fenestration and in the adjacent building space on a time scale short compared with that of the diurnal cycle.

A direct approach to this problem is being undertaken in the U.S.A. A room-sized, twin-chamber calorimeter, the Mobile Window Thermal Test (MoWiTT) Facility, has been developed at Lawrence Berkeley Laboratory [30,31]. This facility is shown in figures 9 and 10. It is designed to expose fenestration systems to outdoor conditions and accurately measure the net energy flow as a function of time, on a time scale short compared to that of a building, with interior conditions which duplicate those of a room as nearly as possible. Simultaneous measurement of two fenestration systems in the twin chambers allows a direct comparison of systems without the need to correct for different weather conditions in sequential tests. The facility can be turned to study fenestrations in different orientations, and can be moved to climates of interest. It will normally be used in Reno, Nevada, which has both cold winter and hot summer conditions. Preliminary hot-weather tests were carried out in Livermore, California.

Both the U-value and the shading coefficient can be extracted from the MoWiTT measurements of net energy flow by taking into account the basic assumption of the shading coefficient methodology, namely,

$$\phi = A\ (U\Delta T + SF\ I_S), \tag{1}$$

where ϕ is the net energy flow per unit time, A is the area of the fenestration, ΔT is the difference between exterior and interior air temperatures, and I_S is the incident solar intensity. The U-value U and and solar factor SF are independent of solar flux and air temperature, respectively, by assumption. (If this is not true,

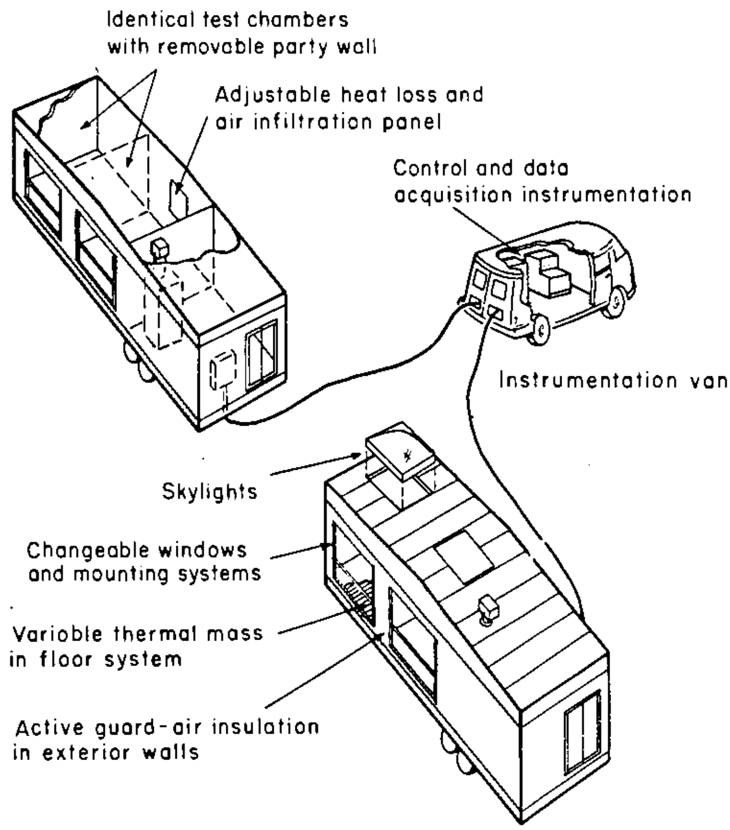

Figure 9a: Conceptual drawing of the MoWiTT Facility [24]. One of the two measurement modules shown has been built to date.

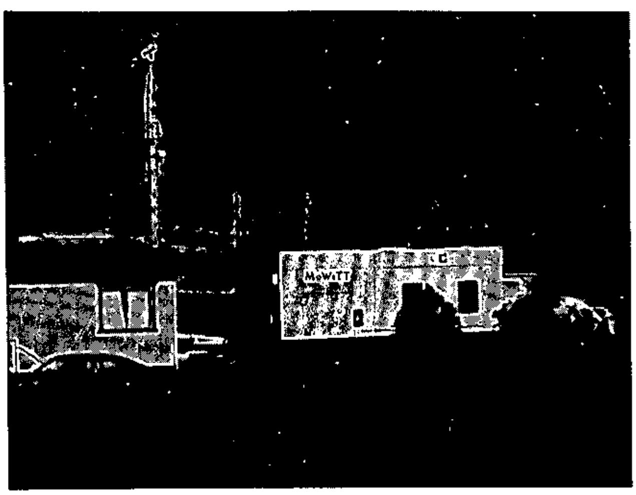

Figure 9b: MoWiTT Facility at its field test site in Reno, Nevada, U.S.A. Portable building at left contains data acquisition and support facilities.

then it is not possible to define either a solar factor or a shading coefficient.) Equation (1) is then fit to the (time-dependent) measured values of ϕ, ΔT, and I_S to determine the constants U and SF. If this is done for the fenestration in question and for a simultaneous measurement of a single-glazing sample of equal area, then the shading coefficient SC is given by

$$SC = \frac{SF_{fenestration}}{SF_{single\ glazing}}. \tag{2}$$

If the data fitted is taken over those hours of the day during which shading coefficients were normally measured with a solar calorimeter, then the resulting shading coefficient should be comparable to that used by ASHRAE. In addition, the quality of the fit to the data will give some estimate of the adequacy of the constant-shading-coefficient approximation. By accumulating data over an extended period, dependence of U and SF on other environmental conditions such as wind speed, sky temperature, solar incidence angle, and beam/diffuse ratio can be studied.

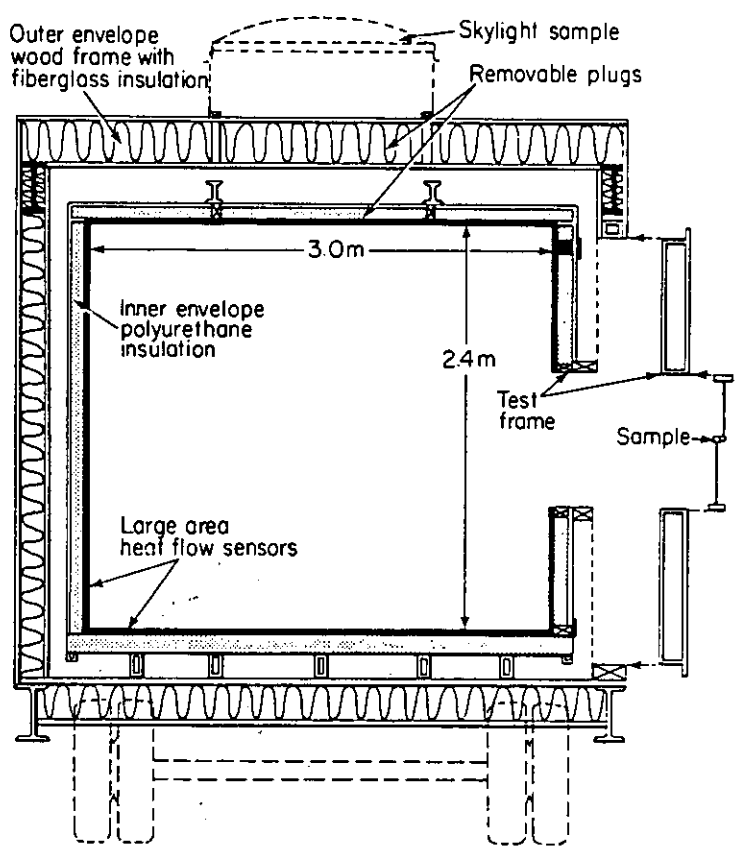

Figure 10: Cross section of a MoWiTT calorimeter chamber, showing mounting of a small-sized fenestration sample [24].

3. FENESTRATION FIELD PERFORMANCE DATA

Data from the MoWiTT facility have recently become available [32-34]. Since these represent the first short-time-scale measurements of the net heat flow through fenestrations under field conditions (even the ASHRAE calorimeter measurements are pseudo-steady-state), we will consider them in some detail.

Figures 11 and 12 [32] trace the diurnal behavior of the heat flow through single glazing under summer conditions in south- and east-facing orientations in Livermore, CA. These figures point out some of the complications attending a fit of Eqn. 1 to measured data, namely, that diffuse solar radiation and partial shading of the window due to its setback in the adjacent wall must both be accounted for.

In the later measurements of figures 13, 14, and 15, from [34], the effect of shading is minimized by having essentially no window setback. These measurements were made in Reno, Nevada, and are for spring/summer conditions. The measurements include the simultaneous operation of both calorimeters; figures 13 and 14 represent simultaneous measurements. The curves in these figures represent Eqn. 1 with values for U and SF assumed *a priori* rather than derived by fitting the data. As can be seen, the form of the curve appears to represent the shape of the data quite well, but the magnitudes of the day and nighttime maximum and minimum heat flows are not represented well, indicating the difficulty of predicting the magnitudes of the heat flows using "textbook" values for U and SF, even when detailed on-site measurements of temperature and solar flux are available.

The particular problem the experimenters encountered in this data was the fact that when the measurements were taken solar incident angles were much higher than generally assumed, resulting in a shading coefficient for beam solar radiation which is not slowly-varying with solar angle. In figure 14, for which the daytime peaks seem to be reasonably well represented, a shading coefficient of 0.60 was used to generate the curve, while the standard ASHRAE value (assuming an incident angle of 30°) would be 0.85. The details will be found in the references.

A similar correspondence between the general form of the Eqn. 1 calculation and the measured data also holds for north-facing measurements, shown in figures 16, 17 and 18.

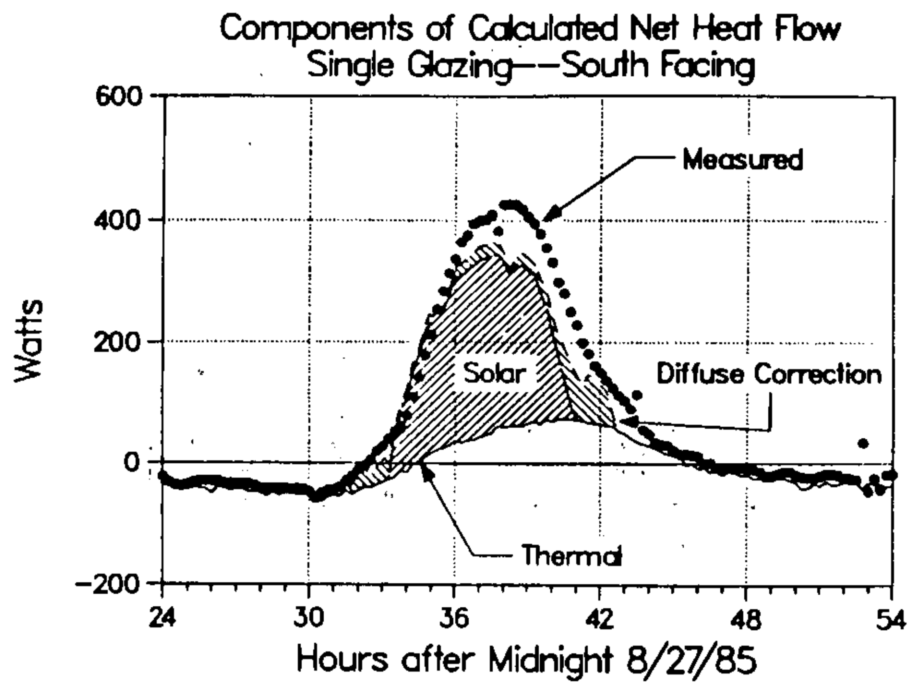

Figure 11.

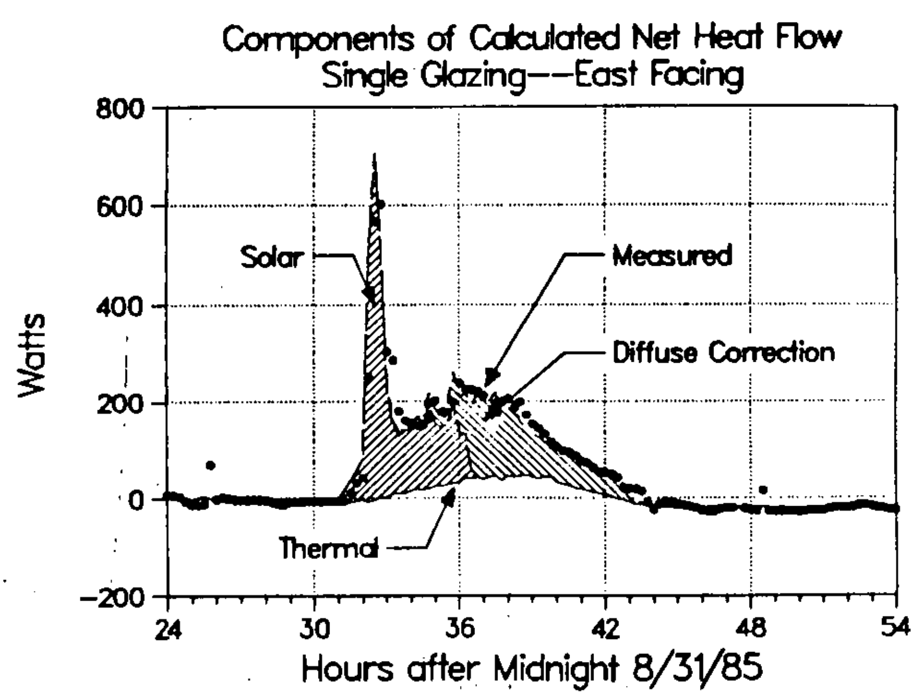

Figure 12.

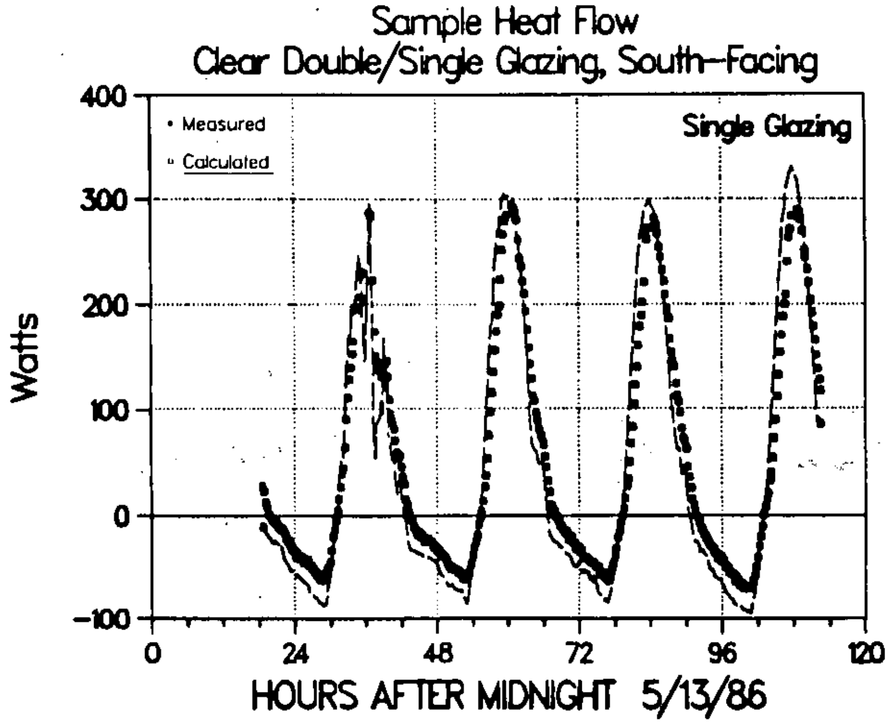

Figure 13.

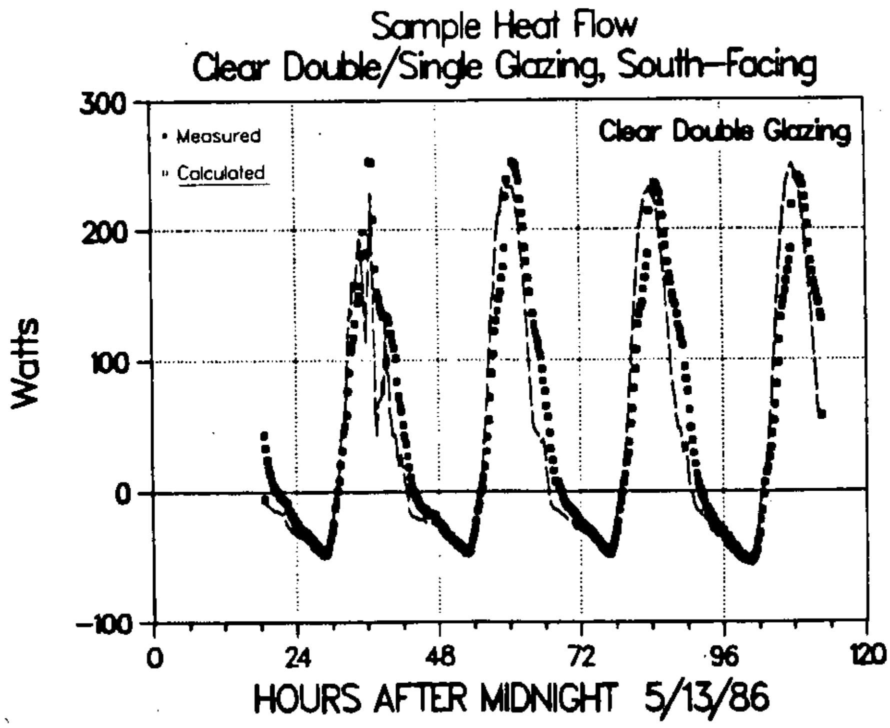

Figure 14.

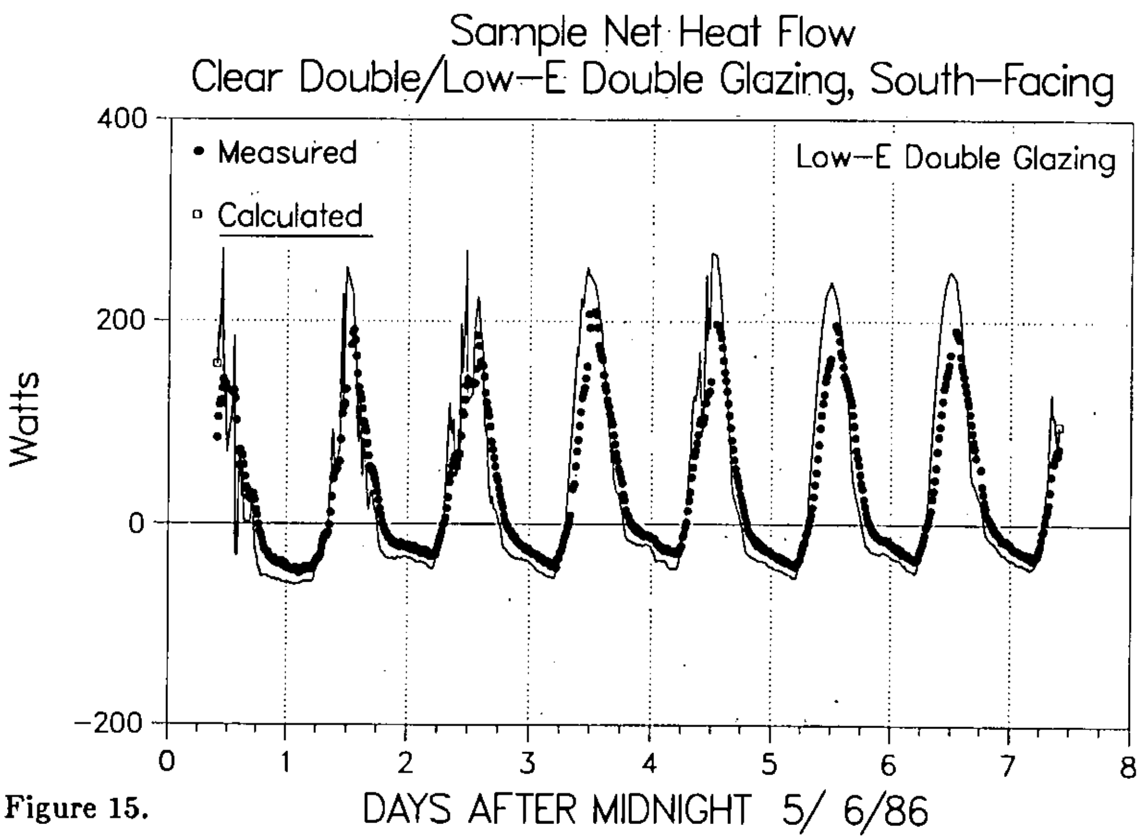

Figure 15.

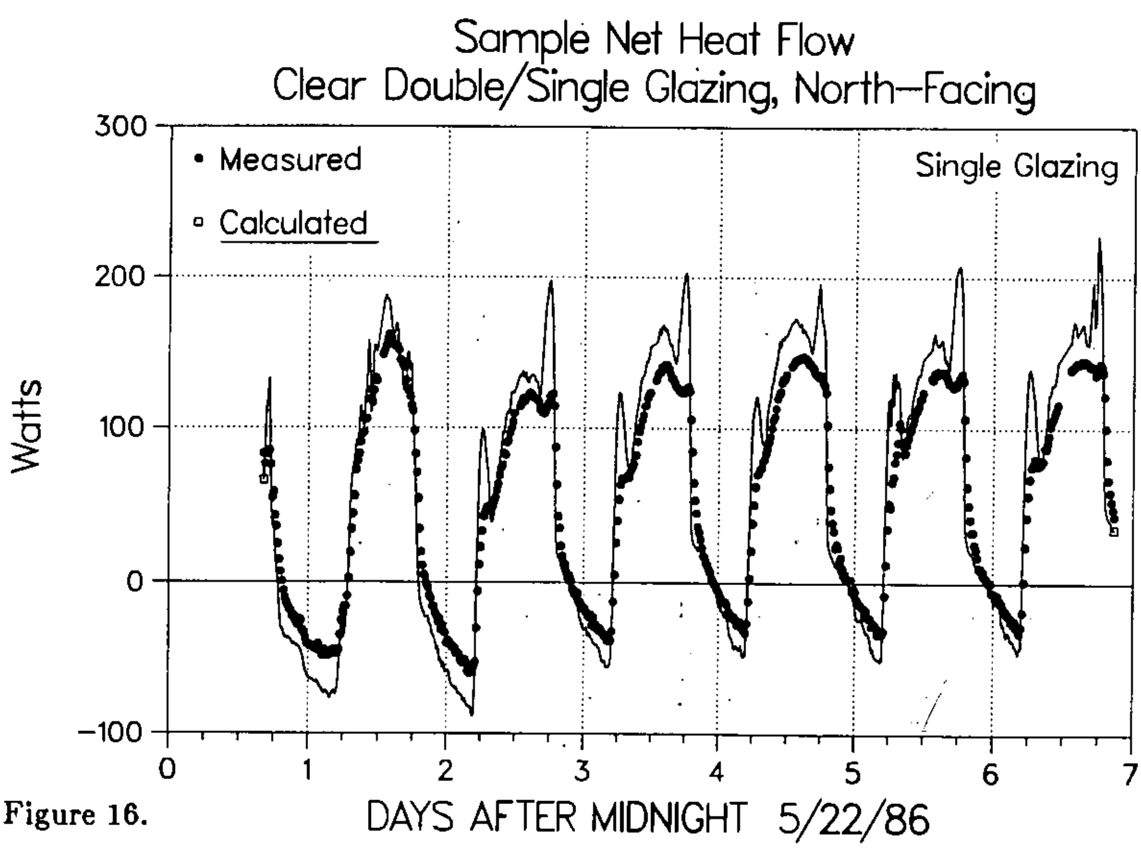

Figure 16.

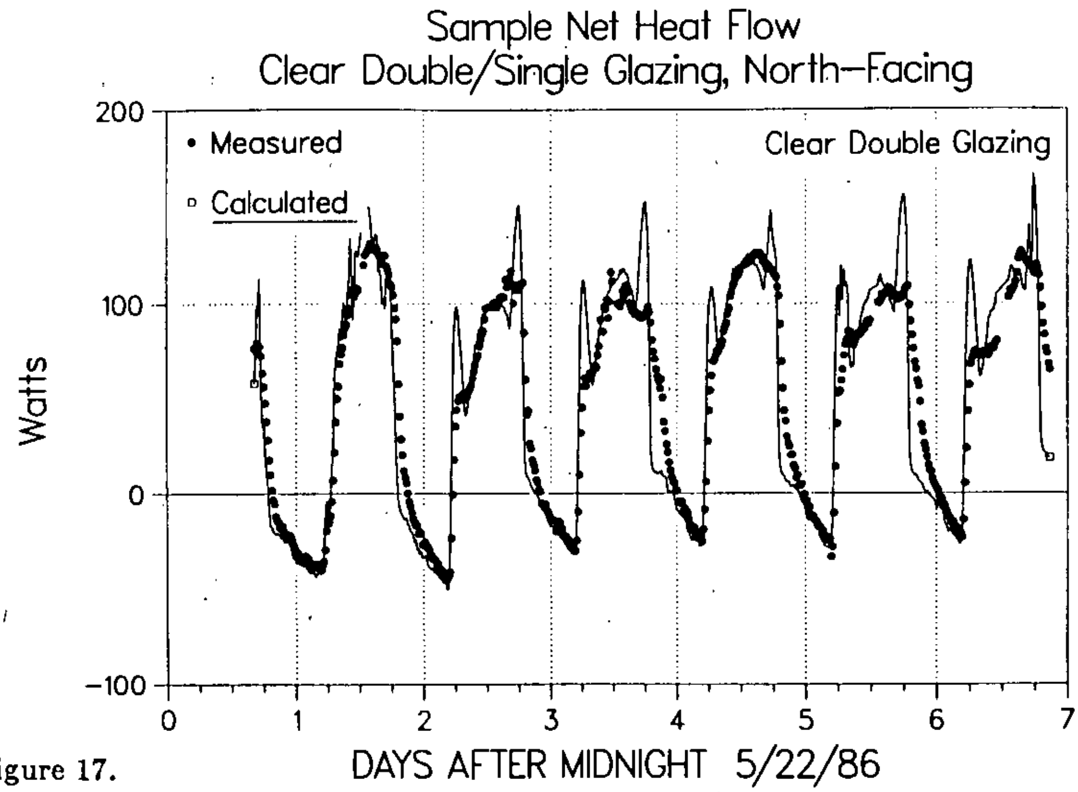

Figure 17.

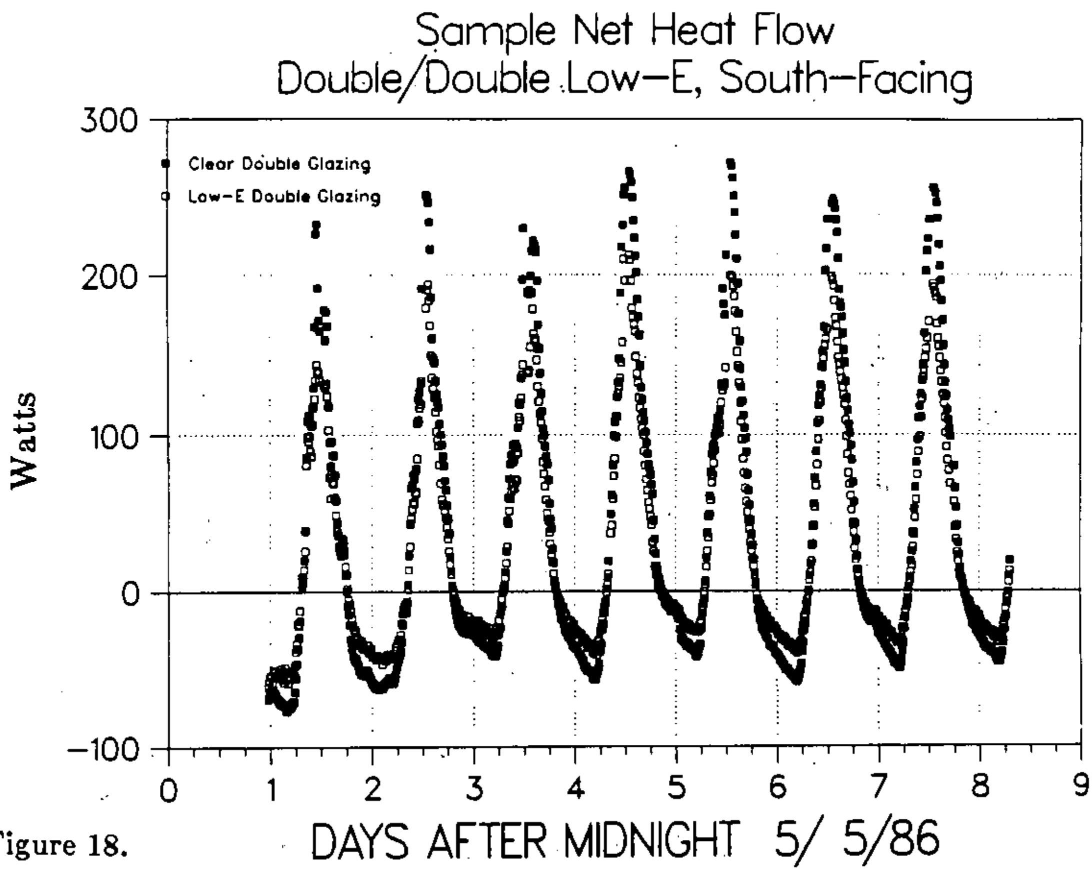

Figure 18.

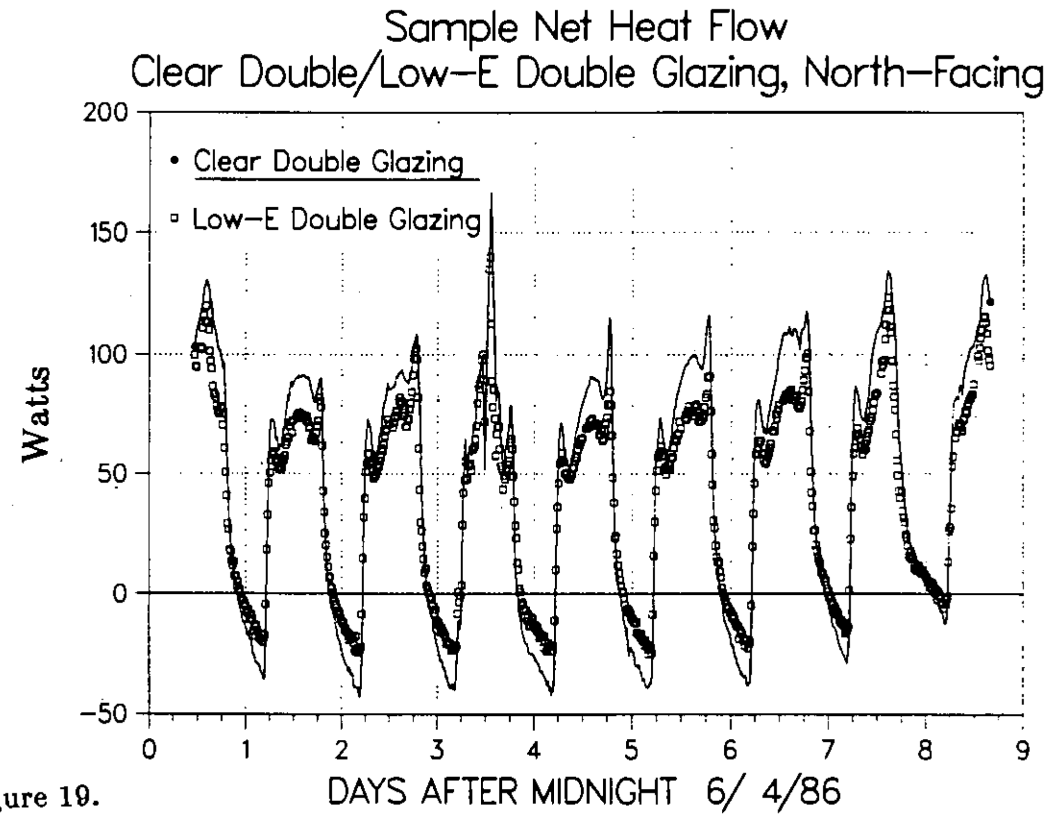

Figure 19.

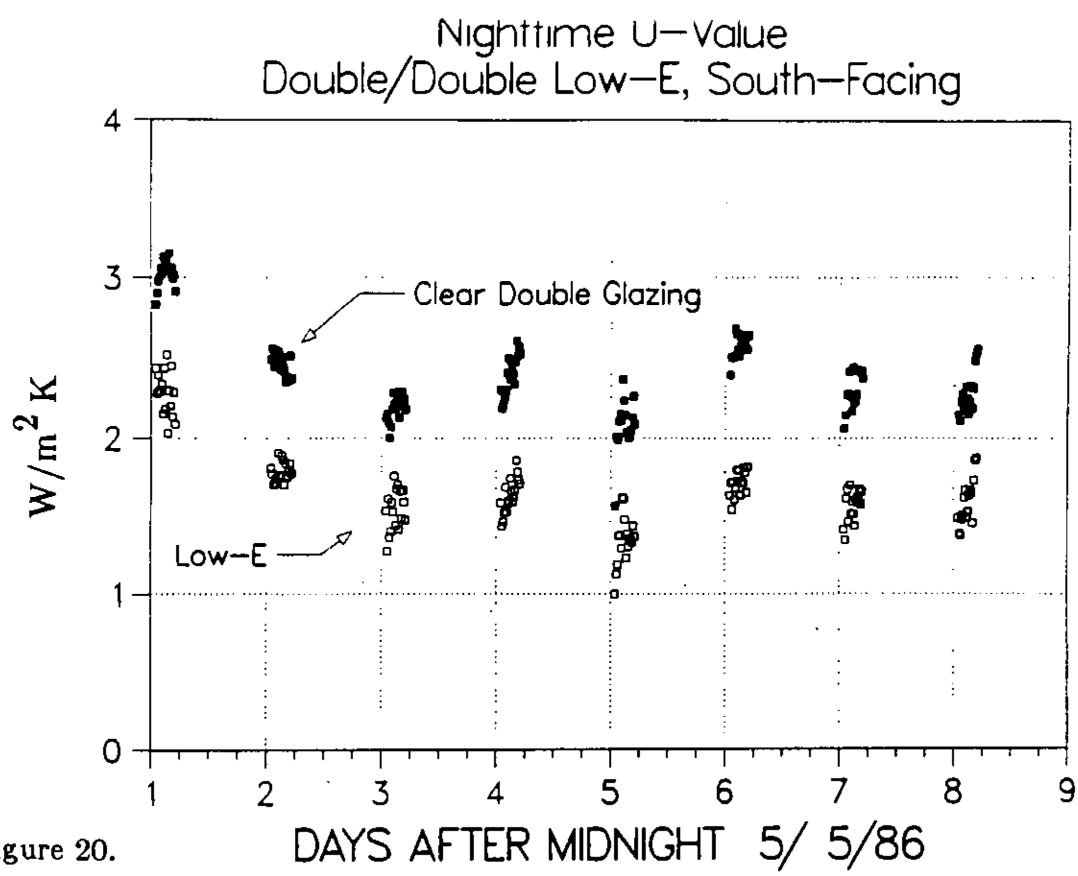

Figure 20.

One of the interesting features of these measurements includes a direct comparison between frameless sealed insulating glass units which are of identical construction except that in one unit the number 3 glazing surface (as counted from the outdoor side) has a low-emissivity (Low-E) sputtered coating. The overall heat flows through this unit are those of figures 15 and 18.

The direct measured comparison between the two units is shown in figure 19, taken from [33]. This figure demonstrates that the effect of adding a low-emissivity coating is to reduce the magnitude of both daytime heat gain (due to absorption in the coating) and nighttime heat loss. While these measurements were made under summer conditions, the same effect will occur under winter conditions, when the solar heat gain may be beneficial. The evaluation of these coatings should therefore be based on overall diurnal performance (including comfort considerations affecting the utilizability of daytime solar gain) rather than on a simple comparison of nighttime U-values. Figure 20 graphs instantaneous measurements of nighttime U-value [33].

4. ACKNOWLEDGEMENTS

This work was supported by the Assistant Secretary for Conservation and Renewable Energy, Office of Buildings and Community Systems, Building Systems Division of the U.S. Department of Energy under Contract No. DE-ACO3-76SF00098.

5. REFERENCES

[1] George V. Parmelee, Warren W. Aubele and Richard C. Huebscher, *ASHVE Transactions,* Vol. 54, p. 158, 1948.

[2] George V. Parmelee and Warren W. Aubele, *ASHVE Transactions,* Vol 54, p. 407, 1948.

[3] G. V. Parmelee and W. W. Aubele, *ASHVE Transactions,* Vol. 55, p. 39, 1949.

[4] George V. Parmelee and Warren W. Aubele, *ASHVE Transactions,* Vol. 55, p. 435, 1949.

[5] G. V. Parmelee and W. W. Aubele, *ASHVE Transactions,* Vol. 56, p371, 1950.

[6] G. V. Parmelee and W. W. Aubele, *ASHVE Transactions,* Vol. 57, p. 209, 1951.

[7] G. V. Parmelee and W. W. Aubele, *ASHVE Transactions,* Vol. 58, p 85, 1952.

[8] G. V. Parmelee, W. W. Aubele, and D. J. Vild, *ASHVE Transactions,* Vol. 59, p. 221, 1953.

[9] G. V. Parmelee and D. J. Vild, *ASHVE Transactions,* Vol. 59, p. 403, 1953.

10 G. V. Parmelee, *ASHVE Transactions,* Vol. 60, p. 341, 1954.

[11] D. J. Vild and G. V. Parmelee, *ASHAE Transactions,* Vol. 62, p. 89, 1956.

[12] Necati Ozisik and L. F. Schutrum, *ASHAE Transactions,* Vol. 64, p. 463, 1958.

[13] Necati Ozisik and L. F. Schutrum, *ASHAE Transactions,* Vol. 65, p. 311, 1959.

[14] N. Ozisik and L. F. Schutrum, *ASHRAE Transactions,* Vol. 65, p. 714, 1959.

[15] N. Ozisik and L. F. Schutrum, *ASHRAE Transactions,* Vol. 66, p. 228, 1960.

[16] N. Ozisik and L. F. Schutrum, *ASHRAE Transactions,* Vol. 66, p. 359, 1960.

[17] L. F. Schutrum and N. Ozisik, *ASHRAE Transactions,* Vol. 67, p. 465, 1961.

[18] L. F. Schutrum, *ASHRAE Transactions,* Vol. 68, p. 167, 1962.

[19] Erich A. Farber, William A. Smith, C. W. Pennington, and John C. Reed, *ASHRAE Transactions,* Vol. 69, p. 392, 1963.

[20] C. W. Pennington, William A. Smith, Erich A. Farber, and John C. Reed, *ASHRAE Transactions,* Vol. 70, p. 54, 1964.

[21] John I. Yellott, *ASHRAE Transactions,* Vol. 71, p. 260, 1965.

[22] John I. Yellott, *ASHRAE Transactions,* Vol 72, part 1, p. 72, 1966.

[23] M. E. McCabe, C. E. Hancock and M. Van Migom, "Thermal Performance Testing of Passive Solar Components in the NBS Calorimeter", National Bureau of Standards Report NBSIR 84-2920, U.S. Department of Commerce, Gaithersburg, MD, 1984.

[24] A. Faist, J.-B. Gay, A. Razafindraibe, J.-L. Scartezzini and F. Thévenon, "The passive solar energy building 'LESO'-- a new tool for passive and hybrid systems investigation," *Proceedings of the 2nd International Congress on Building Energy Management*, p. 1.17, Ames, Iowa, 1983.

[25] J. H. Klems, "Error Analysis of *in Situ* Field Tests of Fenestration Net Energy Performance", *Energy and Buildings 8*, pp. 165-173, 1985.

[26] R. Gicquel, "Conceptual Framework for PASSYS", ARMINES, Ecole des Mines de Paris, Centre d'Energetique, unpublished report, April, 1986.

[27] K. Schreitmuller, F. Mehlhorn, and G. Linder, "Design of an Advanced Passive Solar Test Facility," DFVLR, April 1985.

[28] J. H. Klems, "Measurement of Fenestration Net Energy Performance: Considerations Leading to Development of the Mobile Window Thermal Test (MoWiTT) Facility", ASME Meeting paper 84-WA/Sol-7 and Lawrence Berkeley Laboratory Report LBL-18144, 1984.

[29] H. A. L. Van Dijk et. al., "A Test Facility for Passive Solar Energy Systems in the Netherlands", Report 403.219, TPD-TNO, Delft, Netherlands, 1985.

[30] Joseph H. Klems, Stephen Selkowitz and Sy Horowitz, "A Mobile Facility for Measuring Net Energy Performance of Windows and Skylights," *Energy Conservation in the Built Environment,* Vol. III, p. 3.1, An Foras Forbartha, Dublin, Ireland, 1982.

[31] J. H. Klems, *Measurement of Fenestration Performance Under Realistic Conditions,*, Lawrence Berkeley Laboratory Report No. LBL-17429, 1984 (Presented at Windows in Building Design and Maintenance, Gothenburg, Sweden, June 13-15, 1984).

[32] J. H. Klems and H. Keller, "Measured Net Energy Performance of Single Glazing Under Realistic Conditions," *Thermal Performance of the Exterior Envelopes of Buildings III,* (Clearwater, Fla.,Dec. 2-5) 1985, ASHRAE, Atlanta, GA.

[33] J. H. Klems and H. Keller, "Thermal Performance Measurements of Sealed Insulating Glass Units with Low-E Coatings Using the MoWiTT Field Test Facility," Lawrence Berkeley Report LBL-21583, *ASHRAE Transactions* 1987, V. 93, Pt. 1.

[34] J. H. Klems and H. Keller, "Measurement of Single and Double Glazing Thermal Performance under Realistic Conditions using the Mobile Window Thermal Test (MoWiTT) Facility," Lawrence Berkeley Laboratory Report LBL-22149, to be presented at the 1987 ASME Solar Energy Conference, Honolulu, Hawaii, March, 1987.

4.5. Influence of solar protections

H. Erhorn

R. Stricker

M. Szerman

Fraunhofer Institute of Building Physics
Department of Heat and Climate
(Director: Prof. Dr.-Ing. habil K.A. Gertis)
Nobelstrasse 12
D-7000 STUTTGART 80
FEDERAL REPUBLIC OF GERMANY

LIST OF SYMBOLS

SF	solar factor (whole system)	[-]
g	total solar energy transmission coefficient (for glazing)	[-]
z	reduction factor	[-]
SC	shading coefficient	[-]
f	fraction of window area in relation to facade area	[-]
τ_e	direct solar transmission coefficient	[-]

Subscripts

w	window
e	exterior
i	interior

1. INTRODUCTION

Summerly heat protection depends on the energy permeability of transparent external areas of the building (windows and fixed glazing including sunshading), its ratio to the total external area of the building, its orientation to the cardinal points, the ventilation inside the rooms, the heat storage capacity (particularly of inside partitions of the building) as well as on heat conduction of the non-transparent external areas of the building under variable boundary conditions (day-time temperature course and solar radiation).

Admittedly, the evaluation of solar gains through glazings and solar protections may be based on energetical aspects; it is, however, recommended to consider the lighting performance as well.

The determination of values is carried out calorimetrically, spectrophotometrically and, for some special cases, derived calculation procedures are given [1]. In this chapter the estimations are carried out in an international comparison. In chapters 4.3, 4.4.1 and 5.1 the phenomena and measurement methods concerning energetic and daylighting properties are described in greater detail.

2. EFFICIENCY OF SOLAR PROTECTIONS

An effective sunshading for transparent external areas of a building can be achieved through structural forms (as cantilevered roofs, balconies) or by means of exterior or interior sunshading devices (as e.g. window shutters, slattered roller blinds, louvers, marquises and solar glazings). Automatical sunshading devices can have an exceptionally favourable effect, but they are expensive and could cause control problems. The multifunctional usage of building elements as constructive and overhang types looks promising at first sight but they lack adaptability to actual solar angles or overcast conditions. Moreover, those elements represent classical thermal bridges which cause increased heat transfer during the heating season.

2.1 Energetic Evaluation

To make energetic evaluations of solar gains through glazing with and without sunshading devices, different parameters are used internationally. In most countries the Solar Factor (SF) is taken as a basis. Sometimes this factor is determined as "total solar radiant heat transmission" [2] and is defined as:

Fraction of solar radiant heat at normal incidence that is transferred through the glazing by all means. It is composed of the direct transmittance and an appropriate fraction of the absorptance determined for the "normal" exterior and interior surface resistances. Where the glass surfaces have an emittance different from that of ordinary glass, the surface heat transfer has to be modified appropriately (see also chapter 4.3).

In most countries the SF-factor is determined for the complete system (glass including device). But in some countries the values for glazing and sunshading device are given separately to reduce the measurement effort. For glazing the total solar energy transmission coefficient (g), and for sunshading devices a reduction factor in connection with glazing (z) is determined. The SF-factors for the combination glass inclusive sunshading result from multiplication of factors g and z:

$$SF = g \cdot z \qquad 1)$$

Physically seen, this method is not exact because the z-factor is influenced by the glass itself in case of a glass sunshading combination [3] and therefore cannot be stated independently of the glass.

In some countries the shading coefficient (SC) is used as common criterion of window performance. The shading coefficient is the total solar heat transmission of the window expressed as a fraction of the total solar heat transmission through clear single glazing. The total transmission is the sum of the direct transmission and the part of the absorbed radiation that is released inwards. The reference level is that of a notional clear single glass that has a total transmission of 87 per cent of the incident energy.

Therefore the shading coefficient results to:

$$SC = \frac{SF}{0.87} \tag{2}$$

The shading coefficient depends upon the solar optical properties of the glass and the material of the blind, on the coefficients of the geometry of the blinds and the angular position of the sun [9].

The most efficient operation of louvered blinds is achieved when they are so adjusted that the reflected radiation passes normally through the glass as shown in Figure 1. Because the position of the sun changes continually it is impracticable to keep louvers in the most efficient position and it is general practice to make an initial setting, probably to somewhere near the 45° position assumed in this report, and then leave the blind unchanged until the sun is off the facade [9].

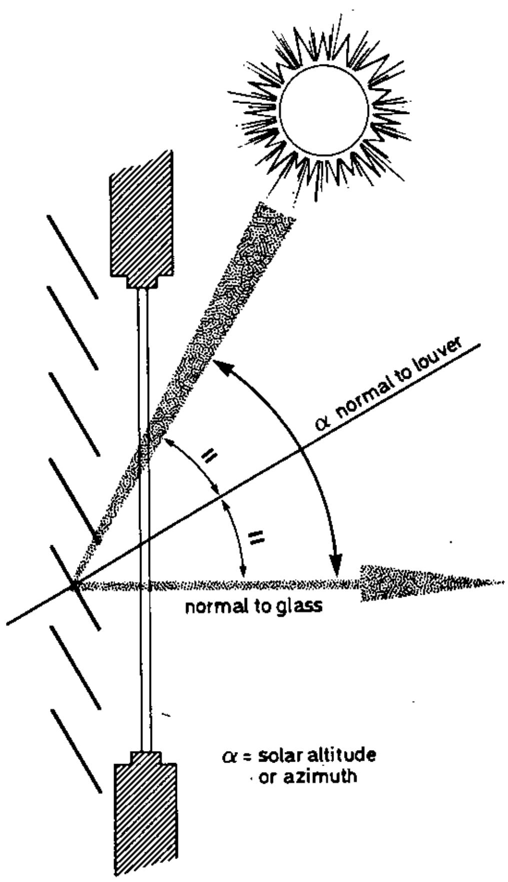

Figure 1: Louvered blinds adjusted for maximum rejection of solar radiation.

In the following, the parameters used derived from the different standards or publications in the participating countries are described:

- Federal Republic of Germany:

In Germany the standard values for g- and z-factors are combined in DIN 4108 [4]. Productspecific deviations can occur in single investigations or standard measurements [5]. In Table 1 the standardized z-factors are shown. The thereby resulting SF-factors for double and triple glazing are shown in Table 2. Investigations [6] rendered z-factors, shown in Figure 2, for different sunshading devices in conjunction with a double glazing.

Table 1: Total solar energy transmission coefficient of glazing (g-Value), according to [4].

line		glazing	g
1	1.1	double-glazing out of clear glass	0.8
	1.2	triple-glazing out of clear glass	0.7
2		glass blocks	0.6
3		multiple glazing with special glass (heat absorbing glass, antisun glass)	0.2 - 0.8

Table 2: Reduction factors of sunshading devices in connection with glazing (z-Factor), according to [4], and the equivalent SF-(SC-)factors for combination with double and triple glazing

line	sunshading devices	z	SF (SC) double glazing	SF (SC) triple glazing
1	lacking sunshading devices	1.00	0.80 (0.92)	0.70 (0.80)
2	internal and between panes			
2.1	woven fabric or foil	0.40-0.70 (0.46-0.80)	0.32-0.56 (0.37-0.64)	0.28-0.49 (0.32-0.56)
2.2	jalousies	0.50 (0.57)	0.40 (0.46)	0.35 (0.40)
3	external			
3.1	jalousies, venetian slats, ventilated	0.25 (0.29)	0.20 (0.23)	0.18 (0.21)
3.2	jalousies, slatted roller blinds, window shutter, fixed or venetian slats	0.30 (0.34)	0.24 (0.28)	0.21 (0.24)
3.3	canopies, loggias	0.3 (0.34)	0.24 (0.28)	0.21 (0.24)
3.4	marquises, ventilated from the top and sideways	0.40 (0.46)	0.32 (0.37)	0.28 (0.32)
3.5	marquises in general	0.5 (0.57)	0.40 (0.46)	0.35 (0.40)

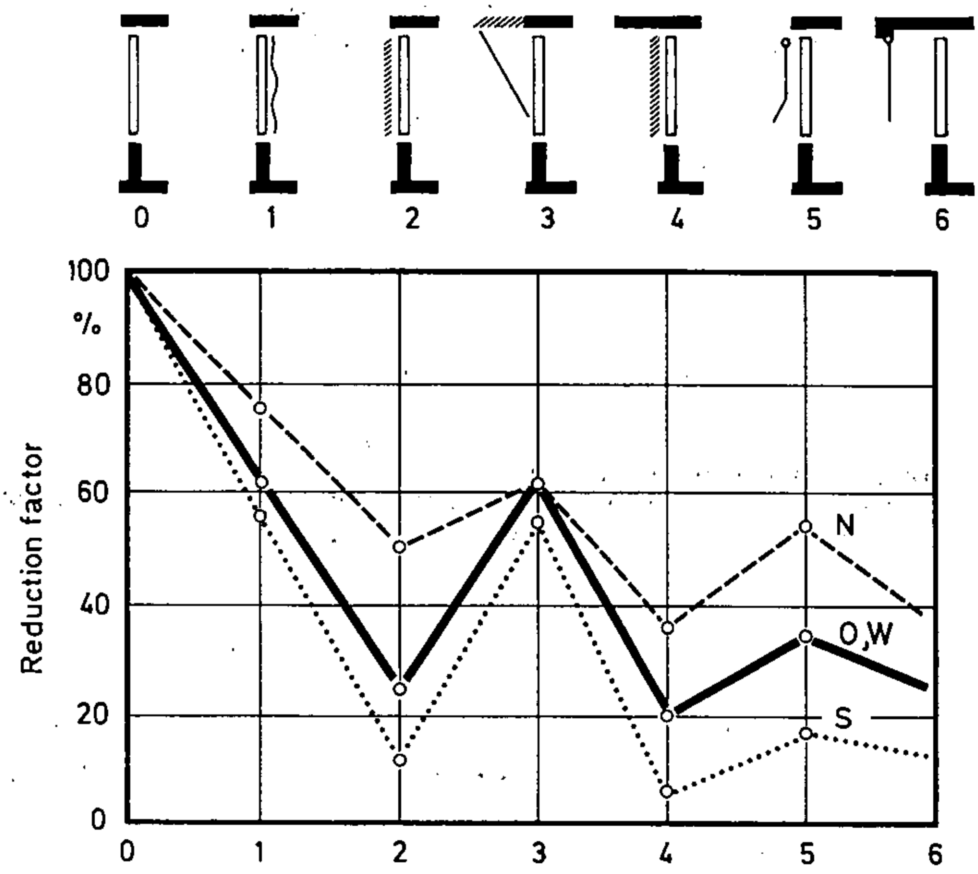

Figure 2: Reduction factor (z-factor) of various sunshading devices and different orientations in combination with double glazing, according to [6].

- Italy:

In Italy normally the combined SF-factor for glass incl. sunshading devices is used. In chapter 4.3. extensive examples in respect to this are listed.

- Netherlands:

In the Netherlands the concept ZTA is commonly used for the solar transmittance. ZTA is determined for 75 per cent direct radiation at an angle of incidence of 45° plus 25 per cent diffuse radiation. A computer model has been developed for calculation of the SF-factor of window systems including venetian blinds [7]. Results are compiled in Table 3. The different definition of ZTA compared to g is the reason why the values for unshaded glazing units are lower than those for example given in the German standard DIN 4108 [4] and ASHRAE standard [8]. It appears that the SF-factor for double glazing with internal blinds is higher than for the same system with single glazing only.

Table 3: Solar factor (SF) for a single and double glazed window system with internal and external venetian blinds, calculated for angles of incidence of 45° plus some diffuse radiation (in the Netherlands ZTA-concept), according to [7].
For comparison, the shading coefficient (SC), calculated by way of equation (2), is given as well.

no.	window	SF	SC
1	single clear glass, 6 mm	0.80	0.92
2	as 1, with internal venetian blinds light coloured, slat angle 45°	0.44	0.51
3	as 1, with external venetian blinds light coloured, slat angle 45°	0.15	0.17
4	double clear glass 6-12-6	0.70	0.80
5	as 2, with double glass	0.46	0.53
6	as 3, with double glass	0.13	0.15

- Switzerland:

In Switzerland a solar factor is used which results from calorimetric measurements under natural conditions at a measuring duration of 2 hours.

In Table 4 values for external and internal sunshading devices are listed.

Table 4: Solar factors used for cooling load calculations in Switzerland [3] and, for comparison, the shading coefficient (SC), calculated by way of equation (2).

Glass type	type of shading device	Solar factor (SF)	Shading Coefficient (SC)
Clear glass (4 / 12 / 4)	-	0,72	0,93
	-external blinds slat angle 60 °	0,11	0,13
	-external blinds slat angle 45 °	0,13	0,15
	-external drapery, closed weave fabric	0.18 - 0.22	0.21 - 0.25
	-internal blinds or drapery light	0,46	0,53
	medium	0,52	0,60
	dark	0,59	0,68
	-internal reflective drapery (silver)	0,50	0,57
Heat - absorbing glass (4 / 12 / 4)	-	0,50 - 0,65	0,57 - 0,75
	-internal glare protection*	0,40 - 0,55	0,46 - 0,63
Heat reflective glass (4 / 12 / 4)	-	0,25 - 0,50	0,29 - 0,57
	-internal glare protection*	0,20 - 0,45	0,23 - 0,52

* internal blinds or drapery

- United Kingdom:

In the U.K. normally the SF-factor is used. As an alternative, the SC-factor is often to be seen in application. Glass manufacturers, e.g. [2] [9], offer extensive tables for different types of glazing units and sunshading devices. In Figure 3 SF-factors (total solar radiant heat transmission), exemplary for different glazing types, are shown. In the diagram on the bottom one can see very clearly the influence of the angle of incidence on the parameters.

Glazing with Blinds

Double window with 6mm clear float inner and blind between panes

OUTER GLASS	Solar Radiant Heat: Direct Transmittance	Reflectance	Absorptance	SF: Total Transmittance	Shading Coefficients SC: Short wavelength	Long wavelength	Total
CLEAR FLOAT							
6mm	0.07	0.39	0.54	0.25	0.08	0.21	0.29
12mm	0.06	0.29	0.65	0.25	0.07	0.21	0.28
SPECTRAFLOAT							
6mm 51/66 (Bronze)	0.05	0.25	0.70	0.23	0.06	0.21	0.27
ANTISUN FLOAT							
6mm 72/62 (Green)	0.04	0.16	0.80	0.23	0.05	0.22	0.27
6mm 41/61 (Grey)	0.04	0.15	0.81	0.23	0.05	0.21	0.26
6mm 50/62 (Bronze)	0.04	0.15	0.81	0.23	0.05	0.21	0.26
REFLECTAFLOAT							
6mm 33/53 (Silver)	0.05	0.39	0.56	0.20	0.05	0.18	0.23
SUNCOOL FLOAT							
6mm 10/23 (Silver)	0.01	0.32	0.67	0.12	0.01	0.13	0.14
6mm 20/34 (Silver)	0.02	0.20	0.78	0.17	0.02	0.17	0.19
6mm 10/24 (Bronze)	0.01	0.21	0.78	0.13	0.01	0.14	0.15
6mm 20/33 (Blue)	0.02	0.22	0.76	0.16	0.02	0.16	0.18
6mm 30/39 (Blue)	0.02	0.21	0.77	0.18	0.03	0.17	0.20
6mm 40/50 (Blue)	0.03	0.16	0.81	0.21	0.04	0.20	0.24
Properties of Blind at 45° Louvre Angle	0.11	0.50	0.39	—	—	—	—

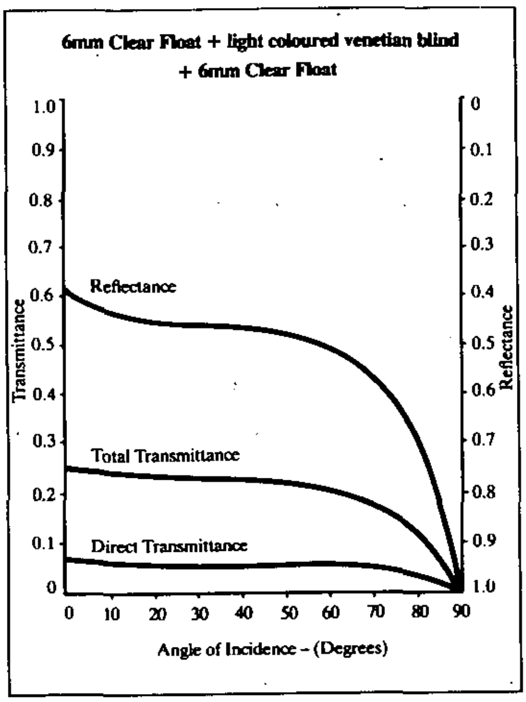

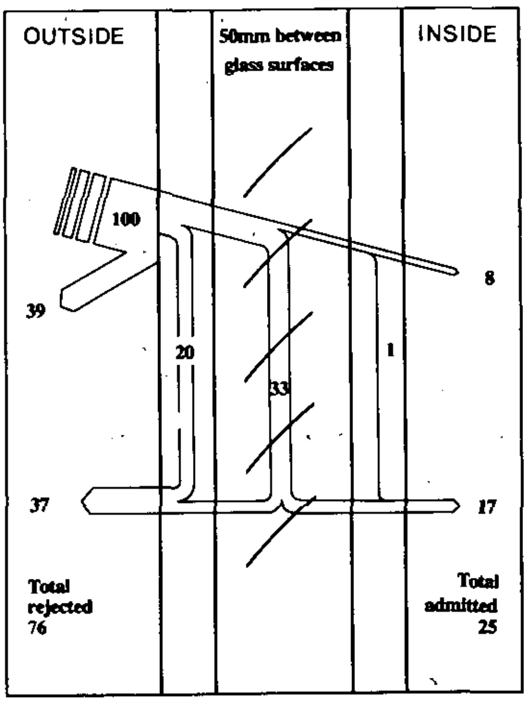

Figure 3: Transmission properties of windows used in United Kingdom, according to [2], exemplary for a double glazing with sun-shading between the panes.

*) Special brandname of Pilkington Brothers Ltd.
Other producers offer similar products with analogous glazing data.

- United States of America:

In the USA the SC-factor is predominantly used. As an example in Table 5 SC-factors and, in brackets, SF-factors are compiled for various indoor shading types according to the American standards [3].

Table 5: Shading coefficient (and solar factor) for combinations of single and double glazings with various indoor shading types, according to [8].

glass type (clear)	type of indoor shading				
	venetian blinds		roller shade		
			opaque		translucent
	medium	light	dark	white	light
single double	0.64 (0.56) 0.57 (0.50)	0.55 (0.48) 0.51 (0.44)	0.59 (0.51) 0.60 (0.52)	0.25 (0.22) 0.25 (0.22)	0.39 (0.34) 0.37 (0.32)

- ISO:

In the ISO draft [10] the total solar energy transmission coefficient g is defined as the sum of the direct solar transmission coefficient, τ_e and of the secondary heat transfer coefficient q_i of the glazing towards the inside, the latter resulting from heat transfer by convection and longwave IR radiation of that part of the incident solar radiation which has been absorbed by the glazing

$$g = \tau_e + q_i$$

2.2 Lighting Evaluation

Apart from the energetic evaluation, knowledge of the influence of sunshading devices on the supply of daylight for a room is important. Mostly, these two influences compete with each other, i.e. from the energetic point of view a good sunshading often drastically reduces the supply of daylight for a room and this occasionally requires additional lighting. In chapter 5, daylighting strategies are explained in detail. For various glazing types Table 6 shows that for low SF-values sometimes a pronounced loss of supply of daylight has to be accepted. The selection of a sunshading device has to be optimized by considering energetic and lighting evaluations in a way that a reduction of solar irradiation will not require additional lighting.

Table 6: Comparison between light transmission and SF-factors of different double glazing types, according to [2] and, for comparison, the shading coefficient (SC), calculated by way of eq. (2)

Double glazing with clear float inner pane (6 mm)

Outer glass	thickness (mm)	light transmittance	SF	SC
Clear float	6 10	0.76 0.73	0.72 0.66	0.83 0.76
Antisun float green	6	0.63	0.49	0.56
Antisun float bronze	6	0.44	0.49	0.56
Antisun float bronze	10	0.29	0.38	0.44
Suncool float silver	6	0.18	0.25	0.29
Suncool float bronze	6	0.09	0.16	0.18
Suncool float blue	6	0.27	0.29	0.33

3. ADDITIONAL RECOMMENDATION

In various countries maximum window sizes in connection with SF-factors of the window system are introduced to avoid summer overheating of rooms. In Germany, for example, a maximum value for the product of solar factor SF and proportional window area is recommended [4]. In Table 7 these values are shown in dependence on the mass of the internal parts of a building and the possibility of ventilation. In other countries similar procedures can be found, e.g. in the Netherlands a graphical procedure for office buildings [11].

Table 7: Recommended maximum values (SF · f) dependent on natural ventilation possibilities and on the inner type of construction, according to [4]

inner type of construction	recommended maximum values (SF · f)	
	without increased natural ventilation	with increased natural ventilation
light	0.12	0.17
heavy	0.14	0.25
f = window area / (facade area inclusive window area)		

4. CONCLUSION

Usually, sunshading devices are energetically appreciable. Here, the quantity of the solar energy transmitted is determined in relation to the solar energy incident onto the window. Various factors are internationally used to describe these phenomena, but the solar factor (SF) is the value which is most frequently used. The splitting of the SF-factor into a value for the glazing (g) and into a reduction factor for the sunshading device (z) is incorrect from a physical point of view. Always, SF-factors are only valid for the total unit of glazing including sunshading. Besides the energetic valuation, a sunshading device's influence on the lighting performance must not be neglected. A sunshading device can necessitate additional lighting which causes an increase in electricity costs and in internal heat loads which are undesirable in summer.

REFERENCES

[1] Owens, P.G.T.:
Solar Control Performance of Open and Translucent Louver Systems. Environmental Advisory Service, 1974.

[2] Pilkington:
Transmission Properties of Windows.
5th edition (1985).

[3] SIA Dokumentation 70:
Kühlleistungsbedarf von Gebäuden. Zürich (1983).

[4] DIN 4108: Wärmeschutz im Hochbau.
Thermal Insulation in Building Construction Part 1/2/3 Aug. 81/ Part 4 Dec. 85/ Part 5 Aug. 81/ Supplement 1 Apr. 82.

[5] DIN 67507: Lichttransmissionsgrade, Strahlungstransmissionsgrade und Gesamtenergiedurchlaßgrade von Verglasungen.
Light Transmittance, Radiation Transmittance, and Total Solar Energy Transmission Coefficient of Glazings, June 1980.

[6] Schmid, J.; Krebbers, J.:
Windows and Window Systems - State of Technology and Development. Rosenheim, FR Germany, January 1985.

[7] SBR42: Zonwering bij gebouwen.
Sunshading for Buildings.
Stichting Bouwresearch, Publication Nr. 42, 1974.

[8] ASHRAE Handbook 1985: Fundamentals SI-Edition, American Society of Heating, Refrigerating and Air-Conditioning Engineers (1985), Atlanta.

[9] Pilkington: Solar Control Performance of Blinds.
Environmental Advisory Service, 1973.

[10] ISO: Light Transmittance, Direct Solar Transmittance, Total Solar Energy Transmittance, Ultraviolet Transmittance and Related Factors of Glazings. ISO/TC 160/WG2/AH2/N21E, Draft.

[11] SBR 74: Zon en Ramen, Regels voor de keuze van raam grootte en zonwering voor gebouwen zonder mechanische koeling. (Sun and Windows, Guidelines for the Selection of Window Size and Sunshading for Buildings without Mechanical Cooling). Stichting Bouwresearch Publication Nr. 74 (1980).

5. DAYLIGHTING

S. Selkowitz
Windows and Lighting Program
Applied Science Division
Lawrence Berkeley Laboratory
University of California
Berkeley, CA 94720
USA

LIST OF CONTENTS I

1. INTRODUCTION

The effective use of daylight supplied by fenestration in buildings is important to energy conservation because it may replace or supplement the energy required for electric lighting. This presupposes that there is a means to control the light switching either manually or automatically. The design of the lighting should provide a distribution and intensity that are appropriate to the visual requirements of the space, both for task illumination and for general lighting purposes, without creating either disability glare from veiling reflections or discomfort glare from sources of excessive brightness. This design process requires that the daylight transmitting properties of windows be well understood. If these fundamental principles of lighting design are achieved the potential energy savings through lighting control employing direct on/off switching or preferably continuous dimming can be achieved.

There may be additional savings attributable to a daylighted building in addition to direct savings of electric lighting energy.
A fraction of the thermal energy associated with electric lighting will typically be removed by the building cooling and ventilating system. If electric lighting energy requirements are reduced, these additional cooling loads may also be reduced. The magnitudes of these potential loads may also be reduced. The magnitudes of these potential cooling load savings are highly dependent on the installed lighting power density, the use of the fenestration in the building and the optical properties of the fenestration system, specifically the spectral transmittance properties and the light distribution effects. Properly designed fenestration can provide cooling load savings but the combination of oversized fenestration and very efficient electric lighting systems may result in an increase, rather than a decrease in cooling loads (of course a building with lighting controls will always result in a cooling load lower than the identical building with identical fenestration but without the controls). In winter the heat from the electric lighting system will reduce heating requirements and the use of daylight control strategies to reduce electric lighting will increase heating loads.

However, it will almost always be more cost efficient to provide the heat requirements directly through an efficient central heating system rather than using lights as a source of resistance heat.

Since the overall performance of the fenestration depends on a careful balance between the daylight admitting properties of the fenestration and the solar heat gains it is important to be able to accurately characterize both effects for any fenestration system under a wide range of sun and sky conditions. There are many architectural design strategies that will further enhance the use of daylight. These include the use of reflecting projections and light shelves, courtyards and atria, etc. but each must be analysed and used with appropriate caution to ensure not only a sound energy saving design but one that achieves the lighting design objectives in terms of quality and quantity.
These issues are treated thoroughly in a forthcoming report by the CIE [1].

2. VISIBLE TRANSMITTANCE

The visible transmittance of a window system is defined by weighting a spectral transmittance function by the photopic response function of the eye [2]. Determining the window spectral transmittance is a routine calculation for the case of planar, homogeneous glazings but becomes much more complex as the glazing elements become more optically and geometrically complex.
These difficulties are shared in the analysis of solar heat gain so will not be discussed further here. A further distinction in analyzing daylight performance compared to solar heat gain is the issue of instantaneous vs. time averaged properties. Much of the thermal analysis is performed with a time step of one hour which suggests that hourly average solar data and hourly average transmittance values are adequate. Daylight must be analysed from more of an instantaneous perspective since there is not an equivalent to 'thermal storage' to justify longer time averaging. In fact in many instances it is both practical and necessary to use averaged data but there are equally instances in which their use could produce substantial errors.

Transmittance for visible light can vary significantly compared to accepted values for solar transmission. This difference can be created using selective absorption or reflection in the glazing layers themselves or in coatings applied to the glazing. Furthermore the total visible transmittance of two or more glazing layers, each with spectrally selective properties may differ from the result obtained by simply multiplying the individual transmittance properties. A transmittance calculation through the multiple glazed system should be done on a spectral basis to provide the correct result.

3. DEFINITION OF SKY CONDITIONS

The CIE has defined standard overcast and clear sky luminance distributions [3, 4]. These are widely utilized in computer models that are used to calculate daylight transmission/admission. The clear sky model is driven by humidity and turbidity data that are not always available, so often standard climate conditions are assumed. There is not a single generally accepted model for solar beam properties; many different models are in use. For normal glazing materials without much spectral dependence the visible transmittance properties calculated from any of these models will not vary much. However, if one uses selective coatings with a strong wavelength dependence then the calculated transmittance may vary by noticeable amounts.

There are two sources of uncertainty in the calculation of transmittance as a function of sky luminance distribution. One is the development of data to convert from the normalized distributions provided by the CIE formulae to absolute engineering data. The CIE distributions are normalized with respect to zenith luminance; one must therefore use an equation for zenith luminance as a function of appropriate local climate variables. Many individuals have developed such equations but there is no generalized agreement on a single model [5]. The second problem is the case of partly cloudy and average sky conditions, which in many locations may occur more frequently than the standard overcast and clear. This is now being examined by a CIE technical committee.

Furthermore, both the clear and the overcast standards are idealized conditions; not all observable full cloudy skies will match the CIE distribution and it is difficult to know if these variations will produce a significant variation in interior daylight effects. The greatest potential error will occur under partly cloudy conditions when the sky luminance conditions and the presence and absence of direct sun may vary widely.

4. TRANSMITTANCE PROPERTIES OF FENESTRATION SYSTEMS

The transmittance properties of fenestration systems determine the amount of light that reaches the building interior and the angular distribution of that light. From the perspective of the building envelope, the window is a light transmitting element and we tend to ask the question, how much of the incident light is transmitted? However, from the perspective of interior lighting analysis, the window is a light emitting surface and the appropriate question is, what is the candlepower distribution of the light source? Of course one of the significant differences between windows and other interior light sources is that the window intensity and distribution change rapidly with time over a wide range.

For the purposes of this discussion we consider the window to be the collection of exterior shading, glazing and interior shading elements. The window will then have three distinct effects. It will act as a light collecting element, as a light filtering element and as a light redirecting element. Furthermore we consider here the optical performance relative to the windows role only as a light source. Window optical properties will also influence the occupant's visual environment in terms of providing a view (clear, obstructed, distorted) and as a potential source of glare.

Each of these functions will also be relevant to its solar transmittance performance, but most solar calculations are not as interested in the distribution related effects. For each of the three categories mentioned above we review briefly the types of effects on optical properties. As a light collector the geometry and surface properties of the window will influence performance. Window elements need not be planar, they can include effects such as fins which can reach out to intercept light that would otherwise not be available to the window. The transmittance vs. angle of incidence function for a window with white fins would be very different than a flat sheet of glass at high incident angles. One can alter the geometry of the glazing, which in turn will alter the incidence angle and thus the transmittance. The surface texture can also be changed so that the traditional angle of incidence transmittance relationships no longer hold.

As a light filtering and redirecting element windows will normally reduce the intensity of the transmitted flux. But they may also change the directional properties and the spectral properties. For example a tinted absorbing glass will reduce transmitted intensity without altering directional properties. Some tinted glasses may be spectrally neutral, others such as bronze glass will have higher solar/light ratios, while others such as blue-green glass will have higher light/solar ratios.
Coated glazings have similar effects but add the possibility of a wider range of spectral control. Diffusing materials and any other opaque reflecting element in the window will alter the directionality of transmitted flux. Simple combinations of geometry changes and changes in the diffusivity of the glazing can have major effects on light transmittance. A domed diffusing skylight, for example, will provide 50-100% more light at low solar altitudes than a flat diffuser and even more relative to flat clear glazing.

The redirecting properties of windows are probably the most important effects that influence daylight performance greatly, while being of little interest in most thermal calculations. In most thermal analysis it is enough to know the total transmittance of the window system. For daylighting analysis it is usually essential to have some knowledge of the directional nature of the transmitted flux which requires that one be able to calculate or measure these properties for complex, multi-element window systems. With the exception of simple systems for which properties can be calculated directly, these optical data are generally not available today, although research studies are in progress to develop a standard approach to determine these properties.

5. EFFECTS OF ADJACENT BUILDING SURFACES AND LANDSCAPE ON TRANSMITTANCE

The overall daylight performance of the fenestration system is dependent on the total luminous flux incident on the fenestration system. There are four primary flux sources: the sun, the sky, the ground and other surfaces seen by the fenestration system. In the last category we include other buildings, landscape, e.g. trees and shrubs, and other elements of the building in which the subject fenestration is located. These 'other sources' can serve two contradictory functions. They can obstruct flux from one or more of the other three sources, e.g. a tree blocking the sun and they can be an indirect source of reflected flux originating elsewhere, since they are not normally light emitting sources themselves. In most practical cases they will serve both functions and their net contribution will depend upon the specifics of each case.

Several examples will illustrate the potential effects. Consider a north facing window looking out over a dark ground. During most of the year the primary light source will be the sky, with the ground contributing less than 10%.

Now add a three story building adjacent and parallel to the existing building such that the roofline forms a cutoff angle of 45° with respect to the window. The adjacent building now obstructs 50% of the sky view and reduces the useful daylight by an even greater factor due to the average angle of incidence of light from the remaining sky. If the adjacent building is very dark in color the reflected sunlight and skylight will be small, thus resulting in a net decrease in interior illuminance relative to the previous case. The effects on indoor illuminance levels may be even more pronounced since low obstructions may eliminate the direct light received at a task indoors even if the overall effect on incident flux is less dramatic. Window size, shape and location, as well as task location in the indoor shape will influence these results.

Now consider the identical case but change the adjacent building to a very high reflectance white. Under overcast conditions the reflected light from the white building will be less than the sky it obstructs. However, under sunny conditions the south facing white obstruction could be as much as ten times brighter than the deep blue north sky that it obstructs, thus raising daylight levels relative to the sky alone. If we rotate both the window and the obstructing building by 180° then the effect of the obstruction changes again. Now the obstruction blocks low angle winter sun and allows midday summer sun to reach the window. Thus the effects of adjacent building elements or landscaping can serve to increase of decrease both the flux available at the window and the spatial distribution and efficiency with which the flux can be effectively utilized within the space.

The ground reflected component can also be influenced both by design and by variable outdoor conditions over which the designer has little control. Consider the difference in ground reflected light between a dark bare earth and the same ground covered by fresh snow. In many cold northern climates snow cover may be a permanent part of the landscape for many months, in other climates it may be a highly variable phenomenon.

The effect of snow is multiplied when direct sun is present, particularly on the north elevation which would otherwise receive substantially less total flux. Designers can also create permanent 'snow-like' surfaces using crushed rock with high reflectance or by using appropriate painted surfaces. One should also note that incidence angle for ground reflected light comes from below the 'horizon'. For typical planar glazings this will not pose a problem, but if angle selective materials are used, such as some types of screens or blinds, they will have highly directional transmittance properties. One might then have to specify transmittance vs. altitude angle from -90° to +90°.

As a light reflecting landscape element snow introduces an additional difficulty due to its variable surface texture that will greatly alter its surface reflectance properties. We normally assume most landscape materials act as diffuse sources. At least some types of snow and ice, however, will behave more like specular or semi-specular surfaces which should be accounted for in window optical properties when estimating transmittance.
Similar effects can be expected for bodies of water adjacent to buildings. In both cases the light will be transmitted through the glazing at negative altitude angles and first strike the ceiling or walls.

6. REFERENCES

[1] Commission Internationale de l'Eclairage, Technical Committee. TC-4.2., Guide on Daylighting of Building Interiors, to be published.

[2] Commission Internationale de l'Eclairage, Principles of light measurements, CIE publication no. 18 (E-1.2), Paris, 1970.

[3] Commission Internationale de l'Eclairage, Daylight: International Recommendations for the calculation of natural light, CIE publication no. 16 (E-3.2), Paris, 1970.

[4] Commission Internationale de l'Eclairage, Standardization of luminance distribution of clear skies, CIE publication no. 22 (TC-4.2), Paris, 1973.

[5] CIE Technical Committee 4.2, Circular letter no. 3/82, Commission Internationale de l'Eclairage, Paris, March, 1982.

6. AIR INFILTRATION

P. Wouters
Belgian Building Research Institute
Lombardstraat, 41
B-1000 BRUSSELS
BELGIUM

LIST OF CONTENTS

List of symbols

A, B	: regression constants	
H	: percentage of open windows	
Φ_v	: heat flow rate due to ventilation	(W)
Φ_{AIR}	: air flow rate of fresh external air	(m^3/h)
Φ^*_{AIR}	: air flow rate of fresh external air	(m^3/s)
Q_v	: Seasonal heating demand	(Wh)
ΔP	: pressure difference	(Pa)
	index T = total	
	W = caused by the wind	
	S = caused by temperature difference	
C_p	: shape factor or wind pressure coefficient	
v	: wind velocity	(m/s)
	index w = windward side	
	l = leeward side	
v*	: friction speed	(m/s)
τ	: shear stress	(N/m^2)
h	: height	(m)
k	: constant of Von Karman	
Co, Zo, Hg, α, a, k	: constants	
G	: mass flow	(kg/s)
N	: exponent in the power low equation	
C	: leakage coefficient	(m^3/sPa^N)
DD	: number of degree-days	
n	: ventilation rate	(h^{-1})
s	: standard deviation	
Φ_{50}	: air flow rate for a pressure difference of 50 Pa.	

1. INTRODUCTION

Ventilation and air infiltration is an important area within the IEA program "Energy conservation in buildings and community systems". Within the IEA Executive Committee (Building and Community Systems) there was an unanimous agreement that infiltration was the area about which least was known.

As a result of it different working groups were created to study this problem in detail :

IEA Annex 5 : "Air Infiltration Centre (AIC)"

IEA Annex 8 : "Human behaviour with regard to ventilation"

IEA Annex 9 : "Minimum ventilation rates".

Especially the AIC has published a large number of publications concerning ventilation and infiltration. Therefore, it is logical to limit this chapter and to refer to these publications for those who wish to know more of this topic. Especially the Calculation Techniques guide [1.] may be very helpful.

The reference list contains an overview of the publications of the Air Infiltration Centre. The name of AIC changed in 1986 into Air Infiltration and Ventilation Centre (AIVC).

It seems useful to give in this introduction an overview of the reasons for obtaining ventilation levels within a certain range.

1.1. Energy consumption

Since the energy crisis of 1973 everyone has become aware that thermal comfort must be paid for (sometimes at high expense). To limit energy costs people started lowering the temperature set point, reducing the number of heated rooms, insulating thair walls and .. improving the airtightness of the windows by weatherstrips or the replacement of the window frames.

This reaction was logical !

Ventilation and infiltration in wintertime involves the heating up of cold external air. A few simple calculations show us the required energy consumption :

$$\phi_v = 0.34\ \Phi_v\ (\theta_i - \theta_e) \qquad \text{(for explanation see 2.4)}$$

Suppose :

- an airflow Φ_v = 10 m³/h
- θ_i = 20 °C
- θ_e = 5 °C
- D = 2500 degree-days

→ heat losses Φ_v = 0.34 . 10 . (20 - 5) W

Φ_v = 51 W

Seasonal heating demand Q_v = 0.34 x 10 x 24 x 2500

Q_v = 204 kWh/year (MJ/year) (see 2.4).

1.2. <u>Air quality</u>

Air quality is strongly related to ventilation levels. In the IEA annex 9 "Minimum ventilation rate" the different pollutants are discussed in detail. Therefore we refer to the publication in that annex. [2.].

Table 1 gives a list of the pollutants which are analysed in the framework of annex 9 [2.].

<u>Table 1</u> : Pollutants analysed in the IEA-annex 9 "Minimum ventilation"

- Carbon dioxide
- Tobacco smoke
- Formaldehyde
- Biocides
- Ionizing radiation
- Micro-organisms
- Hydrocarbons and other organic substances
- Combustion products
- Humidity
- Body odour

1.3. Comfort and health requirements

Although 1.2. also deals with health aspects we prefer a specific paragraph for the more "classical" comfort and health requirements :
- enough oxygen for the human metabolism
- enough fresh air to avoid odours.

In many cases the latter requirement is the severest of all the requirements (including those mentioned in 1.2.).
In table 1 requirements and/or recommendations for some countries are given.

1.4. Draught

Draught is in many cases a cause of thermal discomfort.
Some reasons of draughts :
- poor airtightness of windows and doors
- bad adjustment of the mechanical ventilation system
- stack effect due to an open staircase
- ...

It is important to emphasise that draught problems aren't necessarily related to high ventilation rates, although there is usually a correlation.

Table 2 : Minimum ventilation rates [4.]

		Canada	Denmark	Finland	Netherlands	Norway	Sweden	Switzerland	UK	USA	W. Germany
Residential	Whole dwelling	1 ac/h [3]	0.5 ac/h	0.35 $dm^3/s\ m^2$ [2]			0.35 $dm^3/s\ m^2$ ≈ 0.5 ac/h				
Residential	Living room				21 - 42 $dm^3/s\ m^2$				3 - 8 dm^3/s pers. [4]	5 dm^3/s	1 - 1.5 ac/h
Residential	Bedroom				1 $dm^3/s\ m^2$				3 - 8 dm^3/s pers. [4]	5 dm^3/s	1 - 1.5 ac/h
Residential	Kitchen		15 - 20 dm^3/s [3]	8.8 dm^3/s	21 - 28 $dm^3/s\ m^2$	22 dm^3/s [3]	10 dm^3/s	22 - 33 dm^3/s	6 ac/h [1,4]	50 dm^3/s [1]	33 dm^3/s
Residential	Bathroom/WC		15 dm^3/s [3]	6.4 dm^3/s	14 $dm^3/s\ m^2$	17 dm^3/s [3]	10 dm^3/s	17 dm^3/s	3 ac/h [1,4]	25 dm^3/s [1]	17 dm^3/s
Offices	No smoking	refers to ASHRAE Standards		0.8 $dm^3/s\ m^2$		1.4 $dm^3/s\ m^2$				2.5 dm^3/s pers.	8.3 dm^3/s pers.
Offices	Smoking			1.6 $dm^3/s\ m^2$						10 dm^3/s pers.	13.9 dm^3/s pers.

Notes: [1] Installed capacity for intermittent use

[2] Values also given per person related to occupancy density for smoking and non-smoking

[3] If mechanical ventilation is used, otherwise ventilation openings are specified (see Table 2)

[4] Scotland only, for England and Wales see Table 2 . Separate regulations apply to Inner London.

1.5. Condensation and mould growth

Humidity levels in buildings are strongly related to ventilation levels. The energy crisis has encouraged the people to improve the insulation of their buildings. Unfortunately, this is not always done according to the rules of good practice and a lot of thermal bridges exists nowadays in many buildings. This means low surface temperatures. Two other effects, namely lower internal temperatures in several countries (United Kingdom, Belgium,...) and a reduced ventilation rate have resulted in an extreme high number of condensation problems.

A classical example is the replacement of windows in social housing estates :

- before replacement these mostly small houses with a high occupation rate have wooden, not-airtight windows with single glazing. Also a rather high ventilation rates.
- after replacement there are perfectly airtight windows with at least double glazing. There is no longer an indicator of high humidity levels (= surface condensation on the single glazing) and the improved airtightness means a lower ventilation rate. As a result of it, many houses have after replacement condensation problems on walls.

More information with regard to condensation is given in the chapter on condensation.

Remark

This exemple does not mean that such a replacement has to be avoided but that an overall approach is necessary, which includes an inspection of the building and appropriate information for the occupants.

The importance of condensation is illustrated by the fact that the IEA has organised a workshop on condensation in Leuven (Belgium) in September 1985 [5.].

1.6. Conclusion

This limited analysis can be summerised as follows :

1) There are requirements concerning the ventilation level from different points of view. However, some of the requirements conflict : minimisation of the energy consumption and optimisation of the air quality can not be provided at the same time.
A compromise has to be found.
2) Air change rates are strongly related to climatological conditions : wind speeds and temperature difference.
One can reduce this dependence on the one hand by making the building envelop as airtight as possible, and on the other hand by providing the building with special ventilation arrangements (ventilation grids, fans,..).
This approach means that the windows must be as airtight as possible (depending on the climate and the economic situation).

In the framework of this annex it is therefore useful to indicate the physical process of air flow through components, especially windows (2.) to indicate the standards and requirements concerning airtightness of window (3.) to relate laboratory results to results obtained in occupied houses and to relate airtightness levels to practical ventilation rates (4.).
These different topics will be discussed in the following paragraphs.

2. THEORY

Air flow through building components is influenced by a large number of parameters :

- climatological data :
  - . wind velocity
  - . wind direction
  - . outside temperature
- air tightness of the components
- inside temperature
- surroundings
- ...

However, under steady state conditions the problem is very simple to describe physically :

- there is the potential field : a pressure difference across the component
- there are the various different resistances within the building component to air penetration.

The pressure difference across the building component is discussed in 2.1. and the air flow through leakage openings is analysed in 2.2.

2.1. The pressure difference across building components [3.].

Pressure difference across components can be caused by two reasons :

- pressure difference caused by the wind : ΔP_W
- pressure difference caused by temperature differences : ΔP_S

In formula :

$$\Delta P_T = \Delta P_W + \Delta P_S$$

ΔP_T = total pressure difference.

2.1.1. deals with the wind effects, the stack effect is discussed in 2.1.2.. A literature reference with regard to the effect of fluctuating pressures is given in 2.1.3. and a brief summary of the impact of molecular diffusion in 2.1.4.

2.1.1. Pressure differences caused by the wind

Pressure differences across the climatic shield which are caused by the wind are calculated according to the formula :

$$\Delta P_w = P_w - P_i$$

where :

P_w is the pressure of the wind on the outer side of the building component (reference : atmospheric pressure) (see 2.1.1.1.)

P_i is the pressure in the dwelling or room (reference : atmospheric pressure). P_i is function of the distribution of the air leakages and the pressure distribution P_w around the building. It can be calculated by applying the continuity equation : total outward flow = total inward flow (for the whole dwelling). This definition is only valid if $\theta_i = \theta_e$.

A lot of information can be found in the proceedings of the AIC 1984 wind pressure workshop [6.].

2.1.1.1. **Wind pressure on the outer side.**

The wind pressure on the outer side of an element can be expressed as follows :

$$P_w = 1/2\ \rho\ C_p\ v^2$$

ρ : density of the air (kg/m³)

C_p : shape factor (-) (see 2.1.1.3.)

v : wind velocity at a reference height (m/s).

By assuming $\rho = 1.28$ kg/m³, one obtains :

$$P_w = 0.64\ C_p\ v^2.$$

2.1.1.2. The **wind velocity at a certain height.**

In meteorology is the windspeed measured at the height of 10 m. Different formulas exists to estimate the wind speed at other heights.

a) Formulas based on "Law of Prandtl"

- Law of Prandtl

$$v(h) = \frac{v^*}{k} \ln \frac{h}{h_o}$$

where :

v(h) : windspeed at height h (m/s)

h : height (m)

v* : friction speed (m/s)

$= \sqrt{\frac{\tau}{\delta}}$ where τ : shear stress (N/m²)

δ : density (kg/m³)

k : constant of Von Karman ($\simeq$ 0.4)

h_o : equivalent height, which is a function of the roughness of the terrain (m) (table 3.).

Table 3 : h_o values for Law of Prandtl

Terrain	h_o
free water surface	0.2 - 0.6
uncovered terrain	0.5 - 2
grass (10 cm)	2.3
(100 cm)	10 - 16
wood	50 - 100
urban area	100

For practical applications is the formula simplified to :

$$v = v_{ref} \cdot c_o \ln \frac{z}{z_o} \qquad \text{(m/s)}$$

v_{ref} : measured windspeed : 10 m above the terrain (m/s)

c_o and z_o : terrain parameters

z : height above the terrain.

The parameters c_o and z_o are a function of the environment. The values applied in Belgium and Denmark are given in table 4.

Table 4 : $v = v_{ref} \cdot c_o \ln \frac{z}{z_o}$ [3] and [7].

Class	Terrain classification	c_o	z_o
I	B : coastal area (≤ 2 km from the sea) DK : "smooth" terrain : e.g. stretches of water and moor without windbreak	0.166 0.17	0.005 0.01
II	B : rural area with individual houses and DK : agricultural land with windbreak, farms with gardens, etc...	0.20 0.19	0.07 0.05
III	B : cities, suburbs, industrial states, woods DK : built-up area, wood	0.23 0.22	0.30 0.33

The differences are almost neglectful.

b) Formula of Davenport

$$v\ (h) = v_g \left(\frac{h}{H_G}\right)^{\alpha}$$

When H_G and α are function of the roughness of the terrain. Davenport proposes the values mentioned in table 5.

Table 5. : Values of α and H_G (m)

	α	H_G (m)
Flat land	0.16	270
Suburban area and small towns	0.28	390
Center of the city	0.40	420

B.R.E. [8.] and the LBL-infiltration model [9.] use the same type of formula for estimating wind speeds :

Building Research Station [8.]

$$\frac{v}{v_{10}} = K \cdot h^{a}$$

v_{10} : wind velocity 10 m above the ground in a flat and open land (m/s)
K and a : constants function of location (table 6.).

Table 6 : Constants in B.R.E.-formula

	K	a
Flat and open land	0.68	0.17
Agricultural and with small obstacles	0.52	0.20
Suburban area and small towns	0.40	0.25
Center of the city	0.31	0.33

LBL-infiltration model [9.] [10.]

The free-stream wind speed at ceiling height V_R is given by :

$$v_R = v_M \frac{\alpha_R \left[\frac{H_R}{10}\right]^{\gamma_R}}{\alpha_M \left[\frac{H_M}{10}\right]^{\gamma_M}}$$

where :

v_R : free-stream speed at ceiling height (m/s)
v_M : wind speed at measuring station (m/s)
H_R : ceiling height (m)
H_M : height of measurement sensor (m)
α_M, γ_M : constants from table 7. appropriate to location of measurement station
α_M, γ_R : constants from table 7. appropriate to location of building

Table 7 : Terrain parameters for Standard Terrain Classes

Class	γ	α	Description
I	0.10	1.30	Ocean or other body of water with at least 5 km of unrestricted expanse
II	0.15	1.00	Flat terrain with some isolated obstacles (e.g. buildings or trees well separated from each other)
III	0.20	0.85	Rural areas with low buildings, trees etc...
IV	0.25	0.67	Urban, industrial or forest areas
V	0.35	0.47	Center of large city (e.g. Manhattan)

Wind velocities :

a) Monthly averages

Table 8. gives as an example the measured average wind speed for 2 locations in Belgium [3], Denmark [11] and West-Germany.

Table 8

Average wind speed (m/s) for locations in Belgium (Kleine Brogel : rural area with low buildings, Middelkerke : Coastal area), Denmark and West-Germany.

Location	JAN	FEB	MAR	APR	MAY	JUN	JUL	AUG	SEP	OKT	NOV	DEC	AV	Period
Belgium														
Kleine Brogel	3.4	3.4	3.8	3.3	3.0	2.9	2.7	2.7	2.7	2.9	3.5	3.4	3.1	'63 - '72
Middelkerke	5.7	6.0	6.5	5.8	5.2	5.2.	4.8	5.1	5.0	5.3	6.3	6.1	5.6	'63 - '72
Denmark														
Coastal stations	6.5	6.1	5.4	4.9	4.3	4.5	4.5	4.6	5.3	6.0	6.2	6.3		'31 - '60
Inland stations	4.5	4.5	4.2	4.2	3.9	3.8	3.7	3.6	3.7	4.0	4.1	4.2		'41 - '60
West-Germany														
Wuerzburg	3.5	4.1	3.1	2.5	2.5	2.6	2.5	2.5	2.5	3.1	2.5	4.1	3.1	
D. Hof	4.7	4.4	3.2	3.1	3.2	3.0	2.8	2.8	3.2	3.7	3.8	4.4	3.6	
Freiburg	1.8	3.4	3.1	2.7	2.0	2.7	3.2	2.8	1.9	2.5	2.4	3.5	2.8	

b) Distribution of the wind velocity

It is important for some applications to know the time of the heating season during which the wind speed is higher than a certain value. Fig. 1 gives a graphical presentation of this information for the Belgian situation. The three curves correspond to the three typical areas in Belgium for wind velocity.

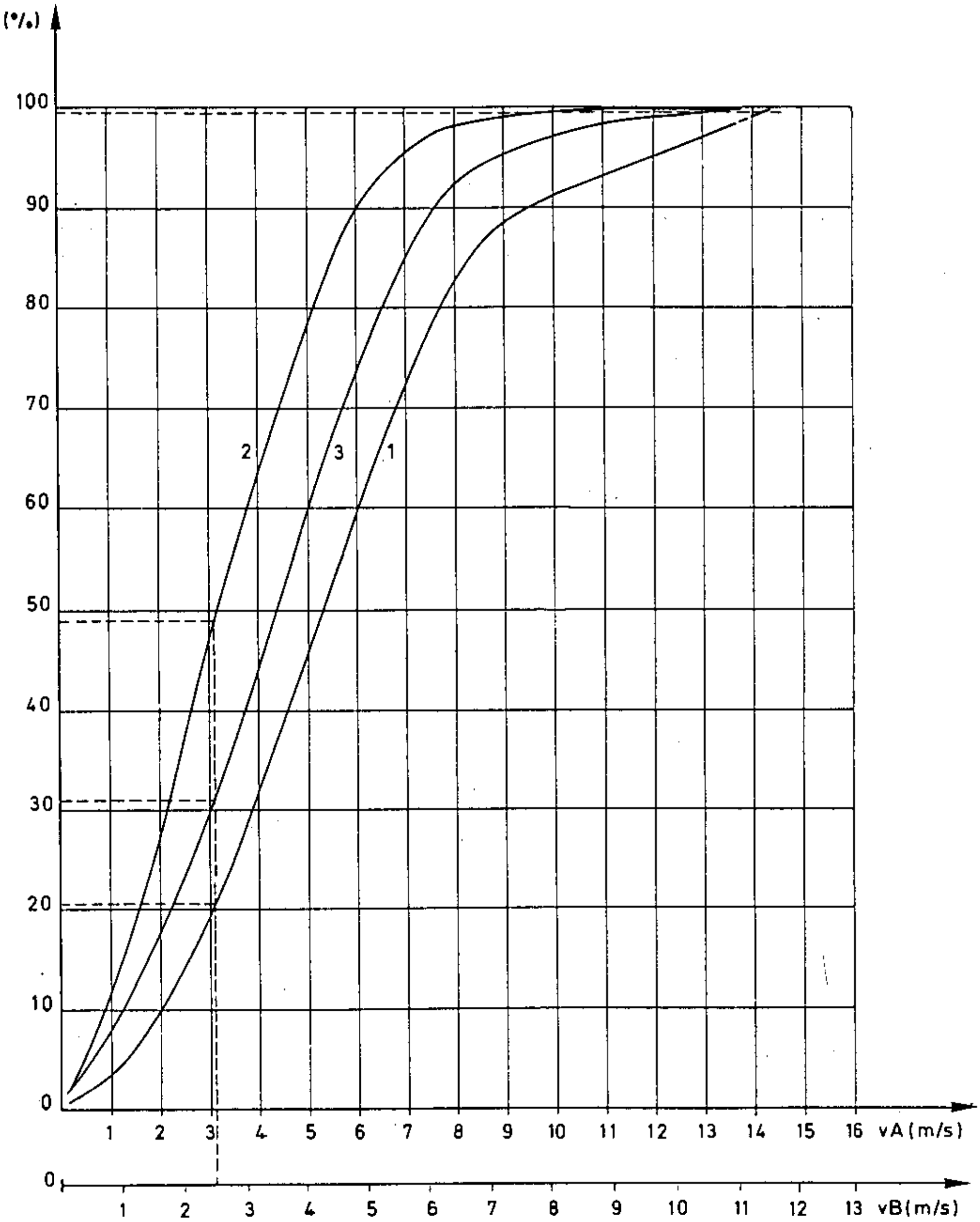

Fig 1 : Percentage of the heating season during which the wind velocity is lower than the value indicated on the x-axis.

Curve 1 : coastal region - Curve 2 : the Campine and the region between the Samber and the Maas - Curve 3 : the rest of the country.

2.1.1.3. **The shape factor or pressure coefficient**

The general form of the pressure coefficient for a point on a building is defined by the equation [12]

$$C_p = \frac{P - P(0)}{0.5\ \rho\ v^2}$$

where :

P(0) : usually the static pressure of the free stream without the building (Pa)

v : reference wind (m/s).

2.1.1.3.1. Reference wind [17]. The choice of reference wind has varied widely. Each method has its advantages and disadvantages. The different methods are only mentioned here :

1. windspeed at 10 meters
   a. simultaneous mean wind
   b. meteorological standard wind speed for the site.
2. windspeed at roof ridge height upstream
3. wind at ceiling height
4. gradient wind
5. local wind profile
6. a modified local reference pressure.

Fig. 2. gives an example of the distribution of the C_p-value based on fullscale measurements [13].

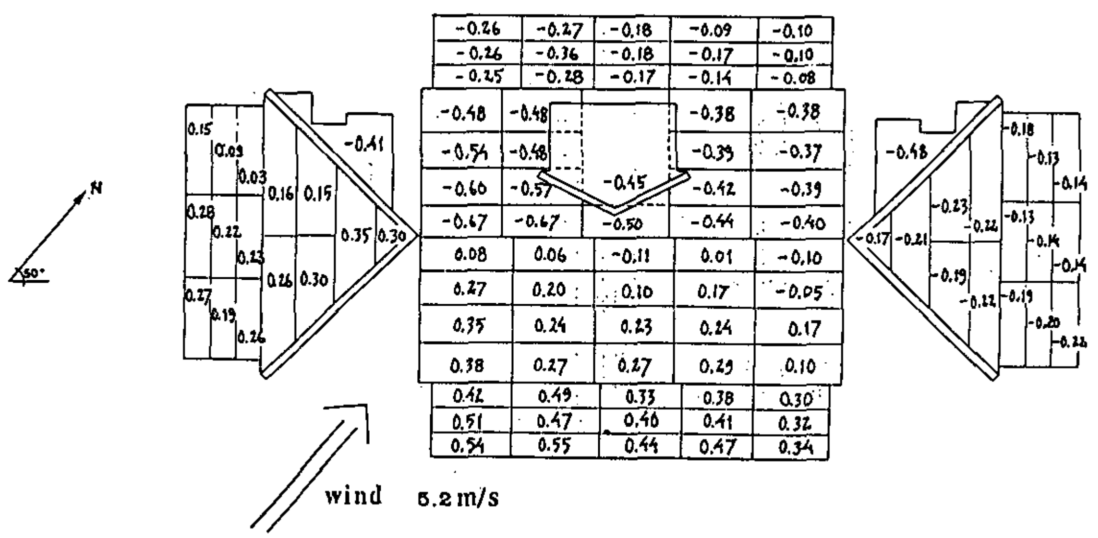

Fig. 2. : C_p-values based on full-scale measurements. The values measured are entered on each house surface - walls, gable, roof, etc...

Practical data for estimating wind pressure coefficient are given in the calculation techniques guide, published by the AIC [1.]

2.1.1.4. **Pressure differences : practical values**

2.1.1.4.1. Pressure differences across the whole building.

a) Average values.

If one assumes for the windward side an average C-value $C_w = 0.5$ and for the leeward side $C_l = -0.3$, it is possible to estimate the average pressure difference across a building.

In table 9. values are given for the Belgian situation.

Table 9. : Pressure difference across the whole building, Belgian situation. [3]

$C_w - C_l = 0.8$ average situation.

Region	Average wind velocity (m/s)		Pressure difference for average wind speed (Pa)
Coastal region	- unprotected	5.3	14
	- protected	4.4	10
Campine + Samber-Maas	- unprotected	3.2	5.2
	- protected	2.6	3.5
Rest of the country	- unprotected	4.4	10
	- protected	3.6	6.6

b) Upper level.

An idea of the maximum pressure difference can be found by taking the 99.5% level. This is the wind speed which is only 0.5 % of the time exceeded. Results for the Belgian situation are given in table 10.

Table 10 : Pressure differences across the whole building which are only exceeded in 0.5 % of the duration of the heating season $C_w - C_l = 0.8$

Region		Air velocity (m/s)	Pressure difference (Pa)
Coastal region	- unprotected	14.2	103
	- protected	11.4	67
Campine + Samber-Maas	- unprotected	9.8	49
	- protected	7.9	32
Rest of the country	- unprotected	12.7	83
	- protected	10.2	53

2.1.4.2. Pressure difference across the building element

The pressure difference across a wall depends on the distribution leakage of the whole building.

minimum : $\Delta P_w \rightarrow 0$

maximum : $\Delta P_w \rightarrow$ pressure difference across the building.

Fig. 3. presents 2 different situations [3.]

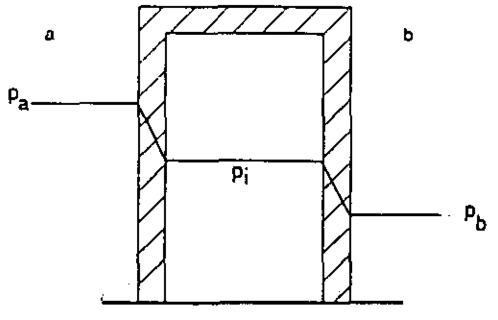

Facades a and b have an identical air tightness

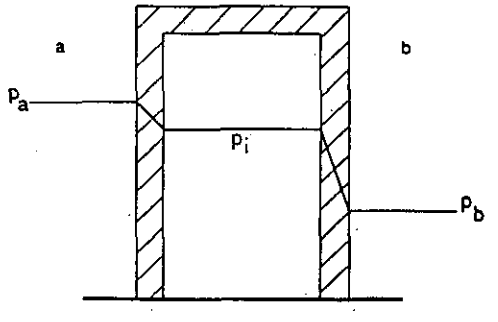

Facade a is more leaky than facade b.

Fig. 3. [3.]

2.1.2. Pressure differences caused by temperature differences : ΔP_t [3]

2.1.2.1. Airtight room with 1 opening

Assuming a completely airtight room with the exception of one opening just above the floor (fig. 4.).

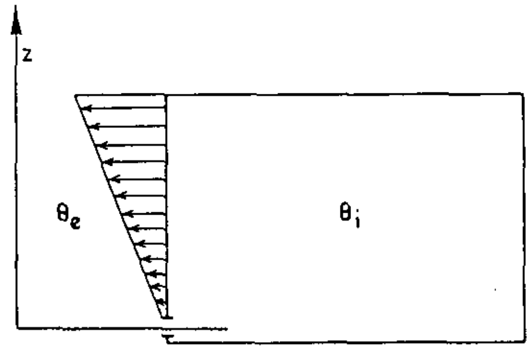

Fig. 4. [3.]

θ_e : external temperature

θ_i : internal temperature

Triangle with arrows : variation of $P_{iz} - P_{ez}$

with : P_{iz} = internal air pressure at height z

P_{ez} = external air pressure at height z.

Other assumptions : - steady state condition

- Ti > Te.

Under steady-state conditions there is no airflow through the opening. At the height of the opening, $P_{io} = P_{eo}$ (z = 0). For a height z, one obtains :

- $P_{iz} = P_{io} - z \cdot \rho_i \cdot g$

ρ_i = density of the air at temperature T_i (kg/m²)

g = gravitational acceleration (9.81 m/s²)

- $P_{ez} = P_{eo} - z \cdot \rho_e \cdot g$

or, because $P_{io} = P_{eo}$:

$$\Delta P_z = P_{iz} - P_{ez} = z\,(\rho_e - \rho_i)\,g$$

Conclusions :

1) a room with only one opening just above the floor is subjected to overpressure with respect to the environment.

2) the overpressure varies linearly with the height z, as illustrated in fig. 4.

3) an additional opening made just under the ceiling would create an air-flow through this opening from the exterior towards the interior.

2.1.2.2. **Airtight room with two openings**

a) Two identical openings, one just above the floor, the other just under the ceiling.
This situation will create a pressure profile as illustrated in fig. 5..
The air enters the room through the lower opening and leaves it through the upper one.
One has : $\Delta P_{lower} + \Delta P_{upper} = h\ (\rho_e - \rho_i)\ g$ (Pa)

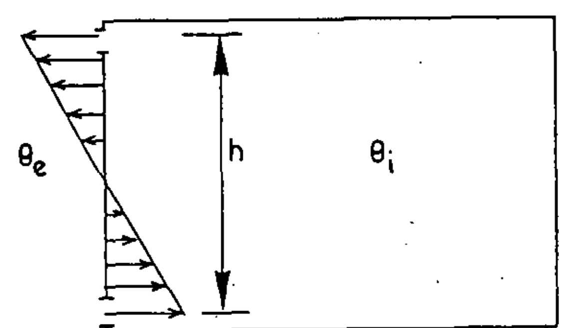

θ_e = external temperature
θ_i = internal temperature
h = vertical distance between the two openings.

Fig. 5 [3.]

b) Two openings with different air resistances
Such a situation is presented in fig. 6.
- lower side : large section, small resistance
- upper side : small section, large resistance.
One obtains again : $\Delta P_{lower} + \Delta P_{upper} = h\ (\rho_e - \rho_i)\ g$ (Pa)

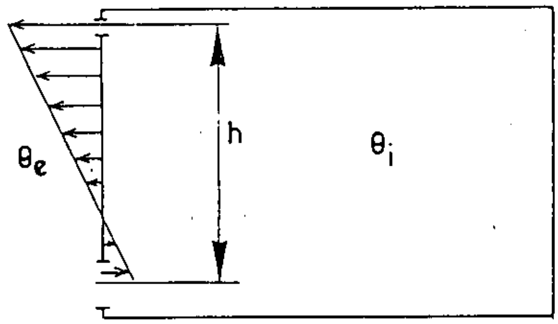

θ_e : external temperature
θ_i : internal temperature
h : vertical distance between the two openings.

Fig. 6. [3.]

2.1.2.3. Generalisation

1) In a room at a higher temperature than the surroundings the overall driven pressure for air movement is :

$$\Delta p = h\ (\rho_e - \rho_i)\ g \qquad \text{(Pa)}$$

Values for ρ are given in table 11. [3].

Table 11 : Density of dry and saturated air (kg/m³) [3]

Temperature (°C)	ρ dry air (kg/m³)	ρ saturated air (kg/m³)
- 20	1.396	1.395
- 15	1.368	1.367
- 10	1.342	1.341
- 5	1.317	1.315
0	1.293	1.290
+ 5	1.270	1.266
+ 10	1.248	1.242
+ 15	1.226	1.218
+ 20	1.205	1.195
+ 25	1.185	1.171
+ 30	1.165	1.146
+ 35	1.146	1.121
+ 40	1.128	1.097
+ 45	1.110	1.070

2) This pressure will create an inflow of air through the lower leakage openings (cracks, joints) and an outflow through the upper leakage openings.
3) The overall pressure difference increases if the vertical distances h increases and if the temperature difference Ti = Te increases.
4) The formula given in 1) can be transformed :

we know $\rho_i = \frac{G_i}{\Phi_i}$ and $\rho_e = \frac{G_e}{\Phi_e}$

where
- G_i and G_e : mass flow (kg/s)
- Φ_i and Φ_e : volume flows (m^3/s)

with $G_i = G_e$

and $\Phi_i = \frac{\Phi_e \cdot T_i}{T_e}$

Therefore : $\Delta p = gh \frac{G_e}{\Phi_e} \left(\frac{T_i - T_e}{T_i}\right)$

or $\Delta p = gh\ \rho_e \left(\frac{T_i - T_e}{T_i}\right)$ (3)

2.1.2.4. **Example**

Assume : θ_i = 15°C, θ_e = 0°C
h = 1 m (window)
h = 5 m (one family dwelling)
h = 50 m (appartment building)

Application of the formula gives :

h = 1 m Δp = 0.7 Pa
h = 5 m Δp = 3.3 Pa
h = 50 m Δp = 33 Pa.

2.1.3. Fluctuating pressure

During the last few years the contribution arising from fluctuating flow on air infiltration has been studied. A good overview of this research in this field is given in [1]

2.1.4. Molecular diffusion

According to [7.] and [14.] the effect of molecular diffusion in practice is neglectible.

2.2. Air flow through leakage openings

If a pressure difference is applied across a leakage opening, the induced air flow rate may be approximated by the power low equation.

$$\Phi = C \, . \, \Delta P_T^{\,N} \quad (m^3 \, s^{-1}), \; (m^3 \, h^{-1})$$

Φ : flow rate $(m^3 \, s^{-1})$ $(m^3 \, h^{-1})$
ΔP_T : applied pressure difference (Pa)
C : leakage coefficient $(m^3 \, s^{-1} \, Pa^{-N})$ $(m^3 \, h^{-1} \, Pa^{-N})$
N : flow exponent.

C and N are determined by the shape and size of the opening. The exponent N varies with the flow regime as follows :
laminar : N = 1
turbulent : N = 0.5

Unfortunately, the dimensions and velocities found under ordinary conditions are such that one can only say that there exists a concave function that can be approximated by the form given above with some compromise N between 0.5 and 1 [15]. The C- and N-values are determined from measurement results.

2.3. The estimation of air flows in buildings

The two reasons for pressure differences are in practice always observed together. Due to the non-linear relationship between pressure difference and air flow (see 2.2.) it is not possible to add the air flows obtained in the two separate systems.
Several mathematical models have been developed for estimating air flows. A comparison of 10 of these models is described in the AIC Technical Note 10 [16]. [63 - 74]
Table 12 shows the results which were obtained when applicating these models on 3 specific buildings for a lot of climatological situations.

Table 12 : Comparison of calculated and measured air change rate [16]

Model	Swiss data set	Canadian data set	UK data set
1. BSRIA	100	49	–
		63[1]	80[2]
2. NRC[3]	100	49	–
NRC[4]	56	86	87
3. IMG-TNO	83	–	–
4. Oscar Faber[5]	–	–	–
5. British Gas[6]	–	78	67
British Gas[7]	–	76	80
6. NBRI	83	78	–
7. IGT	100	76	67
8. LBL	100	81	80
9. BRE	89	73	87
10. Reeves et al[8]	100	57	33

1. *'Exposed' wind directions only. Calculation restricted.*
2. *Stack effect only.*
3. *BS5925 pressure coefficients.*
4. *NRC pressure coefficients.*
5. *Component leakages only modelled.*
6. *Without turbulent correction.*
7. *With turbulent correction.*
8. *First infiltration measurement of data set used as input data.*

The figures give the percentage of calculations of which the difference between the calculated values and the measured values is less than 25%. One can conclude that these models are able to give a rather good estimation of the air flows in buildings.

2.4. Energy loss due to ventilation and seasonal energy demand

2.4.1. The energy losses due to ventilation can be estimated by applying the next formula :

$$\Phi_v = \rho\ c\ \ \Phi_{AIR}\ (\theta_i - \theta_e) \qquad \text{(W)}$$

where :

Φ_v : heat flow rate due to ventilation (W)

ρ : density of the incoming air (kg/m^3)

c : specific heat capacity of the incoming air (J/kgm^3)

θ_i : internal air temperature (°C)

θ_e : external air temperature (°C)

Φ^*_{AIR}: air flow rate of fresh external air (m^3/s).

For practical purposes this formula can be simplified assuming

ρ = 1.23 kg/m^3 (θ = 15°C)

C = 1000 J/kgK

and expressing the air flow rate in m^3/h : Φ_{AIR}.

Then :

$$\Phi_v = \frac{1.230}{3.600}\ \Phi_{AIR}\ (\theta_i - \theta_e) \quad \text{(W)}$$

$$= 0.34\ \Phi_{AIR}\ (\theta_i - \theta_e) \qquad \text{(W)}$$

2.4.2. The seasonal heating demand Q_v can also be estimated.

$$Q_v = \rho \cdot C \cdot \Phi^*_{AIR} \sum_k 24 \, (\theta_i - \theta_{e,k}) \qquad \text{(Wh)}$$

where : $\sum$ = summation over the whole heating season day per day k.

For practical purposes this formula can be simplified :

$$Q_v = 0.34 \, \Phi_{AIR} \cdot 0.024 \cdot DD \quad \text{(kWh)}$$

where DD = number of degree days.

2.4.3. The above mentioned formula is valid if there is no cooling demand. If one wants to take also cooling into account, another formula should be used.

The ASHRAE proposal SP 110 uses the definition "infiltration degree-days" which include heating and cooling periods. A good description of this method is given in [18].

3. MEASUREMENT TECHNIQUES [4]

3.1. Laboratory testing

Tables (international standards) and (national standards) give an overview of standards concerning airtightness of windows. The comments with regard to the measurement techniques are copied from the paper of Mr. P. Jackman [4].

Table 13 : International standards for window airtightness.

Organisation	Standard nr	Year	Title
International Organisation for Standardisation	ISO 6613	1980	Windows and door height windows-air permeability test
European Committee for standardisation	EN 42	1975	Methods for testing windows: air permeability

Table 14 : National standards for window airtightness

Country	Standard nr	Year	Title - description
Belgium	NBNB25-204	1977	Method of testing windows : air permeability tests
Denmark	DS (EN 42)	1976	Methods of testing windows : air permeability test
Germany	DIN (EN42)	1976	Methods of testing windows : air permeability test
Italy	EN 42	1976	Methods of testing windows : air permeability test
Norway	NS 3206	1974	Methods of testing windows : air tightness
Netherlands	NEN 3660	1975	Windows : Air permeability, water tightness, rigidity and strength method of test
New-Zealand	NZS 4211	1979	Specification for performance of windows (appendix 9)
Sweden	SS 818126	1983	Windows and doors-airtightness-testing
Switserland			
UK	BS 5368	1976	Methods of testing windows : Part 1 Air permeability test
	BS 4315	1968	Methods of test for resistance to air and water penetration : Part 1 : Windows and structural glasket-glazed systems
USA	ASTM E283	1973	Standard test method for rate of air leakage through exterior windows, curtain walls an doors

The two international standards EN 42 and ISO 6613 are virtually identical and as most of the European member countries have adopted these as the basis for their national standards, there is a substantially common approach to the air leakage testing of windows.

Specifically, the standards of Belgium (NBN B25-204), Denmark (DS/EN 42), Netherlands (NEN 3660), Norway (NS 3206), Sweden (SS 81 81 26), UK (BS 5368) and West Germany (DIN EN 42) are either identical to or closely related to the international versions. The windows under test is installed over the opening of a chamber by which controlled pressures are applied across the window assembly.

Before the main testing commences, extraneous air leakage from the chamber is measured and preferably eliminated. In addition, three pressure pulses are applied - each of 3 seconds duration and up to at least 500 Pa. The window is then opened and closed five times and finally secured in the closed position. Pressure is applied in stages of 50, 100, 150, 200, 300 and 100 Pa intervals thereafter up to the maximum test pressure difference. Then the pressure is reduced to the same levels in reverse order. Of these standards, the Swedish version is unique in also specifying tests with pressure differences in the opposite direction. The international and other national standards include the reversal of pressure as an option.
The remaining standards while not so clearly akin to the international standards, specify a very similar test procedure though without the initial pressure pulsations.
The New Zealand (NZS 4211), UK (BS 4315) and USA (ASTM E283-73) standards are specific in requiring the extraneous leakage from the test chamber to be substracted from the leakage rate measured with the window in place.
The maximum test pressures specified range from 1000 Pa in BS 4315 (UK) to 75 Pa in ASTM Standard E283-73 (USA) if no other pressure difference is designated.

3.2. On-site testing

The one standard specifically related to component air leakage testing on site is ASTM E783-81. It describes a procedure for determining the air leakage characteristics of exterior windows and doors but it is stated that the method may also be adapted for other leakage routes in the building structure. The test involves sealing a substantially airtight enclosure to cover the internal or external face of the window of door and maintaining a specified pressure difference across the component by supplying air to, or exhausting air from, the enclosure. The required air flow rate is measured and recorded as the leakage through the component. The measurement and correction for extraneous leakage through the test enclosure is also detailed.

4. REVIEW OF PRESENT STANDARD VALUES [4]

4.1. Introduction

A detailed overview of standards and requirements with regard to airtightness is given in the AIC Technical Note 14 : "A review of building airtightness and ventilation standards". [19]

A more condensed overview was presented by Mr. P. Jackman, head of the AIC, at the 5th AIC Conference "The implementation and effectiveness of air infiltration standards in buildings". [4]

The major part of this paragraph is a copy of his paper with regard to the airtightness of windows.

4.2. Airtightness requirements for buildings : overview. [4]

Belgium : STS 52.0
External joinery - general principles
INL Draft 1983

Canada : Measures for energy conservation in new buildings
Associate Committee on the National Building Code
National Research Council of Canada, n° 16574,
Ottawa, 1978

Netherlands : NEN 3661
Windows : Air permeability, water tightness,
rigidity and strength
Requirements
Netherlands Standards Institute (NNI), 1975

New Zealand : NZS 4211 : 1979
Specification for performance of windows
Standards Association of New Zealand, 1979

Norway : Chapter 54. Termal insulation and airtightness (revised 1980)
Building Regulations of 1st August 1969
Royal Ministry of Local Government and Labour

Sweden : Chapter 33. SBN 1980. Thermal insulation and airtightness
Swedish Building Code with Comments
National Swedish Board of Physical Planning and Building (1981)

SIS 81 81 03
Windows. Classification with regard to function
Swedish Standards Commission, 1977

Switzerland : SIA 180/1
Thermal insulation of buildings in winter
Swiss Engineering and Architectural Association, 1980

United Kingdom : BS 6375 : Part 1 : 1983
Performance of windows. Part 1 : Classification for weathertightness
British Standards Institution, 1983

United States of America : ASHRAE Standard 90-80
Energy conservation in new building design
The American Society of Heating, Refrigerating and Air-conditioning Engineers Inc., 1980

West Germany: DIN 18055
Windows : Air permeability of joints and driving rain (water tightness) protection. Requirements and testing
German Standards Institute (DIN), 1981.

4.3. <u>Whole building</u>. Currently Norway and Sweden are the only countries that have recommendations for the airtightness of whole buildings.

Tabulated summaries of the Norwegian and Swedish requirements are given below :

Norwegian Building Regulations	
Building type	Airchange rate/hr at 50 Pa
Single family dwellings	4
Buildings up to 2 floors	3
Buildings exceeding 2 floors	1,5

Swedish Building Code	
Building type	Airchange rate/hr at 50 Pa
Freestanding single-family houses and linked houses	3
Other residential buildings of not more than 2 storeys	2
Residential buildings of 3 or more storeys	1

The Swedish specifications are the more stringent.

4.4. <u>Windows</u>. The standards of several countries specify the maximum allowable leakage of windows with some grading according to application. In others, a leakage classification system is detailed but with no reference to acceptability for particular uses.

The following list summarises the requirements or classifications given in the relevant standards.

Belgium : Standard STS 52.0

Maximum rate of leakage at 100 Pa for different grades of window

	Window classification		
	PA2	PA2B	PA3
Exposure level - height of building in which window is situated (m)	0-10	10-18	>18
Air leakage m^3/h per meter (dm^3/s m)	6 (1.67)	3 (0.83)	2 (0.56)

Canada : Measures for energy conservation in new buildings

Air leakage of windows is not to exceed 0.755 dm^3/s per meter of joint at a 75 Pa pressure differential.

Netherlands : Standard NEN 3661

Test pressures for different window categories for which air leakage must not exceed 5 dm^3/s m.

Height of building in which window is situated (m)	Exposure	Pressure difference Pa
15	Normal	150
40	Normal	200
100	Normal	250
15	Coast	300
40	Coast	350
100	Coast	400

New Zealand : Standards NZS 4211

The rate of leakage at all test pressure differences up to 150 Pa shall not exceed those in the Table below.

Grade	dm^3/s per meter of opening joint	dm^3/s per m^2 of of total window area
A	0,6	2
B	2,0	8
C	4,0	17

Norway : Norwegian Building Regulations - Chapter 54

Windows shall be sufficiently airtight so that air leakage at a pressure difference of 50 Pa does not exceed 1.7 $m^3/h\ m^2$ (0.47 $dm^3/s\ m^2$)

Sweden : Standard SBN 1980

The maximum air leakage of windows is specified as follows :

Pressure difference Pa	Leakage rate $m^3/h\ m^2$ ($dm^3/s\ m^2$) for windows in building height (number of floors)		
	1 - 2	3 - 8	> 8
50	1.7 (0.47)	1.7 (0.47)	1.7 (0.47)
300	5.6 (1.56)	5.6 (1.56)	5.6 (1.56)
500	-	-	7.9 (2.19)

Standard SIS 81 81 03 (1977)

Windows are classified as A, B or C and the permissible air leakage (q) for windows in each class is determined by the equation :

$$q = kp^{2/3}$$

where q = air leakage in m^3/h per m^2 of window area.
k = a coefficient (0.2 for Class A and 0.125 for classes B and C)
p = pressure difference in Pa between inner and outer surfaces of window.

The lines corresponding to these classes have been plotted in Figure 8.

The values quoted above from SBN 1980 coincide with classes B and C.

Switzerland : Standard SIA 180/1

Maximum leakage rates for the various classes of windows.

	Class			
	A	B	C	D
Test pressure difference (Pa)	150	300	600	>600
Height of building (m)	< 8	8 - 20	20 - 100	-
Allowable coefficient of air permeability ($m^3/h\ m\ Pa^{2/3}$)	0.44	0.22	0.22	0.22
($dm^3/s\ m\ Pa^{2/3}$)	(0.12)	(0.06)	(0.06)	(0.06)

UK : Standard BS 6375 Part 1

Four categories are specified with the following test pressure classifications. The acceptable rates of air leakage are expressed graphically and are shown on Figure 7.

Class	Test pressure
I	150
II	200
III	300
IV	600

The standard also specifies that the air leakage through fixed lights shall not exceed 1 m^3/h (0.28 dm^3/s) per meter length of the visible perimeter of the glass when tested at the same pressure as for opening lights.

USA : ASHRAE Standard 90-80

Leakage rate of windows at 75 Pa pressure difference to be no more than 0.77 dm^3/s per meter of sash joint.

West Germany : Standard DIN 18055

The classification of windows is as follows :

	Window classification			
	A	B	C	D
Test pressure (Pa) up to	150	300	600	unspecified
Height of building (m) up to	8	20	100	

The air leakage requirements are presented graphically and these have been reproduced in Figure 7.

Most standards specify the leakages in relation to unit length of the opening joint while a few specify them in terms of unit window area. Thus direct comparison of all the standards is not possible.

However, comparison has been made in each of the two forms by plotting the allowable leakage values on Figures 7. and 8. The plot of leakage expressed

per meter of joint length show, surprisingly, that the highest classifications are to be found in countries having relatively mild climates, i.e. Belgium, New Zealand and UK. The high Scandinavian standards are evident in the other figure where they are compared with the New Zealand classifications which are expressed in both forms.

Figure 7. : Window air leakage rates - per m joint length

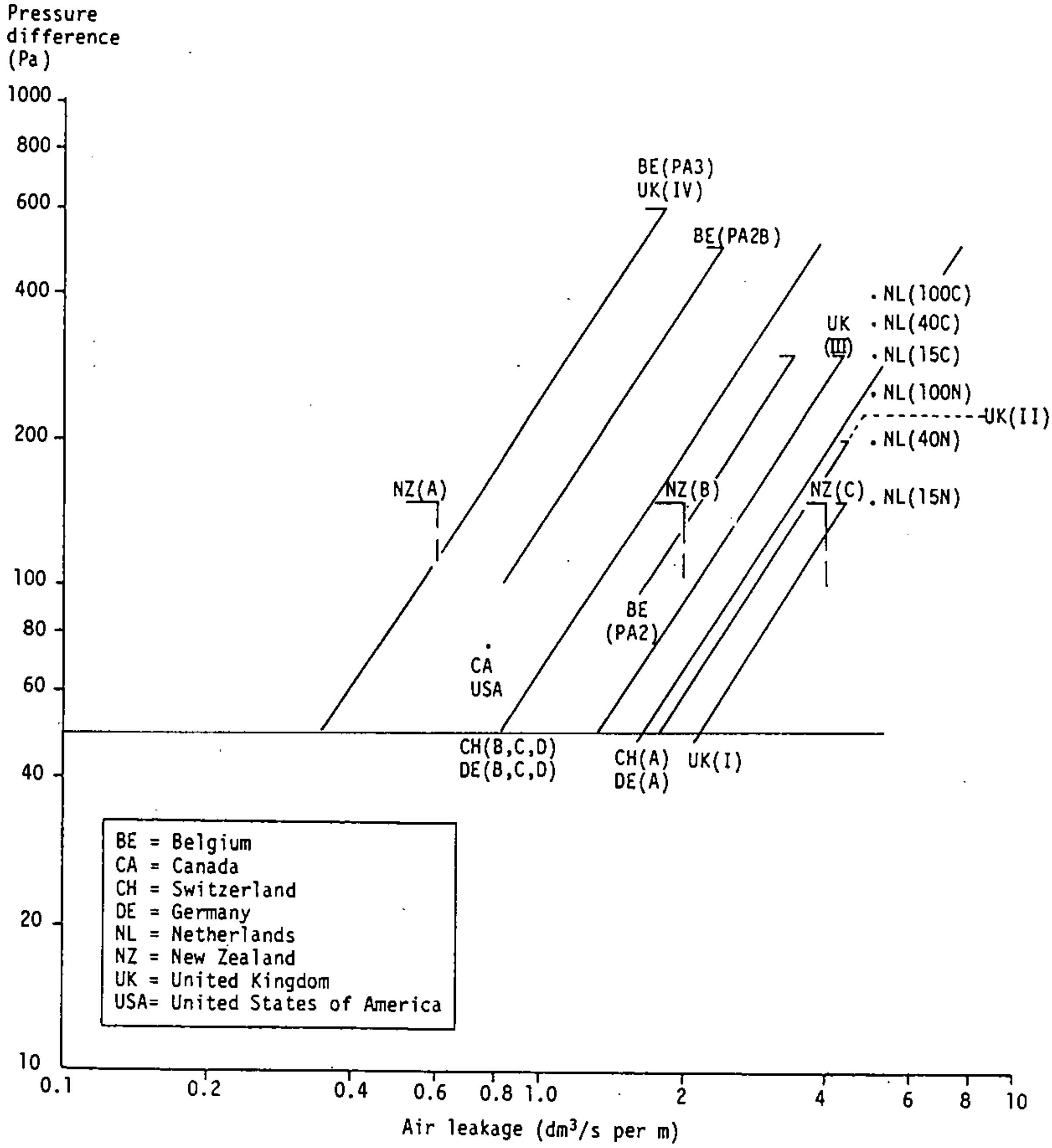

Figure 8 : Window air leakage rates - per m² window area

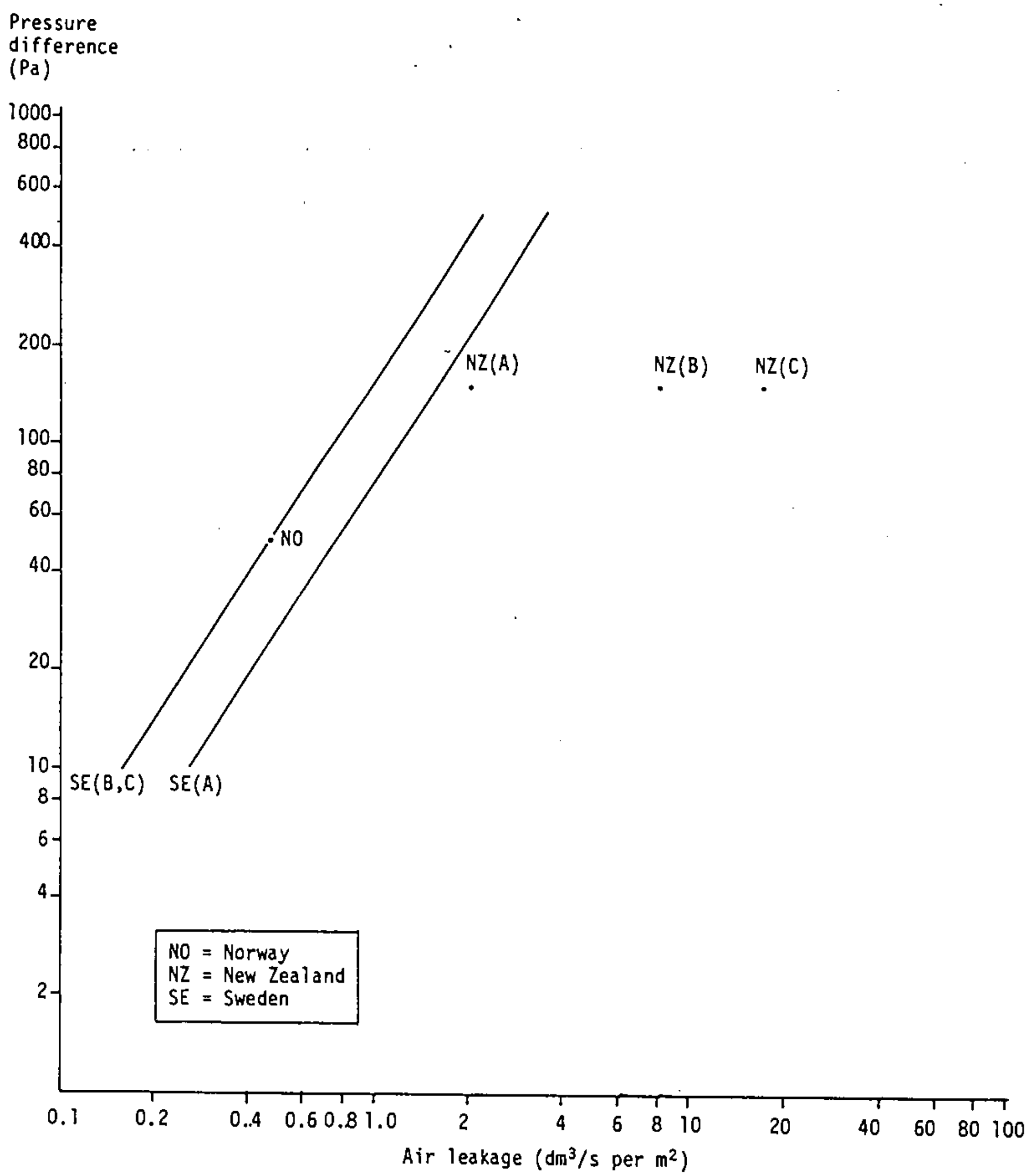

All these standards assume N = 2/3. Therefore, it is possible to express these criteria by giving 1 figure.

Table 15 gives the air flows for $\Delta P = 50$ Pa. This is a usefull value while the building airtightness is in many countries expressed as a ventilation rate for $\Delta P = 50$ Pa.

Table 15 : Window air leakage rates (m^3/h) at 50 Pa.

	per m joint length	per m^2 window area
Belgium	1.3 - 3.8	
Canada	2.1	
Netherlands	4.5 - 8.7	
New Zealand	1.0 - 6.9	3.5 - 2.9
Norway		1.7
Sweden		1.7 - 2.7
Switzerland	3.0 - 6.0	
UK	1.3 - 7.6	
USA	2.1	
West-Germany	3 - 6	

Fig. 9 gives a visual overview of the requirements. They are all presented as allowable leakage rates per meter joint length. The requirements expressed per m^2 window area are transformed to meter joint length by assuming 3 to 4 m joint length per m^2 window area.

Fig. 9 : Overview of the requirements for window leakage.

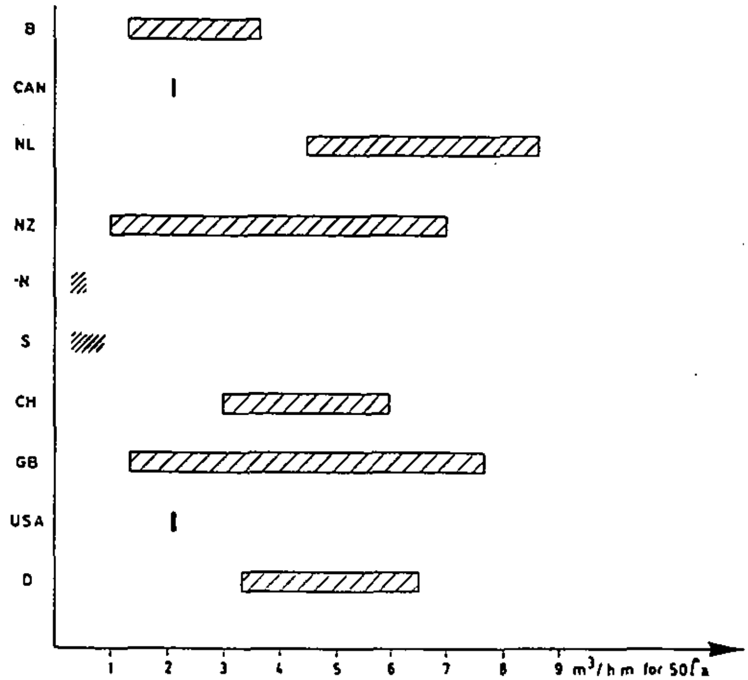

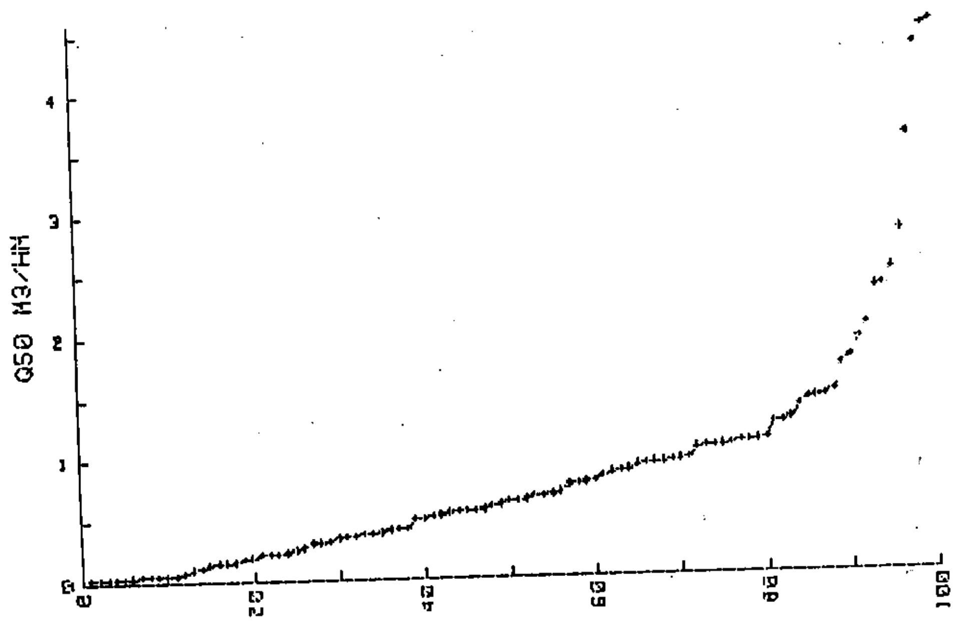

Fig. 10 - Measured air leakage at 50 Pa [20]

Table 16 - Air leakage rates as a function of profile.

Openingswijze / Soort materiaal	Enkele vleugel	Dubbele vleugel met vaste middenstijl	Dubbele vleugel zonder vaste middenstijl	Draai-kipvenster	Horizontaal schuifvenster	Horizontaal wentelraam	Vertikaal wentelraam	Valraam	Kombinaties	Gemiddelde
Aluminium zonder termische onderbreking	2,07	—	—	1,10	3,41	1,94	1,66	—	2,30	2,08
Aluminium met termische onderbreking	—	—	—	0,91	2,27	0,79	—	—	0,40	1,09
Hout	0,85	0,98	1,04	0,98	1,46	1,95	—	—	1,27	1,22
Polyurethaan	—	—	0,61	0,29	—	—	—	—	1,21	0,70
PVC	—	0,30	1,09	0,84	0,22	0,83	—	1,39	—	0,88
GEMIDDELDE	1,46	0,64	0,91	0,82	1,84	1,38	1,66	1,99	1,30	

5. THE LEAKAGE OF WINDOWS WITH RESPECT TO THE TOTAL BUILDING LEAKAGE

5.1. Measured window leakages in practice

Standard values give an indication of good quality levels. Laboratory and on site measurements give a better idea of the achieved airtightness. Firstly the results of laboratory measurements are given and afterwards in situ measurements.

5.1.1. Laboratory measurements

P. Verougstraete [20] has analysed 100 laboratory measurements which have been carried out at the Belgian Bulding Research Institute.
Fig. 10. shows the measured air leakage for a pressure difference of 50 Pa.
The curves according to STS are also presented.
The air leakage as a function of profile and window type is given in table 16.

Major conclusions :

- 90 % of the tested window have an air leakage lower than 1.9 m^3/hm at 50 Pa which is required for a building with a total height less than 18 m. Even 15% have an air leakage below 0.13 m^3/hm at 50 Pa which is less than 1/10 of the allowed leakage rate for buildings higher than 18 m.
  This clearly indicates that windows with an extreme airtightness can be built.
- A certain tendency of air leakage as function of profile and window type can be observed. However, the limited sample number makes a generalisation rather dangerous.

5.1.2. On-site measurements

As opposed to laboratory measurements, 2 types of leakages are observed in practice :

- air which passes through the cracks between the movable and the fixed parts of the windows (the sash perimeter) and which can be subject to weatherstrip application

- air which passes through the cracks between the frame and the surrounding wall.

Van Gunst [43] has measured in 1959 the airtightness of more than 100 windows in experimental dwellings in the Netherlands. Sixteen different types were represented. Only the leakage through the cracks between the movable and the fixed part was measured.
His results are summarized in table 17.

Table 17 : Φ_{50}-values [43]

	Average	Min.	Max
Wooden frames			
. simple frame : single glazing	15.5	1.2	34
double glazing	4.9	1.6	6
. double frames	12.2	4.3	19
Steel frames	6.1	1.4	8
Total	11.7	1.2	34

The major part of these windows don't fulfill at the present Dutch requirements [Φ_{50} : 4.5 to 8.7 m³/hm]. Even the average value is higher than the value allowed for the small buildings in well protected areas.

Knoll and De Gids [21] have reported results of measurements on 21 window systems in Dutch houses.
Their results can be summarized as follows :
- In contradiction with the Dutch NEN 8661 the leakage between frame and surrounding wall is important. On the average : about 40 % of the leakage through the cracks between movable and fixed part (per meter length).

- A large variation was found : The following air flows at 50 Pa (N - 2/3) were derived :

  cracks frame/wall : between 0.2 and 15 m^3/hm (1 to 65)

  cracks fixed/movable : between 1.6 and 36 m^3/hm (1 to 20).

  40 % of the tested windows don't fulfill the required standard.
- A unique variation of the air tightness as a function of the season doesn't exist.

5.1.3. Conclusions

As one could expect indicate on the one side laboratory measurements that the standard values for window airtightness are relatively easy to achieve and that even a ten times higher airtightness is possible.
On the other hand in situ measurements show us that :

a) the existing housing stock contains windows with a large variation of airtightness. A lot of windows do not arrive at the required airtightness.
b) the cracks between frame and wall contribute in many cases to an important increase of the air leakage.

5.2. Building airtightness

A good indication of the airtightness of building envelopes can be obtained from the pressurisation test method. Several countries have standards for the pressurisation test method (Sweden, Norway, United States), while Canada has a draft standard and the Netherlands' standard is in preparation.
The procedure differs somewhat from one country to another, so that the results are not fully comparable :

1) Canada includes the basement in the house volume even though it is not heated. The rest of the countries uses heated volumes.
2) When pressure testing a building in Canada, Norway or Sweden occurs, the ventilation system is sealed of to get the leakage of the enveloppe.

The United States, United Kingdom, the Netherlands and Belgium prefer not to make any modifications to the dwelling.
Several countries have results for a large number of dwellings.
Table 18 resumes the results.

Table 18

Country	Localisation Type	Ref.	Sample size	Average and standard deviation	Min	Max
Belgium	Namur all types	5.23	39	$\bar{n}$ = 10.9 s = 7.3	3	35
Canada	Saskatoon residences	5.24	176	< 1945 $\bar{n}$=10.4 1945-1960 $\bar{n}$= 4.6 1960-1980 $\bar{n}$= 3.6 airtight $\bar{n}$= 1.5	4.2 2 16 0.3	33 12 10 4.7
Netherland	Amersfoort dwellings		130	$\bar{n}$ = 12 s = 4.6	3	33
Norway	Randomly detached dwellings	5.25	61	$\bar{n}$ = 4.7 s = 1.5	2.1	8.0
	Randomly flats		34	$\bar{n}$ = 1.3 s = 0.4	0.5	1.8
Sweden	Different types	5.26	91	< 1920 : $\bar{n}$ = 11.6 1921-1940 $\bar{n}$= 7.8 1941-1960 $\bar{n}$= 6.1 1961-1975 $\bar{n}$= 5.7		
United Kingdom	all types 60-80	5.27	19	$\bar{n}$ = 13.9 s = 3.4	8	20
United St.	randomly	5.28	204	$\bar{n}$ = 22.5	5	> 50
New Zeal.	3 cities	5.29	81	$\bar{n}$ = 9.7	4	30

The average heated volume is between 250 and 400 m³. This gives the following air flows at 50 Pa : Φ_{50}.

- United States : $\bar{n}$ = 20 ac/h → Φ_{50} = 5.000 .. 10.000 m³/h (including HVAC)
- Belgium
- Netherlands
- New Zealand
- Can., SW, Norway older dwellings

$\}$ $\bar{n}$ = 10 ac/h → Φ_{50} = 2.500 .. 4.000 m³/h

- Canada new houses
- Sweden
- Norway
  new dwellings

$\left.\right\}$ $\bar{n} = 2.5$ ac/h → $\Phi_{50} = 500 \,..\, 1.500$ m³/h

5.3. <u>Contribution of the window leakage in the total building leakage</u>

In 1.2. was indicated that the standard value for the air leakage of windows at 50 Pa varies between 0.5 and 10 m³/hm. The total length of the cracks between the movable and the fixed window parts in most houses is less then 100 m, in a lot of cases even less than 50 m. This means that the total leakage rate through the window cracks is for windows according to the standard between 50 and 1000 m³/h at 50 Pa. A comparison with the values for the total house indicate that the window leakage through new windows is on the average not the major path of air infiltration in houses.

A simple calculation for a Norwegian single family dwelling built according the standards leads to the same conclusion :

- building :
  - . requirement (4.3.) : $n_{50} \leq 4\ h^{-1}$
  - . for a volume between 200 and 400 m³ : $\phi_{50} < 800 \ldots 1600$ m³/h
- windows :
  - . requirement (4.4.) : $\phi_{50} \leq 1.7$ m³/hm²
  - . window area ≤ 30 m² → $\phi_{50} \leq 51$ m³/h
  - . relative contribution of the windows

    $\frac{51}{1600} \ldots \frac{51}{800}$ or 3 ... 7 %

On site measurements reveal the same conclusion : the Air Infiltration Centre has published the Technical Note AIC 16 [30], in which information on leakage distributions measured in situ, taken from papers in the Air Infiltration Centre's bibliographic database AIRBASE, is summarised.

A summary of these results with regard to window (and door) leakage is given in table 19 and fig. 11.

Tabel 19 : Contrib. of windows and/or doors in tot. building leakage (%).

Ref.	Windows %	Doors %	Windows + doors
44			20, 22, 19, 24 24, 22
45	6	16, 4	
46	12	5	
47			27
48			40
49	18		
50	89, 33		
51			5
52	15, 22		46 - 73
53			20
54			11
55	14, 7		
56			17, 23
57	25		
58	10, 14	11, 10	
59			37
60			15
61	5-10		
62	45, 50, 11, 33 32, 20, 16	22, 20, 23, 38 18, 15, 3	

Fig. 11 : Contrib. of windows and/or doors in tot. building leakage (%).

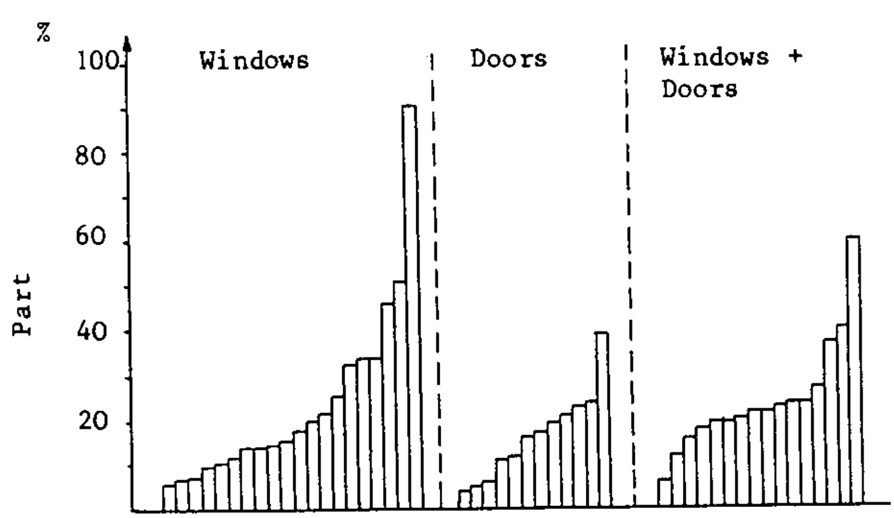

6. PRACTICAL EXECUTION OF JOINTS BETWEEN WINDOW FRAMES AND WALLS - WEATHERSTRIPS [22]

6.1. Introduction

There are a number of possibilities in order to obtain joints which are well airtight.
Several techniques are described in "Air Infiltration control in Housing" (Swedish Council for building research and AIC) [22].
These techniques are mostly based on the Swedish tradition.
Nevertheless they give a good indication of the possibilities and limitations.
The parts which deal with windows are represented hereafter.
They are an integral reproduction of the information in the handbook "Air infiltration control in housing".

6.2. Joints between window (door) frame and wall [22]

There are many different solutions for joints between window or door frames and walls [31], [32]. Some of these solutions are discussed in the following, and the advantages and disadvantages of the respective methods are given. In this handbook we only describe the problems concerning airtightness and thermal insulation in the joints.

SEALING WITH MINERAL WOOL STRIPS BETWEEN FRAME AND WALL
The joint is covered with a batten and/or adjacent plaster.

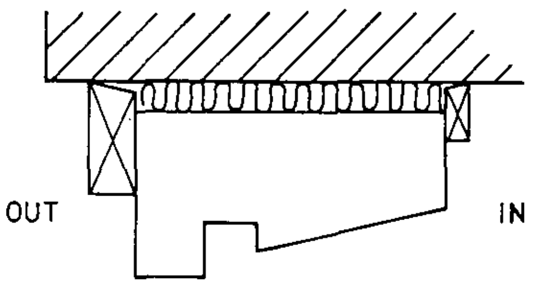

Fig. 12. : Mineral wool strip sealing [22]

The joint will be neither air - nor vapour-tight. A certain degree of airtightness can, however, be achieved with caulking, particularly if mineral wool is used. Hard caulking demands extra anchorage of the frame to stop it bulging outwards.

Current Swedish requirements for energy management are usually fulfilled. The method does have an advantage in that temporary dampness if the joint is not catastrophic since drying out take place relatively unhindered.

INTERNAL SEALING WITH MASTIC AND MINERAL WOOL CAULKING

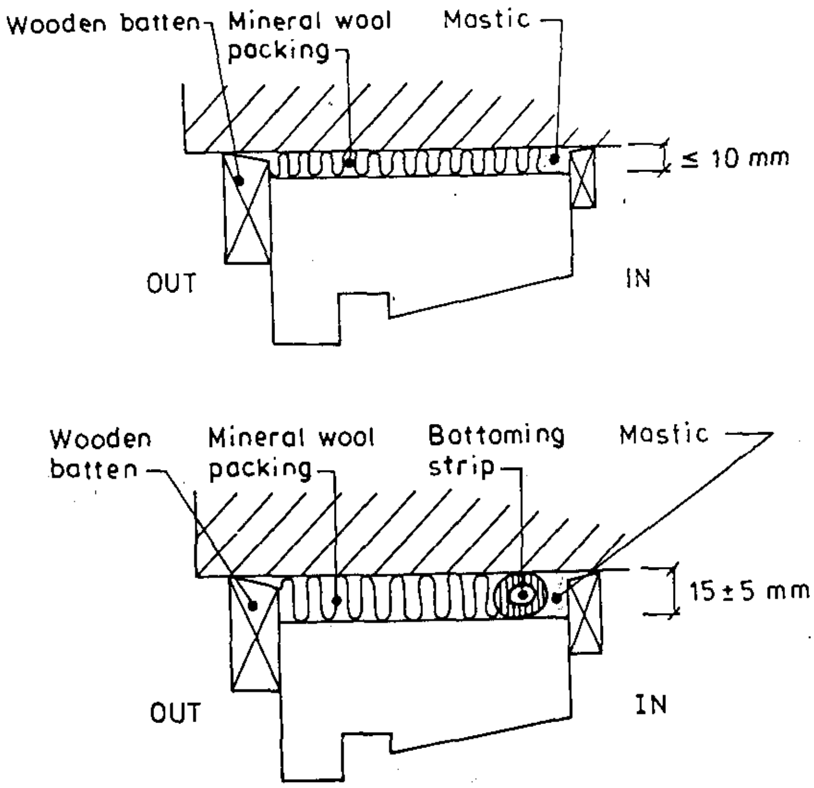

Fig. 13 : Two methods for jointing with mastic. [22]

To facilitate good sealing, it is recommended that the joint dimension is 15 $\pm$ 5 mm and the joint is sealed with mastic. The actual airtightness is achieved with the mastic which forms an elastic, tight join if the appropriate mastic is used.

The intended purposes of the mastic are diffusion sealing and airtight-ness. In some cases, the wall's corresponding layers are joined - often an air/vapour barrier. The best method is to bake the film into the joint. Mastic must close tight and adhere well to the wall and frame without separating as a result of movement between the frame and the wall. Particular attention is paid to joints in corners where wedges and attachment devices might remain.
The purpose of the bottoming strip is to provide a rear barrier to the mastic in the joint. The bottoming strip is selected so that it sits tight even if the joint width is 15 + 5 = 20 mm. Two sizes of bottoming strip should be available during installation work.

Caulking is done with mineral wool and is stopped about 15 mm from the edge of the joint. The prime function of caulking is thermal insulation. Correctly applied caulking provides good insulation.
Airtightness is significant in a joint without any other sealing but, when compared with mastic, is of minor importance to the total airtightness.
The inner moulding is used for aesthetic reasons and to cover and protect the mastic.
The outer gap leads to the outside air. Its most important function is to facilitate drying the air. The outer moulding is intended to provide protection against driving rain.
For the joint to function as intended, it is assumed that stated joint tolerances are maintained.

JOINTING WITH POLYURETHANE FOAM

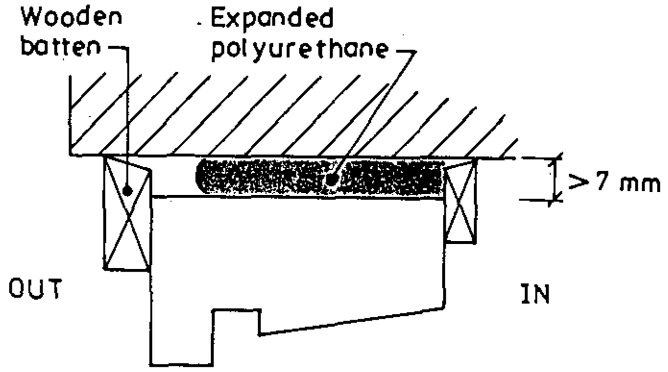

Fig. 14 : How a polyurethane foam joint should be made. [22]

The joint width should not be less than 7 mm, bearing in mind the application of the foam.
The joint has very good thermal insulation properties compared with frame timber and adjacent wall material. The joint is normally sufficiently diffusion tight and airtight even when joints are relatively wide (> 20 mm).
In unfavourable cases, the jointing foam can prolong the drying time of timber that is too moist. Foam should be applied to reasonably dry timber. It is not easy to adjust window frames when foam has been applied.

JOINTING WITH GLASS FIBRE ENCLOSED IN THIN PLASTIC FILM

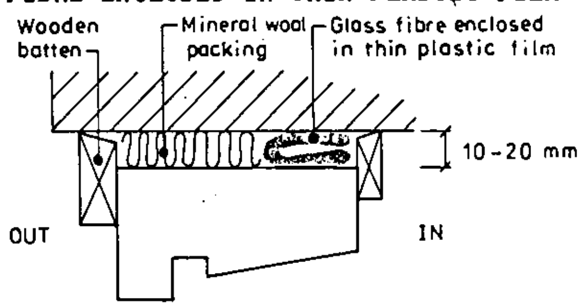

Fig. 15 : Airtightness achieved with glass fibre enclosed in thin plastic film. [22]

Thermal insulation in joints is provided by mineral wool. The actual airtightness (and diffusion seal) is achieved through the plastic film around the internal mineral wool strip.
Good airtightness is achieved for joints between 10 and 20 mm. Point leakage often occurs at window corners and around wedges.

JOINTING WITH TUBULAR STRIP, ANGULAR STRIP, ETC.

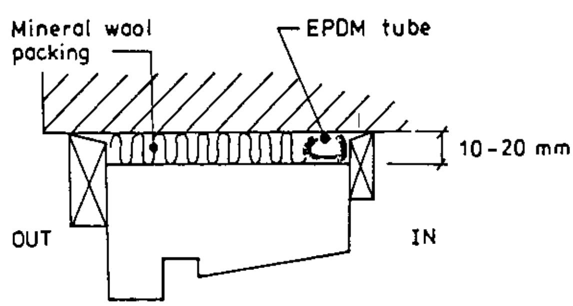

Fig. 16 : Tubular strip. [22]

Joint sealing between frame and wall by using profiles of EPDM rubber to provide the actual airtightening in the joint. The gap should be between 10 and 20 mm. At least two different mouulding sizes are required for installation, bearing in mind different tolerances. To achieve good airtightness, both frame and adjacent wall should be very smooth. The tube should not be stretched too much during installation. Plastic films in timber walls would be joined to the tubular moulding in the joint. Mineral wool provides thermal insulation in the joint.

JOINTING USING PLASTIC FILM

A technique has been developed in Canada where a plastic film strip is applied to the window frame with staples and using glass fibre tape and mastic. This plastic film strip is joined by overlapping and edge sealing to the plastic film in the wall. It is necessary to fit the plastic strip against the frame before it is installed in the wall. See figure 17.

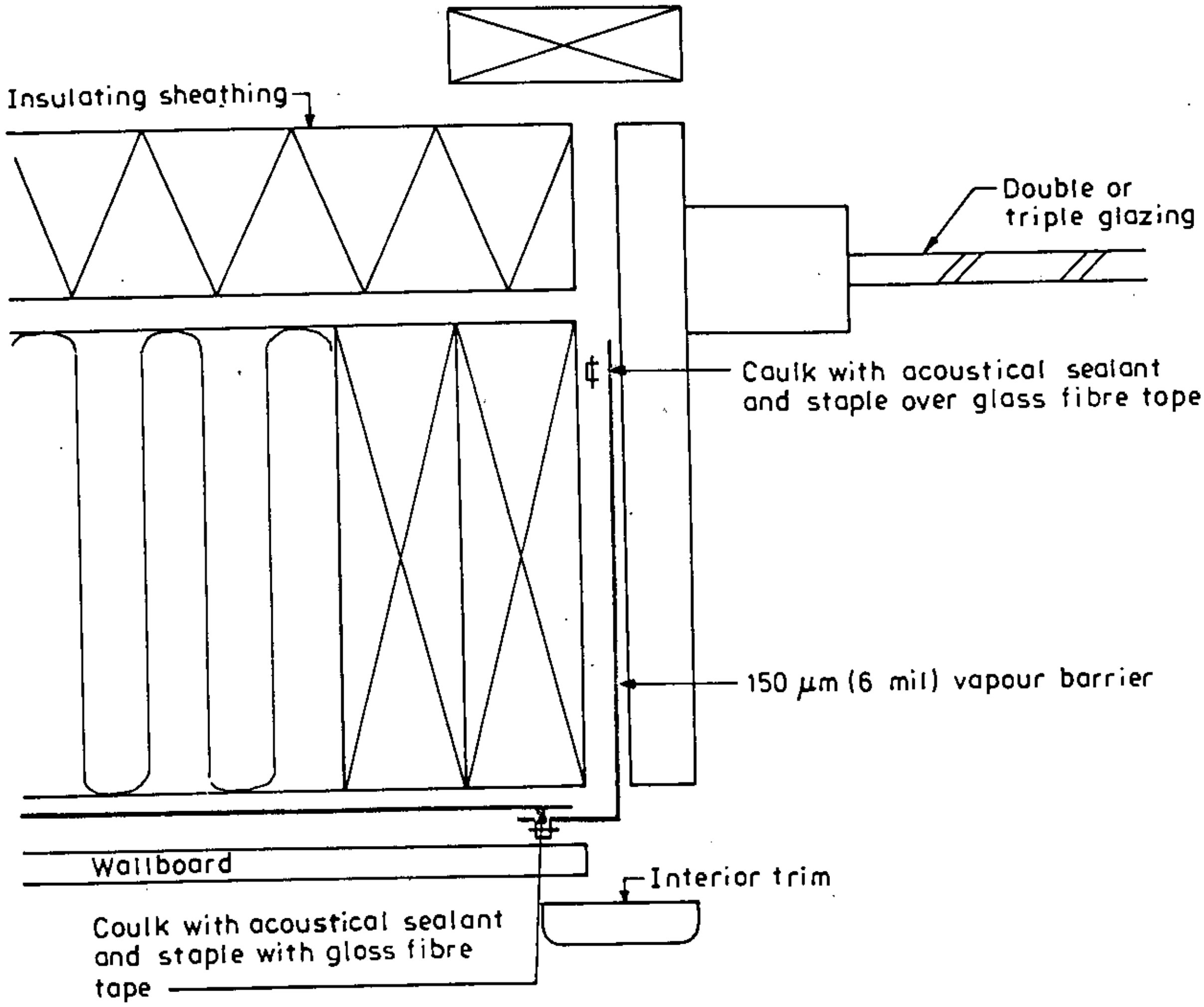

Note : Attach vapour barrier strip to window casing before being inserted into rough opening. Allow sufficient material at corners to fold vapour barrier.

Figure 17 : Air/vapour barrier installation at window (Canadian example)

6.3. Weatherstrip for windows and doors [22]

Types of weatherstrips on the building market

Weatherstrips in the modern sense of the term have a relatively short history in building technology. The strips were first made of spun wool or cotton fibre. They bear a close ressemblance to a soft string and often have a diameter of 8 mm. Nowadays they are also made of synthetic fibres and may have a core of foamed plastic or porous rubber. Self-adhessive weatherstrips of foamed plastic and foam strips were also used in the early days.

Naturally, these types of strips caused an appreciable improvement in airtightness at the time. However, it is a common characteristic of fibre strips and foam strips that they are permeable to air and must therefore be extensively compressed to perform as intended. Foam strips are nowadays mainly sold as dust excluders and are placed between the casement in double glazed windows.

The modern types of strips are made of impermeable materials and have a profile of such design that they can be deformed relatively easily so that the door or window is easy to close while providing a satisfactory seal. The strip must at all times endeavour to regain their original shapes (i.e. they must be resilient). Strips of this type often have a tubular or angular profile. Different types of strips are shown in figure 15.

Tubular strips are made in profile heights of about 5 mm upwards, and angle strips about 7 mm upwards. The materials most commonly used are synthetic rubber (EPDM and chloroprene) and plasticized PVC. EPDM probably has the greatest share of the market. Silicone rubber is also used, but this material is considerably more expensive than those mentioned above and is therefore used to a less extent.

Expanded strips, i.e. porous rubber strips with closed pores, are also relatively new on the market. These strips must not be compressed more than 30 %, or the pores may rupture. They are made in heights ranging from 3 mm upwards.

Types

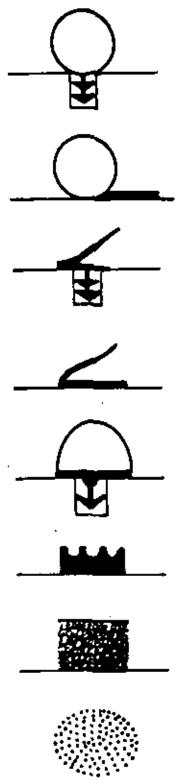

Tubular strip (O strip) with toe for mounting in a groove. It is pressed into the groove

Tubular strip (O strip) for mounting on a flat surface. Self-adhesive, or mounted by stapling, nailing or gluing

Angle strip (V strip) with toe for mounting in a groove. It is pressed into the groove

Angle strip (V strip) for mounting on a flat surface. Mounted by stapling, nailing or gluing

Tubular strip (D strip) with toe for mounting in a groove. It is pressed into the groove

Expanded strip for mounting on a flat surface. Self-adhesive

Foam strip for mounting on a flat surface. Self-adhesive

Fibre strip for mounting on a flat surface. Mounted by nailing or stapling

Figure 18. : Types of weatherstrips for windows and doors. [22]

Airtightness of windows

Studies of airtightness of windows have been made by Höglund & Wäggren [33]. In determining the leakage of air through windows the guarded pressure box method was used. The measurements were made in wood windows which had a design in conformity with the appropriate Swedish standard. Both double-glazed and triple-glazed windows were used. The weatherstrips were placed where the casement abuts on the frame. The gap for the weatherstrips varied from about 2 mm to over 4 mm.

The results are summarized in figure 19. The types which best satisfied the airtightness requirements in the Swedish Building Code were strips of tubular or angular profile. A properly chosen expanded strip could also provide satisfactory airtightness. In most cases foam and fibre strips did not satisfy the requirements stated in the regulations.

The results also showed that it was extremely important for mounting to be done with care. A good result was easier to reach with tubular strips than with angular strips.

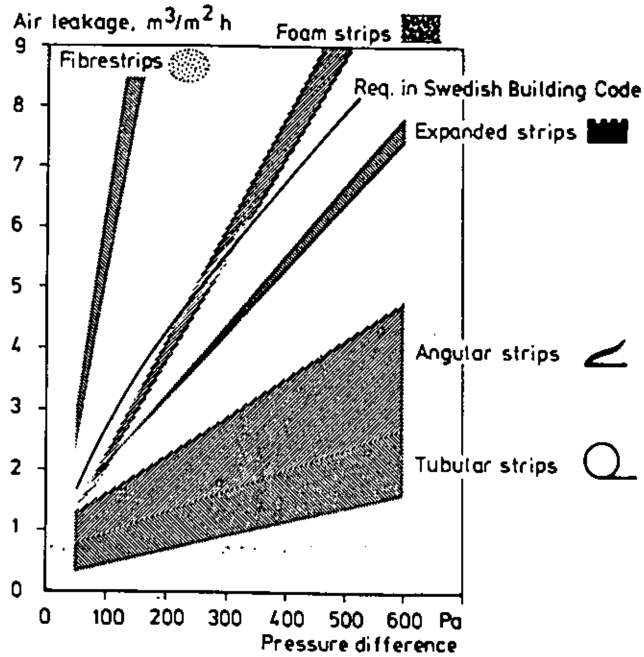

Figure 19 : Summary of test results for weatherstrips in windows. [22]

Structural solutions

Gaps between frames often can be detected by inspecting the opening and closing action and weatherstrips. Gaps can also be detected by using a candle or smoke, or by applying thermography. Detection is faciliated if the room is subjected to negative pressure.

Resealing of windows and doors should include the following steps :

a) Inspect the windows and doors. Do they require repainting or the putty replacing ?

b) Check that the casement/door can be closed and opened easily and adjust were necessary

c) Check that the window/door furniture works properly and adjust and lubricate where necessary

d) Check that the air gap between the casements of all double windows/doors has not been rendered ineffective as a result of repainting etc.. A gap of 1-2 mm is required. If the gap between the casements is greater than 2 mm, 2 previous dust-tight strips can be fitted in order to reduce the air circulation between the panes thereby achieving certain savings in energy.

e) Always paint exposed wood surfaces (surfaces which lack finishing coat, glazing paint, etc...) before reapplying putty and fitting weatherstripping
f) Select suitable strips dimensions bearing in mind the width of the gap between the casement/door and frame. The size of the gap when the window/door is closed can be measured by using Plasticine pressed onto a few places on the rebate in the frame.
g) Select the weatherstripping. When selecting strips for use between the casement and the door, the gap width measured in f) must be considered. When selecting weatherstrips, strips of silicone rubber and EPDM rubber have exhibited the best sealing and ageing properties. Tubular strips provide the best seal but angular strips are also effective. Angular strips are recommended for doors where a low closing pressure is required.
h) The way in which weatherstrips are fitted is important for their correct function. Special attention must be paid to the corners where gaps often occur.

6.4. Retrofits in existing buildings [22]

Air leakage in older buildings has often been found to be unnecesserily high, considering the requirements for air quality for both heating and air conditioning [34].
Considerable energy savings are possible in many cases using relatively cheap and simple sealing measures. As example of this is the "House Doctor's Program" carried out in the United States. Another example is given in table 20 which shows that energy consumption is lower in houses in which good quality weatherstripping has been fitted to windows [35], [36].
Since there are few data on true energy savings that result from carrying out sealing measures, this chapter only discusses the measure themselves without considering their cost-effectiveness.

Problems that arise from inadequate ventilation must always be considered when sealing measures are used in a building. In houses with natural ventilation, air is supplied partly through leaks in the structure and partly through openable ventilation provisions. This limits how far sealing measures can be taken without having to install special supply air devices.
In houses with mechanical exhaust ventilation, the influence of the fan has a dominating effect on the amount of ventilation. Flow through the fan is not changed significantly as the building envelope is further sealed. However, the negative pressure in the house does increase. This also limits how tight the building shell can be made.

Further sealing does not provide any more energy savings. There may be other valid raisons, apart from energy savings, for sealing the building, e.g. draughts in occupied areas, desired ventilation distribution, see figure [37].
Houses with balanced exhaust and supply ventilation should, however, be made as tight as possible to avoid unnecessarily ventilation. This is particularly important if energy recovery using a heat exchanger fitted to the exhaust air is to be optimized.
The main principle for sealing existing buildings must be to ensure that sufficient but not excessive ventilation is achieved and that the supply air enters the building where it causes the least draught, cold downdraught or other discomfort. If these criteria are fulfilled, the airtightness of the house can be improved to the extent that is economically and technically feasible.

Table 20 : Average energy consumption and heated volume with standard deviations after retrofit for existing single-family houses in Sweden with different types of weatherstrips in windows. Almost all of the houses have natural ventilation. [22]

Principal type of weatherstrips between window-frames and casement	Number of houses surveyed	Energy consumption after measures being undertaken litre oil/dwelling		Heated volume per dwelling m^3	
		Average	Standard deviation	Average	Standard deviation
Weatherstrips non-existent	23	4220	2726	426	215
Foamstrips surrounded with fibre	47	4071	1114	473	-
Fibre strips (wool or cotton)	93	3877	1075	454	-
Foamstrips(foamplastics with open pores)	107	3802	1152	466	158
Tubular strips (synthetic rubber)	124	3761	1069	415	144
Angular strips (synthetic rubber)	51	3624	977	464	152
Expanded strips (porous rubber with closed pores)	211	3541	1047	418	-
Fixed windows (not openable)	11	3294	1165	409	142

Common points where air leakage occurs (apart from the wall, ceiling and floor structures themselves) are joints between building sections and penetrations in structures for installations, etc..

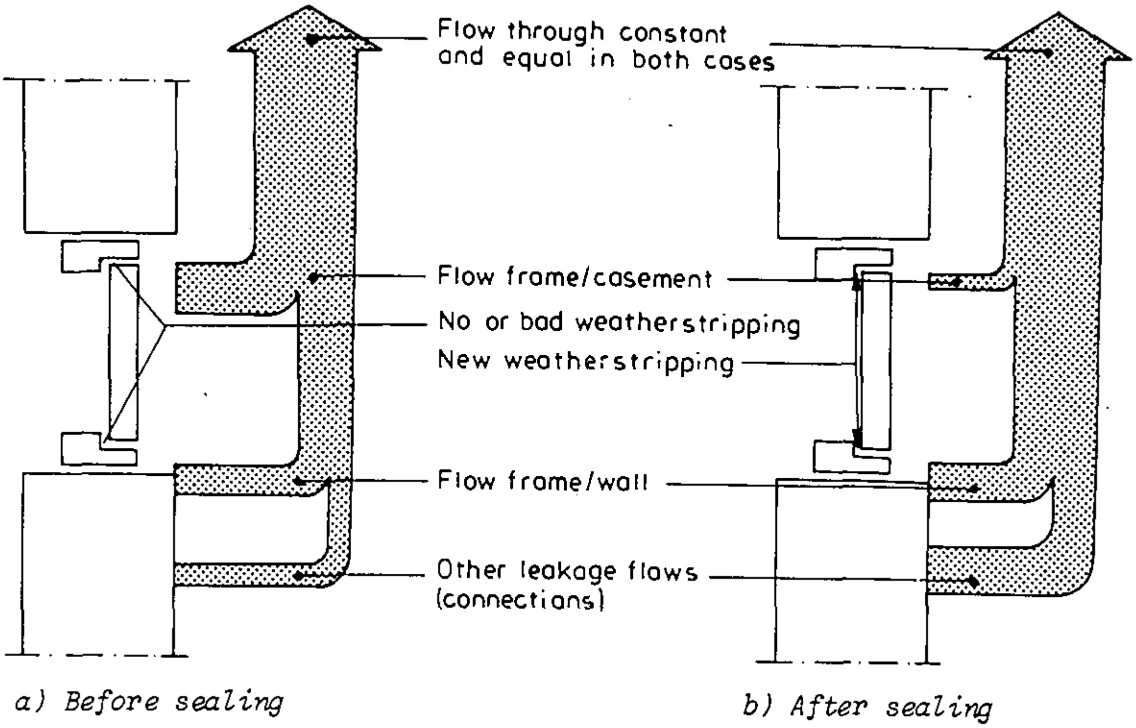

Figure 20 : Flow change in an exhaust air ventilated house when windows are fitted with new weatherstripping. The relatively constant total flow is redistributed in proportion to the previousness of the different leakage locations. Wind forces are often of subordinate importance as the driving force of the air leakage. [22]

Joints between different building sections and between different materials are usually weak points with respect to air leakage. In buildings made of brick or concrete, for example, air leakage is often greatest around windows and doors and at joints between building elements.

(...)

Moisture should also be carefully considered when selecting tightness measures.

Windows and doors

Methods for sealing between window and door frames in new houses have been described earlier. Different types of weatherstripping, and methods of fitting these to doors and windows, are discussed in detail. Such methods are also sometimes applicable when improving existing buildings. Careful consideration of material choice is necessary since many windows and doors in existing buildings have not been designed for the installation of weatherstripping.

Different types of weatherstripping in windows seem to affect energy consumption in different ways.

Investigations in single-family houses have shown that expanded angular and tubular strips of synthetic rubber (EPDM) result in lower energy consumption than when weatherstripping of foam and/or fibre is used [35] (see table 20). These results were confirmed by significance tests on the date given in the table.

There was an obvious difference in energy consumption between houses where weatherstrips did not exist and houses where fixed windows (not openable) were installed, though there were few houses with fixed windows.

Ther result correspond well to the results of an earlier investigation where the efficiency of different types of weatherstrips, in terms of air leakage, has been evaluated in laboratory tests [38].

7. INHABITANTS BEHAVIOUR WITH REGARD TO THE USE OF WINDOWS

As mentioned in the introduction inhabitants behaviour is the topic of IEA annex 8 "Human behaviour with regard to ventilation [39]. This working group will finish their activities in 1986 and the final reports will be published early 1987. Therefore this paragraph discusses only a few topics :

- what is the effect of window opening on the ventilation rate and the energy consumption ?
- the use of windows
- the influence of occupancy on the ventilation rate.

7.1. The effect of window opening on the ventilation rate and the energy consumption

7.1.1. Introduction

A detailed study has been carried out in 1980 by ing. J.C. Phaff, ing. W.F. De Gids, J.A. Ton, P. Van de Ree, L.L.M. Van Schijndel [40]. This paragraph resumes their conclusions.

7.1.2. Description of the project [40]

The aim was to obtain data concerning the ventilation rate, the induced energy consumption and the internal climate if one window is opened in a bedroom.

The measurements have been carried out in three buildings situated in 3 different locations in the Netherlands. About 40 measurements were done for different temperature differences (5, 15°C) and wind velocities (15..10 m/s). The rooms were not heated during the measurements.

7.1.3. Results

The following range of magnitude was measured :

air velocity in window opening	: 0.1 - 0.5 m/s
ventilation rate	: 0.2 - 25 h^{-1}
energy losses due to ventilation	: 200 - 3000 W.

Remark : The room volume varied between 23 and 53 m^3.

The influence of temperature difference and wind velocity for a room of 25 m^3 and an open window of 0.5 m^2 on the ventilation rate and the energy losses are given in tables 21 and 22.

Wind velocity (m/s)	Temperature difference (°C)			
	0	5	10	15
0	3.5	6	7.5	9
2	4.5	6.5	9	9.5
5	6.5	8	9.5	10.5
8	10	11	12	13

Table 21 : Ventilation rate (ac/h) for a 25 m^3 room with an open window (0.5 m^2).

Wind velocity (m/s)	Temperature difference (°C)			
	0	5	10	15
0	-	260	660	1165
2	-	275	690	1200
5	-	355	820	1375
8	-	470	1025	1655

Table 22 : Ventilation losses (W) for a 25 m^3 room with an open window (0.5 m^2)

The seasonal energy demand can also be estimated (Dutch conditions : wind velocity : 5 m/s, temperature difference 12 .. 15°C). Table 23 gives an indication of the energy demand for two 25 m^3-rooms with an open window of 0.5 m^2.

Situation	Windows	Heating demand kWh/year
1	closed	100 .. 600
2	3 hours a day open	1500 .. 2000
3	25 min. a day open	300 .. 800

Table 23 : Estimated heating demand for two 25 m^3 - rooms with window (0.5 m^2)

7.2. The use of windows

Research with regard to the use of windows have been carried out by several researchers. It is also one of the topics under investigation in the IEA-annex 8 working group.
Lyberg [41] and De Gids, Phaff, Van Dongen and Van Schijndel [42] came to the same type of conclusion.
"The weekly mean of the number of open windows is strongly correlated with the mean outside temperature".
However, the formula they derived is not the same :
Lyberg : $H.\Delta T = C^{te} \simeq 1.8 .. 2.6$ (hyperbolic)
De Gids and Cie : $H = A + B\ T$ (linear function) ($A = 10$, $B = 0.65$).
with : H = percentage of open windows (0 .. 1)
T = external temperature (°C)
ΔT = the temperature difference between inside and outside (°C)
A qualitative comparison is given in fig. 21. Basically, there is no fundamental difference for the region where the measurements of De Gids have been carried out (- 5 .. 10°C). The rather important differences for T > 15°C is probably caused by the assumption T_i = 20°C which isn't realistic for T_e > 15°C.

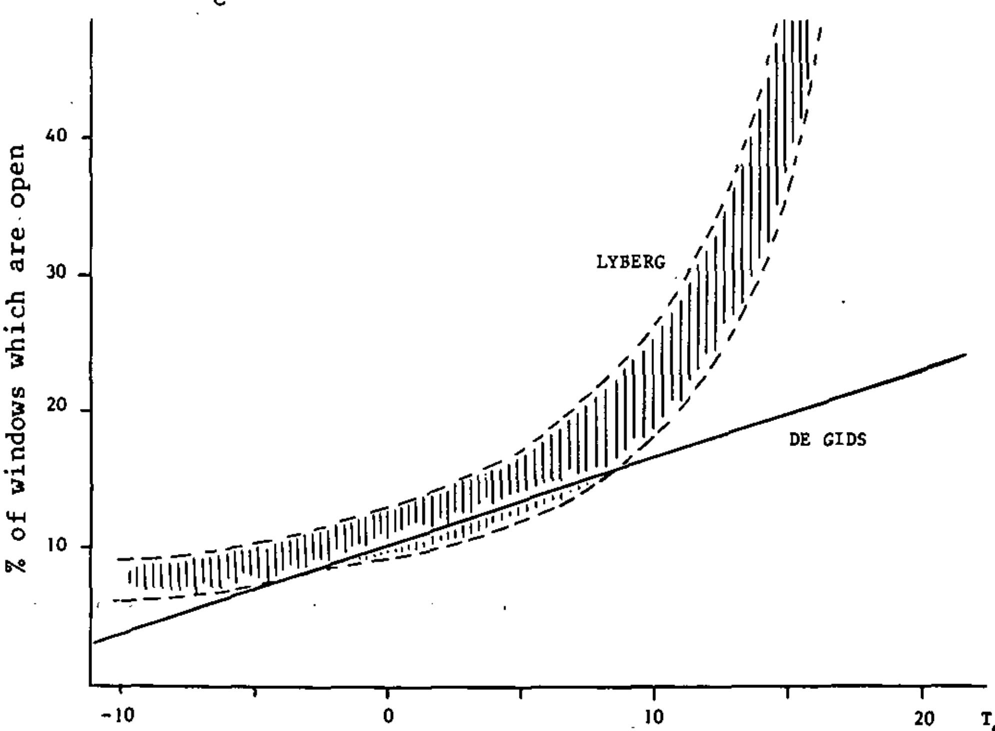

Fig. 21 - Comparison between the formula of De Gids [42] and Lyberg [41]. Assumption for the Lyberg-formula T_i = 20°C.

7.3. The influence of occupancy on the ventilation rate

Kvisgaard, Collet and Kure [7] have measured ventilation rates in 25 dwellings during periods varying between 3 and 18 days. All the dwellings were situated in Denmark whose housing mass is among the most tightly sealed in Europe.

This research resulted in the following conclusions :

a) the occupants' behaviour has a very considerable influence on the total air change rate. On average, the air-change rate is 3-4 times higher than the basic air-change rate. An absolute figure for the behaviour influence is possible by expressing the effect as an absolute increase of the ventilation rate.

   This is done in table 24. Results for the natural ventilated dwellings (14) and the mechanically ventilated ones (8) are given separately.

	n_B		n_{MECH}		n_{TOTAL}		OCCUPANCY	
	Average	s	Average	s	Average	s	Averg.	s
Natural	0.19	0.08	-	-	0.51	0.25	0.32	0.26
Mechanical	0.17	0.09	0.63	0.20	0.97	0.30	0.34	0.23

Table 24 : Summary of results of measured ventilation rates (ac/h)

Remarks :

- the ventilation rate n_{mech} has been estimated intuitively with the aid of the figures in [7.]
- the column "OCCUPANCY" respresents the influence of the effect of occupancy.

This table leads us to the constatation that - on the average - the occupants increase the ventilation rate with 0.3 ac/h.

However the individual results vary largely as illustrated in fig. 19.

b) There is a very large scatter in the results for the table air-change rate. This is showed in table 25.

	Total air change rate (ac/h)				
	0-0.25	0.25-0.50	0.50-0.75	0.75-1.00	> 1.00
Natural and ventilated	2	6	4	1	1
Mechanical ventilated			1	4	3

Table 25 : Distribution of measured total air change rate.

This table indicates that :

- more than 50 % of the natural ventilated dwellings did not arrive during the measurement period at the recommended air-change rate in Denmark of 0.5 h^{-1}
- All the mechanical ventilated dwellings have a ventilation rate above this recommendation.

7.4. Conclusion

This chapter has briefly described some results obtained in the field of human behaviour with regard to ventilation". It clearly indicates that the occupants play an important role with regard to the ventilation of their homes. This becomes more and more important while the air-tightness of the buildings is improving rapidly in a lot of countries. Another aspect of the inhabitants behaviour : draught stripping has not been analysed in this chapter nor the changed behaviour due to the energy crisis with regard to window use, heating patterns,... Práctice in a lot of countries indicates that a reduced ventilation pattern together with the presence of thermal bridges are probably the 2 most important reasons for the large number of condensation and mould growth problems of the last decennium.
More information concerning this subject will be given in the IEA-annex 8 publications : Human behaviour with regard to ventilation.

8. WINDOWS IN RELATION WITH VENTILATION PROVISIONS

There is in a number of countries tendency to construct buildings with an airtight envelope. The required ventilation levels are achieved by adding ventilation provisions : ventilation grills, ventilation chimneys, exhausted ventilation system, balanced ventilation system.

In a number of cases these provisions are integrated in the window design.
Two examples are given as illustration.

a) Ventilation grills integrated in the window

a.1. Ordinary model

Fig. 22 shows a grill which is mounted in the frame.

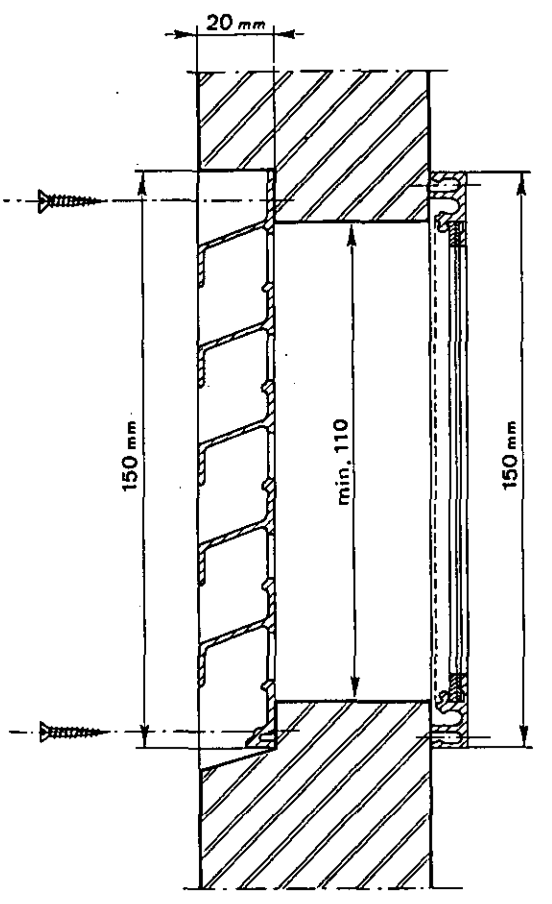

a.2. <u>Model with thermal barrier</u>

Fig. 23 shows a grill with 2 special features :

a) thermal barrier to reduce the heat losses and the condensation risks

b) the glass can be directly mounted in the grill (for renovation purposes).

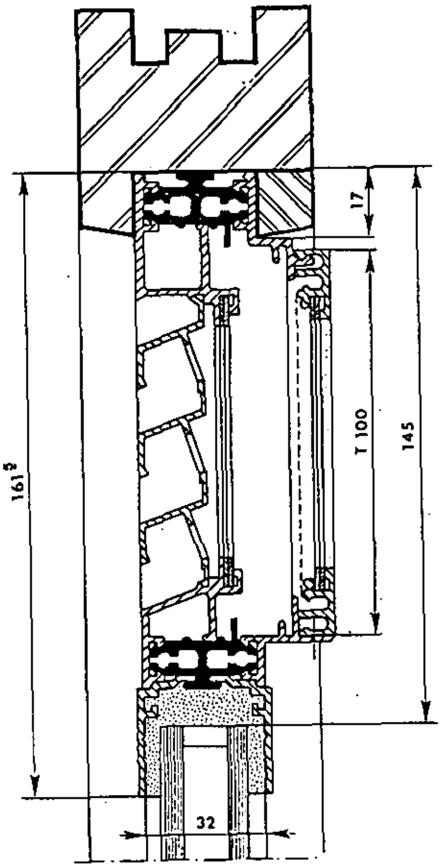

a.3. Grill with noise reduction

In cases with a high external noise level, ventilation grills are in many cases undesired given the low acoustic insulation. However improved versions exist as illustrated in fig. 24

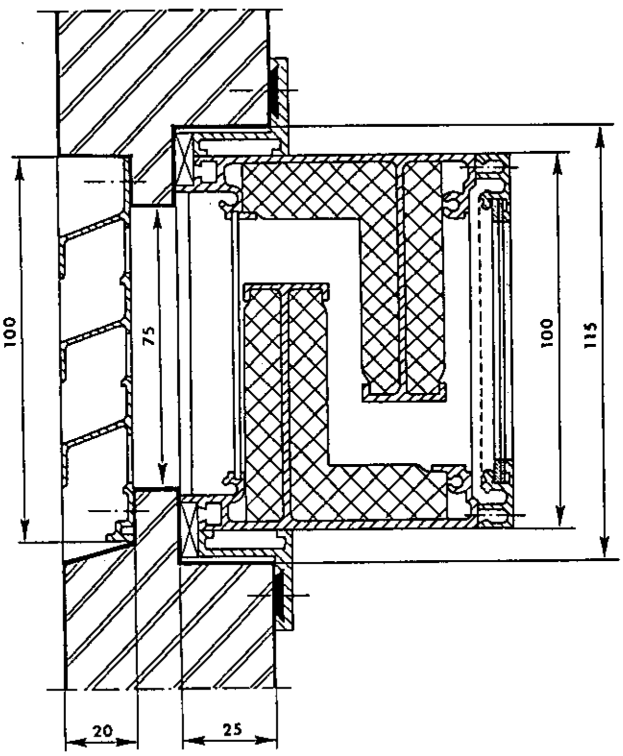

b) Windows as part of the mechanical exhaust system

Several systems are developed which use the glazing system as a first heating exchanger in order to obtain a lower heating demand. This can of course be combined with a second heat exchanger if a further heat exchange with the incoming air is desired.

Two possibilities are illustrated in fig. 25 and fig. 26

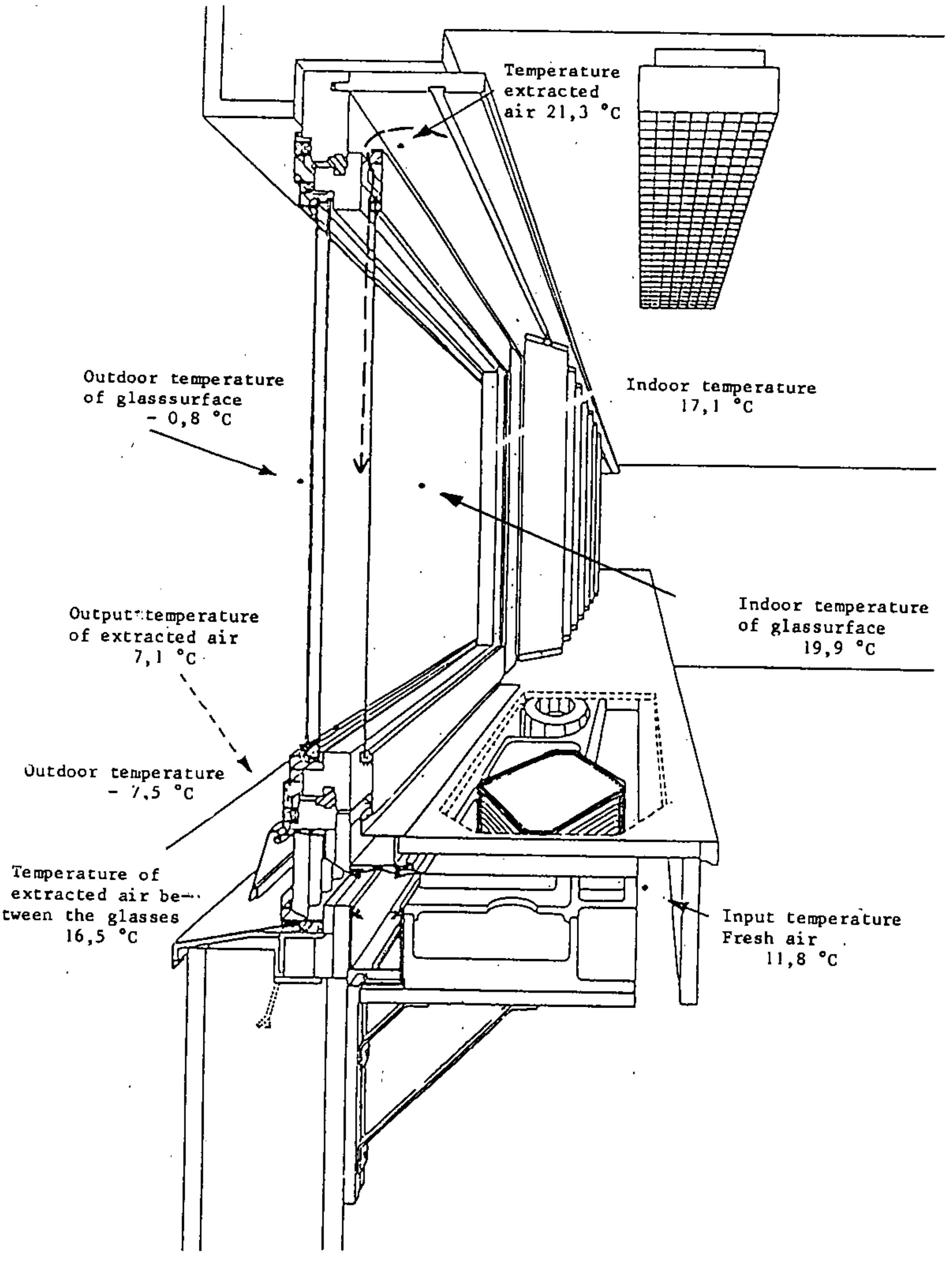

Fig. 25 - Windows as part of the mechanical exhaust system.

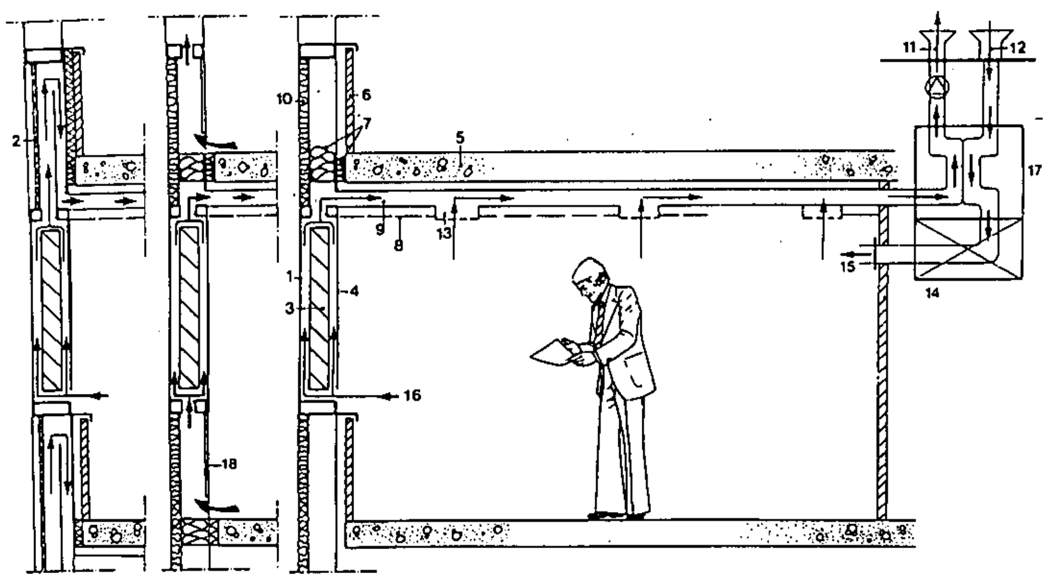

1. Double isolating glass
2. Single hardened and coloured glass
3. Sunshading
4. Single moving or removing glass
5. Floor
6. Selfsuporting fireproof panel
7. Fireproof material
8. Suspended ceiling
9. Extraction conduct of vicious air
10. Insulation panel
11. Output of vicious air
12. Suction of fresh air
13. Luminous element on extraction conducts
14. Air conditioning installation
15. Input fresh air
16. Indication of vicious air in hollow space of the curtain facade
17. Heat exchanger for eventual energy-recuperation
18. Solid panel

Fig. 26 - Windows as part of the mechanical exhaust system.

9. ACKNOWLEDGEMENTS

This work was supported by the Belgian National Energy R&D Program (Prime Minister's Office - Science Policy Planning) who also sponsors our participation in the IEA-Annex 5 (Air Infiltration Center) and IEA-Annex 8 (Human Behaviour with regard to Ventilation).
We like to thank the Air Infiltration Centre and the Swedish Council for Building Research whose publications were a great help to us.
Also the individual contribution of Mr. P. Jackman simplified our work.

We are grateful to the IEA-annex 12, annex 8 and annex 5 colleagues for their comments on the manuscript.
We hope that their support has resulted in an overview without important gaps nor errors.

Finally, but not at least, we would also like to thank the following persons without whose practical assistance this chapter would not have been completed : Mrs. Olislaegers, Mrs. M. De Jonghe, Mr. P. Voordecker and Mr. D. L'Heureux.

10. REFERENCES

[1] A.I.C., Calculation Techniques guide, Air Infiltration Centre, 1986.

[2] IEA-Annex 9 : Minimum ventilation rates : literatuure revies to special research fields and proposal of R&D projects. Final report, August 1983.

[3] B.B.R.I., T.I.N. Humidity problems in buildings. Causes of deterioration. Thermal bridges. Internal Climate. Data for the design and execution of buildings. Occupational conditions in rooms. Brussels, 1984.

[4] Jackman P., Review of building airtightness and ventilation standards, 5th AIC Conference, Reno, 1984.

[5] IEA News, Issue 3, December 1985.

[6] AIC TN 131 : Wind pressure Workshop. Proceedings, Air Infiltration Centre, 1984.

[7] Kvisgaard G., Collet P., Kure J., Research on fresh-air change rate : 1, Occupants' influence on air-change, EEC-contract n° EEA-5-052-DK EFP-80, NO 5723, Technological Institute, Tåstrup, 1984.

[8] Principles of natural ventilation, Building Research Establishment, summary 210, Building Research Station, Watford, 1978.

[9] Sherman, M., Air Infiltration in Buildings, Doctoral thesis, LBL-10712, October 1980.

[10] Klems J.H., Methods of estimating air infiltration through windows, Energy and Building, 5 (1983), 243-252.

[11] Frydendahl K., Denmarks' climate in Wind, Klimatologiske meddeleser nr. 1, Copenhagen.

[12] Lawson T.V., Wind effects on buildings, Vol 1 : Design Applications, Vol 2 : Statistics and meteorology, Applied Science Publishers, London 1980.

[13] J. Janda, Gusten J., Estimation of rate of air infiltration based on full-scale wind pressure measurements, 3rd AIC conference, London, September 1982.

[14] Hunt, Burch, Air infiltration measurements in a four bedroom townhouse using SF6 as tracer gas, ASHRAE transactions, nr. 2338.

[15] Saving Energy in the Home, Princeton's Experiments at Twin Rives, Princeton, USA, Ballinger Publishing Company, Cambridge, Massachusettes, 1978.

[16] Liddament M., Allen C., The validation and comparison of mathematical models of air infiltration, Air Infiltration Centre, 1983.

[17] AIC, Wind pressures for air infiltration calculations : an analytical review and development of a pressure coefficient prediction procedure, Air Infiltration Centre, 1984, not published.

[18] Sherman M., Description of ASHRAE's Proposed airtightness standard, 5th AIC Conference, RENO (V.S.), 1984.

[19] AIC TN-14 : A review of building airtightness and ventilation standards, Air Infiltration Centre, February, 1984.

[20] Verougstraete P. , Commentaire de plusieurs essais de laboratoire relatifs à l'étanchéité des fenêtres au vent et à la pluie, BBRI, revue p. 10-21, March 1983.

[21] Knoll B., De Gids W.F., Luchtdoorlatendheid van 21 gevels met gevelelementen in 3 seizoenen, IMG-TNO, Delft (Netherlands), November 1981.

[22] Air Infiltration Control in Housing : A guide to International Practice Air Infiltration Centre and Swedish Council for Building Research, 1983.

[23] Wouters P., Voordecker P., L'Heureux D., Airtight measurements in 40 houses in the region of Namur, IEA annex 8 report, BBRI, Brussels, 1986.

[24] Dumont R., Orr H. & Figley D., Air Tightness Measurements of Detached Houses in the Saskatoon Area (National Research Council of Canada, Division of Building Research), Building Research Note nr. 178, Ottawa, 1981.

[25] Brunsell J. & Uvsløkk, S. Boligers Lufttetthet. Resultater fra lufttetthetsmalinger av nyere norske boliger. Airtightness of Buildings, Results from Airtightness Measurements in New Norwegian Houses (in Norwegian). (Norwegian Building Research Institute). Arbeitsrapport 31. Oslo 1980 (Translated into English by AIC).

[26] Hammarsten S. & Pettersson B., Testing of Retrofits in Buildings. Methods and Results, Paper to the Energy Audit Workshop. Copenhagen, April 1981.

[27] Warren P., A Simple Method for Predicting Infiltration Rates in Housing. Proceedings of the CIB W-67 Third International Symposium on energy Conservation in the Built Environment, Dublin, 1982.

[28] Grimsrud D., Grot R. & Harrje D., Air Infiltration Site Measurements Techniques. Second AIC Conference, Building Design for Minimum Air Infiltration. Stockholm, September 1981.

[29] Basset M., The Infiltration components of ventilation in New Zealand houses, 6th AIC-conference. Het Meerdal Park (Nl), September 1985

[30] AIC TN 16 : Leakage disstribution in buildings, Air Infiltration Centre June 1985.

[31] The Application of Structural Measures for Energy Conservation in Existing Buildings (Swedish Council for Building Research), D4 : 1982. Stockholm 1982.

[32] Holmberg A., Fönsterhalet. Inbyggnad av träfönster i nya hus. Wooden Windows in New Buildings (in Swedish Council for Building Research). R15:1981. Stockholm 1981.

[33] Höglund I. & Wanggren B., Studies of the Performance of Weatherstrips for Windows and Doors (Swedish Council for Building Research). D4:1980. Stockholm 1980.

[34] Hammarsten S. & Pettersson B., Testing of Retrofits in Buildings, Paper presented at the Energy Audit Workshop in Copenhagen, April 13-15, 1981.

[35] Elmroth A., Forslund J. & Rolen C., Effects of Energy Conservation Measures in Existing Buildings. Contribution to the 2nd AIC Conference : Building Design for Minimum Air Infiltration. Stockholm 1981.

[36] Höglund I., Johnsson B. & Lagerström J., Ulvundaprojektet - Effektivare energianvänding i ädre byggnader. Etapp I. The Ulvsunda Project - More Effective Energy Use in Older Buildings. Phase I (In Swedish) (Swedish Council for Building Research). T5 : 1981, Stockholm 1981.

[37] Elmroth A. & Nylund P.-O., Ventilation och byggnad är ett enda totalsystem. The ventilation system and the building are parts of the same system (In Swedish). *Byggindustrin nr.* 24, 1980. Stockholm 1980.

[38] Höglund I. & Wanggren R., Studies of the Performance of Weather-strips for windows and doors. (Swedish Council for Building Research). D4 : 1980, Stockholm 1980.

[39] Meunier B., Van Houtte O., Inhabitants' behaviour with regard to ventilation - a report with regard to the work of annex VIII, 6th AIC conference, Het Meerdal Park (NL), September 1985.

[40] Pfaff J.C., De Gids W.F., Ton J.A., Van de Ree D., Van Schijndel L.L.M., Ventilatie van Gebouwen. Onderzoek naar de gevolgen van het openen van één raam op het binnenklimaat van een kamer. IMG/TNO Rapport c 448, Nederland, 1980.

[41] Lyberg M.D., Residents and windows. Airing windows, Swedish Institute for building research, Stockholm, 1983.

[42] De Gids W.F., Pfaff J.C., Van Dongen J.E.F., Interim rapport "Bewonersgedrag en ventilatie", IMG/TNO rapport C 581, Nederland, Juli 1985.

[43] Van Gunst E., Het raam in onze woning in verband met gezondheid en ekonomie, De Ingenieur, nr. 11 and 14, 1959.

[44] Tamura G., Measurements of air leakage characteristics of house enclosures. ASHRAE transactions 1975, 81, part 1., 202-208.

[45] Shaw C.Y., Jones L., Schools : Air tightness and infiltration. ASHRAE J., April 1979, vol. 21, nr. 4, P. 40-45, Air tightness and air in school buildings, ASHRAE Trans. 1979, vol. 85, nr. 1, p. 85-95.

[46] Caffey, G.E., Residential air infiltration, ASHRAE, 1979 (1), 41-57.

[47] Guillaume M., Measurements of ventilation rates in houses with natural and mechanical ventilation systems. In "Ventilation and infiltration in dwellings", Proceedings of CIB Steering Group S17 meeting "Heating and Climatisation", Holzkirchen, September 1977, 68-93.

[48] McIntyre I.S., Newman C.J., The testing of whole houses for air leakage. Building Research Establishment note, 21/75.

[49] Tietsma G.J., Peavy B.A., The thermal performance of a two bedroom mobile home. National Bureau of Standards, Building Science Series 102.

[50] Nusgens P., Guillaume M., Natural ventilation of single family houses. Ventilation naturelle des maisons individuelles, CSTC, Trim. vol. 15, nr. 1, p. 4-16.
Translation nr. 12.

[51] Treado S.J., Burch D.M., Hunt C.M., An investigation of air infiltration characteristics and mechanisms for a townhouse. National Bureau of Standards, Technical Note, 992, August 1979.

[52] Warren P.R., Webb B.C., Ventilation measurements in housing. CIBS Symposium "Natural ventilation by design", London 2nd December 1980, p. 22-34.

[53] Jones W.R., Stricker S., Ventilation requirements and natural air leakage in residences. Ontaria Hydro Research Review, nr. 4, December 1981, p. 9-13.

[54] O'Sullivan P., Jones P.J., The ventilation performance of houses, a case study, 3rd AIC Conference "Energy efficient domestic ventilation systems for achieving acceptable indoor air quality", September 20-23.1982, UK.

[55] Hedberg H.O., Variaton of airtightness with time. Tathetens tidsberoende, Unpublished report Tyrens Foretagsgrupp AB Stockholm, 1982, 40 pp.

[56] Bassett M., Air Infiltration in New Zealand houses. 4th AIC Conference "Air infiltration reduction in existing buildings, Switzerland, 26-28 Sept. 1983.

[57] Murakami S., Yoshino H., Airtightness of residential buildings in Japan, 4th AIC Conference "Air Infiltration reduction in existing buildings", Switserland, 26-28 Sept. 1983.

[58] Reinhold C., Sonderegger R., Component leakage areas in residential buildings. 4th AIC Conference "Air Infiltration reduction in existing buildings", Switserland, 26-28 September 1983, p. 16.1 -16.3.

[59] Basset M.R., Building site measurements for predicting air infiltration rates. Preprint ASTM Symposium on measured air leakage performance of buildings, Philadelphia USA, April 2-3, 1984.

[60] Goss P., Air leakage characteristics of window treatment products. Preprint ASTM Symposium on measured air leakage performance of building, Philadelphia, USA, April 2-3, 1984.

[61] Saarnio P., Airtightness, pressure differences and indoor climate in the experimental building Kaarminkatu 24. Proc. CIB Workshop on indoor air quality and energy conservation, Helsinki, June 1983, ESPoo Report B3, p. V.1-V.15.

[62] Yoshino H., Hasegawa, F., Utsumi Y., Verification of calculation models of air infiltration standards in buildings, Reno, Nevada, 1-4 October 1984, pp. 20.1-20.21.

[63] Jackman P.J., A study of natural ventilation of tall office buildings. Inst. Heat Vent. Eng., Vol. 38, pp. 103-118, 1970.

[64] Sander D.M., Fortran IV Program to calculate air infiltration in buildings. National Research council, Division of building Research, Canada, Computer Program Nr. 37, Ottawa, 1974.

[65] Kusuda T., NBSLD, The computer program for heating and cooling loads in buildings. NBS Building Science Series 69, 1974.

[66] de Gids W.F. Calculation method for the natural ventilation of buildings. TNO research Institute of Environmental Hygiene, Delft, Netherlands, 1977

[67] Irving S.J. The computer simulation of smoke movement during building fires. Fire Prev . Sci. Tech., nr. 22, pp. 3-8, 1979.

[68] Etheridge D.W. and Alexander D.K., The British Gas multi-cell for calculating ventilation. ASHRAE Trans, vol. 86, part 2, pp. 808-821, 1980.

[69] Etheridge D.W., Gale R., Theoretical and experimental techniques for ventilation research in buildings. Proc. 1983 International Gas Research Conference, London, UK.

[70] Larsen B.T., Energy consumption of residential buildings. The computer program ENCORE Part 1 : User's Manual and Part 2 : Documentation. Norwegian Building Research Institute, 1977.

[71] Cole J.T., Kinast J.A., Zawacki T.S., Elkins R.H. and Marcris R.A. Development and field verification of a model of house air infiltration for single family residences. Gas Research Institute, Final Report, June 1981.

[72] Sherman M.T. and Grimsrud D.T., Measurement of infiltration using fan pressurization and weather data. AIC Conference "Instrumentation and Measuring Techniques, Windsor, UK, 1980.

[73] Warren P.R. and Webb B.C., The relationship between tracer gas and pressurization techniques in dwellings. AIC conference "Instrumentation and Measuring Techniques", Windsor UK, 1980.

[74] Cole J.T., et al., Application of a generalised model of air infiltration to existing homes. ASHRAE Trans. Vol. 86, Part 2, pp. 765-77, 1980.

AIVC Publications List

PERIODICALS

Air Infiltration Review
Quarterly newsletter containing topical and informative articles on air infiltration research and application. Also gives details of forthcoming conferences, recent acquisitions to *AIRBASE* and new AIVC publications. *Unrestricted availability, free-of-charge.*

Recent Additions to *AIRBASE*
Quarterly bulletin of abstracts added to *AIRBASE*, AIVC's bibliographic database. Provides an effective means of keeping up-to-date with published material on air infiltration and associated subjects. Copies of papers abstracted in 'Recent Additions to *AIRBASE*' can be obtained from AIVC library. *Bulletin and copies of papers available free-of-charge to participating countries* only.*

GUIDES AND HANDBOOKS

AIC-AG-1-86 – Liddament, M.W.
'Air Infiltration Calculation Techniques – An Applications Guide'
A loose-leaf handbook divided into six chapters covering empirical and theoretical calculation techniques, algorithms, references and glossary of terms. *Available free-of-charge to participating countries* only, via your national Steering Group representative.*

HANDBOOK – Elmroth, A., Levin, P.
'Air infiltration control in housing. A guide to international practice'
An international guide to airtightness design solutions of great practical value to all those concerned with the design of pollution – free dwellings with low energy demands. *Unrestricted availability. Price £12.50 hard copy. Also available in microfiche £10.00.*

TECHNICAL NOTES

AIC-TN-5-81 – Allen, C.
'AIRGLOSS: Air Infiltration Glossary (English edition)'
Contains approximately 750 terms and their definitions related to air infiltration, its description, detection, measurement, modelling and prevention as well as to the environment and relevant physical processes. *Available free-of-charge to participating countries.* Price: £10 to non-participating countries.*

AIC-TN-5.1-83 – Allen, C.
'AIRGLOSS: Air Infiltration Glossary (English-German/Deutsch-Englisch) Supplement'
Available free-of-charge to participating countries. Price £7.50 to non-participating countries.*

AIC-TN-5.2-84 – Allen, C.
'AIRGLOSS: Air Infiltration Glossary (English – French/Français – Anglais) Supplement'
Available free-of-charge to participating countries. Price £7.50 to non-participating countries.*

AIC-TN-5.3-84
'AIRGLOSS: Air Infiltration Glossary (Italian Edition)'
Available free-of-charge to participating countries. * *Price £10 to non-participating countries.*

AIC-TN-6-81 – Allen, C.
'Reporting format for the measurement of air infiltration in buildings'
Produced to provide a common method for research workers to set out experimental data, so assisting abstraction for subsequent analysis or mathematical model development. May be used directly for entering results and as a useful checklist for those initiating projects. Example of use of format is included as an appendix. *Available free-of-charge to participating countries.* * *Price: £6 to non-participating countries.*

AIC-TN-10-83 – Liddament, M., Thompson, C.
'Techniques and instrumentation for the measurement of air infiltration in buildings – a brief review and annotated bibliography'
Four-section bibliography contains review papers, information on tracer gas techniques, pressurization methods and miscellaneous approaches. In addition the report contains a list of manufacturers of instrumentation currently being used in air infiltration investigations. *Available free-of-charge to participating countries* only.*

AIC-TN-11-83 – Liddament, M., Allen, C.
'The validation and comparison of mathematical models of air infiltration'
Contains analysis of ten models developed in five participating countries. These range in complexity from 'single-cell' to 'multi-cell' approaches. Also contains numerical and climatic data for fourteen dwellings compiled to produce three key datasets which were used in model validation study. *Available free-of-charge to participating countries* only.*

AIC-TN-12-83 – Liddament, M.
'1983 Survey of current research into air infiltration and related air quality problems in buildings'
3rd worldwide survey by AIVC, containing over 170 replies from 22 countries. Produced in two sections: an analysis in tabular form of survey results, followed by reproduction in full of research summaries, and appendix containing names and addresses of principal researchers. *Available free-of-charge to participating countries* only.*

AIC-TN-13-84 – Allen, C.
'Wind Pressure Data Requirements for Air Infiltration Calculations'
An up-to-date review of the problems associated with satisfying the wind pressure data requirements of air infiltration models. *Available free-of-charge to participating countries* only.*

AIC-TN-13.1-84
'1984 Wind Pressure Workshop Proceedings'
Report of written contributions and discussion at Workshop held in March 1984, Brussels. *Available free-of-charge to participating countries* only.*

AIC-TN-14-84 – Thompson, C.
'A Review of Building Airtightness and Ventilation Standards'
Lists and summarises airtightness and related standards to achieve energy efficient ventilation. *Available free-of-charge to participating countries* only.*

AIC-TN-16-85 – Allen, C.
'Leakage Distribution in Buildings'
Examines those factors which can influence leakage distribution, including building style, construction quality, materials, ageing, pressure and variations in humidity. *Available free-of-charge to participating countries* only.*

AIC-TN-17-85 – Parfitt, Y.
'Ventilation Strategy – A Selected Bibliography'
Review of literature on choice of ventilation strategy for residential, industrial and other buildings. *Available free-of-charge to participating countries* only.*

AIC-TN-18-86 – Parfitt, Y.
'A subject analysis of the AIC's bibliographic database – *AIRBASE.*' 4th Edition
Comprehensive register of published information on air infiltration and associated subjects. The articles are indexed by subject and full bibliographic details of the 2,000 papers are given. A list of principal authors is also included. *Available free-of-charge to participating countries* only.*

LITERATURE LISTS – Listing of abstracts in *AIRBASE* on particular topics related to air infiltration.

No. 1 Pressurization – Infiltration Correlation: 1. Models (17 references).
No. 2 Pressurization – Infiltration Correlation: 2. Measurements (26 references).
No. 3 Weatherstripping windows and doors (24 references).
No. 4 Caulks and sealants (24 references).
No. 5 Domestic air-to-air heat exchangers (25 references).
No. 6 Air infiltration in industrial buildings (42 references).
No. 7 Air flow through building entrances (22 references).
No. 8 Air infiltration in commercial buildings (28 references).
No. 9 Air infiltration in public buildings (10 references).
No. 10 CO_2 controlled ventilation (13 references).
No. 11 Occupancy effects on air infiltration (15 references).
No. 12 Windbreaks and shelter belts (19 references).
No. 13 Air infiltration measurement techniques (27 references).
No. 14 Roofs and attics (34 references).
No. 15 Identification of air leakage paths (23 references).

Available free-of-charge to participating countries only.*

CONFERENCE PROCEEDINGS

No. 1 'Instrumentation and measuring techniques'.
Unrestricted availability. £35.00 sterling.
No. 2 'Building design for minimum air infiltration'.
Unrestricted availability. Price: £15.00 sterling.
No. 3 'Energy efficient domestic ventilation systems for achieving acceptable indoor air quality'.
Unrestricted availability. Price: £23.50 sterling.
No. 4 'Air infiltration reduction in existing buildings'.
Unrestricted availability. Price: £16.00 sterling.
No. 5 'The implementation and effectiveness of air infiltration standards in buildings'.
Unrestricted availability. Price: £16.00 sterling.
No. 6 'Ventilation strategies and measurement techniques'.
Unrestricted availability. Price: £22.00 sterling.
No. 7 'Occupant interaction with ventilation systems'.
Unrestricted availability. Price: £25.00 sterling.

Please note that the proceedings of AIC conferences numbers 1-6 are now also available in microfiche form, price £75.00 per set.

**The participating countries are: Belgium, Canada, Denmark, Finland, The Federal Republic of Germany, Netherlands, New Zealand, Norway, Sweden, Switzerland, United Kingdom and the United States of America.*

7. LIST OF PARTICIPANTS

Apart from the experts who contributed as (co-)authors to the various sections of the report, the following participants were involved in this part of the research project "Windows and Fenestration":

NAME	AFFILIATION	ADDRESS	COUNTRY
P. Wouters	Belgian Building Research Institute	Lombardstraat 41 B-1000 BRUSSEL	BELGIUM
H. Erhorn, R. Stricker, M. Szerman	Fraunhofer Institut für Bauphysik, Dir.Prof.Dr.-Ing. habil, K.A. Gertis	Nobelstrasse 12 D-7000 STUTTGART 80	FR GERMANY
P. Brunello	Istituto di Fisica Tecnica	Viale Ungheria 43 I-35100 UDINE	ITALY
R. Zecchin	Istituto di Fisica Tecnica Università di Padova	Viale Marzolo 9 I-35100 PADOVA	ITALY
H.A.L. van Dijk, K.Th. Knorr	TNO Institute of Applied Physics	Stieltjesweg 1 2600 AD DELFT	THE NETHERLANDS
A. Nielsen	Norwegian Building Research Institute	Hogskoleringen 7 N-7034 TRONDHEIM-NTH	NORWAY
J.B. Gay	Ecole Polytechnique Féderale de Lausanne (EPFL)	LESO CH-1015 LAUSANNE	SWITZERLAND
T. Frank	EMPA Dübendorf Section Building Physics	Überlandstrasse 129 CH-8600 DÜBENDORF	SWITZERLAND
P.G.T. Owens	Pilkington Glass Ltd.	Prescot Road, St. Helens, MERSEYSIDE WA10 3TT	UNITED KINGDOM
J.H. Klems, S. Selkowitz	Lawrence Berkeley Laboratory	1, Cyclotron Road BERKELEY, CALIFORNIA	USA